Feb. 2007, Vol. 2, Issue 1

BioResources

A peer-reviewed Online Journal Devoted to the Science and Advanced Applications of Lignocellulosic Resources

In this Issue ...

Cover image: Switchgrass (*Panicum virgatum*) at NC State University's Raulston Arboretum

BioResources is supported by NC State University, with database retrieval and online hosting at www.***bioresources****journal*.com, and backup files and author instructions at ***ncsu.edu/bioresources***.

BioResources, a peer-reviewed journal devoted to the science of lignocellulosic materials, chemicals, and applications

NC STATE UNIVERSITY
College of Natural Resources
Department of Wood and Paper Science
Campus Box 8005
Raleigh, NC 27695-8005
919.515.7707/919.513.3022
919.515.6302 (fax)

BioResources

Contents: Vol. 2, Issue 1, February 2007

BioResources is a peer-reviewed journal devoted to the science of lignocellulosic materials, chemicals, and applications. The journal is a service of North Carolina State University, College of Natural Resources (http://cnr.ncsu.edu). Articles can be down-loaded without charge as PDF files at www.bioresourcesjournal.com. The *BioResources* website is hosted by Scholarly Exchange, and articles become indexed for scholars through the Open Journal System (http://pkp.sfu.ca/). **Author instructions**, journal policies, an editorial board list, and article files (secondary source) can be found at http://ncsu.edu/bioresources. Correspondence should be directed to co-editors Martin A. Hubbe (hubbe@ncsu.edu, 919-513-3022) and Lucian A. Lucia (lucian.lucia@ncsu.edu, 919-515-7707).

INCINERATE, RECYCLE, OR WASH AND REUSE?

Martin A. Hubbe

What is the best way to minimize the environmental impact of using a product such as paper? Three debating teams were formed within a university class. One team advocated increased recycling of paper. Another team pointed to evidence showing reduced environmental impact and lower net CO_2 emissions if the paper is incinerated rather than recycled. A third team advocated the replacement of paper by items such as porcelain plates and video screens, cutting costs and reducing waste by multiple reuse.

Keywords: Paper recycling, Incineration, Reuse, Life cycle analysis, Pollution prevention, Environmental impact

Contact information: Department of Forest Biomaterial Science and Engineering, College of Natural Resources, North Carolina State University, Campus Box 8005, Raleigh, NC 27695-8005; hubbe@ncsu.edu

ADVENTURES IN TEACHING ABOUT POLLUTION PREVENTION

Values that are formed while one is very young often trump scientific arguments. Nevertheless, it is the job of faculty members, such as myself, to get university students to think about such issues as energy, toxic byproducts, and the value of relying on renewable resources.

In Spring 2003 I had the delightful opportunity to lead a session of "Advances in Pollution Prevention," a class offered to both on-campus and distance education students through NC State University's Engineering Online program. The class included about 22 undergraduate and graduate students, five of whom were participating by means of CDs, e-mail, and discussion forums. Working with Christine Grant, the course instructor, I had assigned students to one of three debating positions. Group 1 was asked to advocate the position that the proportion of paper that becomes recycled should be increased, in order to minimize environmental impacts. Group 2 was asked to advocate for increased incineration of used paper goods in order to minimize both energy use and the accumulation of landfill materials. Group 3 was asked to advocate for the replacement of disposable paper products by various forms of products designed for multiple reuse, sometimes involving washing of the product. In order to include the distance education students effectively in the debate, I assigned them the task of preparing written opening statements for each advocacy position.

The opening arguments introduced the main technical points supporting each of the three advocacy positions. Citing the EPA and various other sources, the team advocating "increased recycling" described how somebody's waste can be transformed into products, using up less landfill space, and reducing the consumption of wood. "You can pick the waste paper up at the curbside, just like trash," and "you avoid the toxic

emissions" associated with either primary pulp production or incineration of wastepaper. The opening statements in favor of "increased incineration of wastepaper" relied heavily upon life-cycle analyses, comparing de-inking to recycling. By incineration it was possible to avoid generation of toxic sludge, reduce overall air emissions, and displace the use of fossil fuels. The third team asserted that "replacing paper with reusable containers and surfaces" achieves superior environmental benefits and sharply reduces the needs for recycling, incineration, or other means of trash disposal. For instance, one porcelain cup can replace hundreds of paper cups.

After a few minutes of discussion within the groups, the on-campus students cautiously began to challenge and rebut statements made by opposing teams. The pro-recycling team pointed out that the trees left in the forest continue to consume CO_2, improving the air quality. Responding to the "reuse" group, they pointed out that reusable items are not necessarily reused, depending on people's habits. Washing of dishes increases the load on wastewater treatment facilities. The "reuse" group countered that high-volume washing facilities, as in a restaurant, can use detergent and hot water quite efficiently, and the chemicals required for de-inking of pulp are a greater environmental hazard. The pro-incineration team continued to cite results of studies indicating a lower net emission of toxic fumes and a lower overall cost compared to the other alternatives.

TAKING STOCK

Judging from the rising energy in the room, today's students care a lot about environmental issues. One student pointed out the somewhat artificial nature of the debate, suggesting that the best approach probably would involve a combination of the three debating positions. Dr. Grant added that different situations, *e.g.* a fast food restaurant *vs.* cooking or studying at home, might favor completely different strategies to minimize the environmental impact of paper use. It was interesting to note that only one of the on-campus students ultimately voted in favor of the incineration option, even though that team had offered the strongest evidence, based on life-cycle analysis. At least five students continued to favor paper recycling at the end of the class session. One of those students mentioned how strongly they had been influenced by presentations that they had heard while in Elementary School. But the largest number, over seven students, declared themselves to be in favor of "source reduction and reuse" at the end of the class.

Dr. Grant urged the students to hold onto their experience of looking carefully at the details and critical arguments for and against different environmental policies. "Some day soon you may find yourself in a position of influence, and you can help formulate policies in a more beneficial way." I urged the students to be especially careful when comparing different sources of energy; renewable energy can have environmental and societal benefits, compared to sources such as coal, petroleum, and nuclear energy. People vary too, with habits ranging from "lazy and cheap" to "crazy about the environment." In order to maintain progress in research areas that are of concern to readers of this magazine, it is essential that each of us take steps to tell our neighbors about both the benefits of and the need to protect our renewable resources.

RACKING STRENGTH OF PAPERBOARD BASED SHEATHING MATERIALS

Wu Bi[a] and Douglas W. Coffin[b*]

Small-scale racking testers were developed for use as a means to evaluate paperboard-based sheathing materials used in framed wall-construction. For the purpose of evaluating the performance of different sheathing materials, the tester provides an economic alternative to standard full-scale racking tests. In addition, results from testing provide practical insight into the racking response of framed and sheathed walls. The load-deformation responses of three commercial sheathing boards were measured, and initial racking stiffness and racking strength were proposed as parameters for characterizing the board. The racking test results showed that the initial paperboard racking stiffness correlated to elastic modulus and caliper, but the response was insensitive to paperboard orientation or test dimensions. Observations and results showed that both panel buckling and paperboard cutting at the staples affected the racking response, but the dominating factor influencing the racking response appears to be load transfer through the staples.

Keywords: Racking, Paperboard, Sheathing, Strength, and Stiffness

Contact information: a: Department. of Chem. Eng., Georgia Institute of Technology, 311 Ferst Drive, NW, Atlanta, GA 30332; *b: Department of Paper and Chemical Engineering, Miami University, Oxford, OH 45056; *Corresponding author: coffindw@muohio.edu*

INTRODUCTION

The walls of buildings must have adequate strength and rigidity to resist wind and seismic forces. Sheathing materials are normally applied to one or both faces of wall framing to limit in-plane shear distortion of the wall. This shear deformation is called racking. Common sheathing materials used in home construction include plywood, gypsum board, and flakeboard, which have thickness on the order of one half inch. Paper-based sheathing materials are now being produced for prefabricated homes. The caliper of these materials is less than one eighth of an inch. Currently, the racking strength of many of these paper-based materials is inadequate for general home construction, but if the racking strength were improved, these materials could be applied to other building applications.

Wall-racking tests are used to evaluate sheathing materials racking stiffness and strength and certify materials for use in construction. Standard procedures such as ASTM E72, and TAPPI T1005 cm-83 are routinely used to measure the racking strength of framed and sheathed walls (2.4 by 2.4m, or 8 by 8ft). Although, the sheathing materials are the main contributor to racking strength and stiffness, the rigid wood frame also adds to the strength and stiffness. According to ASTM E72, at least two or three runs with new testing arrangements should be done for each test. New identical frames built by the

specified wood species with the same average density should be used for each racking test run. Full-scale wall racking tests are expensive and time-consuming to run, except for the purpose of qualifying a board. For product development, there is a need for a more convenient and less expensive test that could be used to evaluate the potential racking strength of different paperboards and fasteners.

One simplified test previously used to help evaluate sheathing materials is the lateral nail resistance test. The lateral nail resistance test according to ASTM D1037 measures the resistance of a nail to lateral movement through a board. The relationship between the racking strength and lateral nail resistance was investigated for applications with relatively thick sheathing materials, such as fiberboards, gypsum boards, and flakeboards, using both linear models (Neisel and Guerrera 1956, Neisel 1958, Welsch 1963, Tuomi and Gromala 1977, Price and Gromala 1980) and a general nonlinear energy-based approach (McCutcheon 1985). None of those models provided good predictions of racking strength because the response of the nail in the resistance test was not the same as that in the racking test. For paperboard, staples are typically used instead of nails, and the response may be different.

Small-scale wall racking tests have been utilized to evaluate sheathing materials and predict full-scale wall racking behaviors (Tuomi and Gromala 1977, Price and Gromala 1980, McCutcheon 1985, Patton-Mallory et al. 1985). The work of McCutcheon (1985) and Patton-Mallory et al. (1985) suggest that it is possible to predict full-scale wall racking behavior by small-scale racking tests. McCutcheon's (1985) work also found that a small-scale racking test yielded a more reliable prediction than the nail resistance test (Patton-Mallory et al. 1985). Currently no small-scale racking test standard is available.

For our work, we were interested in understanding how changes in the paperboard used to produce the sheathing could affect the racking strength. We were not seeking a prediction of racking strength but a method to evaluate racking strength potential. Thus, a small-scale tester that puts the paper into a global mode of in-plane shear deformation seemed appropriate. With traditional sheathing materials, in-plane shear deformation and cutting from the nails will dominate the racking response. Since the paper-based materials are thin, we expected that buckling of the board also impacts the racking response. Thus, this was considered in the design of the racking tester.

Two simplified small-scale racking testers [0.406×0.406m (16×16in), and 0.813×0.813m (32×32in)] were designed, built, and evaluated. The racking responses of three commercial paperboards were then evaluated. Both the effects of buckling and cutting due to the staples were investigated. Paperboard cutting at the staples appeared to be significant, so a staple resistance test was developed and the effects of paperboard staple cutting on racking stiffness and racking strength were evaluated. In the following, the developed methods are described and some results are presented.

EXPERIMENTAL

Materials

Three commercial paperboards were labeled as A, B, and C. The paperboard was cut into 0.406m (16in) or 0.813m (32in) squares and conditioned at a relative humidity of 50% and temperature of 23 ºC for at least one week before testing. Wood inserts used in the racking test frame were also conditioned at the same temperature and humidity for more than one week. The pertinent properties of the paperboard were determined using the methods described below and are given in Table 1.

Moisture content was determined for five samples of each paperboard type, using samples with dimensions of 0.127×0.203m (5.0×8.0in). Both the initial mass and the oven-dry mass were determined. The oven-dried mass was determined by placing samples in a chamber at 103˚C until the mass reached equilibrium. Samples were cooled in a desiccator. For grammage, five samples having dimensions of 0.127×0.254m (5.0×10.0in) were cut, and the mass of each sample was determined. Mass for both moisture content and grammage was determined with the use of an analytic balance. Paperboard caliper for each of the five grammage specimens was measured with a dial caliper gage. A total of 12 measurements taken around the edges with three readings per edge were recorded and the average was computed. For elastic modulus, 10 MD and 10 CD samples (width: 12.7mm (0.5in); length: 0.20m (8.0in)) for each paperboard grade were used for tensile tests, using an Instron 3344 series EM Test Instrument with clamp length of 152 mm with the general loading speed 2.54mm/min. Some additional tests were done with the same loading speed as in staple resistance tests, 25.4mm/min. Elastic modulus multiplied by sample thickness was determined from the maximum slope of the load per unit width versus strain.

The results given in Table 1 show that both caliper and basis weight increase as ranked from A to B to C. The moisture contents of three paperboards are in the range of 8-9%. The measured elastic moduli (KN/m) are given as stiffness per unit width or engineering elastic modulus multiplied by caliper. The elastic modulus of board A was about 20-25% lower in MD and 10-15% lower in CD than that of B and C. There are no large differences between boards B and C for both directionality and geometric mean modulus ($\sqrt{E_{MD}E_{CD}} \times t$).

Small-Scale Racking Testers

The small-scale racking testers were designed to induce in-plane shear in the panel, but allow for fastening and panel widths similar to that in standard racking tests and actual house framing. The apparatus as shown in Fig. 1, consists of a hinged metal frame with wood inserts cut from 2x4 lumber and is essentially a picture-frame shear test. The sheathing was fastened to the frame with staples. The frame is attached to an Instron 1122 universal tester. The diagonal load and deformation in the tensile direction are recorded and used to evaluate the racking response. The stated load limit for the universal tester is a force of 4448N (1000lb), but in several tests we used a maximum load closer to 5783N (1300lb). The load cell has a range of 22200 N (5000 lb). The racking test has the following unique features: (1) free rotation of the metal frame at all four corners, (2) replaceable wood-studs inserted in rigid U-shaped metal frames, allowing for multiple

tests before stud replacement, and (3) the optional use of a middle wooden stud at the center of one span in the 32-inch racking tester. To eliminate the need for the paperboard to accommodate the large deformation at the corners, the corners of the sheathing sample are cut off before testing. Figure 2 shows a close-up of the hinged corners of the frame, in which a metal pin was used to hold the corner together, yet allow free rotation.

Table 1: Properties of three grades of paperboards

Paperboard		(A)		(B)		(C)	
		Mean	S.D.	Mean	S.D.	Mean	S.D.
Basis Weight (g/m^2)		1,390	20	1,810	10	3,020	10
Caliper (t: mm)		1.84	0.02	2.45	0.03	3.18	0.02
Moisture Content (%)		8.5	0.1	8.2	0.2	8.7	0.1
Elastic Modulus	Ratio: E_{MD}/E_{CD}	2.6		2.9		3.0	
	$\sqrt{E_{MD}E_{CD}} \times t$, (kN/m)	3150	150	3800	200	3900	200
S.D. = Standard deviation							

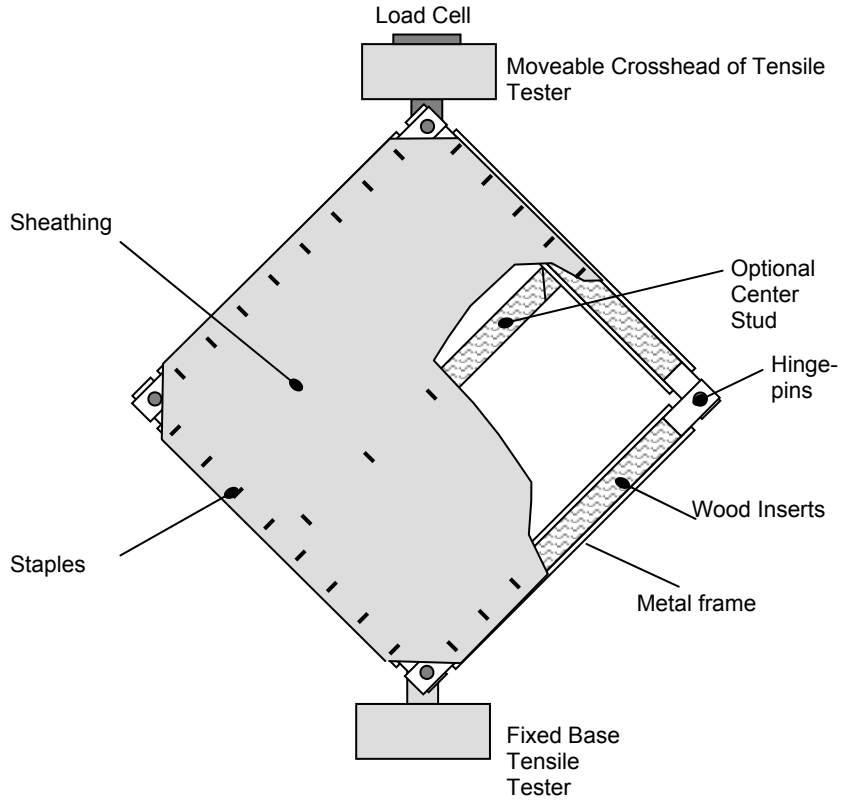

Fig. 1. Designed small-scale test system (left) and the metal frame (right). Shown for 32-inch tester with optional middle stud.

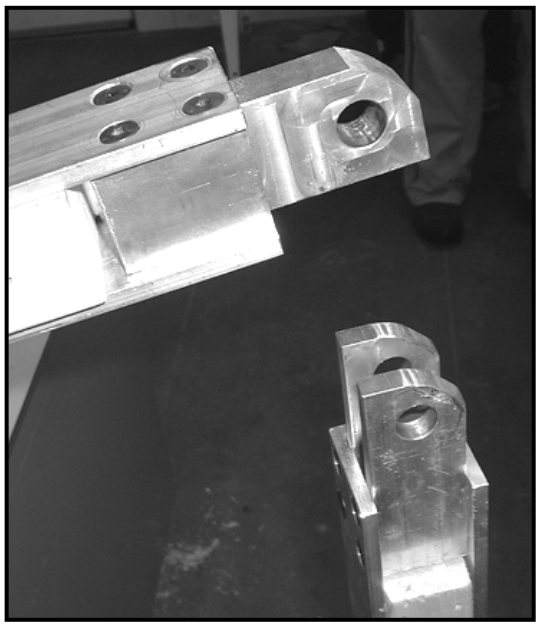

Fig. 2. Hinged corner connection of small-scale racking tester.

No standard is available for the small-scale racking test. The applied racking test procedures followed the general rules used when conducting the full-scale racking test standard. The staples used for the test were 16 gage, with a 1 inch crown and a 1 inch length. Staples were spaced at 7.62cm (3in) intervals along the edges and at 15.24cm (6in) to the middle stud. There were 8 or 4 staples applied at each side in 0.813m (32in) or 0.406m (16in) racking tests respectively, and 4 staples applied to the middle stud in 0.813m (32in). The staple crown was perpendicular to shear stress direction on each side. Staples were centered on the wood stud. After one test, staples and sheathing were removed and stapling positions were shifted about 1.3cm (0.5in) along the stud for the next run. By shifting the staple location, four to six runs could be done before the studs were removed. The depth of wood inserts was 5.08cm (2in) in the 32-inch tester. This depth was double of staple leg length, which allowed for both surfaces of the wood inserts to be used before being discarded. The racking test loading speed was 2.54mm/min (0.1in/min), which was close to the load rate of 790lb in 2min specified in ASTM E72 (2).

To evaluate the buckling extent, out-of-plane displacement was measured using a combination-square and a reference bar clamped to the frame. When a measurement was made, the reference bar was attached to the backside of the tester frame and the combination-square was used to assure the scale was perpendicular to the original plane of the panel. The reference bar provided a reference plane that was parallel to the undeformed plane of the panel. The initial distance from the paperboard surface to the reference plane was measured prior to loading. The difference between the original distance and the distance measured while the tester was under load gave the amount of bulging in the panel at the point of measurement. To compare between samples, the measurements were made at prescribed diagonal displacements. When the extension was reached, the test was paused to hold the racking deformation constant. The measurement was taken at the center of the buckling region where it was a maximum.

Paperboard Staple Resistance Test

During racking tests, cutting of the sheathing around the staples was observed. Therefore, the staple-cutting resistance of the paperboard was investigated and the staple resistance test shown in Fig. 3 was developed**.** The nature of this test is similar to the nail resistance test. Two paperboard strips having the same width of the studs (3.81cm (1.5in)) were aligned with a specimen of wood and stapled to the wood at opposite ends. The free ends of the paperboard were clamped to the jaws of an Instron 3344 series EM Test Instrument. The net paperboard length under tension (net gage length) was taken as the sum of the distances from the clamps to the middle of the staples for both paperboard samples. Different numbers of staples (1, 2, or 3) were used with the crown, either perpendicular, as illustrated in Fig. 3 (a), or parallel, as illustrated in Fig. 3 (b), to the load direction. Paperboard samples were cut in both the machine direction (MD) and the cross machine direction (CD). A range of different gage lengths were used on the staple resistance tests.

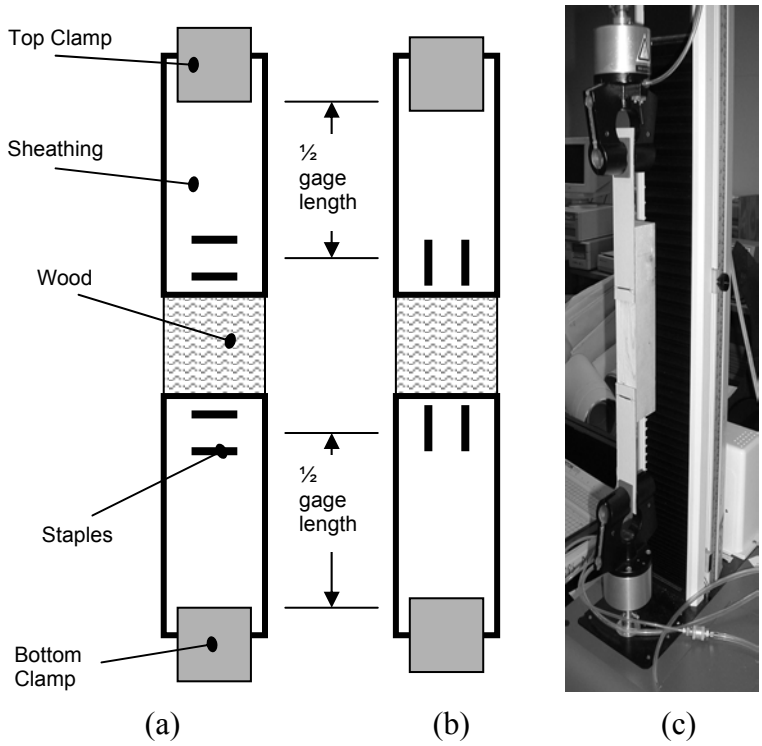

Fig. 3. Staple-resistance test. (a) Schematic with staples in perpendicular position, (b) Schematic with staples in parallel position, (c) Photo with one perpendicular staple.

Techniques of Data Analysis

The analysis of the load-deflection data merits discussion. Given the set-up described above, the load-deflection curve obtained from the racking tester is the diagonal elongation versus the diagonal force. When the test first begins, the whole frame is lifted, and any slack in the system is removed before the paper begins to deform. A typical load-deformation response from the racking test is shown in Fig. 4. This initial

portion of the curve corresponds to lifting the frame off the bottom support. In the next region the load is fairly constant and corresponds to the pulling taut of the frame and the bottom clamp. The load level in the regime corresponds to the dead-load of the frame that had been supported by the bottom clamp. The final region where the load is increasing corresponds to the shear deformation of the sheathing. In the initial loading, there appears to be slack, that is probably due to the deformation needed to fully load the panel. To look at the shear-deformation of the panel, the dead-load and slack was removed. First, the dead load was subtracted from the total load to get the panel load. Next, the point of maximum slope was determined. The intercept of the tangent at the point of maximum slope with the axis of zero panel load were determined and taken as the point of zero-strain location. The corrected load-displacement curve used to determine racking load versus shear strain is shown as the curve shifted to the left in Fig. 4.

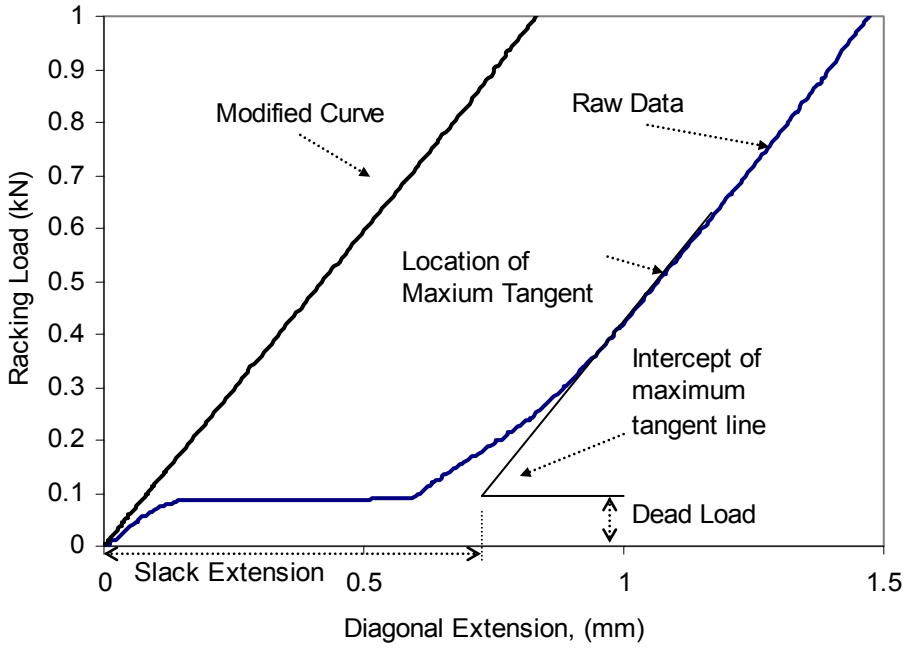

Fig. 4. Typical load-deformation curve before and after analysis.

The correction procedure described above was used to compare curves from different samples. Two other quantities were also taken for the purposes of comparison; racking strength and racking stiffness. Racking strength is the difference in maximum load and dead load divided by the length of the panel sides. The maximum load was not determined for all samples due to the limitation of the load cell, but for many of the samples a maximum was reached. The racking stiffness was determined as the maximum slope of the load versus elongation curve, determined from a running average on the slope versus elongation curve. The deformation interval used in the averaging corresponded to a shear strain of 0.0016.

We define the racking stiffness as the initial slope of the load deformation curves.

$$K_{racking} = \frac{P}{\delta} \quad (1)$$

To first order, the diagonal load, P, versus diagonal extension, δ, can be directly related to the shear stress, τ, and engineering shear strain, γ, in the panel as

$$P = \sqrt{2}at\tau \quad \delta = \frac{a}{\sqrt{2}}\gamma \quad (2)$$

where a is the length of the sides of the panel and t is the thickness of the panel. Assuming that the initial portion of the response can be described as linear-elastic, $\tau = G\gamma$ where G is the shear modulus. For paper, the in-plane shear modulus has been experimentally found and reported to be proportional to the geometric mean of the normal moduli, $G = 0.39\sqrt{E_{MD}E_{CD}}$ (Baum et al. 1981). Substituting Eqn. (2) into Eqn. (1), along with the assumed elastic behavior, provides a prediction of the racking stiffness as

$$K_{racking} = \frac{P}{\delta} = 2Gt = 0.78\sqrt{E_{MD}E_{CD}}\, t \ . \quad (3)$$

According to Eqn. (3), $K_{racking}$ is independent of the size of the test frame. For larger deformations of the panel, we expect the relationship of load to deformation to be nonlinear due to both buckling and yielding in the materials. The buckling will be length dependent, and therefore, scaling will not persist at larger deformations. With the current two test sizes the scaling of stiffness did hold. To check scaling of the load-deformation curve, the results were transformed to shear load and shear strain.

Results from the two-size testers are scaled using the shear strain and a racking shear load ($P_{shear} = \tau t$). Thus, the resulting curves of load and deformation obtained from the racking tests are presented as $P_{shear}(\gamma)$ where

$$P_{shear} = \frac{P}{\sqrt{2}at\tau}, \gamma = \sqrt{2}\frac{\delta}{a} \quad . \quad (4)$$

The initial stiffness of these scaled curves is $\frac{1}{2}K_{racking}$. For the board most prone to buckling (board A), the 32-inch panel results scaled with the 16-inch panel up to a shear strain of about 0.4%. At larger shear strains, the 32-inch panel lost load capacity due to buckling. When a center stud was used in the 32-inch panel, the scaling persisted for the entire load path with strains up to 3%. For the board least prone to buckling (board C), the scaling was valid up to a strain of approximately 1%.

Equation (3) gives an upper bound prediction for racking stiffness. The actual stiffness will be lower, because of the compliance in the fasteners and the frame. For the sheathing material, the factor of 0.78 shown in Eqn. (3) may not hold, because the approximation of Baum et al. (1981) was derived for uncoated paperboard. On the other hand, a linear correlation between geometric mean modulus and initial slope of the racking test was expected.

If the load in the racking test peaks before the limit of the test system is reached, the maximum load is referred to as the racking strength.

RESULTS AND DISCUSSION

Initial Racking Stiffness

A series of racking tests of boards A, B and C were conducted, using both sizes of the racking testers, but without a middle stud. From the load-deflection data, the racking stiffness was calculated. A plot of racking stiffness versus geometric mean modulus is given in Fig. 5. The results indicate that a proportional relationship between geometric mean modulus and racking stiffness as suggested in Eqn. (3) exists. Since there was little difference in the values of geometric mean modulus for boards B and C, there is not enough variation to give a robust test of the relationship, but it is encouraging that B and C have very similar racking stiffnesses and geometric mean moduli despite the large difference in grammage between the two sheets. There is very little difference in the racking stiffnesses for the two different size panels. The proportionality constant is only about 36 percent of the theoretical value given in Eqn. (3). A large portion of this difference is likely due to how well the load is transferred through the staples. Some of it could be due to viscoelastic effects or that the board has a lower shear modulus than the 0.39 value suggested by Baum et al (1981). The difference is not related to panel bulging, which is small in this range and would have caused the 32-inch panel to have a lower slope than the 16-inch panel.

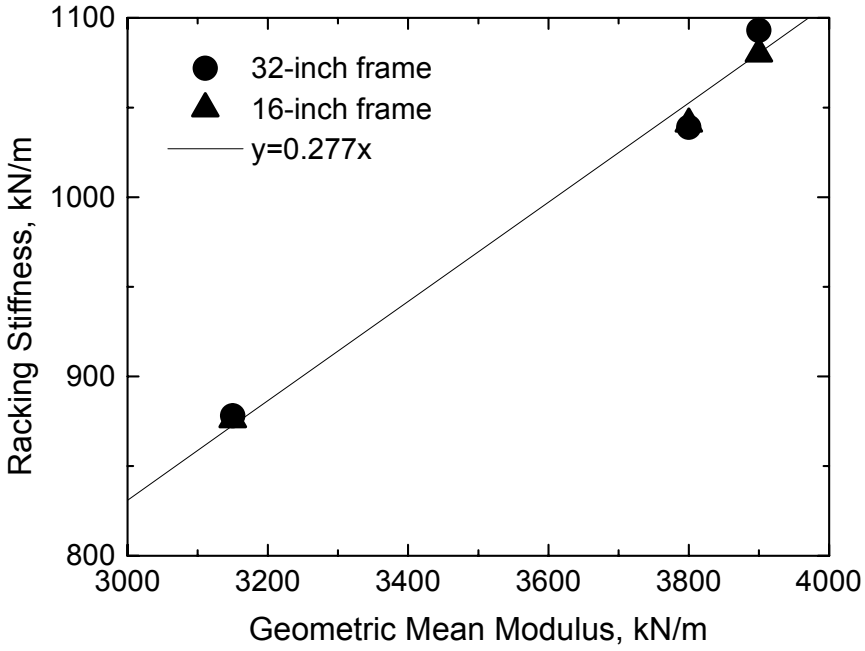

Fig. 5: Plot of racking stiffness against geometric mean modulus

Racking Strength

Panel buckling was observed for all the racking tests conducted in this program. Buckling is resisted by higher bending stiffness and decreased span length. Buckling did not appear to influence racking stiffness, but can be expected to impact racking strength. If buckling impacts strength, one would expect that the 16-inch panels would obtain higher racking strengths than the 32-inch panels. In addition, adding the middle stud should reduce buckling and perhaps improve strength.

For paperboard A, racking strengths for tests which included the middle studs were about 20% higher than those tests that did not use the middle stud. This difference is shown in Fig. 6. For paperboard B, less racking strength differences were observed, however use of the middle stud improved racking strength. For board C, no differences were observed for loads up to the test limit of 4.45KN (1000lb) between tests with and without the middle stud. Paperboard A had the lowest caliper and hence lowest bending stiffness and Paperboard C had the highest bending stiffness. The results given in Fig. 6, suggest that buckling of the panel lowers racking strength.

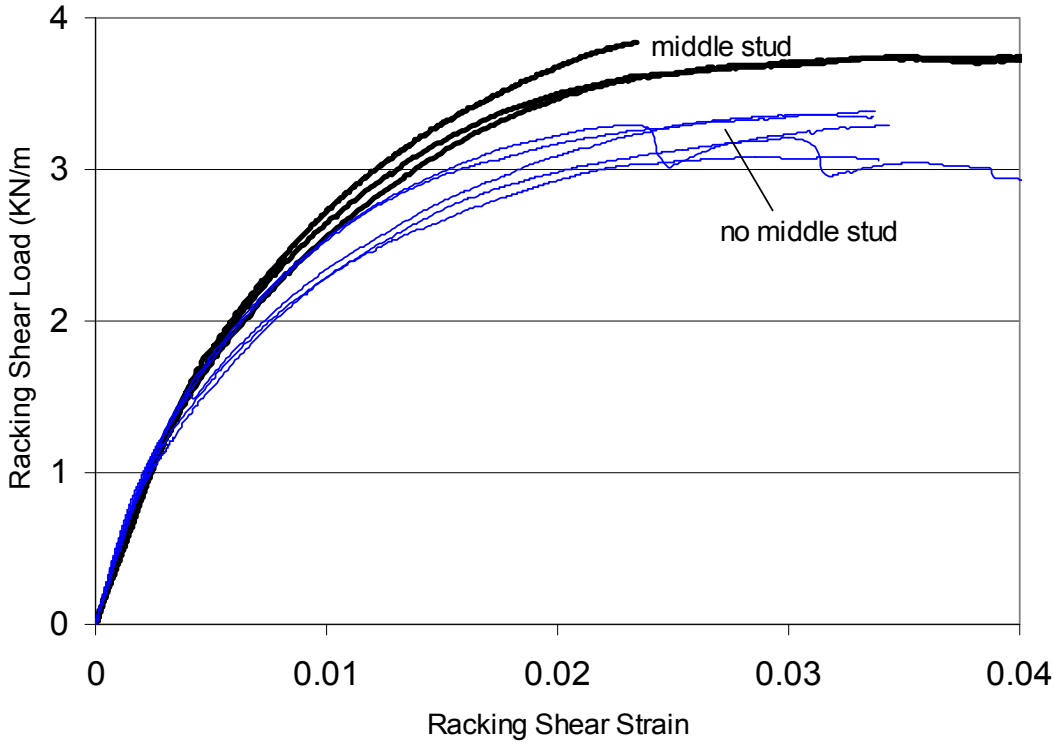

Fig. 6. Effect of middle stud on racking performance for Board A.

The racking strength differences for the three boards are clearly shown in Fig. 7 for both the 16-inch and 32-inch testing with no middle stud**.** The "V" shaped dips in load shown in the figures are due to stress relaxation that occurred when the deformation was held fixed while a buckling measurement was made. Buckling extents were measured at a net shear strain equal to 0.0106 and 0.0159. As expected, much larger buckling extents were observed for the 32-inch test (no middle stud) than those in 16-inch tests. For example, for board B the extent of buckling in the 32-inch test was 15 mm

whereas it was only 1 mm in the 16-inch test. For the 16-inch test, board A had a bulge of 5 mm, which is five times greater than that observed in B and C. Figure 7 also shows that for the 16-inch test boards B and C had similar responses except near the maximum loads where B was slightly weaker. This might be expected since the geometric mean modulus for both boards was quite similar and buckling was minimal. In the 32-inch test frame however, board C is stronger than B for a large range of strain. This is due to the extra buckling that occurs in the 32-inch test. Figure 7 clearly shows that the resistance to buckling offered in the 16-inch test frame leads to higher racking strength. These results combined with the differences in the tests with and without the middle stud and the observation that wrinkles traversed the middle stud during the test indicate that the current practice of spacing staples every 6 inches on middle studs does not provide sufficient resistance to buckling.

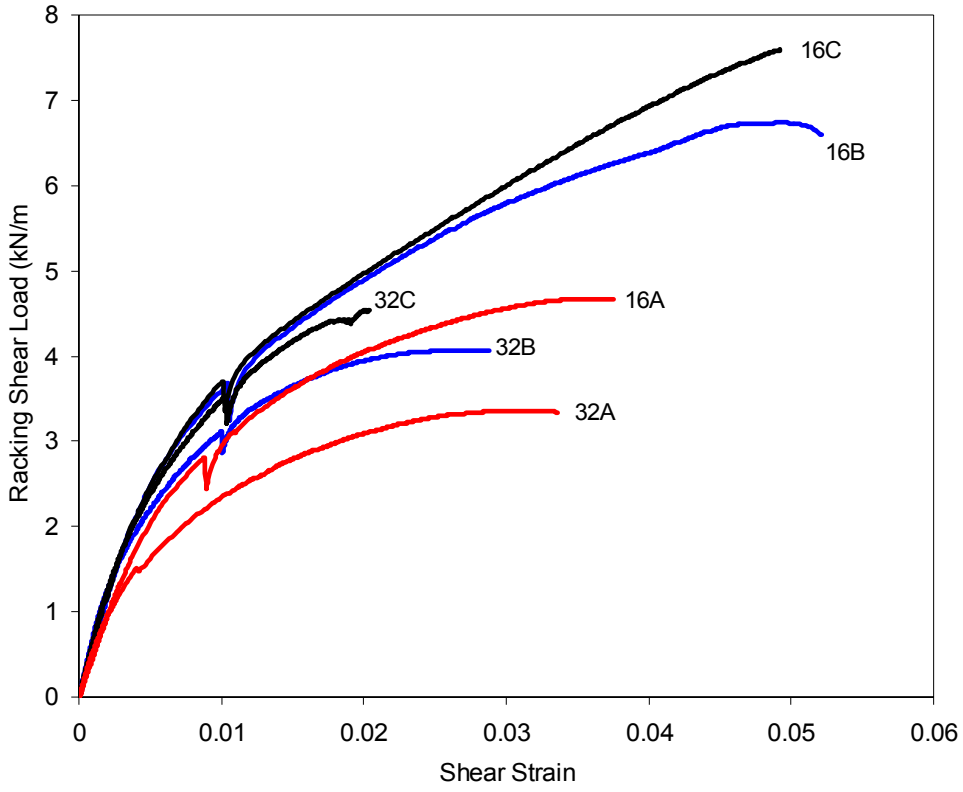

Fig. 7. Representative racking shear load versus shear strain curves of three paperboards without middle stud; 16 indicates 16-inch test size, 32 indicates 32-inch test size, A, B, C indicate board type.

Staple Resistance

Tensile load-strain curve of an MD sample of board A, along with the load-strain curves obtained from the staple resistance tests for three different MD gage lengths with either one, two or three staples are shown in Fig. 8. The staples were parallel to the load direction. The tensile tests and the staple resistance tests were conducted at the same loading speed (1in/min).

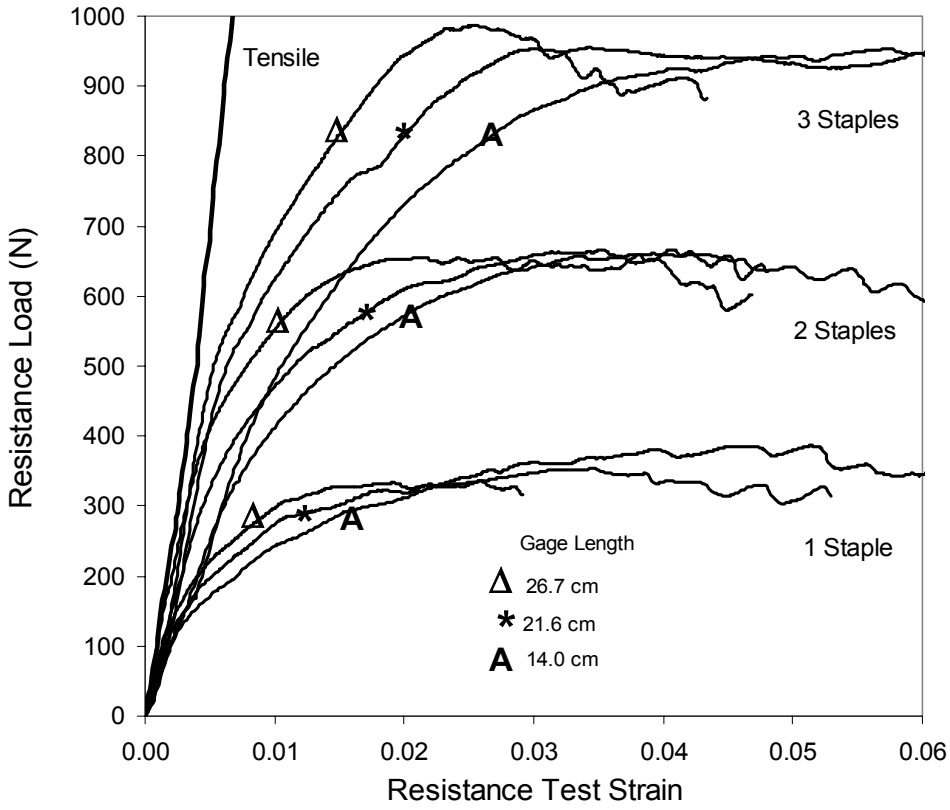

Fig. 8. Staple resistance test curves at varied net gage length and staple numbers

As the gage length increased in the staple-resistance test, the load-deformation curve approached that of the tensile test, but the maximum load did not increase. It appears that staple cutting influences the response even at fairly low load levels. The strength is approximately proportional to the number of staples, and therefore, one can estimate staple-resistance strength. In addition to increased gage length, increasing the number of staples also brought the stress-strain curve closer to that of the tensile test, but the maximum loads in the staple tests were much lower than that of the tensile test (2220N). Therefore, staple cutting appears to severely limit strength and may even influence stiffness.

The maximum cutting forces for a series of staple tests using all three board types, MD and CD samples, and parallel and perpendicular staples were measured. Surprisingly, no significant differences were found between MD and CD samples. On the other hand, perpendicular staple orientation gave higher resistance loads than those with parallel orientation. This is probably due to additional resistance offered by the crown of the staple, which resists movement of the board when it is perpendicular to the load, but allows the paper to slip over the staple when it is parallel to the load.

In racking tests, paperboard (fiber) staple orientations were MD-Perpendicular on two sides and CD-Perpendicular on the other two sides. The staple-resistance strengths obtained from the tests presented in Fig. 8 are given in the second column of Table 2. If we assume that the racking strength is limited by staple cutting, the average maximum

staple cutting force (P_S) from the staple resistance tests can be used to calculate the racking strength (P_U) as follows:

$$P_U = \sqrt{2} \times N \times P_S \quad (5)$$

where, N: number of staples per side in racking tests, which was 8 for the 32-inch test frame and 4 for the 16-inch test frame.

Table 2: Comparison of actual and predicted racking strengths

Paperboard Grades	Nail Resistance, N, From tests	Racking Strength, kN			
		32-inch Test		16-inch Test	
		Observed	Eqn. (5)	Observed	Eqn. (5)
A	400	3.56-4.14	4.5	2.14-2.67	2.3
B	600	4.72	6.8	3.56-3.87	3.4
C	650	5.34	7.4	>4.45	3.6

The measured racking strengths, along with values calculated using Eqn. (3) are given in Table 2. For the 32-inch tests, the measured strengths are less than the calculated values. For the 16-inch tests, the test values are greater than the predicted values. This can be interpreted as follows, the deformation on the frame results in shear deformation, panel buckling, and/or staple cutting. Our observations indicate that the larger the extent of buckling, the lower the degree of paperboard cutting by staples, and vise-versa. In the smaller panel tests, buckling was low, staple cutting was high, and the strength is probably dominated by staple-cutting resistance. In the larger panels, the buckling was much greater, and strength was lower than that due to staple cutting alone. This result also suggests that buckling must have a significant impact on racking strength in the larger panels.

Non-uniform Shear Stress Transfer and Cutting Due to Staples

The predicted initial slopes of three paperboards calculated by Eqn. (3) were 2450, 2950 and 3050KN/m for paperboards A, B and C, respectively. These values were almost triple that of the observed initial slopes. These predicted initial stiffnesses assume uniform and infinitely stiff connections along the sheathing edges. In fact, the shear stress transfer to paperboards occurs only through the staples, and stress concentrations can be expected to impact racking stiffness and strength.

To provide a more uniform shear stress transfer, additional staples were applied to each edge for a sample of board C in the 32-inch tester. Figure 9 provides stress-strain curves of a sample that was loaded and unloaded several times. Each time the sample was unloaded more staples were added to the edges. The results show that adding more staples increased the racking stiffness. The racking stiffness values increased by 15 and 50 percent when using twice and five-times the original number of staples (8/side) respectively.

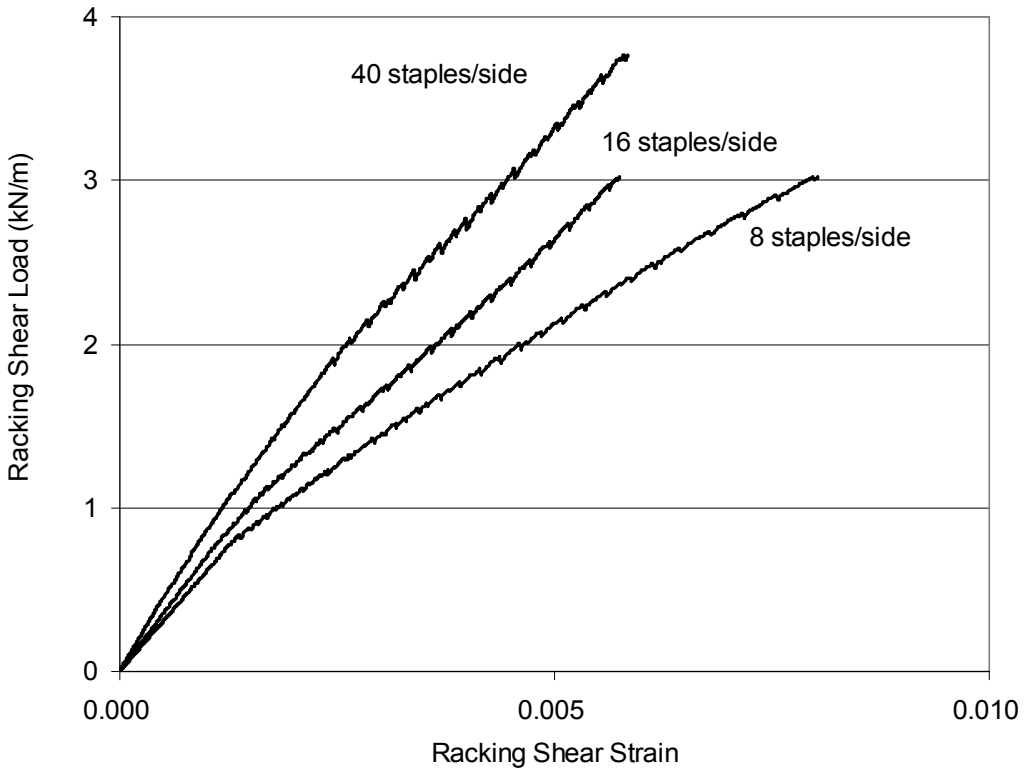

Fig. 9. Racking curves with increased number of staples for the 0.813m (32in) tests with board C

To provide a very uniform sheathing connection the panel was glued to the test frame using Liquid Nail glue with the 16-inch tester. A comparison of the racking response using staples and that using glue are shown for board A in Fig. 10. Clearly the gluing method provided superior racking stiffness and racking strength with a 40-50% increase in racking strength and about a 50% increase in racking stiffness for paperboard A. The average values of buckling extents and initial slopes (average-type) are compared for the two methods in Table 3. The glue test with board B failed quite early and paperboard was peeled away from tester frame at one corner due to the weak gluing at that location. Buckling was not measured for board B. With glued panels, the extra compliance from staple cutting was absent and the extent of buckling was slightly larger than those in the staple tests. Initial racking stiffness values from glue panels were about 50% higher than those from stapled panels for all three paperboards.

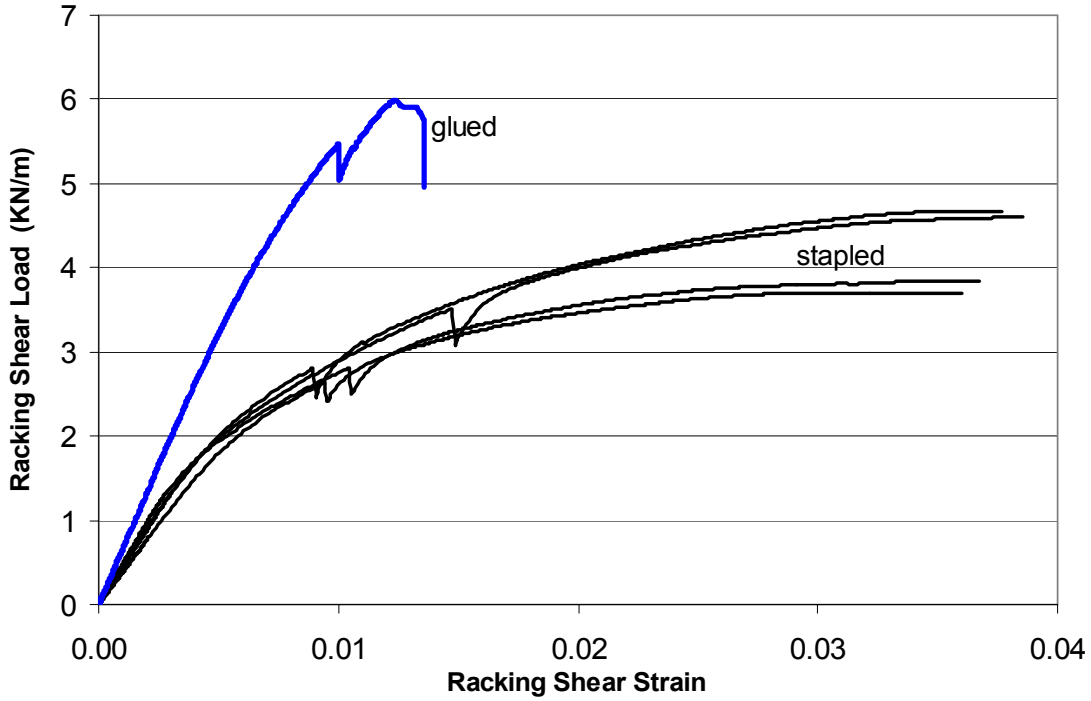

Fig. 10. Comparisons of racking responses between glue and stapling the sheathing for the 16-inch tests of board A

Table 3: Comparisons of initial slopes and extent of buckling using different methods to attach sheathing in 16-inch racking tests

Paperboard Grade	Extent of Buckling (mm)		Racking Stiffness (KN/m)	
	Glue	Staple	Glue	Staple
A	7.1	5.3	1315	876
B	N/A	1.0	1462	1041
C	1.0	1.0	1581	1080

CONCLUSIONS

A small-scale racking tester was developed to evaluate paperboard sheathing materials. It appears that the tester is useful to evaluate racking performance of both the paperboard and the fasteners. The tester provides an economical alternative to the full-scale racking test when one is interested in evaluating differences in sheathing materials. Based on the results and discussions presented above, we conclude the following:

1. The geometric mean modulus multiplied by caliper provides a predictor for racking stiffness.
2. Racking stiffness was unaffected by buckling, test dimension changes, and paperboard MD/CD orientation.
3. Racking stiffness was affected by the number of staples. Lower magnitudes of the observed initial stiffness values were mainly caused by non-uniform shear stress transfer if using staples.

4. Racking strength is negatively affected by both panel buckling and the staple method used to attach the sheathing to the studs.
5. Racking strength could be greatly improved by reducing buckling extents, using thicker boards or gluing the board to the studs.

Given that gluing is probably not acceptable to many home builders, the producer of the sheathing must determine methods to increase fastener resistance of the board. The small-scale tester is probably not sufficient to capture the differences that may be caused by changing the MD/CD orientation of the board with respect to the framing. This is due to the aspect ratio of free spans in 32-inch test with studs is only two while in the real wall is six. In a real wall system, mounting the sheathing so that MD is perpendicular to the framing studs may give higher racking strength.

In summary, the small scale racking test could differentiate differences in the three board types. The small-sale racking tester, along with the staple resistance tester provides alternative methods to evaluate potential sheathing materials before full-scale tests are completed.

ACKNOWLEDGMENTS

This work was completed in partial fulfillment of an MS degree from Miami University. The authors express sincere gratitude to Mr. Rodney Kolb for his participation and to Fibre Converters (Constantine, MI) for providing the paperboard.

REFERENCES CITED

Baum, G. A., Brennan, D. G., and Habeger, C. C. (1981). "Orthotropic elastic constants of paper," *Tappi J.* 64(8), 97-101.

McCutcheon, W. J. (1985). "Racking deformations in wood shear walls," *J. Struc. Eng.* 111(2), 257-269.

Neisel, R. H. (1958). "Racking strength and lateral nail resistance of fiberboard sheathing," *Tappi J.* 41(12), 735-737.

Neisel, R. H. and Guerrera, J. F. (1956). "Racking strength of fiberboard sheathing," *Tappi J.* 39(9), 625-628.

Patton-Mallory, M., Wolfe, R. W., Soltis, L. A., and Gutkowski, R. M. (1985). "Light-frame shear wall length and opening effects," *J. Struc. Eng.* 111(10), 2227-2239.

Price, E. W., and Gromala, D. S. (1980). "Racking strength of walls sheathed with structural flakeboards made from southern species," *Forest Prod. J.* 30(12), 19-23.

Sherwood, G., and Moody, R. C. (1989). "Light–frame wall and floor system: Analysis and performance. General Technical Report FPL-GTR-59," USDA Forest Serv. Forest Prod. Lab., Madison, WI.

Tuomi, R. L., and Gromala, D. S., 1977. "Racking strength of walls: Let-in corner bracing, sheet materials, and the effect of loading rate," U.S. Dept. Agric. Forest Serv. Res. Pap. FPL 301. 20p.

Welsch, G. J. (1963). "Racking strength of half-inch fiberboard sheathings," *Tappi J.* 46(8), 456-458.

STANDARDS CITED

American Society for Testing and Materials. (1997). Test Methods for Evaluating Properties of Wood-Based Fiber and Particle Panel Materials. ASTM D1037. Philadelphia, PA.

American Society for Testing and Materials. (1997). Standard Test Methods of Conducting Strength Tests of Panels for Building Construction. ASTM E72. Philadelphia, PA.

TAPPI. (1983). Racking Strength of Structural Insulating Board. T1005 cm-83. Atlanta, GA

Article submitted: November 5, 2006; Reviews completed Dec. 11, 2006; Revised article accepted Dec. 15, 2006; Article published Dec. 18, 2006.

RHEOLOGY OF CARBOXYMETHYL CELLULOSE SOLUTIONS TREATED WITH CELLULASES

Jung Myoung Lee [a], John A. Heitmann [a], and Joel J. Pawlak [a*]

The effect of cellulase treatments on the rheology of carboxymethyl cellulose (CMC) solutions was studied using a rotational viscometer. The rheological behaviors of CMC solutions of different molecular mass and degrees of substitution where studied as a function of time after various treatments. These solutions were subjected to active and heat-denatured cellulase, a cationic polyelectrolyte (C-PAM), as well as different shear rates. A complex protein-polymer interaction was observed, leading to a potential error source in the measurement of enzymatic activity by changes in the intrinsic viscosity. The interaction was termed a polymeric effect and defined as a reduction in viscosity of the substrate solution without significant formation of reducing sugars from enzymatic hydrolysis. The cause of the reduction in viscosity appears to be related to the interaction between the enzymes as amphipathic particles and the soluble CMC. Thus, the polymeric effect may cause a considerable experimental error in the measurement of enzymatic activity by viscometric methods.

Keywords: Carboxymethyl cellulose (CMC), Endoglucanase activity, Cellulase, Viscosity, Rotational viscometer, Thermal denaturation, Polymeric effects

*Contact information: a: Department of Wood and Paper Science, North Carolina State University, Box 8005, Raleigh, USA; *Corresponding author: jjpawlak@ncsu.edu*

INTRODUCTION

Cellulases are produced by a variety of bacteria and fungi. These enzymes have been used in a number of industrial applications in the fields of food science, textiles, and pulp and paper (Bhat 2000). These enzymes act on cellulosic substrates, both soluble and insoluble. Native cellulose has a complex ultrastructure with both crystalline and amorphous regions. The simultaneous synergistic action of several different isozymes of cellulase is required to complete the hydrolysis of solid cellulose. Based on their activity on cellulose, cellulases can be classified as endoglucanases (EGs), cellobiohydrases (CBHs), and β-glucosidases (Belgiun and Aubert 1994). EGs preferentially hydrolyze the β-(1-4) linkages of amorphous cellulose in a random manner. CBHs hydrolyze crystalline cellulose by cleaving the β-(1-4) linkage of the cellulose to produce cellobiose and may work synergistically with EG to depolymerize the cellulose. The cellobiose released from EG and CBH actions is finally converted into glucose by action of β-glucosidase. Thus, the structure-function relationship between the cellulase isozymes and the cellulosic substrate enhances our knowledge of cellulose biodegradation (Boisset et al. 1998).

Enzyme activity is measured by the production of sugar reducing end group, which is taken to be an indication of cleavage of the cellulose molecules. It is also an indication of the efficiency of the cellulase hydrolyzing reaction. The determination of cellulase activity is a complicated process, because the hydrolysis of insoluble cellulose may not be linear with enzyme dosage and/or reaction time. Thus, the dosage of enzyme and the point in the reaction at which the activity is measured is critical. For such reasons, enzymatic activity should be carefully determined. Several standard substrates are available for the determination of cellulase activity in terms of the overall and EG activity (Ghose 1987). Filter papers have been used as a standard substrate to measure the total cellulase activity (Wu et al. 2006). The filter paper activity, termed as FPase, expressed the summations of the simultaneous synergistic action of EGs, CBHs, and β-glucosidase in a cellulase preparation. Soluble cellulose derivatives, such as carboxymethyl cellulose (CMC) and hydroxyethyl cellulose (HEC), may be used as substrates for determining EG activity. These substrates are rather specific to EG activity, since CBHs are not generally able to degrade substituted cellulose (Rouvinen et al. 1990). The hydrolysis rate of EG was conventionally determined by reduction of viscosity or by increase of reducing sugar end groups of the cellulose derivatives (Sharrock 1988; Mullings 1985). Recently, based on adsorption behaviors of free and bound enzymes on microcrystalline cellulose (MCC), a new measurement of EG activity has been introduced (Zhou et al. 2004). Among these methods, monitoring the reduction in CMC solution viscosity is considered to be the most accurate method to detect EG activity (Almin and Eriksson 1967; Valsenko et al. 1998). However, the viscometric method for measuring activity is not commonly used due to its laborious and discontinuous nature. For this reason, the colorimetric measurement of reducing sugars has been routinely used for measurement of EG activity.

Various types of automated viscometers are available to measure the rheological changes of a polymer solution. Viscosity is a fundamental rheological parameter that characterizes the resistance of the fluid to flow. The viscosity of a polymer solution is related to the polymer concentration, the extent of polymer-solvent interaction, and the polymer structure such as molecular weight, shape, molecular flexibility, and molecular conformation. Under appropriate experimental conditions, it is functionally related to the molecular weight (Browning 1967). However, a more complete understanding of the rheological changes in a cellulase-polymer solution is required to accurately monitor cellulose hydrolysis by viscosity measurements.

Like all proteins, enzymes are basically made up of amino acids linked by peptide bonds between the carboxyl groups of one amino acid and the amino group of the next amino acid. The hydrophobic and hydrophilic nature of amino acids often makes the surface of enzymes have an amphipathic interfacial structure, i.e. proteins tend to adsorb at interfaces as a surface-active polymer (Britt et al. 2003). Moreover, CMC is a semiflexible anionic polymer (Hoogendam et al. 1998). The adsorption of enzymes (protein) on the CMC leads to a change of the polymer behavior. Of particular interest is the effect of enzyme absorption on the rheology of a cellulase-CMC solution. Mixtures of proteins (enzymes) and polymers in aqueous dispersion are often accompanied by either segregative or associative phase separation (Doublier et al. 2000). Thus, physical and chemical parameters of the proteins (enzymes) and substrate and solution characteristics such as solution pH, ionic strength, concentration and protein/polymer

ratio should be considered. Moreover, processing variables such as temperature, shear rate, and time also strongly influence the rheological behavior of the complexes. For example, changes in functional properties due to soluble complexes between a globular protein (BSA) and a polysaccharide (CMC) have been reported (Tuiner et al. 2000; Renard et al. 1997). The protein was adsorbed onto the CMC segments in the dilute regime or entrapped in the polymer network in the semi-dilute region. After thermal treatment of the soluble complexes, a considerable change in the visco-elastic properties of the network was observed (Renard et al. 1998).

When a cellulase is added to a soluble cellulose derivative (e.g. CMC), one might expect that the rheological behavior of the mixture will change considerably as a function of reaction time. The change in the viscosity may be due to the cellulase ad- and de-sorbing or entrapping the substrate. The configuration and conformation of the substrate molecules will then be changed. These interactions between cellulases and substrates may be expected to result in considerable changes in the solution viscosity. Thus, significant changes in the solution viscosity may result without any enzymatic hydrolysis taking place. It should also be noted that reductions of enzymatic activity and its binding ability are expected when enzymes are continuously subjected to shear or exposed to an air-liquid interface during mixing and agitation processes (Kaya et al. 1994; Kim et al. 1982).

The study reported herein investigates the rheological behavior of CMC solutions during enzyme hydrolysis and the influence of enzymes on CMC solutions without hydrolysis. The ability of enzymes to reduce CMC solution viscosity without hydrolysis was investigated in two manners. First a heat-denatured enzyme was applied to the CMC solution. Second, a high degree of substitution CMC was used. This CMC could not be degraded by the enzymes. In addition, the effects of shear rate and contact time were evaluated during the cellulase-polymer interaction.

EXPERIMENTAL

Materials

A commercial enzyme preparation supplied by Dyadic International (Fibrezyme L, Florida, USA) was used in this study. The cellulase preparation was fractionated by using a 10 kD cut-off filter (Amicon, USA) and then used as an active cellulase preparation. In order to make a heat-denatured cellulase preparation, a 10 g l^{-1} solution of the active cellulase preparation was transferred to a glass tube and covered. The tube was then placed in a boiling water bath for 2 hours with vigorous agitation. After the boiling, the suspension was homogenized for 15 minutes with an ultrasonic homogenizer (Omni Ruptor 250, Omni international Inc, USA) in order to make a well dispersed heat-denatured cellulase suspension. The active and heat-denatured cellulase suspensions were refrigerated during storage.

Five commercial carboxymethyl celluloses (CMCs) in the sodium salt form of different average degrees of polymerization (DP) and degrees of substitution (DS) were obtained from Aqualon Hercules Inc. (Wilmington, Delaware, USA): 7L (0.7 DS and 400 DP), 7M (0.7 DS and 1,100 DP), 7H (0.7 DS and 3,200 DP), 9M8 (0.9 and 800 DP), and

12M8 (1.2 DS and 800 DP). The letters L, M, and H correspond to low, medium, and high molecular mass. According to the manufacturer, the typical molecular mass values corresponding to these categories are 90,000, 250,000, and 700,000 Daltons. A cationic polyacrylamide (C-PAM) (Percol® 175, from Ciba Specialty Chemicals) was also used. Its molecular mass is approximately 5,000,000 Daltons.

Methods

Preparation of CMC solutions

An appropriate amount of the CMCs was slowly added into a sodium acetate buffer (50 mM, pH 4.7) to make 1.0 % and 1.4 % concentrations of CMC suspensions under vigorous agitation. After completing the addition, the suspensions were transferred to a blender and vigorously mixed for one minute at room temperature. The blended suspension was stirred for one hour, while heating to 80 °C. In order to make homogenous CMC solutions, the suspension was then filtered through a sintered glass (coarse) funnel into a vacuum filtering flask. The suspension was then agitated for one hour at room temperature under the vacuum to remove entrapped air bubbles. The CMC solutions were stored at 4 °C and used within one week. After one week, fresh CMC solutions were again prepared.

Enzymatic hydrolysis and its viscosity measurement

Enzymatic hydrolysis of CMC solutions was performed using a Brookfield rotational viscometer with a UL adaptor (Brookfield DV-II+2, USA). 20 ml of each CMC suspension was preheated at 50 °C in a water bath before being transferred to the UL adaptor, which was controlled to 50 °C. One ml of each cellulase preparation was added to the CMC suspension to start the enzymatic reaction. The apparent viscosity of CMCs was collected every one minute with an automated program (Rheocalc®, Brookfield instrument, USA). The viscometer used a rotational speed of 10 rpm except during the shear rate dependence experiments. During this set of experiments the shear rates were varied in the range of 1 to 32 rpm.

Reducing sugar measurement

The reaction products of enzymatic hydrolysis were transferred into a test tube as quickly as possible to determine the concentration of reducing sugar end-groups in the sample. The amounts of reducing sugar end groups formed by cellulase action were determined by the dinitrosalicylic acid (DNS) method (Miller et al. 1960) using glucose to generate a standard curve.

RESULTS AND DISCUSSION

Polymeric and Enzymatic Effects of Cellulase

Figure 1 shows the change of the apparent viscosity as a function of time with the addition of active and heat-denatured enzymes. It should be noted that the zero time viscosity of the CMC solutions are indicative of the pure CMC solution viscosity. Also,

at the enzyme concentration used, there was no detectable difference between water and the enzyme solution viscosity. It is clear from this figure that both the active and the heat-denatured enzyme reduce the viscosity of the CMC solution as a function of contact time. This seems to imply that the heat-denatured enzyme preparation retains a portion of its activity, although the preparation was brought to boiling for 2 hours.

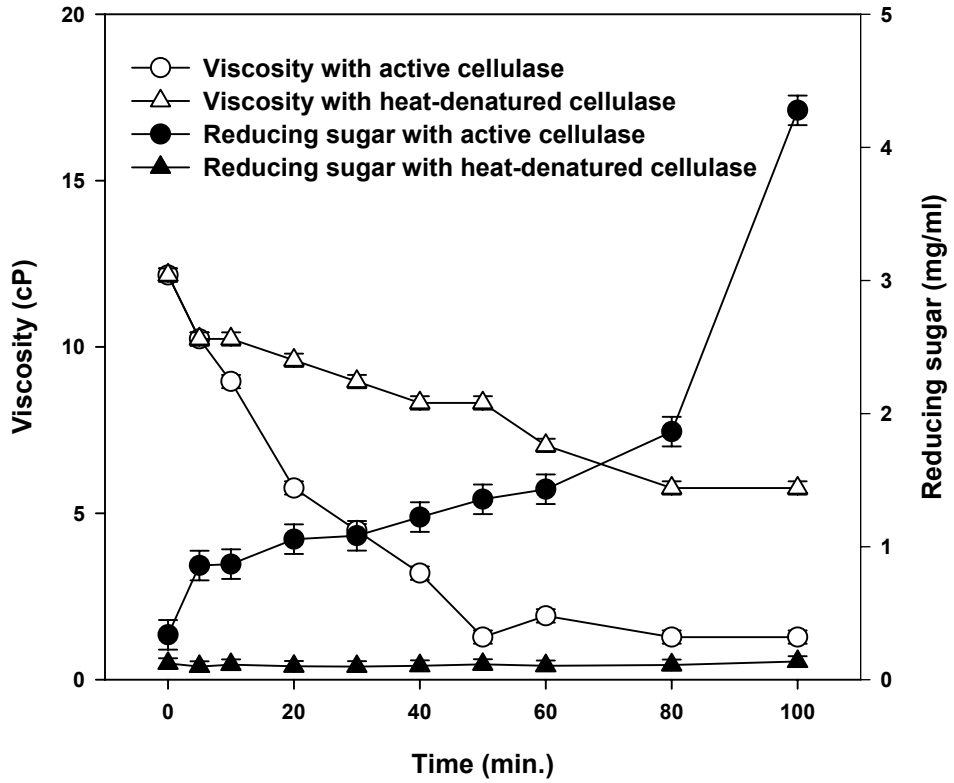

Fig. 1. Changes in apparent viscosity (50 °C and 10 rpm) and reducing sugar of 7 M CMC (1.0 % conc.) treated with active and heat-denatured cellulase as a function of time.

In order to examine whether the change in viscosity of the solution with the heat-denatured enzyme is from its residual activity, the production of reducing end groups in the hydrolysates from the active and heat-denatured cellulases were analyzed by the DNS method. The concentration of reducing sugar (glucose equivalent) liberated from the CMC can be used as a measure of hydrolytic efficiency of the active and heat-denatured cellulase preparations. The active cellulase depolymerized the substrate as a function of reaction time, leading to increased formation of the reducing sugar, whereas the heat-denatured preparation showed no significant change in the reducing sugar. It appears likely that the thermal denaturation of cellulases (Baker et al. 1992; Andreaus et al. 1999) and proteins (Kelly et al. 1994; Shimada and Cheftel 1989) caused partial unfolding of the proteins due to the disruption of the hydrogen bonds responsible for the three-dimensional structure. This may expose highly reactive groups buried inside the protein structure to the solution. This may lead to increased sites available for the CMC to interact with the de-natured enzyme causing conformational changes of the substrate (Kelly et al. 1994). Based on this observation, the results in Figure 1 imply that the heat-

denatured enzyme alters the conformation of the CMC and thus changes the viscosity of the solution. The change in the viscosity due to the amphipathic nature of the enzyme has been the termed the *polymeric effect* in this study.

Effect of Cationic Polymer

A decrease in the viscosity of a CMC solution was also observed when a cationic polymer was added to the solution, cf. Figure 2. In this figure, one can see a decrease in the CMC solution viscosity over time with cationic polymer and heat-denatured enzyme addition. After 90 minutes of elapsed time the solutions were left in the viscometer for 500 minutes without shearing, and then the viscosities of the solutions were again measured. The viscosity with heat-denatured enzyme decreased slightly (3 cPs), whereas the viscosity with the cationic polymer increased over 500 cPs. This indicates that the cationic polyelectrolyte (C-PAM) interacts with the anionic polymer (CMC) as a function of time, forming a complex, and thus leading to an increase in the viscosity. This increase, in the absence of stirring, may be attributed to the high degree of polymerization of the C-PAM.

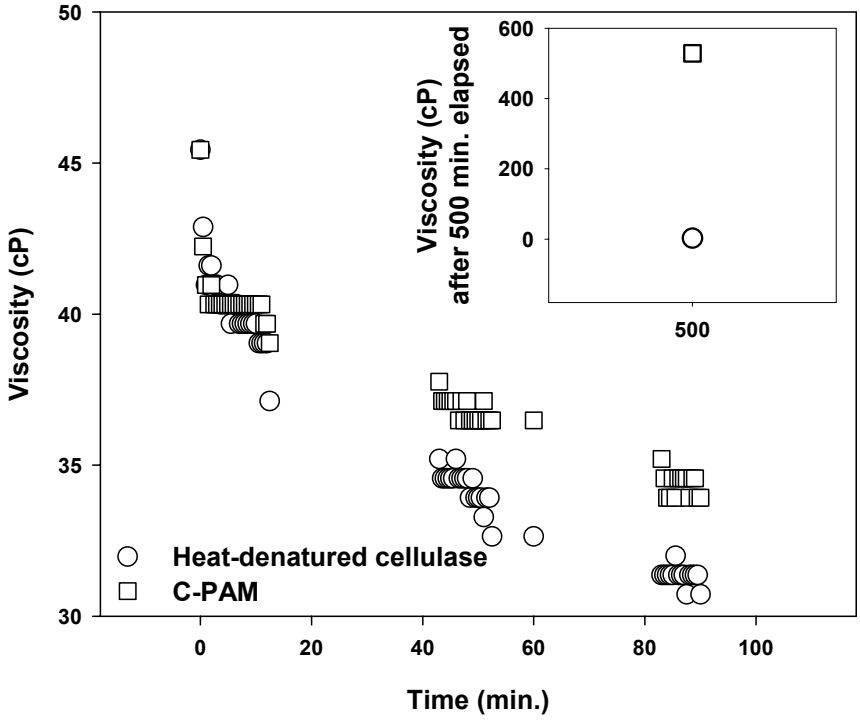

Fig. 2. Changes in apparent viscosity of 7 M CMC (1.4 % conc.) treated with the heat-denatured enzyme or C-PAM (0.1 % conc.) at 50 °C and 10 rpm as a function of time. The inserted plot represents the apparent viscosity of the CMC after 500 minutes elapsed.

Effect of CMCs with Different DS

The polymeric effect, which reduces the CMC viscosity without the creation of reducing end groups, can also be observed using CMC with different degrees of substitution. Figure 3 shows the viscosity of CMC with different degrees of substitution

as a function of enzyme contact time. Also shown in this figure is the concentration of reducing end groups as a function of time. It is known that the susceptibility of CMC to enzyme hydrolysis is dependent on degree of substitution (DS) of the CMC. When the DS of CMC reaches an average of one substitution per glucose unit, steric factors strongly retard the enzyme activity (Focher et al. 1991). Thus the International Union of Pure and Applied Chemistry (IUPAC) recommended CMC having a DS of 0.7 as a substrate for measuring cellulase activity (Ghose 1987). The inhibition of enzyme activity at high DS is shown again here by the lack of increase in reducing end group concentration with increased reaction time for the 1.2 DS CMC. However, it is noted that the viscosities of CMC decreased in a similar manner for all degrees of substitution, regardless of the change in the reducing end groups. This again indicates that a "polymeric effect" plays an important role in determining the viscosity of the CMC solution independent of hydrolytic activity.

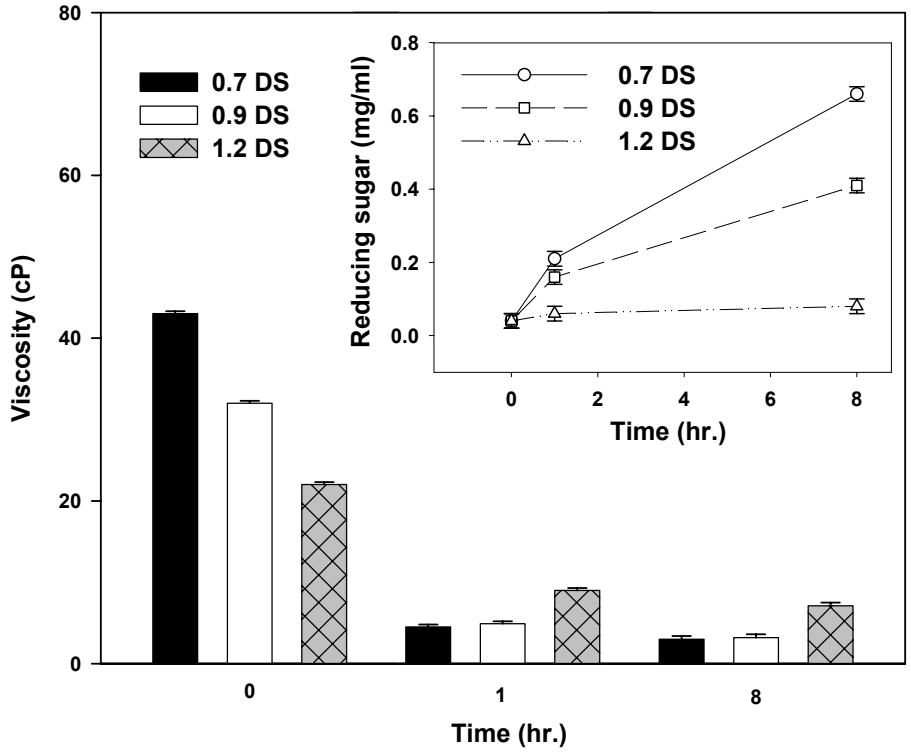

Fig. 3. Changes of apparent viscosity and reducing sugar of 7 M, 9 M, and 12 M CMCs (1.4 % conc.) treated with the active cellulase.

Changes of Intrinsic Viscosity

When measuring the enzymatic activity via changes in solution viscosity, the polymeric effect can result in significant errors in the measured activity, as shown in Figures 1-3. To evaluate the impact of the polymeric effect on the activity measurement, one needs to observe the intrinsic viscosity as a function of time, as the intrinsic viscosity is related to the molecular weight of the polymer. The intrinsic viscosity of a polymer solution is determined by measuring apparent viscosity at a series of different solute

concentrations (0.5, 1.0, 2.0, and 3.0 % with the 7 M CMC). The intrinsic viscosity was evaluated from the extrapolation to zero concentration of ln η_{rel}/C against concentration C, using the Kraemer equation (Kraemer 1938):

$$\frac{\ln \eta_{rel}}{C} = [\eta] + \kappa''[\eta]^2 C \qquad \text{Eq. [1]}$$

where [η] is intrinsic viscosity, η_{rel} is relative viscosity of the polymer solution compared with the solvent, C is the concentration of the polymer solution (in g/dl), and κ" is Kraemer's constant.

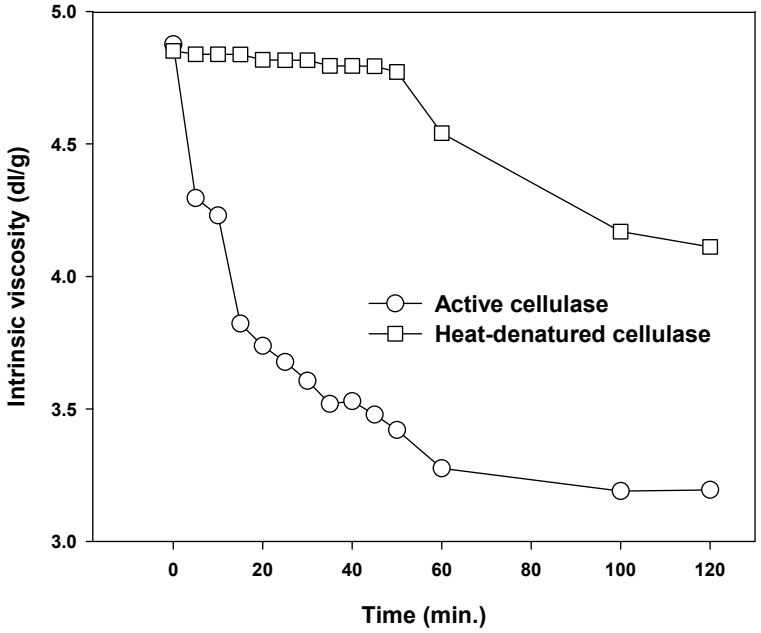

Fig. 4. Intrinsic viscosity of CMC with active and heat-denatured cellulase at 50 °C and 10 rpm.

Figure 4 shows the profiles of intrinsic viscosity of different concentrations of 7M CMC treated with active and heat-denatured cellulases for 2 hours at 50ºC and a shear rate of 10 rpm. One observes a significant decrease in the intrinsic viscosity for both the heat-denatured and active enzymes. Thus, significant errors could occur in measuring the enzymatic activity by solution viscosity, if the polymeric effect is strong or varies from sample to sample.

To accommodate the polymeric effect, the solution viscosity can be adjusted. Assuming that the viscosity of a solution is related to *friction* between molecules within the solution and that the different components contributing to the change in solution viscosity are linear, then one can separate the decrease in viscosity of the active enzyme into two components. The first component is related to the decrease in the molecular weight of the CMC. The second component is related to the polymeric effect. The change in viscosity can be expressed as,

$$\left(\frac{d\eta}{dt}\right)=\left(\frac{d\eta}{dt}\right)_{MW}+\left(\frac{d\eta}{dt}\right)_{polymer} \quad \text{Eq. [2]}$$

where the subscript *MW* indicates the viscosity changes associated with changes in the molecular weight, and the subscript *polymer* indicates viscosity changes associated with polymeric effects. Equation 2 is not applicable when a large amount of enzymatic degradation has taken place, as the magnitude of the polymeric effect is influenced by the molecular weight, cf. Figure 5.

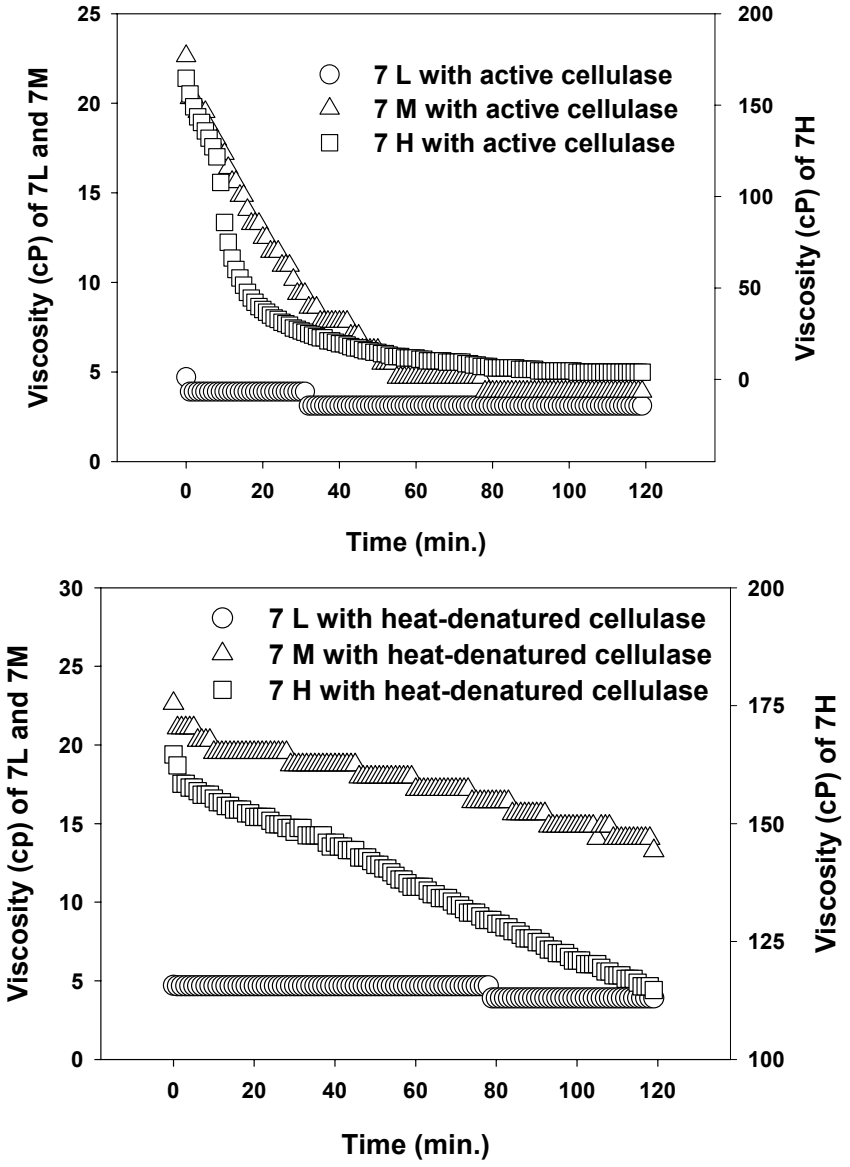

Fig. 5. Apparent viscosity of different molecular weights of CMC (1% conc.) treated with active cellulase (top) and heat-denatured cellulase (bottom) at 50 °C and 10 rpm as a function of time.

For relatively short degradation times, the change in viscosity as measured with the heat-denatured enzyme may be subtracted from the viscosity of the active enzyme solution to provide an estimate of the polymeric effect. For purposes of this estimation it is necessary to assume that the heat-denatured enzymes retain a molecular conformation that is not too different from that of the native enzymes. Using this modified viscosity data, a measurement of the change in viscosity attributed strictly to the catalytic activity can be made. Figure 6 shows the change in the viscosity adjusted for the polymeric effect compared to the unadjusted viscosity. As one can see in the figure, the polymeric effect is significant and should be compensated for in rheological measurements of enzyme activity. However, one also can see that this adjustment for the polymeric effect is nonsensical for large contact times, as the adjusted viscosity becomes negative. Thus, such a correction method should only be used for short contact times.

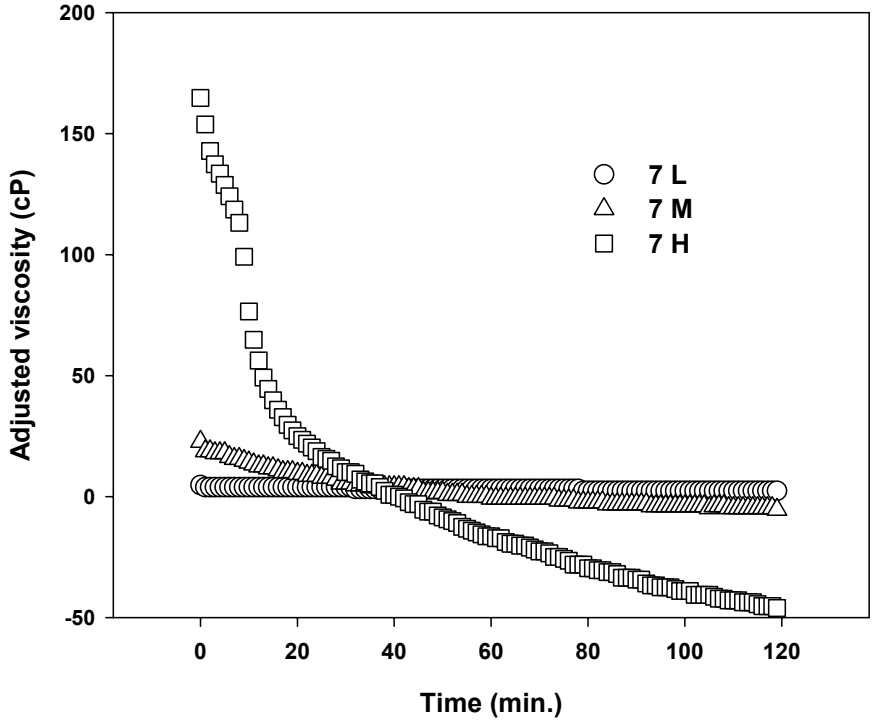

Fig. 6. Adjusted viscosities of the different molecular weights of CMC (1 % conc.) as a function of time.

Effect of Shear Rate on Viscosity

Figure 7 shows the effect of shear rate on the measured viscosity of 1% 7 H CMC at 50 ºC treated with a fixed enzyme dosage. A complex pattern of viscosity change is detected. A possible explanation for this complex pattern is the interaction of enzyme mixing and the effect of shear rate on the disruption of cellulase binding. At low shear rates, the enzymes must diffuse throughout the CMC solution with little assistance from mixing. This results in a slower drop in the viscosity of the CMC solution with time. As the shear rate increases, the mixing assistance becomes better at distributing the cellulase throughout the solution. This results in a more rapid decrease in the solution viscosity.

However, at higher shear rates the viscosity does not decrease as fast as at intermediate shear rates. This may be attributed to the shear rate disrupting the cellulase/CMC binding and thus reducing the cellulase efficiency (Kaya et al. 1994; Kim et al. 1982). Thus, differences in shear rate can affect the measured viscosity change and the perceived cellulase activity.

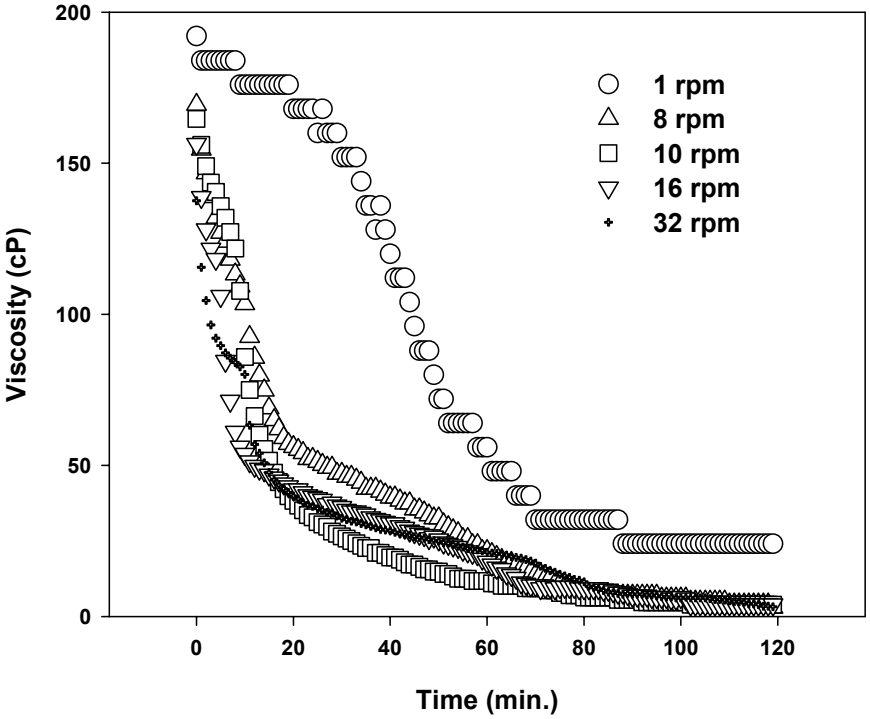

Fig. 7. Effect of shear rates in the range of 1 to 32 rpm of 7 H CMC (1 % conc.) treated with active cellulase as a function of reaction time.

CONCLUSIONS

The rheological behavior of anionic cellulose derivatives during the course of enzyme hydrolysis has been investigated. The effects of the active and heat-denatured cellulases, and a cationic polyelectrolyte (C-PAM) have been examined. Cellulose derivatives with different degrees of polymerization and substitution were examined. A polymeric effect, defined as a reduction in viscosity of the CMCs without significant formation of reducing sugars released from the degradation of the CMCs by enzymatic hydrolysis, has been observed in this study. The polymeric effect may be attributed to the interactions of the enzyme with the polymer in solution. This effect was observed with heat-denatured enzyme, active enzyme and high DS CMC (preventing enzymatic hydrolysis), and with the addition of C-PAM. The intrinsic viscosity, which may be related to the molecular weight of a dissolved material, is reduced by the polymeric effect. This may cause a significant error in the measurement of enzymatic activity with viscometric methods. Assuming a linear relationship between the changes in the solution

viscosity attributed to enzyme hydrolysis and the polymeric effect, a means for correcting for the polymeric effect was proposed. This allows for making a correction for the polymeric effect during the onset of the hydrolysis reaction. Finally, the effect of shear rate on the viscosity change caused by enzymatic hydrolysis was examined. A complex behavior of viscosity change was found with shear rate. The results were interpreted to be a combination of improved mixing with higher shear rates and disruption in binding by higher shear rates.

ACKNOWLEDGMENTS

The authors acknowledge the McIntire-Stennis Program for its financial support of this research.

REFERENCES CITED

Almin, K. E., and Eriksson, K. E. (1967). "Enzymic degradation of polymers. I. Viscometric method for the determination of enzymic activity," *Biochim. Biophys. Acta* 139(2), 238-247.

Andreaus, J., Azevedo, H., and Cavaco-Paulo, A. (1999). "Effects of temperature on the cellulose binding ability of cellulases enzymes," *J. Mol. Catal. B:Enzym.* 7, 233-239.

Baker, J. O., Tatsumoto, K., Grohmann, K., Woodward, J., Wichert, J. M., Shoemaker, S. P., and Himmel, M. E. (1992). "Thermal denaturation of Trichoderma reesei cellulases studied by differential scanning calorimetry and tryptophan fluorescence," *Appl. Biochem. Biotechnol*. 34/35, 217-231.

Beguin, P., and Aubert, J.-P. (1994). "The biological degradation of cellulose," *FEMS Microbiol. Rev.* 13(1), 25-58.

Bhat, M. K. (2000). "Cellulases and related enzymes in biotechnology," *Biotechnol. Adv.* 18(5), 355-383.

Boisset, C., Armand, S., Drouillard, S., Chanzy, H., Driguez, H., Henrissat, B. (1998). "Structure-function relationships in cellulases: The enzymatic degradation of insoluble cellulose." in *Carbohydrases from Trichoderma reesei and Other Microorganisms: Structures, Biochemistry, Genetics and Applications*, M. Claeyssens, W. Nerinckx and K. Piens, eds., Royal Society of Chemistry, Cambridge, 124-132.

Britt, D. W., Jogikalmath, G., and Hlady, V. (2003). "Protein interactions with monolayers at the air-water interface," in *Biopolymers at Interfaces,* M. Malmsten, ed., Marcel Dekker, New York, ch. 16, 415-434.

Browning, B. L. (1967). "Viscosity and molecular weight." in *Methods of Wood Chemistry*, *Vol. 2,* B. L. Browning ed., Interscience Publishers, New York, ch.25, 519-557.

Doublier, J.-L., Garnier, C., Renard, D., and Sanchez, C. (2000). "Protein-polysaccharide interactions," *Curr. Opin. Colloid Interface Sci.* 5, 202-214.

Focher, B., Marzetti, A., Beltrame, P. L., and Carniti, P. (1991). "Structural features of cellulose and cellulose derivatives, and their effects on enzymatic hydrolysis," in

Biosynthesis and Biodegradation of Cellulose, C. H. Haigler, ed., Marcel Dekker, New York, 293-310.

Ghose, T. K. (1987). "Measurement of cellulase activities," *Pure Appl. Chem.* 59(2), 257-268.

Hoogendam, C. W., de Keizer, A., Cohen Stuart, M. A., Bijsterbosch, B. H., Smit, J. A. M., van Dijk, J. A. P. P., van der Horst, P. M., and Batelann, J. G. (1998). "Persistence length of carboxymethyl cellulose as evaluated from size exclusion chromatography and potentiometric Titrations," *Macromolecules* 31, 6297-6309.

Kaya, F., Heitmann, J. A., and Joyce, T. A. (1994). "Cellulase binding to cellulose fibers in high shear fields," *J. Biotechnol.* 36, 1-10.

Kelly, R., Gudo, E. S., Mitchell, J. R., and Harding, S. E. (1994). "Some observations on the nature of heated mixtures of bovine serum albumin with an alginate and a pectin," *Carbohydr. Polym.* 23, 115-120.

Kim, M. H., Lee, S. B., and Ryu, D. D. Y. (1982). "Surface deactivation of cellulase and its prevention," *Enzyme Microb. Technol*. 4, 99-103.

Kraemer, E. O. (1938). "Molecular weights of celluloses and cellulose derivatives," *Ind. Eng. Chem.* 30, 1200-1203.

Miller G. L., Blum R., Glennon W. E., and Burton, A. L. (1960). "Measurement of carboxymethylcellulase activity," *Anal. Biochem*. 1, 127-132.

Mullings, R. (1985). "Measurement of saccharification by cellulases," *Enzyme Microb. Technol.* 7(12), 586-591.

Renard D., Boue F., and Lefebvre, J. (1997). "Protein-polysaccharide mixtures: Structure of the systems and the effect of shear studied by SANS," *Physica B*, 234-236, 289-291.

Renard D., Boue F., and Lefebvre, J. (1998). "Solution and gelation properties of protein-polysaccharide mixtures: signature by small angle neuron scattering and rheology," in *Gums and Stabilizers for the Food Industry 9*, E. Dickinson, and B. Bergenstabl, eds., Royal Society of Chemistry, Cambridge, 189-201.

Rouvinen, J., Bergfors, T., Teeri, T., Knowles, J. K. C., and Jones, T. A. (1990). "Three-dimensional structure of cellobiohydrolase II from Trichoderma reesei," *Science* 249, 380-386.

Sharrock, K. R. (1988). "Cellulase assay methods: A review," *J. Biochem. Bioph. Methods* 17(2), 81-106.

Shimada, K., and Cheftel, J. C. (1989). "Sulfhydryl group/Disulfide bond interchange reactions during heat-induced gelation of whey protein isolate," *J. Agric. Food. Chem.* 37,161-168.

Tuinier R., Dhont J. K. G., and de Kruif C. G. (2000). "Depletion-induced phase separation of aggregated whey protein colloids by an exocellular polysaccharide," *Langmuir* 16, 1497-1507.

Vlasenko, E. Y., Ryan, A. I., Shoemaker, C. F., and Shoemaker, S. P. (1998). "The use of capillary viscometry, reducing end-group analysis, and size exclusion chromatography combined with multi-angle laser light scattering to characterize endo-1,4-β-D-glucanases on carboxymethylcellulose: A comparative evaluation of the three methods," *Enzyme Microb. Technol.* 23(6), 350-359.

Wu, B., Zhao, Y., and Gao, P. J. (2006). "A new approach to measurement of saccharifying capacities of crude cellulase," *BioResources* 1(2), 189-200.
Zhou, X., Chen, H., and Li, Z. (2004). "CMCase activity assay as a method for cellulase adsorption analysis," *Enzyme Microb. Technol.* 35(5), 455-459.

Article submitted: October 23, 2006; First review cycle completed November 20, 2006;
Revision accepted: Dec. 21, 2006; Article published: January 2, 2007.

UTILIZATION OF A CHEMICAL-MECHANICAL PULP WITH IMPROVED PROPERTIES FROM POPLAR WOOD IN THE COMPOSITION OF PACKING PAPERS

R. Boeva-Spiridonova[a*], E. Petkova[a], N. Georgieva[a], L. Yotova[a], and I. Spiridonov[a]

The aim of the present work is to obtain a chemical-mechanical pulp (CMP) from poplar wood with improved properties, to be used in packing papers in place of more expensive softwood or hardwood pulp. For improving the CMP quality indicators, a preliminary treatment of the pulp has been carried out with a mixture of oxidizing enzymes produced from Phanerochaete chrysosporium, including lignin peroxidase, manganese peroxidase, and laccase. The two types of fiber materials obtained were double-stage bleached and then ground to 30°SR. It was found that preliminary enzyme treatment yielded CMP with improved physical, mechanical, and optical properties. The enzyme-pretreated CMP also refined faster, thus reducing the electricity consumption. Bleached CMP from poplar wood, obtained after preliminary enzyme treatment, could be successfully utilized at levels up to 40% in the composition of various packaging papers.

Keywords: Cellulose, Chemical-mechanical pulp, Paper, Production, Utilization, Poplar wood, Phanerochaete chrysosporium

*Contact information: a: Department of Pulp, Paper and Printing Arts, University of Chemical Technology and Metallurgy, 8, Kl. Ohridski Blvd., 1756 Sofia, Bulgaria, *Corresponding author: Tel.: +359 28163307, E-mail address: r_boeva@abv.bg, neli@uctm.edu*

INTRODUCTION

The production of high yield fiber materials (HYFM) can be considered to be desirable from the standpoint of higher wood utilization efficiencies and an introduction of more environmentally sound technologies, generating less pollution. Such fibers have found application in production of different types of papers and cardboards.

Paper is an inseparable part of the daily life of contemporary people. High yield fiber materials, together with conventional lower-yield cellulosic fibers, find wide application in production of numerous types of paper and cardboard. In order to increase the share of these materials it is necessarily to improve their physical, chemical, and optical properties. Practically, this can be realized through addition of various chemical reagents.

Biocatalytic reactions likewise have been applied to an increasing number of industrial processes. These processes allow for development of ecologically clean technologies. Preliminary wood treatment with different enzymes could lead to breaking down of various connections within fiber structures and to improving the delignification processes, helping to obtain fibrous intermediate products that can be used for the production of paper.

Studies of lignin biodegradation have been carried out mostly using white-rot fungi, which produce extracellular lignin-modifying enzymes, such as laccases and peroxidases (lignin peroxidases and manganese peroxidases) (Moreira et al. 1997a,b; Bennet et al. 2002). One application of white-rot fungi and their oxidative enzymes is in biobleaching and biopulping for the preparation of papermaking pulps. In such applications, the new processes, involving biotransformation and bioremediation, have the potential to displace environmentally harmful chemicals, as well as saving mechanical pulping energy costs (Higuchi et al. 1989; Niku-Paavola 2002).

The aim of the present work is to obtain a bleached chemical-mechanical pulp (CMP) from poplar wood with improved properties, to be used in the composition of packing papers. The use of lignocellulose-degrading enzymes from the basidiomycete *Phanerochaete chrysosporium* strain in pulp treatment was studied.

EXPERIMENTAL

Strain and Media

The strain *Phanerochaete chrysosporium*, which has been deposited in the National Bank of Industrial Microorganisms and Cell Cultures, Bulgaria as strain N1038, was used in the experiment. The cultivation of *Ph. chrysosporium* was carried out in a medium as described by Georgieva et al. (2004). The sterile glucose solution ($20g.dm^{-3}$) was sterilized separately and was added to the growth medium. All chemicals were supplied by Merck (Germany).

Cultivation Conditions

The strain *Phanerochaete chrysosporium* was cultivated 96 hours in a batch culture on a rotary shaker (180 rpm at 30ºC). At the 48th hour of the culture development benzyl alcohol was added in concentration $0.5cm^3.dm^{-3}$. It is supposed that benzyl alcohol acts as an inductor in producing lignin-degrading enzymes (laccase, lignin peroxidases, and manganese peroxidases), which are extracellular (Georgieva et al. 2006). The biomass was separated at the end of the cultivation, and the experiments on pulp treatment were conducted with the resulting culture liquid (CL). Furthermore, the culture liquid samples, obtained during the cultivation, were concentrated 5-fold in an ultrafiltration cell without the losses in activity during concentration. The enzyme activities were determined according Bonnarme and Jeffries (1990), and Coll et al. (1993). The strain *Phanerochaete chrysosporium* possibly produced three types of enzymes extracellularly, however, the presence of laccase might not be significant, based on work by Bonnarme and Jeffries (1990).

Production of CMP

The starting material utilized in this research for obtaining of a chemical-mechanical pulp was the poplar wood from the species Populus deltoides cultivar Onda, having an improved density ($474kg.m^{-3}$) (Shamko 1989).

Two kind of fibrous materials were prepared. The first was CMP from poplar wood, following preliminary optimal treatment with 7% NaOH plus 2% Na_2S_4 by 90^oC

and duration 120min, liquor-to-wood ratio 1:5 (Petkova et al. 2001). The second kind of CMP was prepared after the enzyme treatment of poplar chips before grinding according to the determined treatment.

Two kinds of the poplar chips were refined in a Sprout-Valdron laboratory mechanical refiner up to 12^oSR. CMP, BPSW and BPHW were refined separately in laboratory Jokro mill up to 40^oSR.

Twenty grams of the absolutely dry chips were placed in a flask, where $100cm^3$ of a CL with total activity of 179U/mg was added. The flasks were placed in a rotary shaker at 30^0C and pH = 4.5, then continuous aeration and stirring were applied (Georgieva et al. 2004). After 120 hours treatment, the chips were washed sufficiently to reach a neutral pH level and were used for production of a chemical-mechanical pulp, as per the preliminary determined optimization regime: NaOH – 7 %, Na_2S_4 – 2 %, temperature – 90^0C, treatment duration - 120min, and liquor-to-wood ratio – 1:5. The CMP obtained after the preliminary set optimal conditions, according to methods described by Petkova et al. (2001), was bleached in two stages, employing H_2O_2 and rongalit C ($NaHSO_2.CH_2O.2H_2O$).

The reagents Na_2SiO_3 and $MgSO_4$ were applied as stabilizers of the H_2O_2. NaOH was added to reach a pre-determined pH level. In order to chelate the metals ions, the pulp was treated with the complexing agent EDTA. The following fiber materials and chemical reagents have been used for production of the paper samples: bleached sulfate cellulose pulp from hardwood, delivered by plant "Svoliza" JSC – Svishtov city, and bleached cellulose pulp from softwood, imported from Russia.

The paper samples obtained had a basis weight of $60g/m^2$ and sizing level 1.5mm. Test sheets were obtained by means of a Rapid Kothen machine (Bulgarian Standard ISO 536).

Analytical Measurements

The bleaching effect of the treatments was measured by spectrophotometer (Gretag Macbeth Spectroeye) measurement of diffuse blue reflectance factor (Bulgarian Standard ISO Brightness 2470), determination of bursting strength (Bulgarian Standard ISO 2758) on Schopper - Daalen, Laboratory beating Jokro mill method - Bulgarian Standard ISO 5264-3, determination of tearing resistance by the Elmendorf method – Bulgarian Standard ISO 1974, determination of drainability by the Schopper-Riegler method - Bulgarian Standard ISO 5267-1, and determination of tensile properties – part 2, constant rate of elongation method - Bulgarian Standard ISO 1924 – 2.

RESULTS AND DISCUSSION

Enzymatic treatment is one of the newest and most promising methods for bleaching of cellulosic fiber materials, and related technology also has been applied during their production. In Table 1 are shown the data of physical and mechanical properties of CMP.

The physical and mechanical properties of CMP were improved by the enzyme treatment of the wood. It was found that the tensile index was increased by 45%. The tear index was increased by 35%, and the burst index was increased by 9% (Table 1).

It was determined that the chips treated with enzyme were ground faster (refining time – 15min) in comparison with native CMP (refining time 30min). By enzyme treatment the refining time decreased up to 35%. The positive effects of such enzymatic treatment include faster chip refining and increased brightness level of the chemical-mechanical pulp, obtained during the further bleaching. These benefits are explained by the complex action of the three enzymes, which facilitate the weakening of the connections between the lignin and the other wood components, as well as lignin modification and plasticization (Poppius – Levin et al. 1997). It is possible to separate part of the lignin after the chemical and mechanical treatment of wood during the CMP processing. CMP yield, obtained after enzymatic treatment, is lower, a finding that tends to confirm the above-mentioned conclusions (Table 1).

Table 1. Physical and Mechanical Properties of Chemical–Mechanical Pulp from Poplar Wood

Properties	Native CMP	CMP treated with CL
Tensile index, $N.m.g^{-1}$	30.7	44.5
Tear index, $mN.m^2.g^{-1}$	6.5	8.8
Burst index, $kPa.m^2.g^{-1}$	2.3	2.5
Brightness, %	35.4	38.2
Yield, %	92.8	91.2

Results of tests of paperboard properties are shown in Table 2.

Table 2. Physical and Mechanical Properties of Packaging Papers Produced from Chemical-Mechanical Pulp form Poplar Wood Treated with CL

Fiber composition, %	Tensile index, $N.m.g^{-1}$	Tear index, $mN.m^2.g^{-1}$	Burst index, $kPa.m^2.g^{-1}$	Brightness, %	Opaque %
100% bleached CMP	42.8	5.9	2.1	55.5	-
100% unbleached CMP	44.5	8.0	2.5	38.2	-
50% BPSW 50% BPHW	66.7	8.0	4.7	67.5	80.7
60% BPSW, 40% BPHW	68.50	8.0	4.4	66.8	82.0
60% BPSW, 30% BPHW, 10% bleached CMP	66.30	7.2	4.4	65.5	89.9
60% BPSW, 20% BPHW, 20% bleached CMP	61.85	6.4	4.0	63.9	90.6
60% BPSW, 10% BPHW, 30% bleached CMP	57.40	6.0	3.6	60.0	91.5
60% BPSW, 40% bleached CMP	54.80	5.8	3.4	59.6	93.2

The CMP obtained from poplar wood chips, preliminarily treated with enzymes, after two stages of bleaching by H_2O_2 and rongalit C, was applied for production of packaging paper, together with bleached sulfate softwood and bleached sulfate hardwood. This was done aiming to preserve the quantity of BPSW by replacement of BPHW with CMP obtained after enzyme treatment and two-step bleaching. It was observed that the increase of the CMP quantity in the packaging paper caused decreases in the breaking index and the tear index (Table 2).

Such decrease is more significant when the bleached pulp from hardwood is completely replaced by CMP. But even in that case, the parameters remained relatively high: tensile index 54.8N.m.g^{-1} and tear index - 5.8mN.m^2.g^{-1}. Figure 1 shows the changes of the tensile index as a function of the increase of the CMP in paper composition.

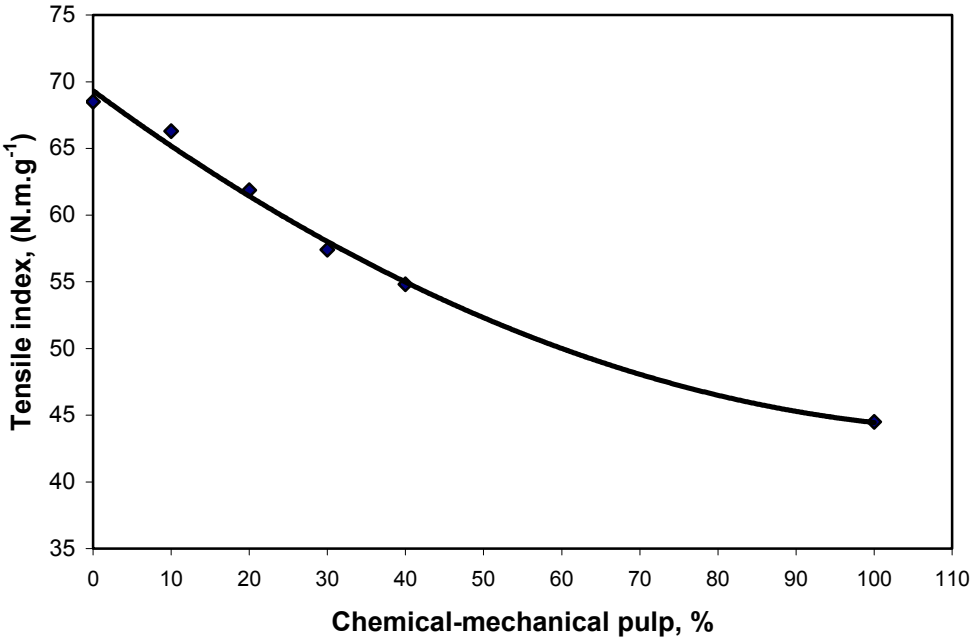

Fig. 1. Changes in the tensile breaking index, depending on the content of chemical-mechanical pulp, treated with CL

The burst index remained relatively high (3.4kPa.m^2.g^{-1}) at the fiber materials ratio of 60% BPSW and 40% bleached CMP. That means that the bleached sulfate pulp from hardwood could be successfully replaced by bleached chemical-mechanical pulp from poplar wood, obtained after preliminary enzyme treatment of the initial chips. The higher parameters of the initial CMP provide grounds for its application in the compositions of various packaging papers with improved properties. In this case, a decrease in the brightness level and increase in the opacity were also observed. The obtained packaging paper had a pleasant yellow color, and it can be successfully utilized for practical

purposes, based in the initial results presented here. When the CMP content is 40%, then a sharper decrease in the levels of the target parameters is observed.

CONCLUSIONS

1. The enzyme treatment of poplar chips was found to be compatible with the grinding process of CMP production.
2. The physical and mechanical properties of CMP were improved. The tensile index increased by up to 45%, the tear index by up to 35%, and the burst index by up to 9%.
3. The quantity of improved CMP could reach up to 40 to 50 % of the total fiber material. In this manner, at least some of the more expensive bleached sulfate pulp from hardwood can be displaced.
4. Bleached chemical-mechanical pulp from poplar wood, obtained after preliminary enzyme treatment, could be successfully utilized in the composition of various high-quality packaging papers.

Symbols used:

CMP - chemical-mechanical pulp

CL - culture liquid

EDTA – ethylene-diamine tetra-acetic acid

^{0}SR – Degree Schopper- Riegler

rpm – revolution per minute

BPSW – bleached pulp from softwood

BPHW - bleached pulp from hardwood

HYFM - yield fiber materials HYFM

REFERENCES CITED

Bennet, J., Wunch, K., and Faison B. (2002). "Use of fungi biodegradation," In: *Environmental Microbiology,* Ch. Hurst (ed.), ASM Press Washington, D.C., 960-971.

Bonnarme, P., and Jeffries, T. (1990). "Mn(II) regulation of lignin peroxidases and manganese-dependent peroxidases from lignin-degrading white rot fungi," Appl and Environ Microbiol 56:210-217

Coll, P., Fernandez-Abalos, J., Villanueva, J., Santamaria, R., and Perez, P. (1993). "Purification and characterization of a Phenoloxidase (Laccase) from the lignin-degrading basidiomycete PM1 (CECT 2971)," Appl and Environ Microbiol 59:2607-2613

ISO 536:1998 – "Paper and board, Determination of grammage."

Georgieva, N., Yotova, L., Betcheva, R., Hadzhiyska, H., and Valtchev, I. (2006). "Biobleaching of lignin in linen by degradation with Trichosporron cutaneum R57," *J. Univ. Chem. Technol. and Met*. 41(2), 153-156.

Georgieva, N., Yotova, L., Valchev, I., Chadjiiska, Ch., and Arizanov, V. (2004). "Biotransformation of lignin in linen by degradation with Phanerochaete chrysosporium," *Proceedings Bioprocess System*, Dec. 6 – 8, 4(10), Sofia.

Higuchi, T. (1989). "Mechanisms of lignin degradation by lignin peroxidase and laccase of white-rot fungi," *Biogenesis and Biodegradation of Plant Cell Polymers*, ACS Symposium Series, 399, 482-502.

Moreira, M. T., Feijoo, G., Sierra, R., Lema, J. M. and Field, J. A., (1997a). "Biobleaching of oxygen delignified Kraft pulp by several whtie rot fungal strains," *Journal of Biotechnology* 53, 237-251.

Moreira, M. T., Sierra, R., Feijoo, G., Lema, J. M. and Field, J. A. (1997b). "Manganese is not required for biobleaching of oxygen delignified kraft pulp by the white rot fungus Bjerkandera sp. Strain BOS55," *Applied and Environmental Microbiology* 63, 1749-1755.

Niku-Paavola, M. L., Tamminen, T., Hortling, B., Viikari, L. and Poppius-Levlin, K. (2002). "Reactivity of high and low molar mass lignin in the laccase catalysed oxidation," in *Biotechnology in the Pulp and Paper Industry*, *Progress in Biotechnology*, Viikari L. and Lantto R. (eds). Elsevier, Amsterdam, 21, 121-130.

Petkova, E., Boeva, R, and Litovski, Z. (2001)." Investigation of possibilities for obtaining of Chemical-Mechanical Pulp prom Poplar Wood", *Celulose and Paper Journal*, (3), 7-8.

Poppius-Levin, K., Wange, W., Tamminen, T., Horling, B., Viikari, L., and Niki-Paovola, M. (1999). "Effects of Laccase /HBT Treatment on pulp and Lignin Structures," J. of Pulp and Paper Science, 25, (3), 90-94.

Shamko, V. E. (1989). "Yield Fiber Materials", Moskow., "Lesnaya promishlenost", (in Russian).

Article submitted Nov. 26, 2006; First round of review completed: January 3, 2007; Revised article accepted: Jan. 16, 2007; Published Jan. 19, 2007

CHEMICAL INVESTIGATION OF WOOD TREE SPECIES IN TEMPERATE FOREST IN EAST-NORTHERN ROMANIA

Ruxanda Bodîrlău, Iuliana Spiridon, and Carmen Alice Teacă*

A quantitative evaluation of wood chemical components for some tree species in a forest area from east-northern Romania is presented here, through a comparative study from 1964 to 2000. Investigation upon the wood tree-rings in a *Quercus robur L.* tree species, as a dominant species, as regards its chemical composition and structure of the natural polymer constituents - cellulose and lignin - was also performed through chemical methods to separate the main wood components, FT-IR spectroscopy, and thermogravimetry. Having in view the impact of climate and external factors (such as pollutant depositions), some possible correlations between wood chemical composition and its further use can be made. The FT-IR spectra give evidence of differences in the frequency domains of 3400-2900 cm^{-1} and 1730-1640 cm^{-1}, due to some interactions between the chemical groups (OH, C=O). The crystallinity index of cellulose presents variations in the oak wood tree-rings. Thermogravimetry analyses show different behaviour of cellulose at thermal decomposition, as a function of radial growth and tree's height. A preliminary chemical investigation of oak wood sawdust shows a relatively high content of mineral elements (ash), compared with a previous study performed in 1964, fact that may indicate an intense drying process of the oak tree, a general phenomenon present in European forests for this species.

Keywords: Tree species, Wood chemical components, Oak wood tree-rings, FT-IR spectroscopy, TG, Thermogravimetric analysis

*Contact information: Romanian Academy, "Petru Poni" Institute of Macromolecular Chemistry 41 A Gr. Ghica Voda Alley, Iasi, RO-700487, Romania; *Corresponding author: cateaca@icmpp.ro, cateaca14@yahoo.com*

INTRODUCTION

Wood represents a significant natural resource, renewable, capable of accumulating carbon by absorption of CO_2 from the atmosphere. Wood anatomy influences its physical and mechanical properties, as well as its chemical reactivity (Durbak et al. 1998; Panshin and de Zeeuw 1980). Technological applications of wood can vary based on their structural differentiation among the different types of wood.

Nevertheless, the tree species may also provide significant functions other than wood production, such as soil conservation, climate stabilization, and social benefits. From an environmental perspective, wood may substitute for fossil fuels as a source of energy, for agricultural fibers for paper production, and for steel or plastics for material applications. The fibrous nature of wood strongly influences how it is used. For more effective and industrially acceptable utilization of wood, the original structure can be

refined into the pure components, having in view its nature as a composite material, given by both chemical and physical components. The contributions of each one of them change with wood species and age, and with the climate of their areas of growing (Meshitsuka 1991).

In most species in temperate climates, the difference between wood that is formed early in a growing season and that formed later is sufficient to produce well-marked annual growth tree-rings. The age of a tree at any cross section of the trunk may be determined by counting these tree-rings (Miller 1999). In canopy forests of temperate latitudes, the radial growth of trees is influenced by a significant interaction of several factors, from which the climate and exogenous alterations (such as pollutant depositions) have a significant impact. Many European forests are predominantly composed of the pedunculate oak (*Quercus robur L.*) and beech (*Fagus sylvatica*) tree species. The relationships between the climatic variability and the radial growth of both tree species in many European regions have been widely studied (Rozas 2001).

Incidences of oak decline have occurred repeatedly during the past three centuries, as well as in the most recent decades. On the basis of historical records and dendrochronological measurements, oak decline in Central Europe has been attributed to the single or combined effects of climatic extremes (winter frost, summer drought), defoliating insects, and pathogenic fungi. Various abiotic (air pollution, nitrogen eutrophication, soil chemical stress, climatic extremes, site conditions) and biotic factors (insect defoliation, borer attack, infection by pathogenic fungi, microorganisms) and their interactions as causes of oak decline in Central Europe have been also discussed (Thomas, Blank, and Hartmann 2002).

Nevertheless, the significant impact of silvicultural practices on wood properties and the volume of juvenile wood produced is important for the forest industry (e.g. problems incurred because of juvenile wood are excessive longitudinal shrinkage, warp, and reduced strength). Due to environmental concerns, the land available for wood production has decreased. In order to meet future wood demand, more wood with target characteristics must be produced by intensive management practices and genetic improvements. The forest products industry is shifting raw materials from mature trees to short rotation plantation or juvenile stock. Compared to mature wood, juvenile wood has different properties, such as lower wood density, shorter fiber length, and higher contents of both lignin and compression wood. The last two mentioned characteristics result, for example, in higher chemical consumption during pulping and lower pulp yield.

Comparative data on the chemical components for some wood tree species from Iasi County, Romania are presented here, having in view a previous study on the native tree species performed by Cr. I. Simionescu and co-workers (Simionescu et al. 1964). The data regarding the forests from Iasi County (as climate and air quality) were also considered. The chemical characterization of pedunculate oak *Quercus robur L.*, the dominant tree species in east-northern Romanian forest, specifically with regard to the tree-annual rings, was performed. The oak wood chemical structure, mainly the major components (cellulose, lignin), was investigated by FT-IR spectroscopy (Nelson and O'Connor 1964; Hergert 1971; Pandey 1999; Colom and Carrillo 2005). The behavior of cellulose to the thermal decomposition has been also investigated through thermogravimetry, evidencing variable properties during the tree's radial growth.

EXPERIMENTAL

Study Site

The forests district, from which the tree species under study were harvested, is located in the Iasi county, on a gentle slope (6-20^0), north-east oriented, with altitudes ranging from 30 to 500 m. The soils are deep brown earths. European pedunculate oak is the dominant tree species in the forest canopy. Forests in the Iasi district represent an area of about 17 % in the administrative area and are situated in the north of the Moldavian Central Plateau. The mean altitude for relief units in Podu-Iloaiei forestry region ranges from 190 to 230 m and a main east-southern exposure of the forests is present.

The forests are mainly composed of: plantations of quercinee (pedunculate oak *Quercus robur L.* and common-oak *Quercus sessiliflora*) – 26 %; hornbeam (*Carpinus betulus*) – 22 %; beech (*Fagus sylvatica*) -14 %; lime – tree (*Tilia cordata*) – 11 %; poplar (*Populus alba*) - 8 %; ash-tree (*Fraxinus excelsior*), sycamore maple (*Acer pseudoplatanus*) - 9 %; tree softwood species – only 2 % (Iasi Forestry Direction, 1997). In Table 1, some data on the air quality are presented (Environmental report from Iasi Environmental Protection Agency 2000).

Table 1. Air Quality for the Iasi Region

Pollutants, measure unit	Pollutants' concentration in the atmosphere				Frequency of overstep of the admissible maximum concentration, %
	Maximum admissible		Effective maximum	Mean annual	
	daily	monthly			
ammonia, mg/m^3	0.30	-	0.642	0.0409	0.09
sedimental powders, g/m^2	-	0.70	79.404	18.39	40.74

Climatic Data

A complete record of temperature and precipitation was obtained at the Iasi Territorial Meteorology Center. The climate in the harvesting area is temperate-continental (namely hills with forests) with periods of flooding phenomena in occasional years only (e.g. 1988, 1989, 1991). Rainfall records evidence both a minimum value (in summer, from June to August) and a maximum value (in autumn-winter from October to December). The mean annual precipitation has a value of 474.4 mm. Maximum temperature values are recorded during summer (from July to September), while minimum temperatures are observed in winter (from December to February), with a mean annual temperature of 9.6 ^{o}C.

Sampling and Chemical Investigation

Dry wood is primarily composed of cellulose, lignin, hemicelluloses, and minor amounts (5% to 10%) of extractives materials. Cellulose, the major component, constitutes up to 50% of wood substance by weight. Cellulose is a high-molecular-weight linear polymer chain which is formed by joining the anhydroglucose units into glucan chains. These anhydroglucose units are bound together by β-(1, 4)-glycosidic linkages. Due to this linkage, cellobiose is established as the repeat unit for cellulose chains. The

degree of polymerization (DP) of native cellulose is in the range of 7,000-15,000. Most of the cell wall cellulose is crystalline. Although lignin occurs in wood throughout the cell wall, it is concentrated toward the outside of the cells and between cells. Lignin is a complex three-dimensional phenylpropane polymer that forms a large molecular structure, giving mechanical strength to wood by gluing the fibers together (reinforcing agent) between the cell walls. Its structure and distribution in wood are still not fully understood (Miller 1999).

Wood represents a composite structure, given by the cell wall polymers, respectively lignin and polysaccharides – cellulose and hemicelluloses (Fengel and Wegener 1984; Pettersen 1984; Sjöstrom 1993). The combined material is known as the lignocellulosic matrix. The different amounts of these biopolymers in the cell wall polymers in wood fibers is influenced significantly by a complex of several factors, both endogenous and exogenous, and vary with wood species. Their proportions vary, but in softwoods there are normally 40-50 % of cellulose, about 20 % of hemicelluloses and 25-35 % of lignin. In hardwoods there are 40-50 % of cellulose, 15-35 % of hemicelluloses and 17-25 % of lignin. There are also lot of other compounds that are found in smaller quantities, e. g. fats, resins, waxes, oils and starches. As a group they are called extractives (Rowell 1984).

Wood samples were prepared for chemical investigation and analysed by using the TAPPI standard methods, as it is described below. Wood round discs were cut from 1.30 m height above ground (for all wood tree species), as well as from different oak tree's height values (1.30 m; 8 m; 15 m), and let to air-dry thoroughly (TAPPI norm T 257 om-85). The wood samples were debarked, then ground in a laboratory ball mill and sieved. For comparative study of the tree species, the fraction which passed through a 0.63 mm sieve was used. The oak wood flour was passed through a 0.40 mm sieve. All wood samples, including the fraction > 0.40 mm for all oak tree-rings domains (0-40 years; 40-70 years; 70-80 years), were investigated according to the analytical methods used in wood chemistry as follows:

- humidity by oven-drying at 105^{o}C (TAPPI norm T 264 om-88);
- cellulose (by gravimetry), after reaction with a 1:4 v/v mixture of concentrated nitric acid and ethyl alcohol (Pettersen 1984);
- extractives by reaction with a 2:1 v/v mixture of benzene and ethyl alcohol, with a Soxhlet apparatus (TAPPI norm T 204 om-88);
- extractives by reaction with one percent sodium hydroxide solution (TAPPI norm T 212 om-88);
- extractives in hot water (TAPPI norm T 207 om-88).

The cellulose content was determined as follows: 1 g (oven-dried) of wood sample was placed in a 200-mL beaker to which 5 mL of concentrated HNO_3 and 20 mL of ethyl alcohol were added. The mixture was heated in a water bath and refluxed for 60 min, after that being filtered using a tared fritted disc glass thimble. The 60-min cycle was repeated for up to 4 cycles. After each succeeding hour, the wood sample was placed again in the 200-mL beaker and fresh portions of 5 mL of concentrated HNO_3 and 20 mL of ethyl alcohol were added with shaking. At the end, the reaction mixture was filtered using a tared fritted disc glass thimble, washed with hot water, and dried at 105^{o}C until the crucible weight was constant, and the cellulose content was calculated.

From the residue remaining after the Soxhlet extraction, the lignin and the holocellulose contents were determined. The lignin was determined by gravimetry after 72% sulfuric acid hydrolysis (by Klason lignin method - in accordance with the previous study of wood tree species performed in 1964, as well as by TAPPI norm T 222 om-88).

According to the Klason method, 1 g (oven-dried) of wood sample was placed in a 100-mL beaker to which 15 mL of 72% H_2SO_4 was added. The mixture was left at room temperature for 2 h with occasional stirring. The solution was then transferred to a 1-L Erlenmeyer flask, diluted with 560 mL of deionized water to a H_2SO_4 concentration of 3%, and refluxed for 4 h. The solution was then filtered, and the acid insoluble lignin was determined gravimetrically.

The holocellulose content (i.e. cellulose and hemicellulose) was also determined by gravimetry, after the reaction of the wood flour with sodium chlorite (Pettersen 1984). A wood sample, 5 g of oven-dried weight, was placed into a 500-mL Erlenmeyer flask, to which 200 mL of deionized water (having a temperature of 90°C) was then added, followed by 10 mL of acetic acid and 2.5 g of 80% (w/w) $NaClO_2$. An optional 25-ml Erlenmeyer flask was inverted in the neck of the reaction flask. The flask was kept in a water bath at 90°C for 60 min, at which time 10 mL of acetic acid and 2.5 g of 80% (w/w) $NaClO_2$ were added with shaking. The 60-min cycle was repeated for up to 6 cycles. At the end, the flask was stoppered and cooled with cold water to stop the reaction. The reaction mixture was then filtered using a tared fritted disc glass thimble, washed with cold water and acetone, and dried at 105°C until the crucible weight was constant, and the holocellulose content was calculated.

All the results are presented relative to the dry matter content (%DM).

The FT-IR spectroscopy (for oak wood cellulose and lignin) was performed by using the KBr (potassium bromide) disk method with a Digilab Fourier Transform Infrared (FTIR) spectrophotometer, Model Excalibur FTS-2000. The samples were mixed with KBr to form the pellets that contained 1% powdered sample. These KBr disks were employed for the FTIR spectroscopy studies.

The thermogravimetric (TG) and differential thermogravimetric (DTG) curves for the cellulose thermal decomposition process were recorded on a Paulik-Erdey-type derivatograph, MOM Budapest (Hungary), under the following operational conditions: heating rate was 12°C/min, temperature range 20-600°C, sample weight 50 mg, using powdered samples in platinum crucibles, 30 cm^3/min air flow. Three or four repeated readings (temperature and weight loss) were performed on the same TG curve, each of them having at least 15 points. Kinetic parameters of thermal degradation for each degradation step were determined by Coats-Redfern method (Coats and Redfern 1964), using a computer program that processed the thermogravimetry data up to 600°C.

RESULTS AND DISCUSSION

Wood Major Chemical Constituents

For many applications a better understanding of the chemistry, properties, and performance of wood fibers is required.

Many wood species from temperate forests have insufficient durability for the intended applications. At this moment this problem is solved partly by using biocides (containing for example: creosote, arsenic, zinc, copper, chromium, etc.) and partly by using tropical hardwoods. Since both the traditional wood preservation and the use of tropical species are under environmental and legislative pressure, the timber industries are seeking alternatives. The use of native grown species with enhanced qualities would be the ultimate solution to this problem.

Wood modification aims at altering the molecular structure of the cell wall polymers. Wood modification can change important properties of the wood, including biological durability, dimensional stability, hardness, and UV-stability by converting hydrophilic OH-groups into larger, more hydrophobic groups. Specific wood modification processes designed for the production of wood plastic composites may be developed, having in view the properties of the wood component in the composites, but also the improved interaction, e.g. by means of grafting processes.

The physical and chemical properties of wood are derived directly from the composition and morphology of the cell walls, depending on the processes of biosynthesis and assembly. Morphological and chemical characteristics of wood can be modified significantly by environmental influence. As wood biomass represents a significant source of energy and raw materials, having a remarkable potential for a continuous recovery, a comparative study on evolution of wood chemical composition for 12 different tree species from the Iasi forestry district was performed (see Table 2).

Table 2. Tree Species Considered for the Comparative Study

Tree species	Tree diameter (m)	Age (years)
Poplar (*Populus alba*)	0.35	18
Cherry-tree (*Cerasus avium L*)	0.35	52
Ash-tree (*Fraxinus excelsior L.)*	0.30	52
Hornbeam (*Carpinus betulus L.)*	0.28	46
Beech (*Fagus silvaticaL.)*	0.345	83
Common-oak(*Quercus sessiliflora*)	0.40	89
Oak (*Quercus robur L.)*	0.355	80
Lime-tree (*Tilia cordata* Mill.)	0.41	70
Willow (*Salix alba L.)*	0.33	19
Elm *(Ulmus foliacea* Gilib.)	0.175	50
Ash-tree (*Fraxinus excelsior L.)*	0.46	102
Common-maple *(Acer campestre L.)*	0.44	96

Comparative data (1964 and 2000) on wood chemical components for the tree species considered in our study are presented in Table 3. The experimental data obtained from this investigation gave evidence of a significant increase in ash content for some tree species considered here (such as poplar, beech, elm, oak, ash-tree, common-oak). The mineral ash content of oak wood, obtained after 1 h at 650^{o}C through a standard method (TAPPI norm T 211 om-85), increased from 0.14 % (as obtained by Cr. I. Simionescu and co-workers in 1964) to 1.30 % (in 2000). This evolution may be correlated with the trees' dryness, a phenomenon found especially for the quercinee tree species (including the pedunculate oak).

Table 3. Wood Chemical Components for Different Romanian Tree Species- Comparative Data (1964 and 2000)

Wood species/ year	Ash (%)		Extractives in : (%) Hot water		NaOH 1 %		Cellulose (%)		Lignin (%)	
	1964	2000	1964	2000	1964	2000	1964	2000	1964	2000
Poplar	0.40	1.00	4.40	2.92	20.05	15.13	46.53	49.26	17.23	25.23
Cherry-tree	0.30	0.41	3.64	3.52	20.79	16.92	48.66	46.64	20.98	18.25
Ash-tree (52 years)	0.39	0.66	6.30	6.38	21.30	18.80	42.41	41.58	26.80	26.39
Hornbeam	0.44	0.60	2.08	4.72	16.68	16.45	47.26	44.88	20.09	19.34
Beech	0.44	1.36	1.75	2.19	16.21	13.15	46.24	47.66	23.49	25.53
Common-oak	0.26	0.73	9.56	7.07	23.91	17.27	44.49	42.30	25.31	26.83
Oak	0.14	1.30	8.12	7.56	23.80	18.27	45.08	42.79	23.32	24.82
Lime-tree	0.46	0.78	2.18	2.26	17.93	13.12	52.43	50.49	20.67	21.41
Willow	1.01	0.91	8. 33	2.68	21.58	15.24	46.76	50.59	28.64	23.45
Elm	0.68	1.41	2.45	3.78	16.76	15.45	49.63	49.03	27.78	26.14
Ash-tree (102 years)	0.39	0.93	6.30	4.99	21.30	14.64	42.41	43.81	26.80	23.18
Common-maple	0.62	0.72	4.28	3.07	18.35	10.57	44.48	49.95	24.56	21.99

As regards the hot water extractives content, there is an obvious increase for beech and elm wood by 25 % and 54 % respectively, as follows from Table 3. The largest values are observed for oak and common-oak, tree species characterized by significant tannins content. A decrease in the NaOH 1 % extractives content is evidenced for all tree species. The major wood chemical components (cellulose, lignin) exhibit a corresponding variation, depending especially on the tree species.

A significant criterion for wood utilization in the pulp and paper industry is represented by the cellulose/lignin ratio (C/L criterion). The estimated values both for C/L_K and C/L_{TAPPI} criterion for all wood samples are presented in Table 4 (fractions sampled from the wood round discs cut from 1.30 m height above ground and passed through a 0.63 mm sieve).

Table 4. C/L_K, and C/L_{Tappi} Criterion Values Determined for the Tree Species

Wood tree species	$C / L_{K\ (1964\ study)}$	C / L_K	C / L_{TAPPI}
Poplar	2.70	1, 95	1, 94
Cherry-tree	2.32	2, 55	2, 60
Ash-tree (52 years)	1.58	1, 58	1, 67
Hornbeam	2.35	2, 32	2, 22
Beech	1.96	1, 97	1, 96
Common-oak	1.74	1, 57	1, 62
Oak	1.93	1, 72	1, 75
Lime-tree	2.53	2, 35	2, 37
Willow	1.63	2, 16	2, 19
Elm	1.78	1, 87	1, 92
Ash-tree (102 years)	1.58	1, 88	1, 87
Common-maple	1.81	2, 27	2, 26

wood sawdust samples < 0.63 mm

Generally, the hardwood species show a C/L criterion value greater than 2. For some tree species presented here, this parameter has values lower than 2.

Preliminarily, the main chemical components of the oak wood sawdust were quantified for each tree-rings domain (see Table 5), showing some differences depending on the height values from which the samples were assayed (in accordance with the previous study performed in 1964). For example, the cellulose content increases with the tree's radial growth. The extractives content both in hot water and percent sodium hydroxide solution increase with tree's height, while the cellulose content decreases. The total extractives content presents an increasing trend with tree's height, mainly for (0-40) years oak wood tree-rings.

The oak tree species gave a wood with poor properties for pulping, both due to the higher extractives content given by tannins and the low cellulose content as evidenced by the minimum value for the C/L criterion as compared with other native Romanian hardwood species.

Table 5. Chemical Components of the Oak Wood Tree-Rings

Oak wood sample /annual tree rings	Extractives %			Total extractives %	Cellulose %	Lignin TAPPI %	C/L ratio	Holo cellulose %
	hot water	NaOH 1 %	alcohol benzene					
1.30 m								
(0-40)	7.91	15.62	4.21	27.74	40.03	21.69	1.845	72.82
(40-70)	7.85	18.95	2.29	29.09	42.81	23.75	1.803	71.57
(70-80)	4.57	13.30	2.89	20.76	44.40	22.12	2.007	72.25
8 m								
(0-40)	9.87	18.35	3.12	31.34	42.04	25.77	1.631	67.03
(40-70)	10.42	17.33	3.15	30.90	40.76	23.82	1.711	58.44
(70-80)	4.61	14.12	2.33	21.06	46.97	20.73	2.265	70.48
15 m								
(0-40)	12.38	21.94	4.26	38.58	37.73	23.47	1.607	73.18
(40-70)	10.72	19.59	3.17	33.48	36.81	24.71	1.489	67.92
(70-80)	5.94	12.70	2.73	21.37	40.96	24.36	1.681	72.56

FT-IR Spectroscopy

Fourier transform infrared (FT-IR) spectra were used to characterize differences between the oak wood tree-rings, with different positions of the absorption bands being observed. Due to the weak differences between the recorded FT-IR spectra for all wood tree-annual rings, only the data obtained for whole wood samples assayed from 1.30 m height above ground and passed through a 0.63 mm sieve (Figure 1) are presented here.

The FT-IR results provide evidence of some frequency domains, as follows: (3430-2922) cm^{-1} given by the OH and CH stretching vibrations ν_{OH} and ν_{CH}; 1730 cm^{-1} characteristic to the C=O stretching vibrations; and (1500-1360) cm^{-1} specific to the deformation vibrations of benzene rings, methylene and methyl groups δ_{CH}, δ_{CH2}, δ_{CH3}.

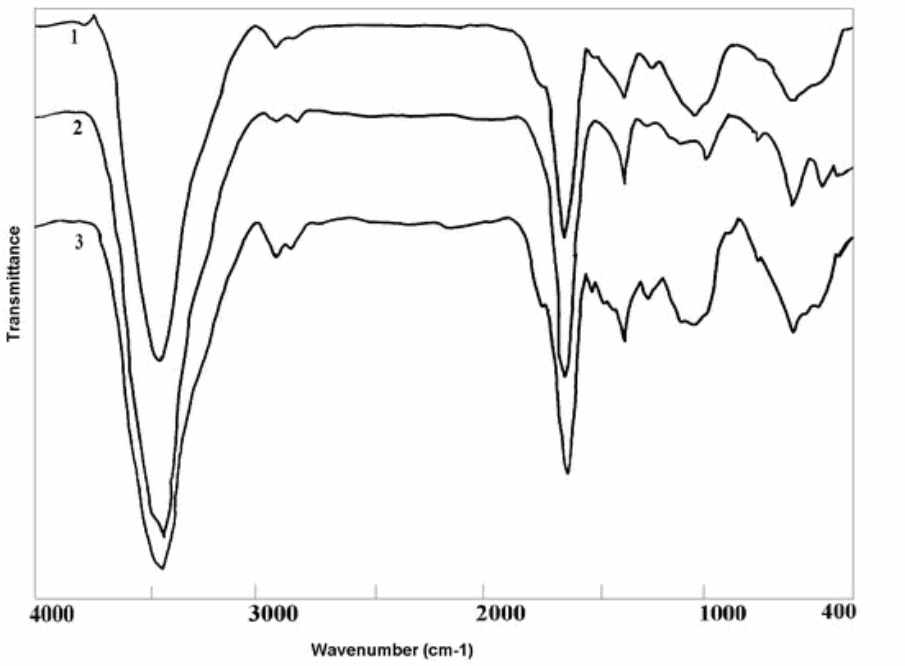

Fig. 1. FT-IR spectra recorded for the oak wood samples (height: 1.30 m - 1. 0-40 years; 2. 40-70 years; 3. 70-80 years).

As the tree becomes older, it is becoming more susceptible to degradation processes. Structural units that undergo various changes are functional groups located on the glucopyranose monomer in cellulose, observable in the FT-IR spectra. Carbon atoms occupying various positions in the ring (denoted as C-1, C-2, …C-6) loose their identity, gradually transforming into various carbonyl groups of different degrees of freedom, namely ketonic, aldehydic, and carboxylic groups.

Next are presented the spectra for celluloses separated from wood specimens assayed from 1.30 m height above ground (Figure 2). Celluloses were separated from the oak wood tree-rings by the common method used in wood chemistry involving concentrated nitric acid and ethyl alcohol. The FT-IR spectra of celluloses show some differences as follows:

1. A shift to the right for spectral bands from 900 cm^{-1}, specific to the atomic vibrations for C-1 from the crystalline network of cellulose in the (0-40 years) wood tree-rings domain - the glucose units in cellulose are joined by β-glycoside bonds between C-1 and C-4 sites of adjacent sugars;
2. a shoulder at the frequency of 1730 cm^{-1}, attributed to the spectral vibrations of CH=O and OH groups during the tree's radial growth. The carbonyl band assignment allows distinguishing aldehydic and carboxyl stretching vibrations as arising around 1710 and 1740 cm^{-1}, respectively. These give evidence to the most profound changes with time upon ageing under various conditions.

For the (0-40 years) oak wood tree-rings, a significant asymmetry is observed for the frequency of 3400 cm^{-1}, specific to the associated hydroxyl groups (O-H stretching hydrogen-bonded).

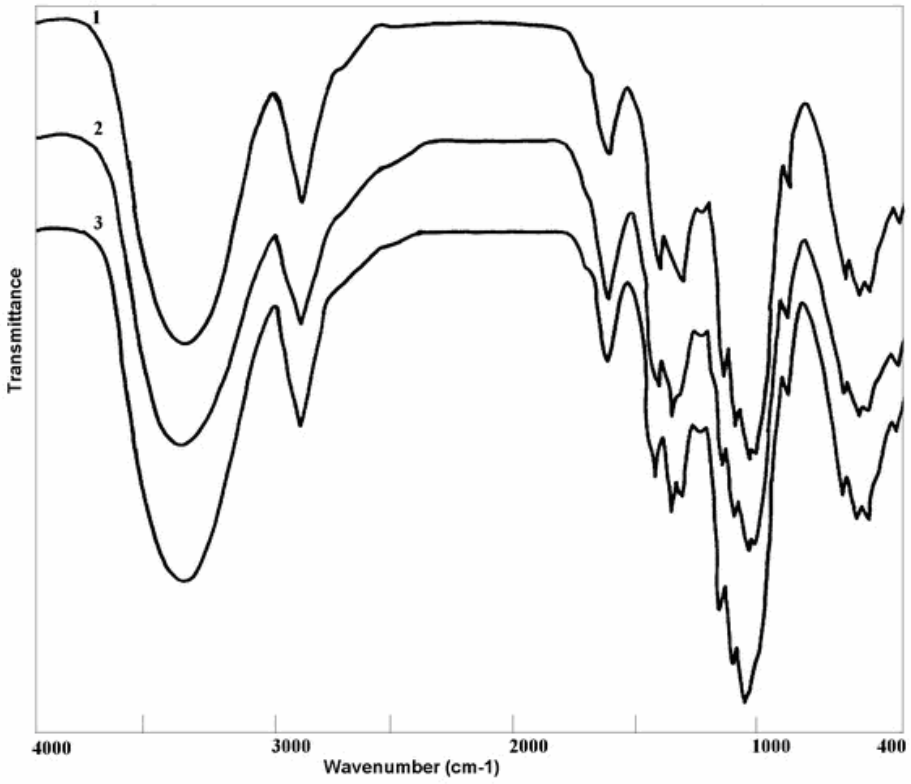

Fig. 2. FT-IR spectra for celluloses separated from the oak wood samples (height: 1.30 m – 1. 0-40 years; 2. 40-70 years; 3. 70-80 years).

The crystalline phase for celluloses reveals some differences depending on the oak wood tree-rings domain and height from which the wood round discs were assayed. The crystallinity index (Cr I), estimated from the FTIR spectra (Rozmarin 1984), presents a slightly decrease with the tree's growth on height (data shown in Table 6).

Table 6. Crystallinity Index for Celluloses Separated from the Oak Wood Tree-Rings

Crystallinity index (A_{1371} / A_{2900})			
Annual tree -rings / height	1.3 m	8.0 m	15.0 m
0-40 years	0.41	0.33	0.36
40-70 years	0.31	0.31	0.29
70-80 years	0.38	0.34	0.36

The FT-IR spectra recorded for lignin isolated from the oak wood samples obtained from 1.30 m height above ground (Figure 3) are quite similar, excepting the intensities for the absorption bands specific to the carbonyl stretching (1722 cm $^{-1}$ attributed to unconjugated ketone and carboxyl groups).

As it can be observed, some small frequency shifts of the absorption bands to the left (at 1031 cm^{-1} attributed to the aromatic C-H in plane deformation, guaiacyl-type, and C-O deformation, primary alcohol), respectively to the right (at 1323 cm $^{-1}$ attributed to the syringyl ring breathing with CO stretching) are correlated with the tree's radial growth, being caused probably by the interactions between the functional groups.

The assignment of the main absorption bands from the FTIR spectra recorded for lignin is in accordance with the literature (Sakakibara 1991), showing sometimes only small variations in the band frequency (e.g., 1502 cm^{-1}, instead of 1510 cm^{-1}, which is a specific band for wood lignin). For the (70-80 years) oak wood tree-rings, a weak peak from a conjugated carbonyl group at 1715-1710 cm^{-1} is observed. This band, which may have originated from polyphenols, could be an indication of the chemical modification of lignin during the heartwood formation process. From the FTIR spectroscopy records, some parameters have been calculated, in accordance with literature data (Rozmarin 1984; Faix and Beinhoff 1988) and are presented in Table 7.

Significant decreases in both phenolic OH group content and S/G (syringyl/ guaiacyl) ratio value is noticed, while the –C-O groups content increases (see Table 7). At the same time, one can observe a decreasing of the aromatic components content during the tree's radial growth.

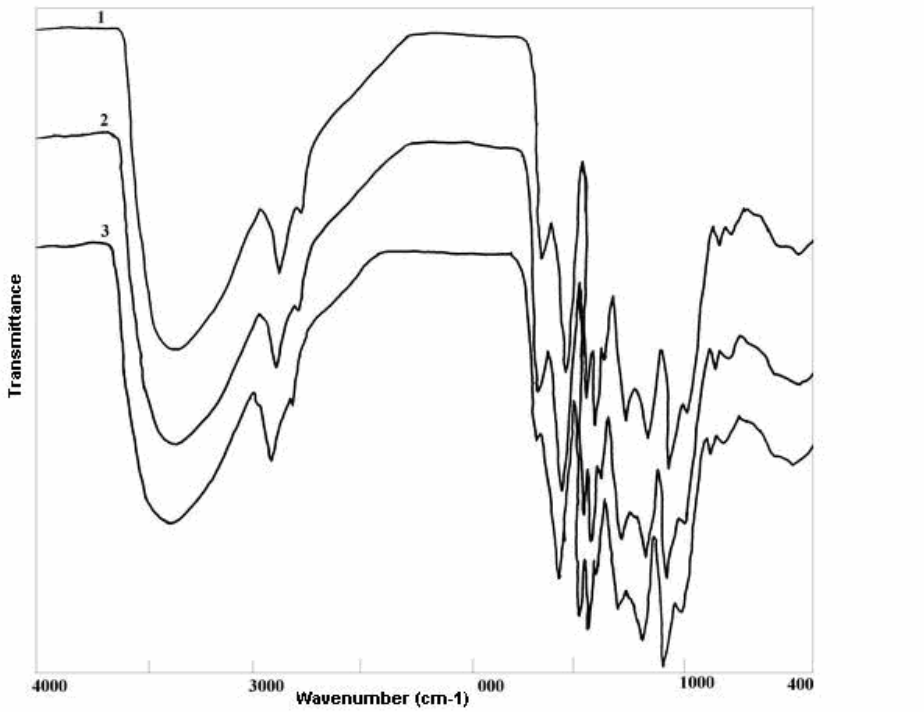

Fig. 3. FT-IR spectra for lignin separated from the oak wood samples (height: 1.30 m – 1. 0-40 years; 2. 40 -70 years; 3. 70-80 years).

Table 7. Absorbance Ratio Representing Indication of Relative Differences in Ratio of Aliphatic to Aromatic Units and Content of Phenolic OH groups and C-O Groups

Wood sample	Ratio of aliphatic to aromatic signals A_{2937}/A_{1502}	Content of phenolic OH groups A_{1323}/A_{1502}	Content of C-O groups A_{1031}/A_{1502}	S/G ratio A_{1323}/A_{1219}
1. 3 m 0-40 years	0.61	0.60	0.42	1.11
40-70 years	0.63	0.72	0.61	1.03
70-80 years	0.76	0.56	0.60	0.72
8. 0 m 0-40 years	0.61	0.63	0.60	1.01
40-70 years	0.66	0.60	0.57	0.96
70-80 years	0.89	0.80	0.77	0.82
15. 0 m 0-40 years	0.58	0.63	0.56	1.06
40-70 years	0.64	0.61	0.55	1.05
70-80 years	0.68	0.51	0.64	0.96

Thermogravimetry Study

Wood thermal decomposition is considered a promising process of efficient and, in the future, economically profitable conversion of this raw material into high quality energetic and chemical products. However, designing technologies based on the pyrolysis of renewable lignocellulosic raw materials requires good knowledge of the kinetics of this process. As cellulose is the main component in wood and crops, its thermal degradation has been the subject of extensive research, which remains of interest in the perspective of reducing the energy production from fossil sources and its associated pollution. Thermal analysis was performed in order to compare the proportions of main active component in the oak wood tree-rings.

The weight loss during the thermal analysis of the wood biopolymers is characterized by three stages of degradation:

1. Up to about 150^{o}C: loss of moisture content in an endothermic reaction;
2. Between 150 and about 400^{o}C: decomposition of the biopolymer, with char formation and the evolution of gas (exothermic reaction);
3. Between 400 and about 500^{o}C: combustion of the char (exothermic reaction).

The cellulose and hemicelluloses components of the whole biomass decompose independently of one another. Lignin decomposition is formally described by a very broad DTG peak at about 300^{o}C (Antal and Varhegyi 1995; Kaloustian et al. 2001).

Thermal degradation of cellulose fits well with apparent first-order kinetics and proceeds essentially through two types of reactions (Shafizadeh 1985). At lower temperatures, between 200 and 280^{o}C, there is a gradual degradation that includes depolymerization, dehydration, etc. At higher temperatures, a rapid volatilization occurs, which is often accompanied by formation of 1, 6-anhydro-β-D-glucopyranose (levoglucosan). The thermogravimetric parameters for the cellulose main thermal decomposition process are presented in Table 8. From these data, one can appreciate that both the initial and final temperatures (T_i and T_f) of the main decomposition process vary significantly with the wood tree-rings.

Table 8. Thermogravimetry Parameters for the Thermal Decomposition Process of Oak Cellulose

Thermal parameters	Oak wood tree-rings								
	0-40 years			40-70 years			70-80 years		
	Tree's height value from which the wood samples were assayed								
	1.3 m	8.0 m	15.0 m	1.3 m	8.0 m	15.0 m	1.3 m	8.0 m	15.0 m
T_i [a], °C	210	191	225	205	262	223	218	257	213
W_{Ti} [b], %	5.8	6,0	5.5	6.0	8.2	7.8	6.5	6.8	10.5
T_{max} [c], °C	318	328	325	324	338	310	320	330	323
W_{Tmax} [d], %	53	50	51	50	52	51.5	56	59	57
T_f [e], °C	410	410	409	400	418	388	397	405	382
W_{Tf} [f], %	81	81	81.5	79	82	77	78.2	81.5	82
Ea [g], Kj/mol	85.27	106.24	82.30	93.07	102.49	82.58	86.27	104.44	79.24
n [i]	0	0.8	0	0	0.9	0	0	0.8	0

[a] Ti = initial temperature; [b] W_{Ti} = initial weight loss; [c] T_{max} = maximum temperature; [d] W_{Tmax} = weight loss at T_{max}; [e] T_f = final temperature; [f] W_{Tf} = final weight loss; [g] E_a = activation energy; [i] n = reaction order.

The higher values for crystallinity index (Cr I) of cellulose isolated from the (0-40 years) oak wood tree-rings are in accordance with the literature data, influencing to a great extent the thermal decomposition process of this biopolymer (Kosic et al. 1973).

The activation energy ranges in the (79.24 - 106.24) kJ/mol domain. Higher values for the activation energy and a first-order reaction for the degradation process are noticed for all celluloses separated from the oak wood specimens assayed from 8.0m height above ground (see Table 8). The weight loss values calculated vary between 77 % and 82 % (Fig. 4-6) at the end of the main thermal decomposition process for cellulose.

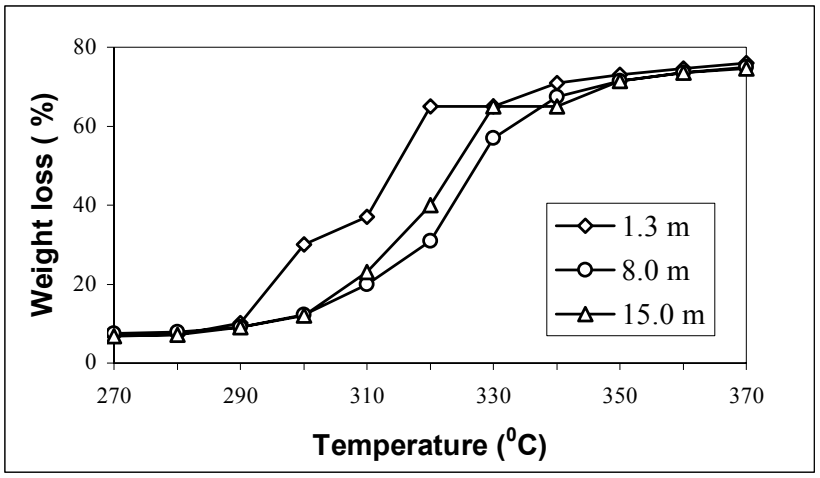

Fig. 4. Weight loss values calculated for cellulose thermal decomposition process (samples from 0-40 years oak wood tree-rings).

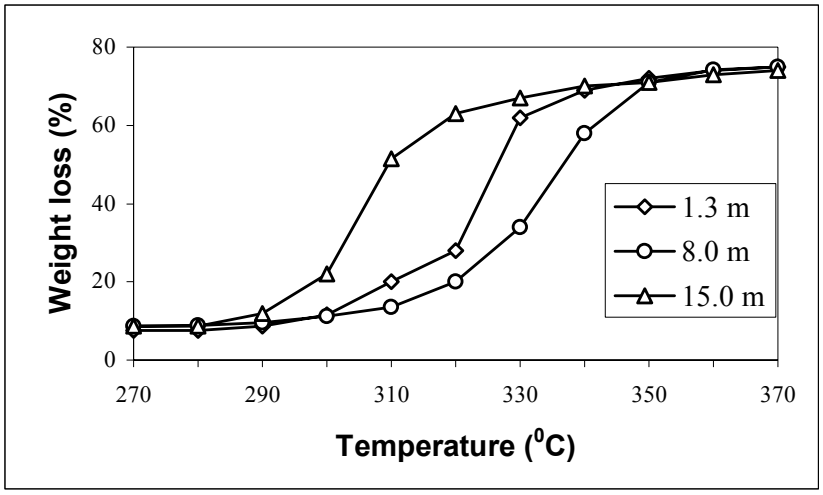

Fig. 5. Weight loss values calculated for cellulose thermal decomposition process (samples from 40-70 years oak wood tree-rings).

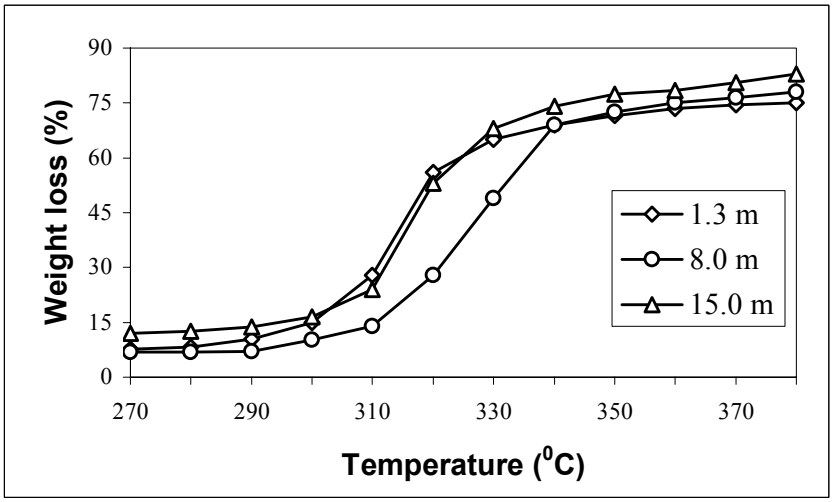

Fig. 6. Weight loss values calculated for the cellulose thermal decomposition process (samples from 70-80 years oak wood tree-rings).

All these aspects may be correlated with the structural associations of the macromolecular chains, as an immediate response to the environmental changes during the trees' growth. The thermal behavior of the wood cell wall polymers is strongly related to their content in the native vegetal biomass (Simpson and TenWolde 1999; Shafizadeh 1982). Nevertheless, the environmental perturbations have a real and huge impact on the trees' growth, the wood cell wall biopolymers - cellulose and lignin- being sensitive to any external variation.

CONCLUSIONS

1. Wood chemical components show significant variations depending on the tree species and the climate conditions (e.g. a decrease of the NaOH 1 % extractives content). The

major wood chemical components (cellulose, lignin) exhibit a corresponding variation. Differences are also noticed by comparison with the previous data on Romanian wood tree species. As general evidence, a special mention should be made on the wood ash content for all tree species which increases. This aspect can be an expression of the trees' dryness process, a fact evidenced mainly for the oak tree species.

2. The cellulose content increases during the oak tree's radial growth, depending on the tree-rings domains, and height from which the wood round discs were assayed. The cellulose/lignin ratio (C/L) values are correlated with the tree's height values ($C/L_{1.30m} < C/L_{8m} < C/L_{15m}$), being higher for the (70-80) tree-rings considered here.
3. The FT-IR spectra for the oak wood samples present differences correlated with the tree species features, and fluctuant environment during the tree's radial growth. Some frequency shifts for the absorption bands both to the right at the frequency of 3430 cm^{-1} and to the left at 1730 cm^{-1}, are observed. These may be correlated with the interactions given by the hydroxyl groups, respectively the carbonyl groups.
4. The FT-IR spectra for celluloses show variable intensities of absorption bands in the frequency domain of 1640-1060 cm^{-1}, for all wood samples, due to the interactions between chemical groups. The crystallinity index (Cr I) of celluloses presents a slightly decrease with the tree's growth on height.
5. The FTIR spectra recorded for the oak wood lignin are quite similar, excepting the intensities for absorption bands specific to the carbonyl groups (1722 cm^{-1}). A decrease both of the phenolic OH groups content and S/G (syringyl/guaiacyl) ratio value is noticed, while the –C- O groups content increases during the tree's radial growth.
6. The thermogravimetry study of celluloses separated from the oak wood samples gives evidence of a main temperature domain for the thermal decomposition process that is influenced to a great extent by the tree's growth process. Weight loss values (W_{Ti}) corresponding to the initial temperature of the main thermal decomposition process are positively correlated with the tree's radial growth. At the end of the main thermal decomposition process, weight loss values (W_{Tf}) of 77-82 % are observed.
7. The chemical properties of wood, such as the hot water and alkali extractives contents, are strongly related to its behavior during the chemical pulping process. Significant correlations can be established between these chemical indications and the frequencies of bands given by the Fourier transform infrared spectra of a series of woods from different sites in Romania. The oak wood is not used in the Romanian pulp industry due to its specific characteristics that cause many difficulties in processing (e.g. due to the large amounts of tannins and lower C/L ratio value). It is mainly used for furniture production.
8. This kind of methodology can be extended to some other tree species for assessing the pulpwood quality of wood from standing trees, because the measurements can be made rapidly and require only small samples. Nevertheless, this approach of the wood tree chemistry may be valuable for investigation of the chemical modification performed both on the wood and its major components (cellulose and lignin). Through this process, materials with given and special properties (e.g. thermal stability, resistance to decay, introduction of some reactive functional groups through addition of different chemicals to the hydroxyl groups of the wood material for further grafting synthetic polymers in order to obtain composites) may be obtained.

ACKNOWLEDGEMENTS

The authors are grateful for the support of the Research and Technology Ministry of Romania - National Agency for Science, Technology and Innovation, Grant No. 5052/1999-2001.

REFERENCES CITED

Antal, M. J., and Varhegyi, G. (1995). "Cellulose pyrolysis kinetics. The current state of Knowledge," *Ind. Eng. Chem. Res.* 34, 703-717.

Coats, A. W., and Redfern, J. P. (1964). "Kinetic parameters from thermogravimetric Data," *Nature* 201, 68-69.

Colom, X., and Carrillo, F. (2005). "Comparative study of wood samples of the northern area of Catalonia by FTIR," *J. Wood Chem. Technol.* 25/1-2, 1-11.

Durbak, I., Green, D. W., Highley, T.L., Howard, J. L., McKeever, D.B., Miller, R.B., Pettersen, R.C., Rowell, R.M., Simpson, W.T., Skog, K.E., White, R.H., Winandy, J. E., and Zerbe, J. I. (1998). *Wood*, Kirk-Othmer Encyclopedia of Chemical Technology, R. E. Kirk-Othmer, F. Kroschwitz, M. Howe-Grant, eds., volume 25, 4th ed., Wiley, New York.

Faix, O., and Beinhoff, O. (1988). "FTIR spectra of milled wood lignins and lignin polymer models (DHP's) with enhanced resolution obtained by deconvolution," *J. Wood. Chem. Technol*. 8/4, 505-522.

Fengel, D., and Wegener, G. (1984). *Wood Chemistry, Ultrastructure, Reactions*, de Gruyter Verlag, Berlin, Germany.

Hergert, H.L. (1971). *Infrared Spectra*, Lignins, K.V. Sarkanen, C.H. Ludwig, eds., Wiley-Interscience, New York.

Kaloustian, J., Pauli, A. M., and Pastor, J. (2001). "Kinetic study of the thermal decomposition of biopolymers extracted from various plants," *J. Therm. Anal. Cal*. 63/1, 7-20.

Kosik, M., Reiser, V., and Michalic, J. (1973). "Thermal and thermooxydation degradation of cellulose. Effect of crystallinity," *Papira Celulosa* 28 /7-8, 29-31.

Meshitsuka, G. (1991). *Utilization of Wood and Cellulose for Chemicals and Energy*, Wood and Cellulosic Chemistry, D. S. Hon, N. Shiraishi, eds., Marcel Dekker Inc., New York.

Miller, R. B. (1999). *Structure of Wood*, Gen. Technical Report FPL–GTR–113 Wood Handbook-Wood as an Engineering Material, U. S. Department of Agriculture, Forest Service, Forest Products Laboratory, Madison, WI, USA, (http://www.fpl.fs.fed.us/documents/).

Nelson, M. L., and O'Connor, R. T. (1964). "Relation of certain infrared bands to cellulose crystallinity and crystal lattice type. Part II. A new infrared ratio for estimation of crystallinity in cellulose I and II," *J. Appl. Polym. Sci.* 8, 1325-1341.

Pandey, K. (1999). "A study of chemical structure of soft and hardwood and wood polymer by FTIR spectroscopy," *J. Appl. Polym. Sci.* 71, 1969-1975.

Panshin, A. J., and De Zeeuw, C. (1980). *Textbook of Wood Technology: Structure, Identification, Uses and Properties of the Commercial Woods of the United States*

and Canada, 4th ed., McGraw-Hill, New York.
Pettersen, R. (1984). *Chemical Composition of Wood*, The Chemistry of Solid Woods, R. M. Rowell, ed., Advances in Chemistry Series 207, American Chemical Society, Washington D.C.
Rozas, V. (2001). "Detecting the impact of climate and disturbances on tree-rings of *Fagus sylvatica* L. and *Quercus robur* L. in a lowland forest in Cantabria, northern Spain," *Ann. For. Sci.* 58, 237-251.
Rozmarin, Gh. (1984). *Macromolecular Basis of Wood Chemistry*, Technical Publishing House, Bucharest, Romania.
Rowell, R. M. (1984). *The Chemistry of Solid Wood*, American Chemical Society, Washington D.C.
Sakakibara, A. (1991). *Chemistry of Lignin*, Wood and Cellulosic Chemistry, N. S. Hon, N. Shiraishi, eds., Marcel Dekker Inc., New York.
Shafizadeh, F. (1982). "Introduction to pyrolysis of biomass," *J. Anal. Appl. Pyrolysis* 3, 283-305.
Shafizadeh, F. (1985). *Thermal Degradation of Cellulose*, Cellulose Chemistry and Its Applications, T. P. Nevell, S. H. Zeronian, eds., Ellis Horwood, Chichester, UK.
Simionescu, Cr. I., Grigoras, M., and Asandei, A. (1964). *Wood Chemistry of Tree Species from Romania*, Romanian Academy Publishing House, Bucharest, Romania.
Simpson, W., and TenWolde, A. (1999). *Physical Properties and Moisture Relations of Wood,* Gen. Technical Report FPL–GTR–113 Wood Handbook - Wood as an Engineering Material, U. S. Department of Agriculture, Forest Service, Forest Products Laboratory, Madison, WI, USA, (http://www.fpl.fs.fed.us/documents/).
Sjöstrom, E. (1993).*Wood Chemistry: Fundamentals and Applications*, 2nd ed., Academic Press, New York.
TAPPI (US Technical Association of Pulp and Paper Industry): Sampling and preparing wood for analysis, norm T 257 om-85, 1985.
TAPPI (US Technical Association of Pulp and Paper Industry): Ash in wood, pulp, paper, and paperboard, norm T 211 om-85, 1985.
TAPPI (US Technical Association of Pulp and Paper Industry): Preparation of wood for chemical analysis, norm T 264 om-88, 1988.
TAPPI (US Technical Association of Pulp and Paper Industry): Wood extractives in ethanol-benzene mixture, norm T 204 om-88, 1988.
TAPPI (US Technical Association of Pulp and Paper Industry): One percent sodium hydroxide solubility of wood and pulp, norm T 212 om-88, 1988.
TAPPI (US Technical Association of Pulp and Paper Industry): Water solubility of wood and pulp, norm T 207 om- 88, 1988.
TAPPI (US Technical Association of Pulp and Paper Industry): Acid insoluble lignin in wood and pulp, norm T 222 om-88, 1988.
Thomas, F. M., Blank, R., and Hartmann, G. (2002). "Abiotic and biotic factors and their interactions as causes of oak decline in Central Europe," *Forest Pathology* 32/4-5, 277-307.

Article submitted: Nov. 29, 2006; First round review completed: Jan. 3, 2007; Revision accepted: Jan. 22, 2007; Article published Jan. 24, 2007

BIOBLEACHING OF FLAX BY DEGRADATION OF LIGNIN WITH LACCASE

Rossica I. Betcheva,[a] Hristina A. Hadzhiyska,[a] Neli V. Georgieva,[b*] and Lubov K. Yotova [b]

Research on lignin biodegradation has become of great interest, due to the fact that lignin is one of the most abundant renewable materials, next to cellulose. Lignin is also the substance that gives color to raw flax fibers. In order to bleach the flax and to keep its tenacity high enough for textile applications, it is necessary to remove the lignin and partially to preserve the pectin. Lignin and pectin are the main constituents of the layer which sticks the flax cells together within the multicellular technical fiber. White-rot fungi and their oxidative enzymes, laccases and peroxidases (lignin peroxidases and manganese peroxidases), are being applied for the biobleaching of papermaking pulp, thereby reducing the need for environmentally harmful chemicals. Some data also suggest that it is possible to use other phenolytic enzymes, such as pure laccase, for this purpose. The objective of the present work was to study the possibility of bleaching flax fibers by pure laccase and combined laccase peroxide treatment, aimed at obtaining fibers with high whiteness and well-preserved tenacity.

Keywords: Laccase, Flax, Lignin degradation, Biobleaching, Laccase, Enzymes

*Contact information: a: Department of Textile Chemistry, b: Department of Biotechnology, University of Chemical Technology and Metallurgy, P. O. Box 1756, Sofia, Bulgaria, *Corresponding author: tel.: +359 2 8163 307, E-mail: neli@uctm.edu*

INTRODUCTION

Flax fibers contain, together with cellulose, considerable quantities of lignin and pectin. It is well known that the lignin is the second most abundant renewable compound on earth. Due to its hydrophobicity and complex random structure, lacking regular hydrolysable bonds, lignin is poorly biodegraded by most microorganisms (Aktas and Tanyolac 2003; Bennet et al. 2002). The lignin, together with the pectin, is located mainly in the layer that sticks the flax cells together within the flax fiber. For obtaining high quality linen textile materials with sufficient whiteness and hydrophilicity, it is necessary to remove pectin (which brings hydrophobicity, due to partial methylation, as well as association of the carboxyl groups with Ca^{2+} and Mg^{2+}) and lignin (which is mainly responsible for the color of raw flax). Conventional pretreatment technologies apply sodium hydroxide combined with oxygen or chloride bleaching for this purpose. For the purposes of textile mechanical technologies (spinning and weaving) it is necessary to preserve the tenacity of flax fibers. This tenacity can be preserved if the flax cells remain stuck together. Such adhesion can be maintained if the pectin is not entirely removed. Therefore, we need a selective hydrolysation, capable of modifying only the lignin. NaOH is not a selective hydrolyser, since it destroys both the lignin and pectin. In

searching for a specific lignin hydrolyser, it has been found that enzymes associated with the white rot fungus, which produces extracellular peroxidases, such as laccases, Mn-peroxidase and lignin peroxidase, are among the best biodegraders of lignin (Georgieva et al. 2004; Hatakka 1994; Heinzkill and Messner 1997; Heinzkill et al. 1998). These enzymes can be used for biopulping, biobleaching, biotransformation, and bioremediation. They can be applied as auxiliaries in different industrial processes, replacing conventional chemicals such as alkalis, oxidizers, reducing agents, or acids (Petit-Conil et al. 2002; Rodrigues et al. 1999; Srebotnik and Hammel 2000). Regarding flax fibers processing, the lignin cleavage and removal are directly related to the degree of whiteness and to the quality of textile materials produced.

The objective of this work was to study the possibility of bleaching flax fibers by pure laccase and combined laccase-sodium peroxide treatment, aimed at obtaining fibers with high whiteness and well-preserved tenacity.

EXPERIMENTAL

Enzymatic Treatment

Unbleached flax fibres from "Rylski len-AD" Bulgaria and linen fabric (cotton/ flax: 50/50) were taken as reference samples. That textile materials were treated in the range of 30-60 ^{o}C for 1-5 h with 0.1g/l laccase (EC 1.10.3.2 *Trametes sp*. Laccase L603P from Biocatalyst; 0.125 g protein per g solid) in 100 mM Na - acetate/acetic acid buffer pH = 5.0. Control (conventional) bleaching was carried out under conditions close to those of the industrial technologies. That bleaching was accomplished by using 1% H_2O_2 (o.w.f.) at 80 ^{o}C for 60 min. at pH=9 without stabilizer in bath ratio 1:10 without shaking. Combined (laccase-sodium peroxide) bleached samples were prepared from enzymatically treated textiles processed additionally with peroxide at 80 ^{o}C for 15 min and 50 ^{0}C for 60 min., while the other bleaching parameters remained the same. Data obtained to characterize the effects of applied treatments were the average results from 3 parallel samples obtained at the same conditions.

Analytical Measurements

The bleaching effect of the treatments was measured by Datacolor equipment, and the CIELab parameter *lightness* (L*) was used to evaluate the effectiveness of enzyme and bleaching treatments. Untreated flax fibers were used as a reference samples.

Kappa Number Assay

The content of lignin in samples studied was characterized by the Kappa Number assay. The flax fibers (1g each) were placed in a vessel containing 500 cm^3 distilled water at 25 ^{o}C with careful stirring to which 100 cm^3 0.1M $KMnO_4$ and 100 cm^3 4N H_2SO_4 were added. The stirring duration was 10 min. Then 20 cm^3 0.1N KI were added to the solution, which was titrated with 0.2N $Na_2S_2O_3$. The Kappa number was measured by SCAN method (SCAN C 1:00) (Testing Committee Finland Sweden, 1977).

Physical and Mechanical Properties

The physical and mechanical properties of textile samples were measured by a Dynamometer apparatus. In order to reveal the advantages of the combined enzymatic-sodium peroxide bleaching, relative changes (R.C.) of the parameters obtained were calculated as follows:

$$R.C. = \frac{\text{Specific Strength of Conventionally Bleached Material}}{\text{Specific Strength of Combined Bleached Material}} \quad X\ 100$$

RESULTS AND DISCUSSION

The first stage of the experiment involved a treatment of flax fibers with pure laccase with enzyme activity 51μmol.min^{-1} at different temperatures. After that, all samples were bleached with H_2O_2, as described above. Colorimetric results, indicating efficiency in increasing the whiteness of fibers, are shown in Table 1. It can be seen that when the temperature of treatment increased, the degree of lightness went through a maximum at 40 ^{o}C. This is the temperature where this enzyme shows maximum activity (Hadzhiyska et al., 2006). For the samples treated with a combination of enzyme and sodium peroxide bleaching, the same dependence could be observed. All results for the *kappa* (κ) number showed the same trend. This could be considered as an indirect demonstration of the dependence between the whiteness of flax fibers and the content of lignin.

If one compares laccase versus lacasse-Na peroxide bleached fibers, one can see the following: Laccase processing was not, by itself, sufficient for obtaining flax fibers with a good appearance (whiteness). As the κ numbers show, the quantity of lignin after the enzymatic treatment decreased, but it was still quite high compared to the value for the control sample. The fact that κ numbers were lower could be explained in terms of changes occurring in the flax lignin.

It was anticipated that enzymatic destruction of lignin could lead to the acceleration of its removal by oxidative bleaching. For this purpose we studied the possibility for a shorter peroxide treatment of the laccase treated fibers. Results in Table 1 show that,

Table 1. Lightness and Lignin Content in Flax Fibers Treated with Laccase at Different Temperatures

T ^{0}C/1h	Enzyme treatment		Additional bleaching with H_2O_2 at 80 ^{0}C/15 min.	
	L*	κ	L*	κ
	[1] ***58.93***	[1] ***15.23***	[2] ***82.40***	[2] ***5.5***
30	58.70	14.40	81.05	6.2
40	60.65	13.69	82.73	6.2
50	60.44	14.86	81.54	6.4
60	59.78	14.87	80.44	6.6

[1] ***Reference*** – untreated flax fibers
[2] ***Control -*** no enzyme treatment - directly bleached with H_2O_2 at 80^{0}C for1h.

for the enzymatically pretreated samples, 15 minutes bleaching with Na peroxide were enough to obtain results for lightness and *kappa* numbers that were similar to those for the control sample. Up to the present, there has been no technology for flax bleaching that can produce textile with good whiteness after only 15 min. of sodium peroxide treatment at 80 ^{o}C.

Data pertaining to the influence of the duration of the enzymatic treatment on the whiteness of flax fibers are given in table 2. The treatments were carried out at 40 ^{o}C, bearing in mind the temperature dependences that were shown in Table 1.

Table 2. The Degree of Lightness of Laccase Treated Fibers at 40 ^{o}C

Duration of treatment (h)	Enzymatic treatment at 40 ^{o}C		Enzymatic treatment at 40 ^{o}C and bleaching with H_2O_2 at 80 ^{o}C/15 min.	
	L*	κ	L*	κ
	1) 58.93	***1) 15.23***	***2) 82.40***	***2) 5.5***
1	60.65	13.69	82.73	6.2
2	61.14	13.53	82.77	5.8
3	61.29	13.52	83.43	5.7
4	61.31	13.52	82.49	5.7
5	61.50	13.21	82.46	5.6

1) ***Reference*** – untreated flax fibers
2) ***Control -*** no enzyme treatment - directly bleached with H_2O_2 at 80^{o}C for1h.

As can be seen from the data, there was not a very well pronounced time dependence of the enzyme effect.

The results obtained on linen fabric treated with laccase are shown in Table 3.

Table 3. CIElab Parameter (L*) of Flax Fabric, Enzymatically Treated at 40^{0}C

Duration of treatment (h)	L*before bleaching with H_2O_2	L*after bleaching with H_2O_2 at 80^{0}C/15 min
	1) 61.04	***2) 73.97***
1	66.43	78.38
2	66.64	78.41
3	66.72	78.63
4	66.98	79.10
5	67.21	79.21

1) ***Reference*** – untreated linen fabric
2) ***Control*** - no enzyme treatment - directly bleached with H_2O_2 at 80^{0}C for1h.

Results in Table 3 show, first of all, that the starting whiteness of the fabric was higher, due to the fact that it contained 50 % cotton, and the flax fibers used were semi-bleached. The time dependence in case of fabric treatment was similar to that for the fiber treatment. Despite the fact that the fabric had a higher whiteness, when considering the untreated reference sample, the flax fibers had higher lightness after treatment, with vary-

ing times of enzymatic treatment before peroxide bleaching. The comparison is given in Fig.1. These results can be rationalized based on the difference between the structure of woven linen textile material and the structure of flax fibers. Woven materials possess a considerably smaller contact reaction surface compared to that of fibrous material. For heterogenic reactions such as the bleaching of textiles in water media, a higher exposed area accelerates reactions occurring at the surface. That could be a possible explanation of the observed lower level of lightness for the fabric, compared to the flax fibers treated under the same conditions (Fig 1).

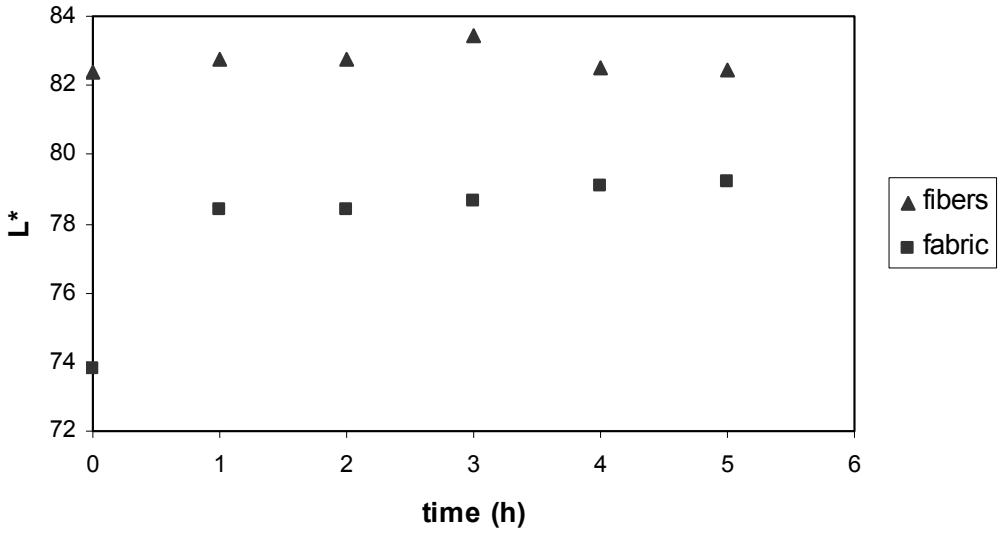

Fig.1. The degree of lightness of flax materials as a function of time of enzymatic treatment, prior to peroxide bleaching

Mechanical properties of flax fibers after treatment with Laccase L603P and after subsequent bleaching with hydrogen peroxide have been characterized by their specific strength. The results obtained are given in Table 4.

Table 4. Physical and Mechanical Properties of Flax Fibers, Treated with Laccase L603P for 1h; Reference Flax Fibers - 0.900 cN/tex

Enzymatic treatment temperature, °C (one hour)	Bleaching with H_2O_2	Specific strength cN/tex	Relative change %
Conventional bleaching(Control)	***80^0 /1h***	***0.400***	***100***
30	80^0 /15′	0.525	131
	50^0 /1h	0.957	239
40	80^0 /15′	0.526	131
	50^0 /1h	0.749	187
50	80^0 /15′	0.526	131
	50^0 /1h	0.708	177
60	80^0 /15′	0.501	125
	50^0 /1h	0.729	182

In the case of combined processing, we explored the possibility for the improvement of bleaching parameters in two ways. First we combined enzymatic treatment with sodium peroxide bleaching at higher temperature but shorter time. The second option that logically could lead to better final mechanical properties was a combined bleaching at lower temperature but longer time.

Experimental results for these treatments, given in Table 5, confirm that the combination of enzyme treatment with peroxide bleaching in all cases produced flax fibers with much higher strength than the conventional bleaching. These results showed also that the temperature of preliminary enzymatic treatment did not influence considerably the fiber tenacity when the bleaching was carried out at 80 ^{o}C. When peroxide was applied at 50 ^{o}C, there is a very strong dependence between the temperature of enzyme application and the fiber strength after bleaching. The decrease of fiber specific strength with the increase of the temperature of enzymatic treatment from 30 to 60 ^{o}C was very well pronounced. Flax fibers were definitely better-preserved when the peroxide bleaching is carried out at 50 ^{o}C.

Table 5. Physical and Mechanical Properties of Flax Fabric, Treated with Laccase L603P for 1h, Reference Flax Fabric - 96.7 dN

Enzyme treatment temperature, ^{o}C (one hour)	Bleaching with H_2O_2	Change in strength dN	Relative change in strength %
Conventional bleaching (Control)	***80^0/1h***	***33.8***	***100***
30	80^0/15′	39.2	116
	50^0/1h	45.0	133
40	80^0/15′	39.2	116
	50^0/1h	45.1	133
50	80^0/15′	34.8	103
	50^0/1h	39.2	116
60	80^0/15′	34.3	103
	50^0/1h	36.3	107

It can be concluded that the enzymatic treatment of samples with Laccase L603P (Biocatalyst) made it possible to carry out peroxide bleaching under milder conditions (a lower temperature and a shorter time for treatment). It can be supposed that the lignin could be destroyed to some extent during the preliminary enzymatic treatment. Probably the enzymatic treatment facilitates the subsequent final removal of lignin and its fragments during the peroxide bleaching. On the other hand, mild conditions could not destroy the pectin entirely, and this could be considered as the main reason for preserving the material's tenacity.

CONCLUSIONS

The bleaching of textile materials containing flax fibers could be facilitated by a preliminary enzymatic treatment with L603P (Biocatalyst). After such a treatment, it was possible to achieve the target level of light reflectance with a just 15 minutes, rather than 60 minutes of treatment by the conventional method, applying only hydrogen peroxide. The combined laccase (L603P) - Na peroxide bleaching could be carried out at a 50 ^{o}C for the oxidative bleaching. That could produce textile materials with high whiteness and very well preserved mechanical properties.

The effect of enzyme treatment could be explained in terms of selective hydrolysis of lignin by the laccase used and better preservation of pectin under these peroxide bleaching conditions.

Symbols Used:

L * - CIELab Lightness
o.w.f. - out of weight of fibers
χ – kappa number
h - time in hours

REFERENCES CITED

Aktas, N., and Tanyolac, A. (2003). "Reaction condition for laccase catalyzed polymerization of catechol," *Bioresource Technology* 87, 209-214.

Bennet, J., Wunch, K., and Faison, B. (2002). "Use of Fungi in Biodegradation," In: *Environmental Microbiology,* Ch. Hurst (ed.), ASM Press Washington, D.C., 960-971.

Georgieva, N., Yotova, L., Valchev, I., Chadjiiska, Ch., and Arizanov, V. (2004). "Biotransformation of lignin in linen by degradation with Phanerochaete chrysosporium," *Proceedings Bioprocess System* Dec. 6 - 8, 4(10), Sofia.

Hadzhiyska, H., Calafell, M., Gibert, J.M., Daga, J.M., and Tzanov, T. (2006). "Laccase-assisted dyeing of cotton," *Biotechnology Letters* 28 (10), 755-759.

Hatakka, A. (1994). "Lignin modifying enzymes from selected white-rot fungi: production and role in lignin degradation," *FEMS Microbiol. Rev.*13, 125-135.

Heinzkill, M., and Messner, K. (1997). "The Lignolytic System of Fungi," In: *Fungal Biotechnology*, T. Anke (ed); Chapman and Hall, Weinheim, 213-276.

Henzkill, M., Bech, L., Halkier, T., Schneider, P., and Anke, T. (1998). "Characterization of laccase and peroxidases from wood-rotting fungi (Finaly Coprinaceae)," *Appl. Environ. Microbiol.* 64 (5), 1601-1606.

Petit-Conil, M., Semar, S., Niku-Paavola, M.L., Sigoillot, J.C., Asther, M., Anke, H., and Viikari, L. (2002). "Potential of laccases in softwood-hardwood high-yield pulping and bleaching," In: *Biotechnology in the Pulp and Paper Industry*, *Progress in Biotechnology* L. Viikari and R. Lantto. (eds.) Elsevier, Amsterdam, 21, 193-201.

Rodriguez, E., Pickard, M., and Vazquez-Duhalt, R. (1999). "Industrial dye decolorization by laccases from ligninolytic fungi," *Curr. Microbiol*. 38 (1), 27-32.

Srebotnik, E., and Hammel, K. (2000). "Degradation of nonphenolic lignin by the laccase/1-hydroxybenzotriasole system," *J. Biotechnol.* 81, 179-188.
Testing Committee Finland Sweden, (1977). Chemical Pulps "Kappa number," Scandinavian pulp, paper and board, June.

Article submitted: Dec. 7, 2006; First round of reviewing completed: Jan. 15, 2007;
Revision accepted: Jan. 23, 2007; Article published Jan. 25, 2007

PELLETIZED PONDEROSA PINE BARK FOR ADSORPTION OF TOXIC HEAVY METALS FROM WATER

Miyoung Oh and Mandla A. Tshabalala*

Bark flour from ponderosa pine (*Pinus ponderosa*) was consolidated into pellets using citric acid as cross-linking agent. The pellets were evaluated for removal of toxic heavy metals from synthetic aqueous solutions. When soaked in water, pellets did not leach tannins, and they showed high adsorption capacity for Cu(II), Zn(II), Cd(II), and Ni(II) under both equilibrium and dynamic adsorption conditions. The experimental data for Cd(II) and Zn(II) showed a better fit to the Langmuir than to the Freundlich isotherm. The Cu(II) data best fit the Freundlich isotherm, and the Ni(II) data fitted both Freundlich and Langmuir isotherms equally. According to the Freundlich constant K_F, adsorption capacity of pelletized bark for the metal ions in aqueous solution, pH 5.1 ± 0.2, followed the order Cd(II) > Cu(II) > Zn(II) >> Ni(II); according to the Langmuir constant *b*, adsorption affinity followed the order Cd(II) >> Cu(II) ≈ Zn(II) >> Ni(II). Although data from dynamic column adsorption experiments did not show a good fit to the Thomas kinetic adsorption model, estimates of sorption affinity series of the metal ions on pelletized bark derived from this model were not consistent with the series derived from the Langmuir or Freundlich isotherms and followed the order Cu(II) > Zn(II) ≈ Cd(II) > Ni(II). According to the Thomas kinetic model, the theoretical maximum amounts of metal that can be sorbed on the pelletized bark in a column at influent concentration of ≈10 mg/L and flow rate = 5 mL/min were estimated to be 57, 53, 50, and 27 mg/g for copper, zinc, cadmium, and nickel, respectively. This study demonstrated the potential for converting low-cost bark residues to value-added sorbents using starting materials and chemicals derived from renewable resources. These sorbents can be applied in the removal of toxic heavy metals from waste streams with heavy metal ion concentrations of up to 100 mg/L in the case of Cu(II).

Keywords: Bark, Sorbent, Adsorption, Metals, Pine, Nickel, Cadmium

*Contact information: USDA Forest Service, Forest Products Laboratory, One Gifford Pinchot Drive, Madison, Wisconsin 53726-2398 *Corresponding author: mtshabalala@fs.fed.us*

INTRODUCTION

Large amounts of bark residues are generated annually by primary timber processing mills worldwide. In the United States alone, an estimated 2.2 million metric tons of bark residues were generated in 2002 (McKeever and Falk 2004). In Canada, approximately 1,200 tons of residual bark was generated daily by Quebec mills (Frigon et al. 2003). Bark residues are therefore one of the most abundant renewable resources that are available for conversion into high-value, environmentally sustainable biomaterials, including low-cost sorbents for treatment of water streams contaminated with persistent organic pollutants (Brás et al. 1999, 2004; Ratola et al. 2003), toxic oily wastes (Haussard

et al. 2003) and reactive dyes (Morais et al. 1999). Several investigators have also shown that bark from various species adsorbs toxic heavy metals from water to different extents (Randall 1977; Deshkar et al. 1990; Reddy et al. 1997; Seki et al. 1997; Gaballah and Kilbertus 1998; Villaescusa et al. 2000; Aoyama and Tsuda 2001; Martin-Dupont et al. 2002, 2004, 2006; Sekar et al. 2004).

In a review of potentially low-cost sorbents for heavy metals, Bailey et al, (1999) concluded that inexpensive, effective, readily available materials such as bark can be used in place of activated carbon or ion exchange resins for removal of heavy metals from solution, although cost comparisons of sorbents are difficult to make due to the scarcity of consistent cost information.

Concentrations of heavy metals in polluted streams vary, depending upon the type of heavy metal, source of pollution, stream location, and time of day. For example Van Hassel et al., (1980) found that heavy metal concentrations in stream water samples collected at three sites adjacent to highways were 2-6 µg/L for Pb; 8-43 µg/L for Zn; 1-7µg/L for Ni; and 0.1-1.1 µg/L for Cd. In a study on the assessment of heavy metal pollution at two South African harbors, Fatoki and Mathabatha, (2001) found that at one of the harbors, heavy metal concentrations in sea water receiving industrial discharges and urban stormwater runoff ranged from 0.2-72 mg/L for Cd; 0.6-42.6 mg/L for Cu; 0.6-16.3 mg/L for Pb; and 0.5-27.6 mg/L for Zn.

Bark flour is effective for removal of toxic heavy metal ions from water because of its high content of polyhydroxy polyphenolic groups that are capable of chelating heavy metal ions (Gaballah, I., and Kilbertus, G., 1998). In addition, bark contains carboxylic groups, which can bind metals by ion-exchange mechanisms (Sakai, K., 2001). However, because bark also contains significant quantities of water-soluble extractives, including soluble tannins, which can be detrimental to aquatic life, the bark needs to be treated before it is used as a sorbent material for removal of contaminants from water. To avoid release of soluble tannins from the bark into the water, Haussard et al. (2003) treated the bark with microorganisms or with copper or chromium solution and Vázquez et al. (2002) used acidified formaldehyde. Earlier studies by Chow (1972) had indicated that water soluble phenolic substances in bark can be condensed into water-insoluble polymers by high-temperature heating. The objective of our study was to investigate whether or to what extent bark powder consolidated into pellets, using citric acid as cross linking agent and subjected to high-temperature heat treatment absorbs toxic heavy metals from water, under both static and dynamic flow conditions, without contributing to high chemical oxygen demand (COD) .

MATERIALS AND METHODS

Air-dried ponderosa pine (*Pinus ponderosa*) bark, obtained from a mill in St. Regis, Montana, U.S.A., was hammer milled into flour that passed through a 20-mesh screen. The flour was consolidated into pellets as described below.

Anhydrous citric acid was purchased from GFS Chemicals (Ohio, U.S.A.) and carboxymethylcellulose (CMC) was purchased from Hercules (Wisconsin, U.S.A.). Standard solutions of Cu (II), Ni (II), Zn (II), and Cd (II) were purchased from Fischer

Scientific (New Jersey, U.S.A.) and diluted with deionized water to the appropriate concentration, as needed. Metal concentration in solution was determined by inductively coupled plasma atomic emission spectroscopy (ICP-AES).

Preparation of Pelletized Bark

Bark flour was mixed with CMC, citric acid, and deionized (DI) water in the proportions shown in Table 1. The ingredients were mixed thoroughly to form a stiff paste. CMC was used as a rheology modifier for pellet extrusion (Kulicke, W-M., et al., 1996). Citric acid was used as crosslinking agent to enhance the wet strength or water-soak properties and dimensional stability of the pellets (Caulfield, 1994). The stiff paste was extruded into cylindrical pellets, which were conditioned for 1 h at 180°C in a forced-draft furnace. The pelletized bark is shown in Figure 1. Type I pellets were selected for further studies because these pellets showed optimal wet strength and hydraulic conductivity in preliminary column experiments, and could be regenerated several times without measurable loss of weight and sorption capacity.

Characteristics of Pelletized Bark

A random sample of 10 pellets was taken for measurement of pellet size and breaking weight. Pellet size was measured by means of an electronic digital caliper, and breaking weight was measured on an Instron testing machine. Breaking weight is defined as the maximum compression load on the pellet just prior to failure.

The liquid-accessible pore volume of the pellets was measured according to the method described by DesMarais et al., (1993). For that purpose, 1.0-g samples of the pellets, weighed accurately to four decimal places, were immersed in DI water at 26.5 ± 0.2°C for 8 h. At the end of this period, the pellets were removed from the water, dabbed lightly with a piece of absorbent tissue paper to remove excess water from the surface, and weighed. Liquid-accessible pore volume V_{acc} was calculated as

$$V_{acc} = (W_{wet} - W_{dry})d_{water} \quad (1)$$

where W_{wet} is weight (g) of the sample after saturation with DI water, W_{dry} is initial weight of the sample at 30% RH, 27 ± 1°C, and d_{water} is density (g/cm^3) of DI water at 26.5°C. Characteristics of the pelletized bark are summarized in Table 2.

Leaching characteristics of the pelletized bark were determined by comparing the chemical oxygen demand and UV–visible spectrum of 40 mL DI water before and after equilibration at room temperature (25±1°C) for 2 h with 1 g pelletized bark. COD of DI water before and after equilibration were 0.55 ± 0.47 and 6.2 ± 3.0 mg/L, respectively.

Table 1. Weight of pellet ingredients

Type of pellet	Weight of ingredient (g)			
	Bark	CMC	Citric acid	DI water
I	200	0.5	40	140
II	200	0.14	20	74
III	200	10	10	200

Fig. 1. Pelletized bark (Type I).

Because the DI water before and after equilibration with the bark pellets did not show the UV–visible absorbance band with λ_{max} = 280 nm, which is characteristic of tannins, it can be concluded that no tannin leached from the bark pellets. The slight increase in COD may have been from soluble carbohydrates leaching from the pellets.

Table 2. Characteristics of Pelletized Bark—Type I

Parameter	Value
Shape	Cylindrical
Length, mm	11.60 ± 2.11
Diameter, mm	3.28 ± 0.16
Breaking weight, kg/pellet	6.15 ± 2.0
Shipping weight, g/L	310
Liquid-accessible pore volume, cm^3/g	0.8–1.0

Equilibrium Adsorption Experiments

Equilibrium adsorption experiments were performed in triplicate by adding 0.5-g aliquots of pelletized bark to labeled 125-mL polyethylene bottles. 20-mL aliquots of Cu(II), Zn(II), Ni(II), or Cd(II) solutions of various initial concentrations (C_0 = 0.1, 0.5, 1.0, 2.0, 5.0, 10, 50, 100, 200, 500 mg/L), pH 5.1 ± 0.02, were equilibrated at 25 ± 1°C with the pelletized bark by shaking the capped bottles for 24 h on a horizontal shaker at 150 rpm. Preliminary experiments had indicated that equilibrium could be reached within 2 h. At the end of this period, equilibrium concentration C_e of the metal ion in the supernatant liquid was determined by ICP-AES (USEPA Method 6010B, 1996).

Adsorption Kinetics Experiments

Adsorption kinetics experiments were performed in 1-L solutions with 1.0 g samples of the pelletized bark. The initial metal ion concentration in solution was 10 mg/L, and initial pH was 2, 4, or 6. The initial pH of the solution was adjusted by adding 0.1 M HNO_3 or KOH as needed. The suspension was stirred using a magnetic bar, and 1-mL aliquots of the supernatant liquid were withdrawn for metal concentration determination by ICP-AES at various time intervals during the 2-h experiment.

Dynamic Adsorption Experiments

Dynamic adsorption experiments were conducted in a glass column, 25 mm in diameter and 400 mm in length. The column was packed with 40 g pelletized bark to a bed height of 300 mm. Five column volumes of DI water were pumped through the column before each metal ion solution of a given initial concentration was pumped through the column at a flow rate of 5 mL/min. The initial metal ion concentration of the solutions was C_{infl} = 1, 10, 25, 50, 70, 100, 250 mg/L. The column effluent was collected in test tubes by means of a fraction collector, and the effluent metal ion concentration C_{effl} was determined by ICP-AES.

RESULTS AND DISCUSSION

Adsorption Isotherms

The amount of metal ions adsorbed at equilibrium, q_e (mg/g), was calculated as

$$q_e = (C_0 - C_e)V/W \quad (2)$$

where C_0 and C_e are concentrations (mg/L) of metal ions in the initial and equilibrium solutions, respectively, V is volume (L) of the initial solution taken for equilibration, and W (g) is the weight of the pellets taken for equilibration.

Experimental results obtained for adsorption of metal ions at equilibrium were analyzed by both the Freundlich and Langmuir adsorption isotherms. The Freundlich isotherm is described by

$$q_e = K_F C_e^{1/n} \quad (3)$$

where K_F is a constant related to the adsorption capacity and n is an empirical parameter related to the intensity of adsorption, which varies with the heterogeneity of the adsorbent. Adsorption is favorable for values $0.1 < 1/n < 1$ (Namasivayam and Yamuna 1992; Raji and Anirudhan 1998). The Langmuir isotherm is described by

$$q_e = q_{max}\, bC_e/(1 + bC_e) \quad (4)$$

where q_{max} is the maximum amount of adsorbate per unit weight of adsorbent and b is a parameter related to the free energy of adsorption of a monolayer of the adsorbate. It

reflects the adsorption intensity and characterizes the affinity of the adsorbent for the adsorbate.

Fig. 2 shows Freundlich and Langmuir adsorption isotherms for Cu(II), Zn(II), Ni(II), and Cd(II) ions on pelletized bark. Isotherm parameters for adsorption of each of the metal ions on pelletized bark are summarized in Table 3. As shown by the values of the root mean squared errors of the nonlinear least squares fit (RMSE), the experimental data for Cd(II) and Zn(II) showed a better fit to the Langmuir than to the Freundlich isotherm. The Cu(II) data best fit the Freundlich isotherm, and the Ni(II) data fitted both Freundlich and Langmuir isotherms equally. According to the Freundlich constant K_F, adsorption capacity of pelletized bark for the metal ions in aqueous solution, pH 5.1 ± 0.2, followed the order Cd(II) > Cu(II) > Zn(II) >> Ni(II); according the Langmuir constant *b*, adsorption affinity followed the order Cd(II) >> Cu(II) ≈ Zn(II) >> Ni(II).

Table 3. Freundlich and Langmuir isotherm parameters for metal ion adsorption on pelletized bark, pH 5.1 ± 0.2

	Freundlich isotherm				Langmuir isotherm			
Ion	K_F	1/*n*	*R*	RMSE	q_{max} (mg/g)	*b*	*R*	RMSE
Cu(II)	84.6	0.79	0.9993	102	24.1	0.0016	0.9982	171
Zn(II)	73.7	0.80	0.9960	238	20.6	0.0018	0.9971	200
Ni(II)	19.8	0.88	0.9964	117	20.6	0.0006	0.9964	120
Cd(II)	203	0.54	0.9947	200	6.8	0.0069	0.9998	41

R is correlation coefficient.
RMSE is root mean squared error of nonlinear least squares fit.

Table 4. Pseudo-first- and second-order kinetic parameters for Cu(II) sorption

	Pseudo-first order				Pseudo-second order			
pH	q_e (mg/g)	k_1 (min^{-1})	*R*	RMSE	q_e (mg/g)	k_2 (g/mg/min)	*R*	RMSE
2	0.728 ± 0.021	0.0641 ± 0.000	0.9835	0.0496	0.786 ± 0.022	0.114 ± 0.003	0.9592	0.0788
4	0.669 ± 0.030	0.0882 ± 0.004	0.9955	0.0250	0.731 ± 0.027	0.170 ± 0.008	0.9770	0.0558
6	0.524 ± 0.004	0.0532 ± 0.006	0.9948	0.0200	0.567 ± 0.002	0.128 ± 0.017	0.9872	0.0313

Table 5. Pseudo-first- and second-order kinetic parameters for Zn(II) sorption

	Pseudo-first order				Pseudo-second order			
pH	q_e (mg/g)	k_1 (min^{-1})	*R*	RMSE	q_e (mg/g)	k_2 (g/mg/ min)	*R*	RMSE
2	0.646 ± 0.011	0.0348 ± 0.000	0.9910	0.0319	0.696 ± 0.013	0.0645 ± 0.000	0.9884	0.0366
4	0.406 ± 0.015	0.0514 ± 0.000	0.9676	0.0403	0.437 ± 0.016	0.158 ± 0.006	0.9316	0.0580
6	0.438 ± 0.030	0.0502 ± 0.001	0.9960	0.0150	0.473 ± 0.034	0.146 ± 0.019	0.9834	0.0296

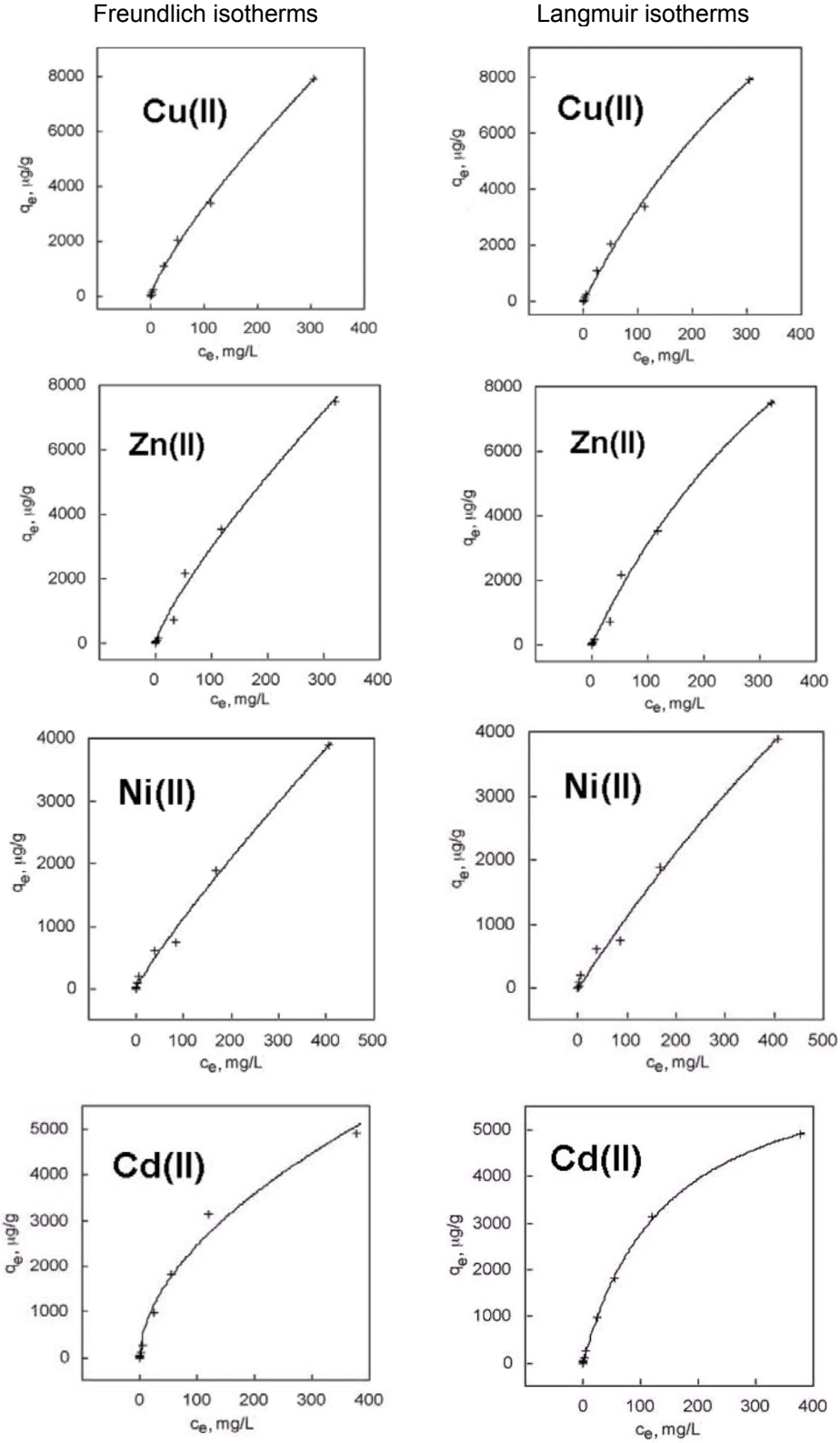

Fig. 2. Freundlich and Langmuir adsorption isotherms for Cu(II), Zn(II), Ni(II), and Cd(II) ions on pelletized bark. [Note: markers (+) represent experimental data points, and the lines (-----) represent the fitted isotherms]

Adsorption Kinetics

Experimental data were analyzed by both pseudo-first- and second-order kinetic models, as described in the following equations, respectively (Ho and McKay 1999):

$$q_t = q_e [1 - \exp(-k_1 t)] + \varepsilon \quad (5)$$

$$q_t = q_e - 1/[(1/q_e) + k_2 t] + \varepsilon \quad (6)$$

where k_1 is the rate constant of the pseudo-first-order model (1/min), k_2 is the rate constant of the pseudo-second-order model (g/mg/min), q_e is the amount of solute adsorbed at equilibrium (mg/g), q_t is the amount of solute adsorbed on the surface of the sorbent at any time t (mg/g), and ε denotes random error.

The kinetic parameters for metal ion sorption on pelletized bark determined by fitting the experimental data to both pseudo-first- and second-order kinetic models are summarized in Tables 4–7. As shown by the values of RMSE, sorption of metal ions on pelletized bark, except for Cd(II), best fit the pseudo-first-order kinetic model under all three pH conditions, 2, 4 and 6. Cd(II) deviated from this trend at pH 4, where it best fit the pseudo-second-order kinetic model.

Adsorption kinetics of a given metal ion on pelletized bark are determined by its characteristic solution chemistry and by the surface chemistry of the pelletized bark. Specifically, solution pH plays an important role in determining both the nature of metal ionic species available in aqueous solution and the nature and concentration of adsorption sites on the bark pellet. Bark pellets have a high content of polyhydroxyl polyphenolic groups that are capable of chelating heavy metal ions. In addition, bark pellets contain carboxylic groups that can bind metals by ion-exchange mechanisms (Vázquez et al., 2002; Martin-Dupont et al 2006). Availability of ion-exchange groups is strongly influenced by pH. Thus at low pH values, carboxylic groups should be predominantly non-ionized, and therefore unavailable for ion-exchange with a metal ion. However as pH increases, more and more carboxylic groups will be ionized and become available for ion-exchange with a metal ion. On the contrary, the distribution of hydrolysis species of metal ions as a function of pH is different for each metal ion. Thus, each metal ion will show its own characteristic adsorption kinetics depending on the distribution of its hydrolysis products at a given solution pH.

Cu(II) adsorption kinetics

The speciation diagram for Cu(II) indicates that in the pH range 2–4.9, Cu(II) ions in aqueous solution may exist in two forms: $Cu(aq)^{2+}$ and $Cu(NO_3)^{+}$. In the pH range 5.0–6.0 an additional two species may appear: $Cu(OH)^{+}$ and $Cu(OH)_{aq}$ (Vuceta and Morgan 1977). Thus, adsorption kinetics of Cu(II) ions will be limited by the rate of adsorption of the dominant species at a given solution pH. As shown in Table 4, q_e values for Cu(II) sorption predicted by both kinetic models decreased with increase in pH. However both pseudo-first-order (k_1) and pseudo-second-order (k_2) rate constants showed a maximum at pH 4. This suggests that the rate of Cu(II) sorption is determined by $Cu(aq)^{2+}$ ion concentration, and as this concentration decreases at pH greater than 4, the rate of Cu(II) sorption decreases accordingly because of formation of other Cu(II) species, such as

Table 6. Pseudo-first- and second-order kinetic parameters for Cd(II) sorption

	Pseudo-first order				Pseudo-second order			
pH	q_e (mg/g)	k_1 (min^{-1})	*R*	RMSE	q_e (mg/g)	k_2 (g/mg/min)	*R*	RMSE
2	0.463 ± 0.032	0.1158 ± 0.004	0.9926	0.0204	0.502 ± 0.036	0.356 ± 0.042	0.9740	0.0378
4	0.398 ± 0.029	0.0730 ± 0.030	0.9798	0.0333	0.458 ± 0.044	0.207 ± 0.117	0.9877	0.0240
6	0.414 ± 0.037	0.0816 ± 0.010	0.9928	0.0184	0.447 ± 0.040	0.272 ± 0.020	0.9798	0.0292

Table 7. Pseudo-first- and second-order kinetic parameters for Ni(II) sorption

	Pseudo-first order				Pseudo-second order			
pH	q_e (mg/g)	k_1 (min^{-1})	*R*	RMSE	q_e (mg/g)	k_2 (g/mg/min)	*R*	RMSE
2	0.434 ± 0.014	0.0765 ± 0.012	0.9938	0.0185	0.471 ± 0.016	0.235 ± 0.054	0.9786	0.0311
4	0.376 ± 0.004	0.0509 ± 0.003	0.9960	0.0127	0.408 ± 0.005	0.167 ± 0.008	0.9884	0.0206
6	0.257 ± 0.018	0.0791 ± 0.022	0.9813	0.0173	0.280 ± 0.018	0.408 ± 0.117	0.9708	0.0215

$Cu(OH)_{aq}$ in solution that are not adsorbed by ion-exchange reaction with H^+ ions on the bark pellets. Gaballah and Kilbertus, 1998 also reported a similar trend in pH dependence of Cu(II) adsorption on modified pine bark

Zn(II) adsorption kinetics

The speciation diagram for Zn(II) indicates that in the pH range 2–6.5, Zn(II) ions in aqueous solution exist only in one form, $Zn(aq)^{2+}$ (Zhang and Muhammed 2001). Thus, adsorption kinetics of Zn(II) ions should be independent of pH in the range 2–6. Indeed, as shown in Table 5, no relationship is apparent between solution pH values and q_e values or pseudo-first- and second-order rate constants (k_1 and k_2, respectively) for Zn(II) sorption on bark pellets. This suggests that interaction of Zn(II) in the pH range 2–4 is not by ion-exchange with H^+ ions on the bark pellets, but rather involves other mechanisms, such as surface complexation or hydrogen-bonding between the hydrated $Zn(aq)^{2+}$ ions and the bark polyhydroxyl-polyphenolic groups (Ravat et al., 2000; Reddy et al., 1997).

Cd(II) adsorption kinetics

Similar to Zn(II), at pH values below 7, Cd(II) exists in aqueous solution only as the $Cd(aq)^{2+}$ species (Leyva-Ramos et al. 1997). Accordingly, its adsorption kinetics on bark pellets should also be similar to that of Zn(II). As shown in Table 6 there was no correlation between solution pH and q_e values or the rate constants k_1 or k_2 for Cd(II) sorption on bark pellets. Thus, a reasonable conclusion is that in the pH range 2–6, adsorption mechanism of Cd(II) is by surface complexation with polyphenolic groups in the bark. This is consistent with observations made by Ravat et al., (2000) that sorption of

Cd(II), Zn(II) and Ni(II) on lignocellulosic substrates showed less dependence on pH than that of Cu(II).

Table 8. Some physical and chemical characteristics of metal ions[a]

Ion	Charge-size function, Z^2/r	Hydration enthalpy, ΔH_h (kJ/mol)	First hydrolysis constant, pK_{pq}
Cu^{2+}	5.48	–2,100	7.9
Zn^{2+}	5.33	–1,807	7.5
Ni^{2+}	5.71	–2,105	9.6
Cd^{2+}	4.21	–2,046	9.0

[a] Huheey 1972; Ahmed et al. 1998; Martin-Dupont et al. 2002.

Ni(II) adsorption kinetics

Although at pH values below 7 Ni(II) exists in aqueous solution only as the $Ni(aq)^{2+}$ species (Ji and Cooper 1996), its adsorption kinetics on bark appeared to be similar to Cu(II) adsorption kinetics because the q_e values showed a decrease with increase in pH from 2 to 6. However, unlike for Cu(II), rate constants k_1 and k_2 showed a minimum at pH 4 (Table 7), which is difficult to explain. However, above pH 4 the increase in the rate constant appears to be consistent with H^+ ion-exchange reaction mechanism.

Table 8 shows some physical and chemical characteristics of metal ions that may have a bearing on their respective rates of reaction with the ligands on the bark. As a first approximation, it can be argued that the ease with which each hydrated metal ion reacts with a ligand on the bark sorbent should be determined by how readily a molecule of water is displaced from its hydration shell. The hydration enthalpy ΔH_h corresponds to the energy required to displace H_2O molecules from cations, and therefore reflects how easily the cation reacts with a ligand located on the bark; the higher the hydration enthalpy, the more difficult for the cation to react with the ligand on the bark. For the cations under consideration in this study, hydration enthalpy follows the decreasing order: Ni(II) > Cu(II) > Cd(II) > Zn(II), which should translate to the following decreasing order of theoretical affinity of the cations for the bark ligand: Zn(II) > Cd(II) > Cu(II) > Ni(II). However this order of theoretical affinity is not in agreement with our experimental data. In the case of divalent cations, the first hydrolysis constant, pK_{pq} represents the extent to which the cation is converted to a monovalent species, $M(OH)^+$ by hydrolysis. For the cations under consideration in this study, the first hydrolysis constant follows the decreasing order: Zn(II) > Cu(II) > Cd(II) > Ni(II), which is in better agreement with our experimental data. This supports the hypothesis that in addition to the effect of pH on the speciation of each metal ion, pH effect on the degree of ionization of the carboxyl (R-COOH), hydroxyl (R-OH) and phenolic (φ-OH) ligands on the bark is equally important. Thus under a given set of solution conditions, such as pH and ionic strength, each metal ion species, depending on its respective physical and chemical

characteristics, will react more readily with those ligands that are available under the given pH conditions.

Dynamic Adsorption Experiments

Breakthrough curves for Cu(II), Zn(II), Ni(II), and Cd(II) are shown in Figure 3. The breakthrough volume, defined as the volume of column effluent where the ratio of the effluent-to-influent concentration of a metal ion is equal to 0.5, was estimated from a logarithmic curve fit of the experimental data. The regression equations and the value of breakthrough volumes, calculated from these equations for each of the ions, are summarized in Table 9. Breakthrough volumes decreased in the order Cu(II) > Zn(II) > Cd(II) > Ni(II) at influent pH 5.1 ± 0.2.

To determine the amount of metal ion adsorbed per unit weight of pellets under flow through column conditions, the breakthrough data were fitted to the linearized form of Thomas equation (Kapoor and Viraraghavan 1998):

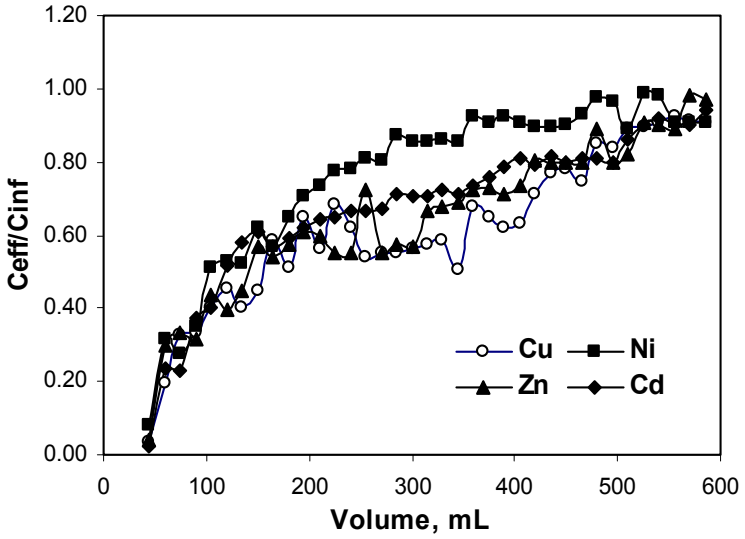

Fig. 3. Breakthrough curves for Cu(II), Zn(II), Ni(II), and Cd(II) at flow rate 5 mL/min, influent pH 5.1 ± 0.2, influent concentration ≈10.0 mg/L.

Table 9. Calculated breakthrough volumes of Cu(II), Zn(II), Ni(II), and Cd(II) on pelletized bark at flow rate 5 mL/min, influent pH 5.1 ± 0.2, and influent concentration ≈10.0 mg/L

Metal ion	Regression equation	R^2	Breakthrough volume, mL
Cu(II)	$y = 0.2857\text{Ln}(x) - 0.9758$	0.8628	175
Zn(II)	$y = 0.2948\text{Ln}(x) - 0.9949$	0.9198	159
Ni(II)	$y = 0.3208\text{Ln}(x) - 1.0263$	0.9542	116
Cd(II)	$y = 0.2952\text{Ln}(x) - 0.9702$	0.9419	146

$y = C_{effl}/C_{infl}$; x is volume of effluent (mL); R^2 is coefficient of determination.

$$\log(C_{inf}/C_{eff} - 1) = kq_0M/Q - kC_{inf}V/Q \quad (7)$$

where C_{inf} and C_{eff} are solute concentrations (mg/L) in the influent and effluent, respectively, k is the Thomas rate constant (ml/min mg), q_0 is the maximum solid-phase concentration of solute (mg/g), M is the mass of adsorbent (g), V is the throughput volume (mL), and Q is the volumetric flow rate (mL/min).

As shown in Table 10, the experimental data did not show a good fit to the Thomas model regression equation. Consequently, q_0 values calculated according to this model should be treated as approximations of the actual values. The amount of metal ion adsorbed per unit weight of pellets decreased in the order Cu(II) > Zn(II) > Cd(II) > Ni(II). This affinity sequence is almost consistent with that obtained from adsorption isotherm experiments described above, with Zn(II) and Cd(II) in reversed positions.

Table 10. Thomas adsorption model parameters for dynamic adsorption of Cu(II), Zn(II), Ni(II), and Cd(II) on pelletized bark at flow rate 5 mL/min, influent pH 5.1 ± 0.2, and influent concentration ≈10.0 mg/L

Metal ion	Regression equation	R^2	k, mL min-1 mg-1	q_0, mg g^{-1}
Cu(II)	$y = -0.0138x + 0.6258$	0.7948	1.383	57
Zn(II)	$y = -0.0153x + 0.6319$	0.8015	1.483	53
Ni(II)	$y = -0.0169x + 0.4040$	0.7965	1.856	27
Cd(II)	$y = -0.0138x + 0.5204$	0.7659	1.314	50

$y = \log (C_{inf}/C_{eff} - 1)$; $x = V/Q$

Pellet Regeneration and Metal Recovery

Pellets were regenerated by gentle stirring in 0.5 M HNO_3 for 12 h. Figure 4 shows breakthrough curves for six influent concentrations of copper (1, 25, 50, 70, 100, 250 mg/L) passed successively through the column packed with virgin or regenerated pellets. There was practically no difference between the performance of the virgin and regenerated pellets, except at the high influent concentration (250 mg/L).

It is also important to note that recovery of the metals in dilute nitric acid has the effect of concentrating the metals in solution from which they could be recovered by suitable precipitation or electrochemical methods. The regenerated bark pellets could then be safely used as hog fuel in cogeneration plants.

CONCLUSIONS

Bark flour from ponderosa pine was consolidated into pellets, using citric acid as cross-linking agent. The pellets were subjected to high-temperature heat treatment.

1. The pellets did not leach tannins when soaked in water. In the pH range 2–6, the pellets showed different capacities for removal of heavy metal ions from synthetic metal ion solutions.
2. The equilibrium amount q_e of Cu(II) adsorbed per gram of sorbent increased from approximately 0.5 mg at pH 6 to 0.7 mg at pH 2, and for Zn(II), from approximately 0.4 mg to 0.7 mg.
3. For Cd(II) and Ni(II), no pH effect was apparent on the amounts adsorbed per gram of sorbent, which ranged from approximately 0.4 to 0.5 mg and 0.3 to 0.4 mg, respectively.
4. This study demonstrated the potential for converting low-cost bark residues to value-added sorbents using starting materials and chemicals derived from renewable resources. These sorbents can be applied in the removal of low-concentration toxic heavy metals from waste streams.

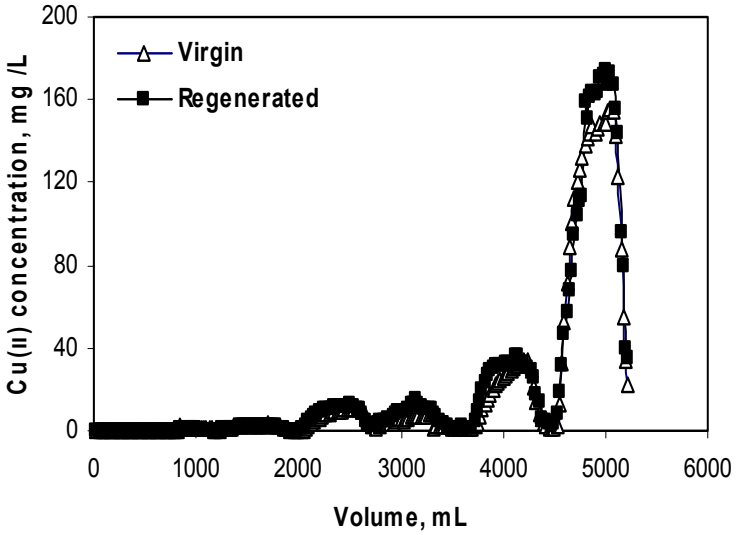

Fig. 4. Breakthrough curves for six influent concentrations (1, 25, 50, 70, 100, 250 mg/L) of Cu(II) passed successively through column packed with virgin and regenerated pellets.

ACKNOWLEDGMENTS

The authors are grateful to the USDA Forest Service, Forest Products Laboratory, for financial support and the opportunity to complete this project. We also thank Dan Foster and Jim Beecher for analytical support, Dan Caulfield for technical advice, Eric O'Neill for technical support, and Steve Verrill for statistical analysis.

REFERENCES CITED

Ahmed, S., Chughtai, S., and Keane, M. A. (1998). "The removal of cadmium and lead from aqueous solution by ion exchange with Na-Y zeolite," *Separation Purification Technol.* 13, 57-64.

Aoyama, M., and Tsuda, M. (2001). "Removal of Cr(VI) from aqueous solutions by bark," *Wood Sci. Technol.* 35, 425-434.

Bailey, S. E., Olin, T. J., Bricka, R. M., and Adrian, D. D. (1999). "A review of potentially low-cost sorbents for heavy metals," *Wat. Res*. 33(11), 2469-2479.

Brás, I. P., Santos, L., and Alves, A. (1999). "Organochlorine pesticides removal by *Pinus* bark sorption," *Environ. Sci. Technol.* 33(4), 631-634.

Brás, I., Lemos, L. T., Alves, A., Pereira, M., and Fernando, R. (2004). "Application of pine bark as a sorbent for organic pollutants in effluents," *Management of Environmental Quality: An International Journal* 15(5), 491-501.

Caulfield, D. F., (1994), "Ester crosslinking to improve wet performance of paper using multifunctional carboxylic acids, butanetetracarboxylic and citric acid," *Tappi Journal*, 77(3), 205-212.

Deshkar, A. M., Bokade, S. S., and Dara, S. S. (1990). "Modified Hardwickia binata bark for adsorption of mercury (II) from water," *Water Res.* 24(8), 1011-1016.

DesMarais, T. A., Stone, K. J., Thompson, H. A., Young, G. A., LaVon, G. D., and Dyer, J. C. (1993). "Absorbent foam materials for aqueous body fluids and absorbent articles containing such materials," *United States Patent* 5,268,224.

Fatoki, O. S., and Mathabatha, S., (2001), "Assessment of heavy metal pollution in the East London and Port Elizabeth harbours," *Water SA*, 27(2), 233-240.

Frigon, J. C., Cimpola, R., and Guiot, S. R. (2003). "Sequential anaerobic/aerobic biotreatment of bark leachate," *Water Sci. Technol.* 48(6), 203-209.

Gaballah, I., and Kilbertus, G. (1998). "Recovery of heavy metal ions through decontamination of synthetic solutions and industrial effluents using barks," *J. Geochemical Exploration* 62, 241-286.

Haussard, M., Gaballah, I., Kanari, N., De Donato, Ph., Barrès, O., and Villieras, F. (2003). "Separation of hydrocarbons and lipid from water using treated bark," *Water Res.* 37, 362-374.

Ho, Y. S., and McKay, G. (1999). "Pseudo-second order model for sorption processes," *Process Biochem.* 34, 451-465.

Huheey, J. E. (1972). *Inorganic Chemistry: Principles of Structure and Reactivity*, Harper & Row, New York.

Ji, J., and Cooper, W. C. (1996). "Nickel speciation in aqueous chloride solutions," *Electrochimica Acta* 41(9), 1549-1560.

Kapoor, A., and Viraraghavan, T. (1998). "Removal of heavy metals from aqueous solutions using immobilized fungal biomass in continuous mode," *Water Res.* 32(6), 1968-1977.

Kulicke, W-M., Kull, A. H., Kull, W., and Thielking, H., (1996)"Characterization of aqueous carboxymethylcellulose solutions in terms of their molecular structure and its influence on Rheological behaviour," *Polymer*, 37(13), 2723-2731.

Leyva-Ramos, R., Rangel-Mendez, J. R., Mendoza-Barron, J., Fuentoes-Rubio, L., and Guerrero-Coronado, R. M. (1997). "Adsorption of cadmium(II) from aqueous solution onto activated carbon," *Water Sci. Technol.* 35(7), 205-211.

Martin-Dupont, F., Gloaguen, V., Granet, R., Guilloton, M., Morvan, H., and Krausz, P. (2002). "Heavy metal adsorption by crude coniferous barks: a modeling study," *J. Environ. Sci. Health Part A* 37(6), 1063-1073.

Martin-Dupont, F., Gloaguen, V., Guilloton, M., Granet, R., and Krausz, P. (2004). "Chemical modifications of Douglas Fir bark, a lignocellulosic by-product—enhancement of their lead(II) binding capacities," *Separation Sci. Technol.* 39(7), 1595-1610.

Martin-Dupont, F., Gloaguen, V., Guilloton, M., Granet, R., and Krausz, P. (2006). "Study of the chemical interaction between barks and heavy metal cations in the sorption process," *J. Environ. Sci. Health Part A* 41, 149-160.

McKeever, D. B., and Falk, R. H. (2004). "Woody residues and solid waste wood available for recovery in the United States, 2002," *Management of Recovered Wood Recycling, Bioenergy and Other Options,* European COST E31 Conference Proceedings, C. Gallis, (ed.).

Morais, L. C., Freitas, O. M., Gonçalves, E. P., Vasconcelos, L. T., and González, B. C. G. (1999). "Reactive dyes removal from wastewaters by adsorption on Eucalyptus bark: variables that define the process," *Water Res.* 33(4), 979-988.

Namasivayam, C., and Yamuna, R. T. (1992). "Removal of Congo red from aqueous solutions biogas waste slurry," *J. Chem. Technol. Biotechn.* 53, 153-157.

Raji, C., and Anirudhan, S. (1998). "Batch Cr(VI) removal by polyacrylamide-grafted sawdust: kinetics and thermodynamics," *Water Res.* 32(12), 3772-3780.

Randall, J.M. (1977). "Variation in effectiveness of barks as scavengers for heavy metal ions," *Forest Products J.* 27(11), 51-56.

Ratola, N., Botelho, C., and Alves, A. (2003). "The use of pine bark as a natural adsorbent for persistent organic pollutants—study of lindane and heptachlor adsorption," *J. Chem. Technol. Biotechn.* 78, 347-351.

Reddy, B. R., Mirghaffari, N., and Gaballah I. (1997). "Removal and recycling of copper from aqueous solutions using treated Indian barks," *Resources Conservation Recycling* 21, 227-245.

Sakai, K., (2001) "Chemistry of Bark" in *Wood and Cellulosic Chemistry*, Edited by David N.-S. Hon, Nobuo Shirashi, Marcel Dekker, Inc., New York, Chapter 7, 243-273.

Sekar, K. C., Kamala, C. T., Chary, N. S., Sastry, A. R. K., Rao, T. N., and Vairamani, M. (2004). "Removal of lead from aqueous solutions using immobilized biomaterial derived from a plant biomass," *J. Hazardous Materials* B108, 111-117.

Seki, K., Saito, N., and Aoyama, M. (1997). "Removal of heavy metal ions from solutions by coniferous barks," *Wood Sci. Technol.* 31, 441-447.

USEPA Method 6010B (1996). "Inductively coupled plasma-atomic emission spectrometry," CD-ROM, Revision 2, 1-25

Van Hassel, J. H., Ney, J. J., and Garling, Jr., D. L., (1980) "Heavy metals in a stream ecosystem at sites near highways," *Transactions of the American Fisheries Society*, 109, 636-643.

Vázquez, G., González-Álvarez, J., Freire, S., López-Lorenzo, M., and Antorrena, G. (2002). "Removal of cadmium and mercury ions from aqueous solution by sorption on treated *Pinus pinaster* bark: kinetics and isotherms," *Bioresource Technol.* 82, 247-251.

Villaescusa, I., Martinez, M., and Miralles, N. (2000). "Heavy metal uptake from aqueous solution by cork and yohimbe bark wastes," *J. Chem. Technol. Biotechn.* 57, 812-816.

Vuceta, J., and Morgan, J. J. (1977). "Hydrolysis of Cu(II)," *Limnol. Oceanog.* 22(4), 742-746.

Zhang, Y., and Muhammed, M. (2001). "Critical evaluation of thermodynamics of complex formation of metal ions in aqueous solutions—VI. Hydrolysis and hydroxo-complexes of Zn^{2+} at 298.15 K," *Hydrometallurgy* 60, 215-236.

Article submitted: Dec. 21, 2006; First round reviewing completed: Feb. 5, 2007; Revised version accepted: Feb. 15, 2007; Published Feb. 17, 2007

FLAX SHIVE AS A SOURCE OF ACTIVATED CARBON FOR METALS REMEDIATION

Wayne E. Marshall[a], Lynda H. Wartelle[a], and Danny E. Akin[b*]

Flax shive constitutes about 70% of the flax stem and has limited use. Because shive is a lignocellulosic by-product, it can potentially be pyrolyzed and activated to produce an activated carbon. The objective of this study was to create an activated carbon from flax shive by chemical activation in order to achieve significant binding of selected divalent cations (cadmium, calcium, copper, magnesium, nickel, zinc). Shive carbons activated by exposure to phosphoric acid and compressed air showed greater binding of cadmium, copper, nickel or zinc than a sulfuric acid-activated flax shive carbon reported in the literature and a commercial, wood-based carbon. Uptake of calcium from a drinking water sample by the shive carbon was similar to commercial drinking water filters that contained cation exchange resins. Magnesium removal by the shive carbon was greater than a commercial drinking water filtration carbon but less than for filters containing cation exchange resins. The results indicate that chemically activated flax shive carbon shows considerable promise as a component in industrial and residential water filtration systems for removal of divalent cations.

Keywords: Flax shive, Activated carbon, Metal ion, Phosphoric acid activation

Contact information: a: USDA-ARS, Southern Regional Research Center, 1100 Robert E. Lee Blvd., New Orleans, LA 70124 USA; b: USDA-ARS, R. B. Russell Research Center, 950 College Station Road, Athens, GA 30605 USA
**Corresponding author:danny.akin@ars.usda.gov*

INTRODUCTION

Flax (*Linum usitatissimum* L.) is a versatile crop that supplies both fiber and seed (i.e., linseed) for important industrial applications (Domier 1997). The desire for natural fibers to replace glass fiber and the promotion of linseed and linseed oil for nutraceutical uses bodes well for increased flax production. Bast fiber and linseed already have value-added markets (Sharma 1992), and interest is increasing for finding value-added uses of the by-products, such as the non-fiber part of the stem, to improve the economics (Domier 1997).

Flax stems constitute the source of bast fibers, which are used in a variety of applications (textiles, composites, specialty paper). To obtain these bast fibers, flax straw is first retted, in which fiber is separated from non-fiber components such as shive. Shive is the woody, lignified inner tissues of the stem and is a by-product of fiber production. Flax fiber constitutes about 25-30% of the stem (Stephens 1997). Therefore, a large amount of shive is available after fiber processing. With estimates of 1 million tons of flax straw available annually from linseed production (Dormier 1997), about 700,000 tons of shive could be available for a variety of uses.

Traditionally, shive is considered a waste product and as such has limited value or is used in low-value applications such as chip board, animal bedding, and burning for thermal energy (Sankari 2000; Sharma 1992). Sharma (1992, 2004) reported that upgrading shive using lignin-degrading, white rot fungi, which include edible mushrooms, was a promising use. The large amount of shive available, the collection and concentration at fiber processing plants, and the requirement to transport waste shive away all call for research into value-added uses. Certainly, the need to make use of this potential resource is recognized (Domier 1997), and internet searches list horse bedding (www.ecolit.com) and reinforced thermosetting (www.freepatentonline.com) as diverse potential uses. Higher value uses may be possible with technology, such as extraction of aromatics (Kim and Mazza 2006) for a variety of uses such as antioxidants and antimicrobial compounds.

Studies by Cox et al. (1999, 2000) and by El-Shafey et al. (2002) demonstrated that flax shive could be converted to carbonaceous material by contact with sulfuric acid. This material used to sorb a variety of divalent cations. A more recent investigation by Cox et al. (2005) showed that a carbon sorbent prepared from flax shive could adsorb precious metals, such as silver. Two papers by Williams et al. (1997, 1998) used waste linseed straw to adsorb copper, nickel and cadmium in a semi-continuous batch adsorption system. Adsorption of the three metals by linseed fiber was not as effective as using a seaweed waste product under similar experimental conditions.

In addition to carbonized flax shive, several other woody plant straw sources have been successfully converted to activated carbon for the removal of metal ions. Johns et al. (1998) used rice straw and sugarcane bagasse and activated this material for carbon production by steam, carbon dioxide, or carbon dioxide plus 38% oxygen. Carbon with the greatest adsorption towards copper ion was produced by activation with carbon dioxide followed by oxidation with 38% oxygen.

Metal ion adsorption of activated carbon from agricultural waste sources can also be enhanced by pyrolysis/activation with phosphoric acid and breathing air (Toles et al. 1998). The activated carbons thus produced can be used to remove high levels of metal ions from aqueous solution.

The objectives of this study were to investigate flax shive prepared by two different retting treatments as a source of activated carbon for metal ion adsorption and to compare our results with the results of Cox and co-workers who used a different carbon activation process. Flax shive carbons were prepared in our laboratory by chemical activation with phosphoric acid and compressed air and their metal ion adsorption properties evaluated.

EXPERIMENTAL

Materials

Flax shive was collected after processing retted flax stems from the USDA Flax Fiber pilot plant, Clemson, SC. Sources of shives included: 1) dew-retted flax, and 2) experimental enzyme-retting using a commercial pectate lyase and chelator (Akin et al., in press). Dew-retting, which depends upon naturally occurring fungi to colonize and partially degrade flax stems, is the primary commercial method used to separate fiber

from shive. Enzyme-retting is an experimental process to provide a more consistent fiber. Waste shive derived from both retting processes was sifted through a sieve with 20 mm x 4 mm openings and then through a sieve with 5 mm diameter openings to remove fiber. Cleaned shive passing through the sieves was milled through a Wiley mill with a 2 mm mesh screen and constituted the material for activated carbon.

Norit C was purchased from Norit Americas Inc. (Marshall, TX). It is a wood-based carbon manufactured by a phosphoric acid activation process. The sample as received contained residual phosphoric acid. Thus, the carbon was treated with several washings of hot water to remove the residual acid before use in this study.

Three commercial drinking water filtration cartridges were used and were purchased at local retail outlets. PŪR RF (Replacement Filter) cartridges are comprised of a coal-based carbon and are used in point-of-use applications to purify residential tap water. PŪR PF (Pitcher Filter) cartridges contain mostly cation exchange resin with some carbon included. They are particularly effective at removing lead from drinking water in a pitcher filter configuration. Both products are made by PŪR, Minneapolis, MN. Brita PF is a water filtration product similar to PŪR PF in composition and use. It is made by Brita Products Company, Oakland, CA. The synthetic cation exchange resin IRC86 was purchased from Supelco, Inc., Bellefonte, PA. According to the manufacturer, IRC86 is used to remove hard water cations to soften water for various industrial processes. All commercial adsorbents were dried in a forced air oven at 60^{o}C for 12 hours before adsorption studies were conducted.

Methods

Particles of non-carbonized shive and phosphoric acid-activated shive carbon were mounted on carbon tabs on SEM stubs, coated in a sputter coater with gold, and viewed in a JEOL JSM 5800 scanning electron microscope at 15 kV.

Proximate analyses of dew-retted and enzyme-retted flax shives were carried out by Eurofins Scientific, Inc. (Des Moines, IA) using standard AOAC methods.

Flax shive activated carbon was made by placing 100 g of 0.85 to 2.00 mm shive particles into a large porcelain evaporating dish. For phosphoric acid activation, 100 g of 30% (w/w) phosphoric acid was added to the 100 g of shive, mixed, and the mixture allowed to stand overnight at room temperature in order to imbibe the phosphoric acid . The evaporating dish was placed in a retort contained within an industrial box furnace (Lindberg/Blue M, Watertown, WI) and heated to 450°C for 4 hr under a flow of compressed air. Compressed air was introduced into the retort at a rate of 40 mL/min.

Activated carbons were allowed to cool overnight in the furnace. The carbons were weighed to calculate an activation yield:

$$\% \text{ activation yield} = (\text{wgt. of carbon from furnace} / \text{wgt. of shive}) \times 100. \quad (1)$$

Phosphoric acid-activated carbons were washed several times with water at 80-90°C to remove excess acid. The carbons were washed until no lead phosphate precipitate was observed when a 0.08 M solution of lead nitrate was added to the wash solution. Washed samples were collected on a 0.18 mm US standard sieve. Carbons were dried at 110°C for 2 hr. The carbons were weighed to determine final yield:

% final product yield = (wgt. of washed carbon / wgt. of shive) x 100 (2)

BET (Brunauer-Emmett-Teller) surface area was determined from nitrogen adsorption isotherms obtained at -196°C using a Micromeritics Gemini surface area analyzer (Norcross, GA). Surface areas were calculated using the BET equation supplied in the Micromeritics software.

Twenty-five mL of 20 mM solutions of the metal ions cadmium, copper, nickel and zinc were prepared in individual beakers and mixed with 0.25 g of activated carbon. The solutions were prepared by dissolving the metal salts in 0.07 M sodium acetate-0.03 M acetic acid buffer at pH 4.8. The slurry was stirred for 24 hr at 300 rpm and 25°C using Teflon stir bars in order to achieve equilibrium between adsorbed metal ion and metal ion free in solution. The pH at the beginning and end of the experiments was recorded and normally differed by about ± 0.2 pH units.

At the conclusion of the adsorption experiments, an aliquot of control solution with no carbon or experimental carbon sample was drawn into a disposable syringe and filtered through a 0.22 μm Millipore filter (Millipore Corp., Bedford, MA). The filtered sample was diluted 1:100 (v/v) with 4 vol% nitric acid (Ultrapure, ICP grade) and analyzed using a Leeman Labs Profile ICP-AES (Teledyne/Leeman Labs, Hudson, NH).

To determine the adsorption of calcium and magnesium ions, a sample of drinking water was obtained from a municipality in Texas. The pH of the water before analysis was 8.4, indicating a high concentration of hard water cations. Two separate analyses of calcium and magnesium were determined on the water and the average values were 2.57 mmol/L (103 ppm) and 4.44 mmol/L (108 ppm) for calcium and magnesium, respectively. The municipal drinking water was not buffered and the pH varied in the range 6.5 to 7.5 during the adsorption studies for all sample examined. All water samples were stirred for 24 hr and determinations made on the calcium and magnesium concentrations after adsorption as described in the previous two paragraphs.

RESULTS AND DISCUSSION

Structure of Flax Shive and Flax Shive carbon

Scanning electron micrographs of flax shive and flax shive phosphoric acid-activated carbon are shown in Fig. 1. The non-carbonized shive is characterized by ordered rows of tubular structures involved in water and nutrient transport up the stem of the flax plant. Carbonization of the shive retains much of the tubular structure but the walls of the tubes are now punctuated by numerous oval-shaped pores. These are the macropores of the activated carbon. In many cases the macropores lead to a complex internal pore structure below the carbon surface that involve channels leading to both meso- and macropores where most of the adsorption takes place.

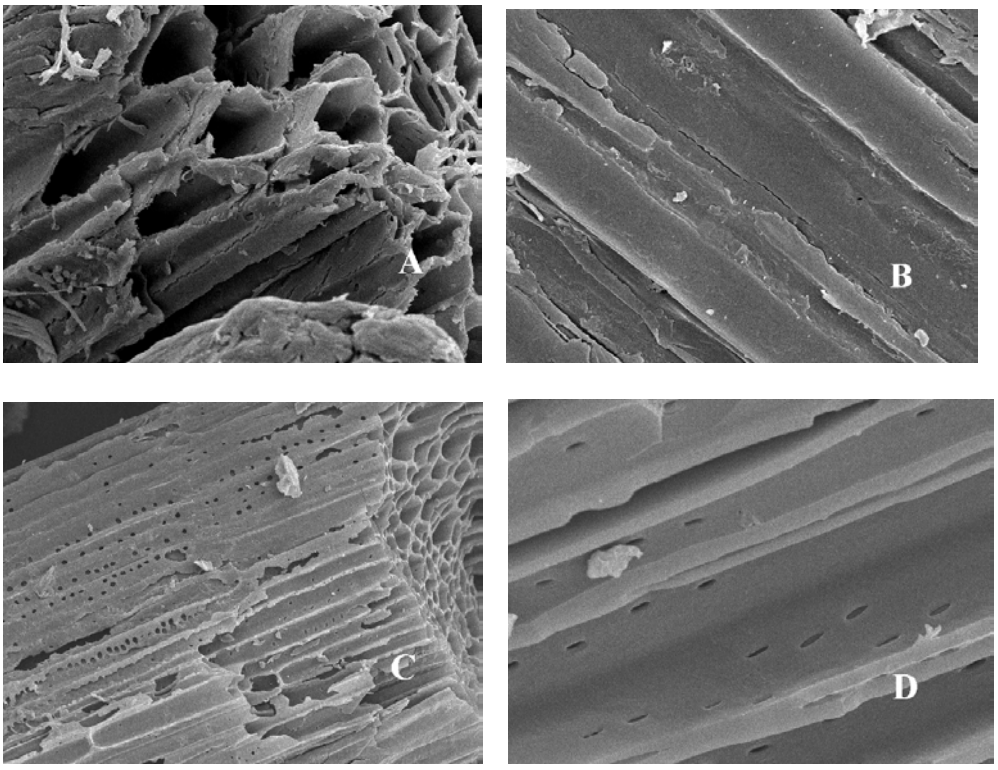

Fig 1. Scanning electron micrographs of untreated shive and phosphoric acid-activated, dew-retted shive carbon. A. Untreated fragment of shive. X 1,200. B. Enlarged area of untreated lignified cell wall showing relatively smooth surface. X 2,700. C. Fragment of shive constituting a particle of phosphoric acid-activated carbon showing numerous pits in the cell walls. X 500. D. Enlarged area of cell wall from phosphoric acid-activated shive carbon showing pitted surface. X 2,700.

Proximate Analysis of Retted Shive

Table 1 shows the proximate analysis for samples of dew-retted and enzyme-retted flax shive. The type of retting appears to have essentially no effect on the cellulose, hemicellulose, lignin, protein and ash composition of the shive. Shive is between 70-75% lignocellulose with about 17% hemicellulose and minor amounts of protein and ash. A high lignocellulosic content coupled with low ash content makes shive a good candidate for carbonization and subsequent conversion to an activated carbon (Marshall, unpublished observations).

Table 1. Proximate Analysis of Dew-Retted and Enzyme-Retted Flax Shive.

	Percent component (dry wgt. basis)				
Sample ID	Cellulose	Hemicellulose	Lignin	Protein	Ash
Dew-retted	47.7	17.0	26.6	3.5	1.0
Enzyme-retted	46.8	16.7	24.1	3.7	2.1

Properties of Activated Carbons from Retted Shive

Dew-retted and enzyme-retted shive were treated with phosphoric acid and activated. Activation yield, final product yield and BET surface area values are given in Table 2. There was little difference in activation yield between the two retting treatments. The activation yield for the phosphoric acid-activated carbon was about three times the final product yield. The additional weight is due to the presence of residual phosphoric acid in the sample. Upon removal of acid with repeated water washes, the final product yield was greatly reduced. Additionally, some carbon particles could be lost through the 0.18 mm mesh sieve and would add to the difference between activation and final product yields. BET surface area was higher in the carbon from dew-retted shive than enzyme-retted shive. Surface area differences were also reflected in a larger pore volume for the dew-retted carbon (data not shown). Although proximate analyses of the carbon precursors were similar (Table 1), differences in precursor structure due to the retting method employed could result in differences in pore structure formation. Since BET surface area is largely dependent on the presence of micropores, structural differences that encourage micropore formation would yield a higher surface area.

Table 2. Activation Yield, Final Product Yield and BET Surface Area of Dew-Retted and Enzyme-Retted Flax Shive Activated Carbons.

Sample ID	Activation yield (%)	Final product yield (%)	BET surface area (m^2/g)
Dew-retted	31.6	12.1	539
Enzyme-retted	33.3	12.1	305

Metal Ion Uptake by Carbons from Retted Shive

Table 3 details the metal ion adsorption of four metal ions implicated in toxic contamination of water and wastewater (cadmium, copper, nickel, zinc). Flax shive carbons (dew- and Bioprep-retted) were compared to two other sets of carbons. One, flax shive carbons prepared by heating with sulfuric acid that was described by El-Shafey et al. (2002) and the other a lignocellulosic-based (wood) carbon (Norit C) that is commercially available. Metal ion adsorption values from the El-Shafey et al. (2002) study were selected by us to represent the highest monolayer adsorption capacities recorded in their paper consistent with a temperature of 25°C, the same temperature used in our experiments. El-Shafey et al. (2002) used solution pH values of 4-5 and solution temperatures of 25-45°C. Metal ion uptake values for all ions were greater in the phosphoric acid-activated shive carbons than for either literature values from El-Shafey et al. (2002) or from Norit C.

Only single values for metal ion adsorption were reported by El-Shafey et al. (2002) as given in Table 3. Thus, no statistical analysis could be made among all three data sets. Statistical comparisons were generated among data obtained in our laboratory only. However, in all cases, our range of adsorption values (Table 3) was still greater than those obtained by El-Shafey et al. (2002).

Table 3. Metal Ion Adsorption by Flax Shive Activated Carbons and a Commercial Carbon.

Sample ID	Metal ion adsorption (mmol/g carbon, dry wgt. basis)			
	Cadmium	Copper	Nickel	Zinc
Flax shive, PA activated				
Dew-retted	0.57±0.03a	1.53±0 a	0.82±0.03a	0.81±0.06a
Bioprep-retted	0.53±0.03a	1.41±0.05b	0.69±0.01b	0.84±0.02a
Flax shive, SA activated	0.40[1]	0.82	0.57	0.50
Commercial				
Norit C	0.14±0.04b	0.27±0.03c	0.33±0.03c	0.20±0.02b

[1] Values from El-Shafey et al. (2002).
PA = phosphoric acid; SA = sulfuric acid
a,b,c = Values within columns with different letters differ at $P \leq 0.05$. Values are from duplicate tests and were analyzed by one-way analysis of variance.

In another experiment, both experimental and commercial carbons were examined for their ability to remove calcium and magnesium ions that are responsible for hard water in both industrial and residential water supplies. In the example given (Table 4), a sample of drinking water from a Texas municipality was used that contained high levels of both calcium and magnesium ions. Based on the results from Table 3, the carbon from dew-retted shive was used, since this carbon performed better than the enzyme-retted counterpart in metal ion adsorption.

Table 4. Calcium and Magnesium Ion[1] Adsorption by a Dew-Retted Flax Shive Carbon and Commercial Carbons and/or Cation Exchange Resins.

Sample ID	Metal ion adsorption (mmol/g carbon, dry wgt. basis)	
	Calcium	Magnesium
Dew-retted flax shive		
PA activated	0.19±0 a (71.5)[2]	0.19±0.01a (41.7)
Commercial		
PŪR RF	0.00±0b (0.0)	0.04±0.03b (9.0)
PŪR PF	0.18±0.01a (71.7)	0.23±0.02c (52.6)
Brita PF	0.20 ±0 .02a (78.1)	0.27±0.01c (61.2)
IRC86	0.18 ±0.05a (71.2)	0.23±0c (52.3)

[1]The calcium and magnesium ion concentrations in the city drinking water supply were 2.57 mmol/L and 4.44 mmol/L, respectively. However, the amounts of calcium and magnesium ions in the assay solution were 0.26 mmol and 0.44 mmol, respectively.
[2]Values in parentheses are the percentages of calcium and magnesium ions removed from the drinking water.
a,b,c = Values within columns with different letters differ at $P \leq 0.05$. Values are from duplicate tests and were analyzed by one-way analysis of variance.

The experimental carbon was compared to adsorbents used in several commercial, potable water filtration systems and also to a commercial cation exchange resin used to remove hard water cations from industrial water supplies (IRC86). The shive-based carbon removed significantly more calcium and magnesium ions than the commercial potable water filtration carbon found in a PŪR RF water filtration cartridge. The experi-

mental carbon performed as well as the other three commercial adsorbents for the removal of calcium ion, but magnesium ion was removed at lower levels ($P \leq 0.05$) compared to the other three commercial products. The most likely reason for the good performance of PŪR PF and Brita PF is that both products are predominantly composed of cation exchange resin with added carbon. Details of the resins used in these products are not known. The industrial resin IRC86 from Rohm and Haas, is a weak cation exchange resin with carboxylic acid functional groups, which removes alkali earth cations, such as calcium and magnesium, that cause hardness in industrial water.

The use of phosphoric acid-activated carbon for drinking water purification would depend on the residual phosphorus content of the carbon. Several commercial phosphoric acid-activated carbons evaluated in our laboratory have been found to contain phosphorus as evidenced by a lead phosphate precipitate formed in the wash water with the addition of lead nitrate. The final wash water of our carbons does not yield a precipitate and thus may be safe for use in potable water filtration. Only actual use of our phosphoric acid-activated carbon as a filtration medium in a continuous drinking water filtration system and monitoring the effluent for residual phosphorus will determine its suitability for a particular filtration system.

CONCLUSIONS

1. Flax shive, the woody, interior portion of the flax plant can be converted to activated carbon by carbonization and activation with phosphoric acid and compressed air.

2. The phosphoric acid-activated carbon proved adept at adsorption of several different metal ions.

3. This carbon outperformed a sulfuric acid-activated flax shive carbon described in the literature and two commercial carbons in metal ion adsorption and was comparable to commercial carbon/cation exchange resin mixtures for the uptake of calcium ion.

4. Shive, which is a low-value lignocellulosic by- product of the flax fiber industry, can be made into activated carbon and used in applications requiring removal of various metal ions from solution, potentially adding profit to an industry that derives little if any profit from the shive.

DISCLAIMER

Mention of names of companies or commercial products is solely for the purpose of providing specific information and does not imply recommendation of endorsement by the U.S. Department of Agriculture over others not mentioned.

REFERENCES CITED

Akin, D. E., Condon, B., Sohn, M., Foulk, J. A., Dodd, R. B., and Rigsby, L. L. "Optimization for enzyme-retting of flax with pectate lyase," *Ind. Crops Prod*. (in press).

Cox, M., El-Shafey, E., Pichugin, A. A. and Appleton, Q. (1999). "Preparation and characterization of a carbon adsorbent from flax shive by dehydration with sulfuric acid," *J. Chem. Technol. Biotechnol*. 74, 1019-1029.

Cox, M., El-Shafey, E., Pichugin, A. A. and Appleton, Q. (2000). "Removal of mercury (II) from aqueous solution on a carbonaceous sorbent prepared from flax shive," *J. Chem. Technol. Biotechnol*. 75, 427-435.

Cox, M., Pichugin, A. A., El-Shafey, E. I. and Appleton, Q. (2005). "Sorption of precious metals onto chemically prepared carbon from flax shive," *Hydrometallurgy* 78(1-2), 137-144.

Domier, K. W. (1997). "The current status of the field crop: Fibre industry in Canada," *Euroflax Newsletter* 8, 8-10.

El-Shafey, E., Cox, M., Pichugin, A. A. and Appleton, Q. (2002). "Application of a carbon sorbent for the removal of cadmium and other heavy metal ions from aqueous solution," *J. Chem. Technol. Biotechnol*. 77, 429-436.

Johns, M. M., Marshall, W. E. and Toles, C. A. (1998). "Agricutural by-products as granular activated carbons for adsorbing dissolved metals and organics," *J. Chem. Technol. Biotechnol*. 71, 131-140.

Sankari, H. S. .(2000). "Linseed (*Linum usitatissimum* L.) cultivars and breeding lines as stem biomass producers". *J. Agron. Crop Sci*. 184, 235-231.

Sharma, H. S. S. (1992). "Utilization of flax shive. In: Sharma, H. S. S., Van Sumere, C. F. (eds.), *The Biology and Processing of Flax*, M Publications, Belfast, Northern Ireland, pp. 537-543.

Stephens, G. R. (1997). "Connecticut fiber flax trials 1994-1995." *The Connecticut Agricultural Experiment Station, Bull.* 946, New Haven, CT.

Toles, C. A., Marshall, W. E., and Johns, M. M. (1998). "Phosphoric acid activation of nutshells for metals and organic remediation: process optimization," *J. Chem. Technol. Biotechnol.* 72, 255-263.

Williams, C. J., Aderhold, D., Edyvean, R. G. H. (1997). "Preliminary study on the removal of copper, nickel and cadmium by waste linseed straw and/or dealginate," *Resour. Environ. Biotechnol*. 1(3), 227-241.

Williams, C. J., Aderhold, D., Edyvean, R. G. H. (1998). "Comparison between biosorbents for the removal of metal ions from aqueous solutions," *Water Res*. 32(1), 216-224.

Article submitted: Dec. 15, 2006; First round of reviewing completed: Feb. 2, 2007; Revised version accepted: Feb. 21, 2007; Published: Feb. 23, 2007.

PRECIPITATED CALCIUM CARBONATE (PCC) – CELLULOSE COMPOSITE FILLERS; EFFECT OF PCC PARTICLE STRUCTURE ON THE PRODUCTION AND PROPERTIES OF UNCOATED FINE PAPER

Ramjee Subramanian[a*], Henrik Fordsmand[b], and Hannu Paulapuro[a]

This work examines the precipitation of PCC – pulp composite fillers with varying crystal habits and their effects on the papermaking properties of printing and writing paper. Colloidal (c-PCC), rhombohedral (r-PCC), and scalenohedral types (s-PCC) of composite PCCs were produced and compared with commercial reference PCCs. Scanning electron microscopy showed the c-PCC to be a high-surface-area nano-structured PCC. The rhombohedral composite was formed in clusters like a spider-web structure. Under similar experimental conditions, composite PCC was formed as individual ellipsoidal crystals and some of the particles had malformed structure, in contrast to the structured reference s-PCC. The co-precipitation and the structure of PCC significantly influence the forming, consolidation, and properties of paper, as well as its performance in printing.

Composite c-PCC showed the highest retention during forming. At higher filler contents, dewatering was reduced significantly with handsheets containing s- and r-PCC composite fillers. Colloidal composite handsheets showed the lowest tensile index and internal bond strength, while the rhombohedral composite gave the highest z-directional bond strength. Compared with the traditional reference samples containing commercial PCCs, paper with s- and r-composites had significantly higher density but similar light scattering ability. Addition of fibrillar fines to fine paper increased print rub fastness significantly in both laser and inkjet printed samples.

Keywords: Composite filler, Calcium carbonate filler, PCC morphology, Fine paper, Uncoated wood free paper, Scanning electron microscopy (SEM), Retention, Dewatering, Fine paper properties, Rubfastness

*Contact Information: a: Laboratory of Paper and printing technology, Helsinki University of Technology, P.O.Box: 6300, 02015 HUT, Finland; [b]J:M.Huber Oy, Denmark; *Corresponding author: rsubrama@cc.hut.fi*

INTRODUCTION

Comparing the market prices of filler and pulp fibers, the advantage of replacing fibers with pigment is evident, and hence, fillers are an important component in practically all printing and writing papers. Pigment properties are important in determining the effects of filler on the properties of paper and paperboard (Bown 1997; Fairchild 1992). In printing and writing papers, precipitated calcium carbonate (PCC) is being increasingly used to reduce raw material costs and basis weight of paper while maintaining thickness, or to customize the products by improving some critical paper

properties. On the other hand, the progressive addition of PCC in paper is limited by its negative effects on the bond strength and bending stiffness of paper (Holik 2006). Several methods have been proposed to increase the filler content in paper (Middleton et al.1985; Allan et al. 1998; Klungness et al. 1993). Composite fillers, formed by the in-situ precipitation of PCC in a suspension of cellulosic fibrils, have been shown to improve the performance of PCC and to allow increased amounts of filler in paper (Silenius 2002; Subramanian et al. 2005). However, the effects of the crystal habit of composite PCC on the properties of printing and writing paper have not been examined in detail in these studies.

In the present work, cellulosic fines were produced with a Masuko refiner (Kang et al. 2004). Three different composite PCCs — colloidal, rhombohedral and scalenohedral — were precipitated in-situ with pulp fines. Similar experimental conditions were employed for the production of composite and reference PCC fillers. The effects of adding composite PCCs on the properties and quality of fine paper were compared with the effects of reference PCCs. Handsheets were printed using HP LaserJet ("LaserJet" is a trademark of HP) and Epson ink-jet printers to compare the effects on toner adhesion and absorption, using reference and composite fillers, the inks being used as a probe material rather than defining printability in this case.

EXPERIMENTAL

Preparation of Composite Fillers

ECF bleached unrefined never dried pine pulp obtained from a mill, in Finland, was ground in a Masuko refiner to produce fines. Bauer-McNett analysis of the fines showed that 92% of the fines passed through a 200-mesh screen. The consistency of the fines-PCC composite was in the range of 0.085% to 0.1%. Equivalent amounts of calcium hydroxide suspension was added to the fines suspension in order to obtain a 2:1 PCC-fines mixture, which was carbonated to crystallize PCCs with colloidal, rhombohedral, and scalenohedral structures.

PCC morphology was controlled through crystallization of intermediary phases as described by Yamada and Hara. Colloidal PCC was thus obtained through amorphous calcium carbonate (ACC) (Yamada and Hara 1985_a).

$$Ca(OH)_2 \rightarrow ACC \rightarrow \text{Colloidal PCC} \quad (1)$$

It is believed that the ACC is transformed into colloidal PCC through a spinodal decomposition reaction of the ACC. Rhombohedral PCC was obtained through amorphous calcium carbonate (ACC) and basic calcium carbonate (BCC) (Yamada & Hara, 1985_b).

$$Ca(OH)_2 \rightarrow ACC \rightarrow BCC \rightarrow \text{Rhombohedral PCC} \quad (2)$$

Scalenohedral PCC was precipitated directly from $Ca(OH)_2$ (Yamada & Hara, 1985_c; Meuronen Jari, 1997). The progress of the reaction was monitored by conductivity

measurement, as shown in Fig. 1 for the production of 2:1 colloidal composite filler. The reaction was terminated when the conductivity suddenly dropped and approached 0 S/m, as shown in Fig.1.

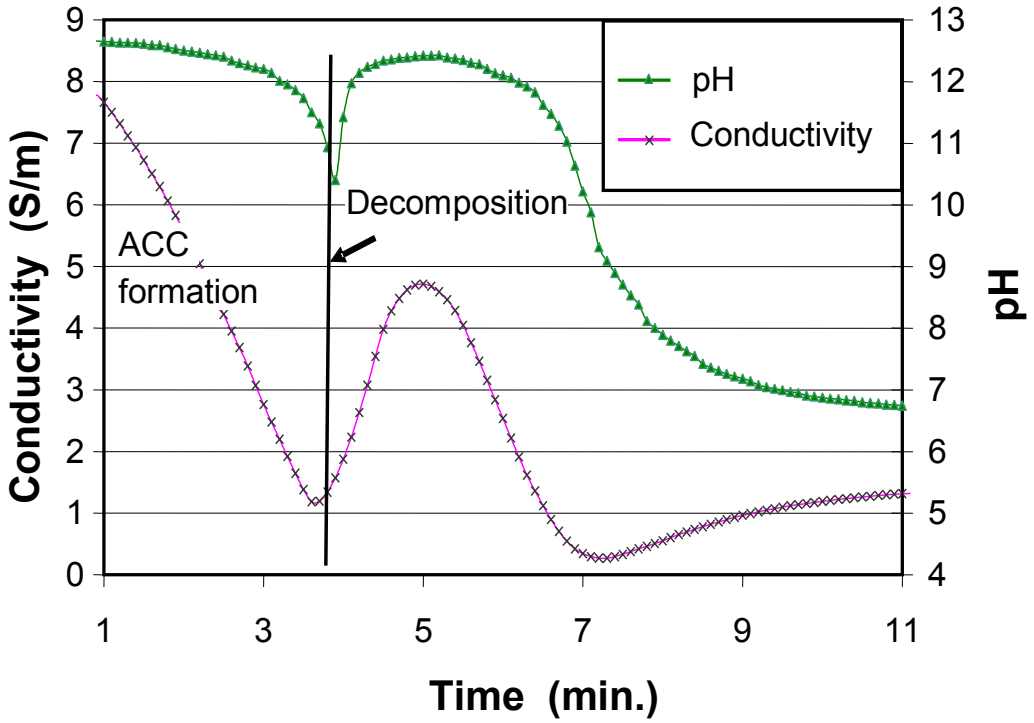

Fig. 1. Parameters observed during the crystallization of composite calcium carbonate filler with colloidal morphology

Sheet Forming and Testing

Refined pine softwood (23º SR) and birch hardwood pulp (18º SR) in a 30:70 ratio were used as the base furnish. Cationic acrylamide copolymer (C-PAM, 250g/t paper) was used as the retention aid in forming handsheets. The polymer solution was mixed in the handsheet mould, by air mixing, for 20 seconds. No other additives were used. Reference fillers, provided by J.M. Huber, produced under similar conditions as composite PCCs were used in the reference experiments.

Handsheets (80g/m^2) were produced in a standard handsheet mould with addition of retention aid, according to the ISO standard (ISO 5269-1). The samples were pressed twice in a Material Testing System (MTS) press at a pressure of 3.3 Mpa for 0.02 seconds with two blotting papers on each side. The handsheets were dried under standard conditions in a drum drier (ISO 5269-1). The first-pass retention was calculated as a percentage of the PCC retained in the handsheets to the total amount present in the stock suspension. In case of composite fillers, the total filler was measured from the whole composite sample, by ashing at 550^{o}C, and used to compute the amount of filler added to the base furnish. The handsheets were tested according to ISO standards. Internal bond strength was measured according to TAPPI T569 pm-00 standard method.

The PCC attached to the fibers was separated from them by oxidizing the cellulosic fibers for 2 hours in atmospheric air at low temperature (300ºC), followed by oxidation for 1 hour at 500°C.

The specific surface area of the PCC attached to the fibers was determined with the Brunauer-Emmett-Teller (BET) nitrogen adsorption method. The measurement was carried out with a Micromeritics Gemini 2375. The particle size distribution was determined by sedimentation of the ash residue with a Sedigraph 5100.

The method of ashing was used to assess the primary particle size distribution properties of the filler. The functionality of the filler, especially when combined with fibre, will additionally depend on the structures formed, including agglomerates and/or composites. Interpretation of the role of particle size in this case needs to be viewed in close relation with the microscopic analysis of composite particle structures. From the log-normal graph of the particle size vs. cumulative mass percentage we determine the median particle size (MPS), which represents the equal division of the mass of all particles present in the suspension. The particle size "75/25 ratio" was calculated from the Sedigraph as the measured value of the pigment particle size measured in microns at the 75 percentile divided by the particle size measured in microns at the 25 percentile. The 75/25 ratio is a measure of the breadth of the particle size distribution, and lower and higher values of 75/25 slope indicate that the particle size distributions are narrower and broader, respectively.

It is our experience (Maloney et al. 2005) that the slow ashing preserves the particle size of the PCC. Therefore, Sedigraph particle size results can be directly compared with particle sizes measured in the conventional way on standard fillers, while BET values should be treated with more care, preferably only by comparing the data obtained from slowly ashed samples.

Absorption and Structural Properties of the Handsheets

The handsheets were printed by HP LaserJet (4350dtn) and inkjet (Epson stylus C44UX) printers. The density and gloss were measured using Viptronic 4-794 and Vipgloss-I (4 -778), respectively. Printing ink rub resistance was tested with a PATRA print rub tester, using VTT test method 4716-94, with 2696g weight and 200 disc revolutions.

RESULTS AND DISCUSSION

Scanning Electron Microscopic (SEM) Study of the Composite Precipitated Calcium Carbonates

The colloidal calcium carbonates were seen to consist of precipitated nano-crystals aggregated into ellipsoidal shapes, as shown in Fig. 2. The precipitation occurred at random sites, mostly on the end of fibrils and, hence, the fibrils were partially covered with calcium carbonate fillers. The particle size of colloidal PCCs was less than 100nm.

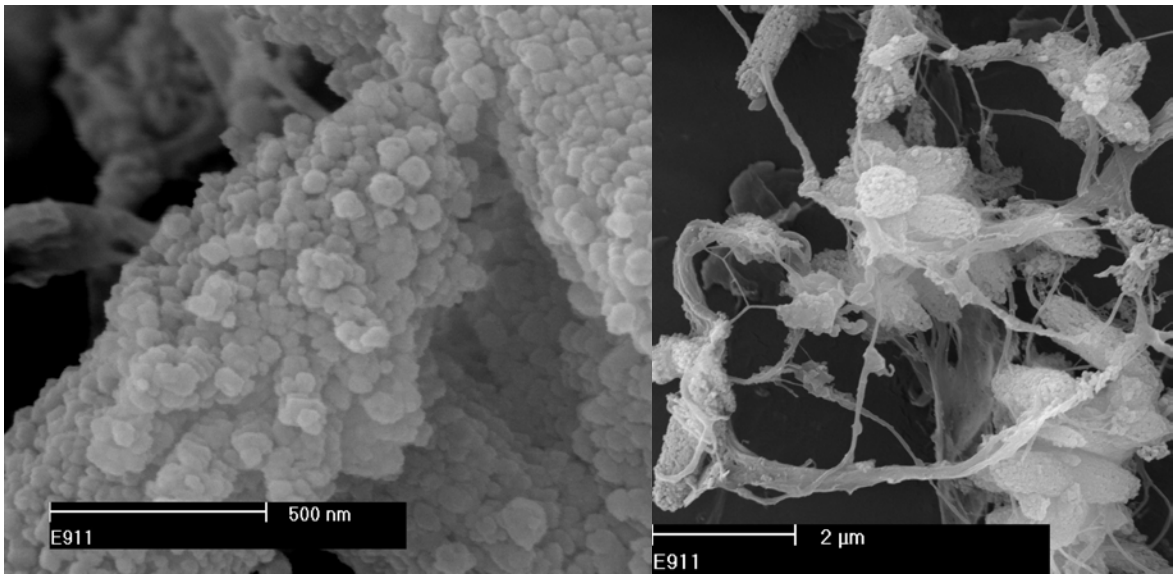

Fig. 2. Colloidal precipitated calcium carbonate composite

The rhombohedral PCCs were found in clusters, forming a pearl necklace structure with the fibrils, as shown in Fig. 3. Some fibrils covered PCC particle surfaces. In addition, films of microfibrils covering PCC surfaces were seen in the micrographs. The particle size of rhombohedral PCCs was below 2µm.

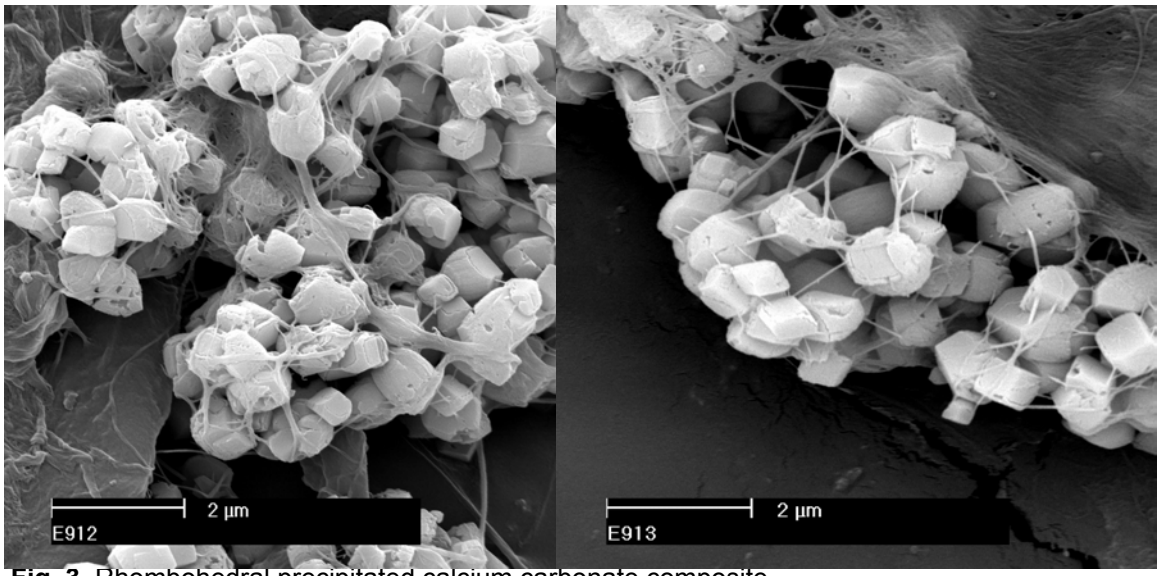

Fig. 3. Rhombohedral precipitated calcium carbonate composite

Alince has described that the light scattering ability of a pigment is a function of its refractive index and size (Alince, 1986), and in the case of agglomerates, also the particle spacing. Unbonded fibre surfaces contribute to light scattering due to debonding and their micrometre dimensions (Alince et.al. 1985). The SEM picture, Fig. 3, shows that the fibril width connecting the PCCs was below 200nm, and hence, may not contribute to light scattering, in contrast to the unbonded fibre surfaces.

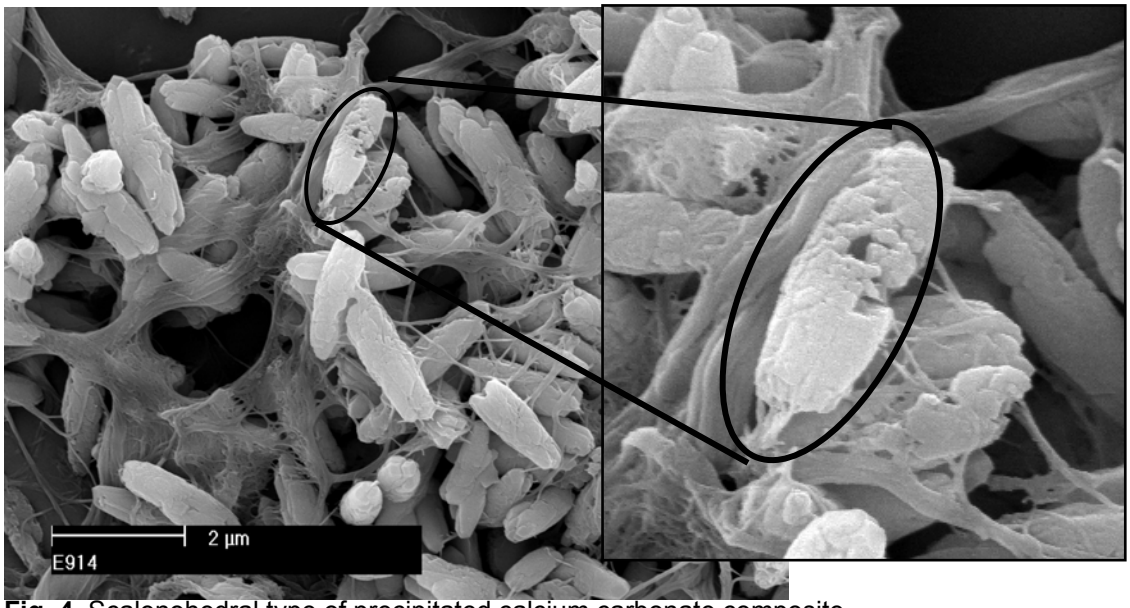

Fig. 4. Scalenohedral type of precipitated calcium carbonate composite

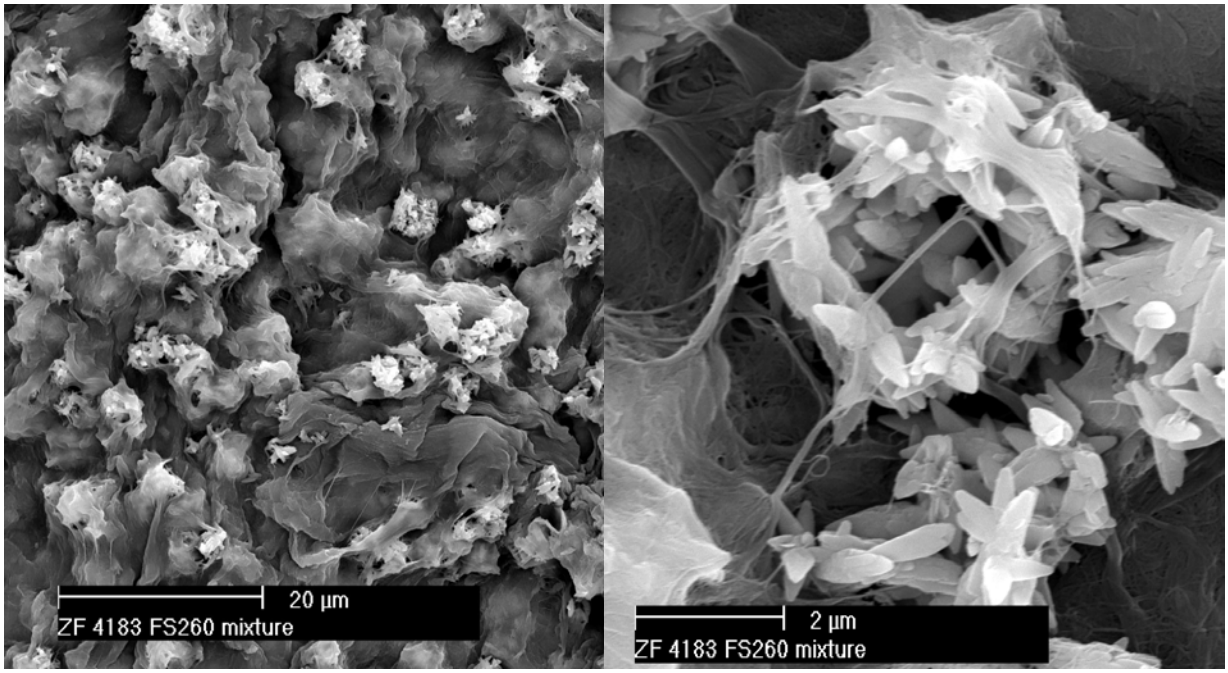

Fig. 5. Reference scalenohedral PCC mixed with cellulosic fines

The structure of the scalenohedral type of composite PCC formed under the experimental conditions was similar to that of the reference scalenohedral PCC, as shown in Fig. 4. Due to low solids and the presence of fines in the suspension, the precipitate appeared to have ellipsoidal form and was not structured, in contrast to the structured reference s-PCC. The presence of fibrils appeared to disrupt and inhibit the growth by covering the particle surfaces, as shown by the dark voids in the picture. Therefore, the particle size of these precipitates was lower, compared to the reference commercial PCC.

The precipitates were intertwined in a network structure. The fines surface coverage was higher with s-PCC composite than with other morphologies.

Fig. 5 illustrates mixing of fines and reference filler. It is seen that the filler was embedded into the fines network and partially covered by the fibrils. The filler was structured with a mean particle size of 2µm. It is to be noted that, during mixing, the PCC penetrated into the fibril network and prevented the collapse of the fibrils.

Filler Characteristics

The properties of the precipitated composites are compared with those of their respective reference PCC in Table I. The particle size distribution of the composite and reference particles was steep, as shown by the 75/25 ratio, with the exception of colloidal PCC. The measured surface areas of the reference fillers were larger than those of the composite PCCs. As stated above, this may, however, be a consequence of the preparation procedure. The colloidal PCCs had the largest surface area, as measured with the nitrogen absorption technique, among the various crystal habits in both composite and reference fillers. Also, at the same particle size, colloidal composite and reference fillers showed significant difference in their surface areas. Colloidal PCCs may thus be described as small aggregates of nano-sized crystals, a description that is also supported by the SEM investigation. The PCCs in fine and coarse rhombohedral composites did not differ significantly in size characteristics, in comparison to the reference rhombohedral PCCs.

Table 1 Characteristics of Composite and Reference PCC Filler

Type of filler	BET surface area (m^2/g)	Median particle size (µm)	75/25 ratio
composite c-PCC	12.02	1.42	3.0
composite fine r-PCC	3.91	1.31	1.75
composite coarse r-PCC	3.36	1.73	1.82
composite s- PCC	3.87	1.35	1.78
reference c-PCC	20.76	1.32	2.74
reference fine r-PCC	9.1	0.97	2.65
reference coarse r-PCC	4.32	2.29	2.16
reference s-PCC	5.81	2.19	1.74

Retention and Dewatering

The first-pass retention of the different types of filler is shown in Fig. 6. PCC-fibrillar fines composite filler gave higher retention than reference PCC, due to the higher flocculation index of fines with C-PAM retention aid (Solberg 2003). It was observed that the colloidal composite filler showed the highest first-pass retention, which is probably due to the PCC morphology (Fig. 2) and agglomeration. It has been shown that the retention of particles increases with increase in particle size, aggregated pigments, platy type filler, and coarse particles (Bown 1996).

On the other hand, the retention of reference PCCs decreased significantly with increased addition of filler. The mixture of reference filler and fines had a higher retention than reference filler, but lower than the composites. Mixing of filler with fines trapped the filler into the fines network (Fig. 5), resulting in higher retention than with addition of reference filler by itself.

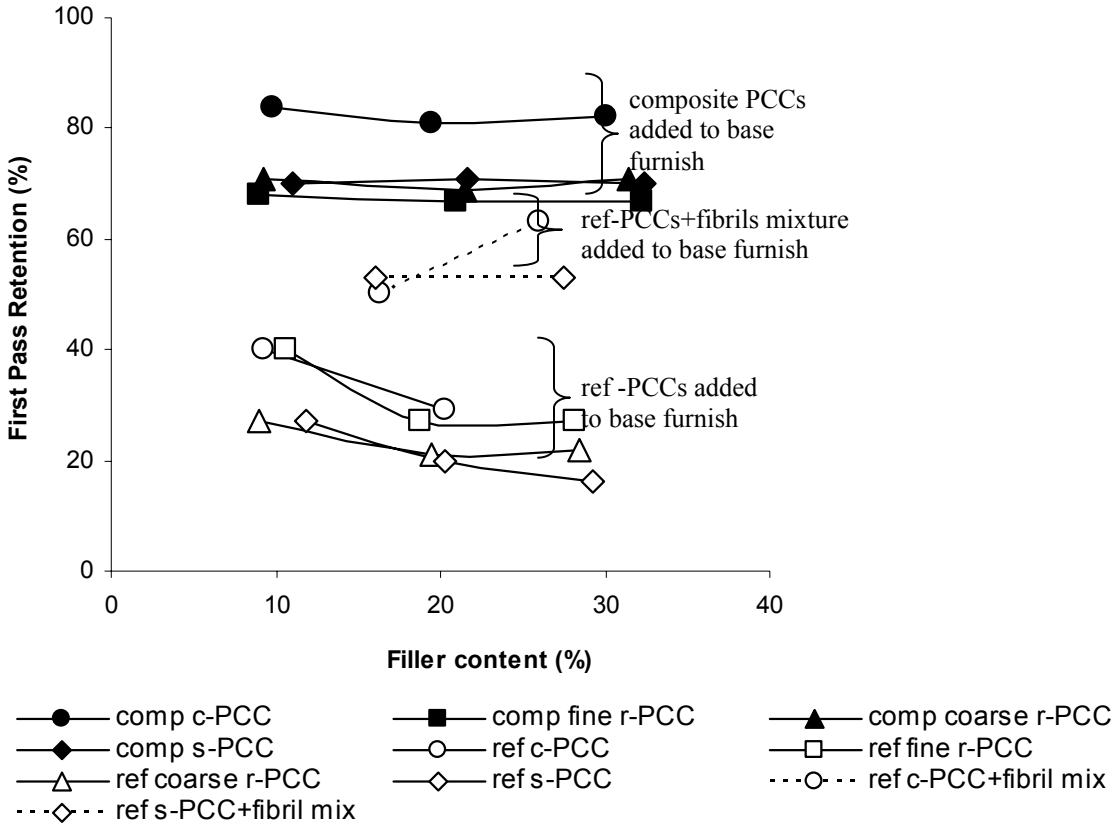

Fig. 6. First-pass retention of composite PCCs, ref-PCC's and ref-PCCs+fines mixture. Abbreviations: comp = composite; ref = reference; c= colloidal PCC; r = rhombohedral PCC; s=scalenohedral PCC; mix = mixture

Dewatering of the handsheets with various fillers after the first press is illustrated in Fig. 7. It is seen that the reference PCC gave the highest dry solids with increasing filler fraction in the paper. Mixing of fines with PCC significantly reduced the dry solids of handsheets after pressing. Among the reference fillers, structured s-PCC showed lower dry solids because of the water retention in the pores of the particles.

Among the composites, at lower handsheet filler content the colloidal composite showed the lowest dry solids, probably due to the homogeneous distribution of fillers leading to poor drainage. At higher filler contents, the drainage of colloidal fillers increased due to the expansion of the network structure. The expansion of the structure was confirmed by the increased bulk shown by the colloidal composite filled handsheets. At high filler contents, greater than 20%, the drainage of s- and r-PCC composite samples decreased significantly, probably due to the higher amount of film-forming fines in the structure.

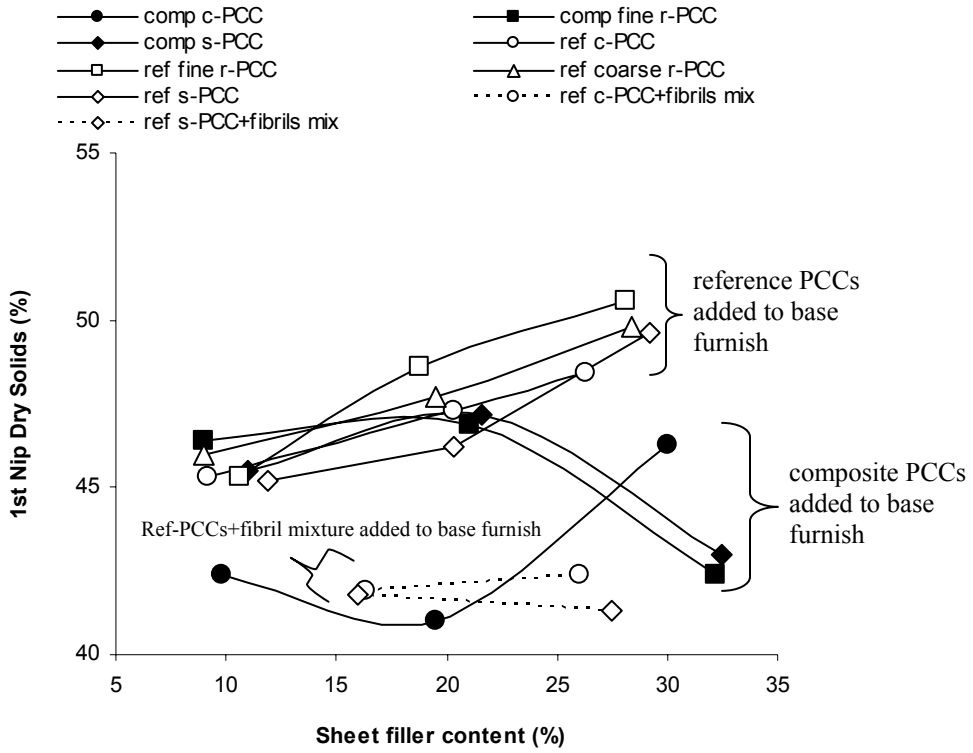

Fig. 7. Dewatering of composite fillers, reference PCCs and PCC-fines mixture handsheets at first press nip. For abbreviations, refer to Fig. 6

Paper Properties

The effect of addition of fines, in the form of composites or as a mixture of reference filler and fines, on the structural properties of paper is shown in Fig. 8. In contrast to reference PCC, a composite filler containing kraft fines enhances Campbell's forces, and thus aids in forming a dense network structure (Retulainen 1997). Among the reference fillers, addition of s-PCC caused a significant increase in the air permeability and a decrease in density. Addition of colloidal PCC resulted in a minimal increase in the air permeability of paper.

Addition of fines improved bending stiffness, as shown in Fig. 8, due to stronger bonding (Xu et al. 2005_b) and improved sheet consolidation (Seth, R.S., 2003). Mixing of fines and reference PCC gave the highest bending stiffness resistance. Reference r- and c-PCC gave the lowest bending stiffness, which decreased with increased addition of filler.

Comparing the internal bond strength and tensile index of various morphologies of PCC (Fig. 9), composites were found to give higher tensile strength than the reference fillers. These results correlate with earlier research findings (Xu et al. 2005_a) showing that fines contribute to strength by acting as a sealent-glue that increases the bonding area in filled paper. Among composites, at all filler contents, colloidal PCC and rhombohedral PCCs added to paper showed minimum and maximum internal bond strength respectively. Colloidal PCC composite gives reduced tensile strength at low filler contents.

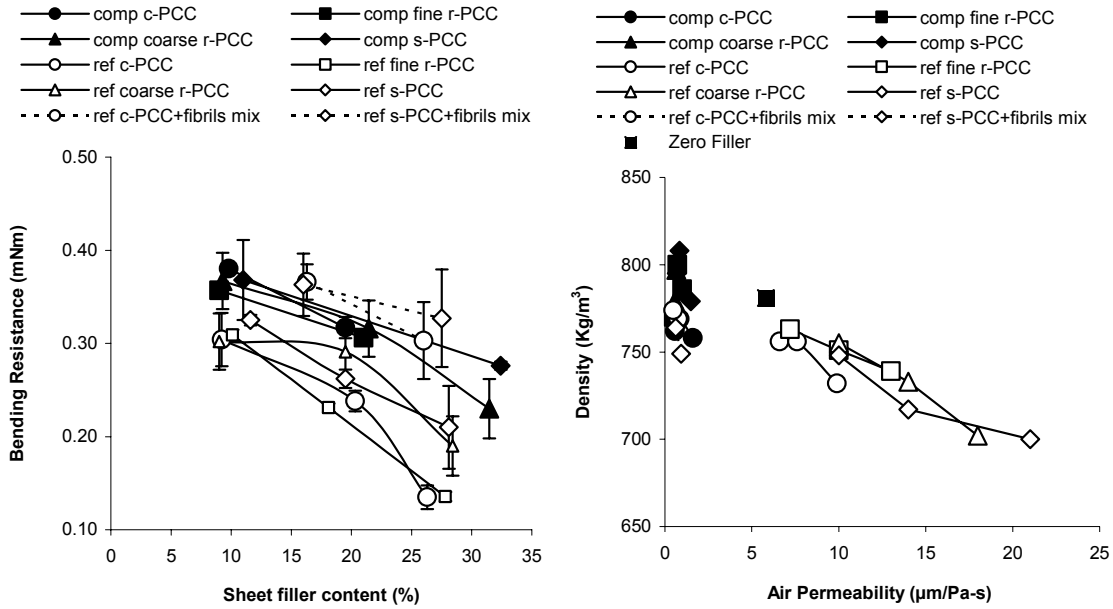

Fig. 8. Impact of PCC filler loading, as a function of PCC particle morphology, on the structural properties of paper. For abbreviations, refer to Fig. 6

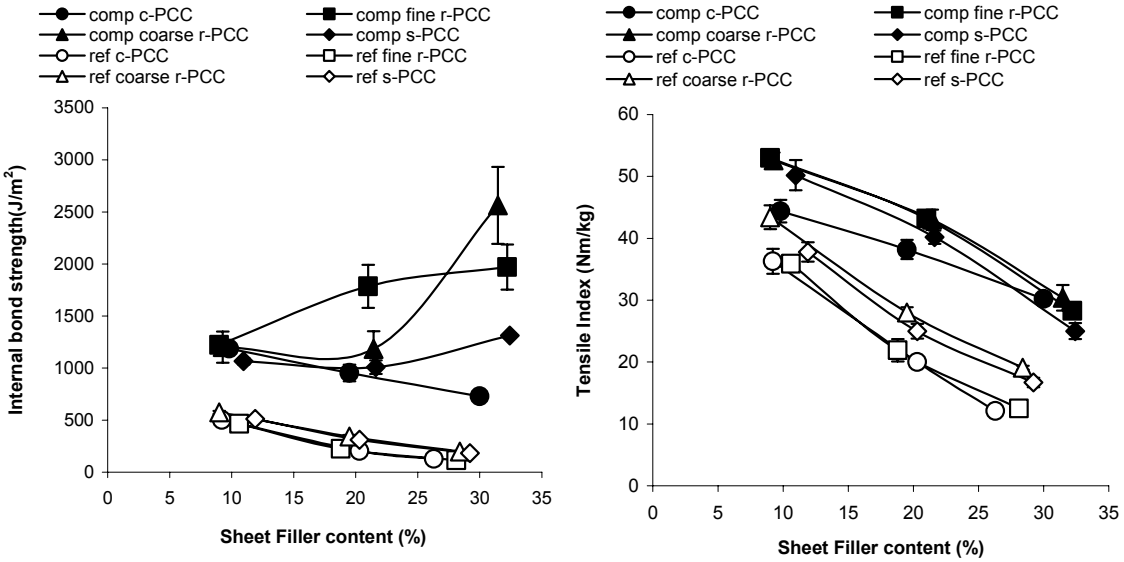

Fig. 9. Comparison of the strength properties of handsheets as a function of filler amount for composite and reference PCC filler with three different morphologies. For abbreviations, refer to Fig. 6

According to Fig. 10, increased addition of filler enhanced the light scattering of paper when using reference and composite fillers. Silenius (2002) has noted that the light scattering of composite fillers depends upon the particle size of the precipitated calcium carbonate particles. In our results we found that in-situ precipitation can lead to lowering

of surface area and particle size of the composite particles. Also, the dimensions of the fibrillar fines used in the co-precipitation of composites had a significant impact on the light scattering of the composite handsheets. As explained earlier (Fig. 3), less than 200 nanometer sized dimensions of the fibrils might not contribute to the light scattering, in contrast to the micrometer sized fiber dimensions. Thus, we found that the light scattering was similar for composite and reference filler added paper, in contrast to earlier experiments (Subramanian, et al. 2005).

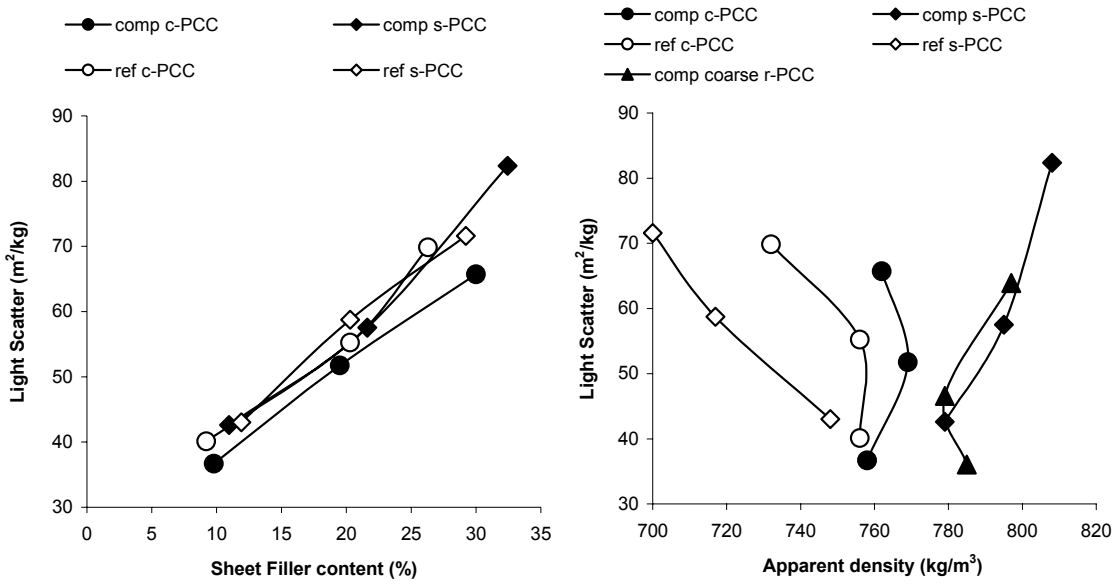

Fig. 10. Impact of PCC particle morphology on the light scattering properties of composite and reference PCC filled handsheets. For abbreviations, refer to Fig. 6

However, even with increased density, addition of composite filler to sheets imparted light scattering similar to that of reference fillers. This is due to the higher number of optical pores generated in the PCC-composites network structure, as shown in Fig. 4. The number of optical pores has a direct impact on the light scattering property of paper (Alince et al. 2002).

Print Rub Fastness

HP LaserJet and Epson ink-jet printed samples had an average density of 1.5, and an average gloss of 3 and 2 respectively. The suitability of these uncalendered and unsized handsheets for print analysis, per se, is not the aim of the exercise. However, the relative changes of absorption (ink jet) and of toner adhesion (laser printing) are of relevance in understanding the role of the different filler types. The whiteness of the rub-off samples is shown in Fig. 11, where the whiteness of a contact sheet is quoted, i.e. decreasing whiteness indicates high intensity of rub-off from the printed samples onto the contact sheet.

Addition of fibrillar fines, in the form of a composite or in a mixture of PCC and fines, was seen to enhance the rub resistance of the printed samples. This effect was more pronounced at higher filler contents.

Addition of fines increased sheet density of handsheets formed with composites and reference PCC-fibril mixtures. On the other hand, as shown in Figs. 3, 4, and 5, mixing of fines or in-situ PCC precipitation created network structures consisting of higher numbers of fine pores in the handsheets. Lowering of pore size, and thereby increasing the capillarity and adsorbing surface area had a positive effect on print rub resistance (Gane et al. 2006). Coarser colloidal PCC agglomerates added to handsheets resulted in lower print rub fastness with a significantly higher negative slope.

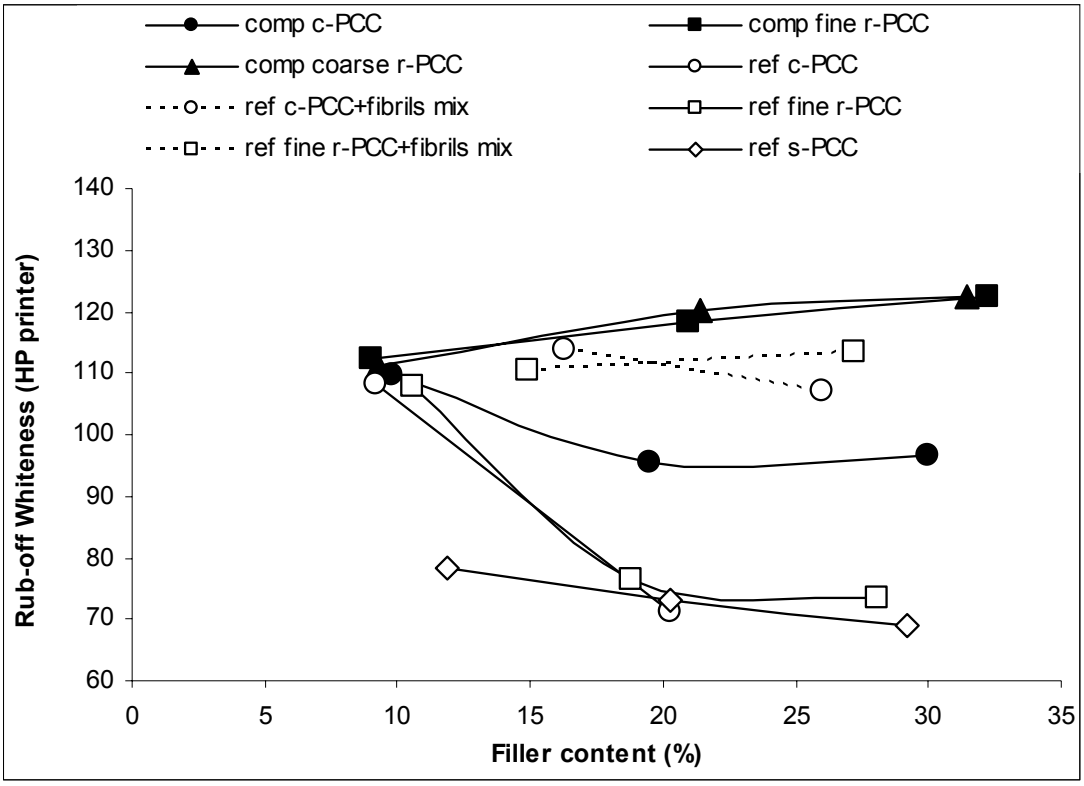

Fig. 11. Rub fastness, measured as the whiteness of copy paper rubbing surface, of HP laser-jet printed handsheets formed with the addition of composite filler, reference PCC's, and a PCC-fines mixture. For abbreviations, refer to Fig. 6

Similar trends were observed with inkjet printed samples. With inkjet printing, due to the lower strength of the base paper, the surface of the reference sample was completely scuffed below 100 revolutions.

CONCLUSIONS

1. In this work colloidal, rhombohedral, and scalenohedral types of PCC composites were precipitated. The characteristics of composite PCCs and their influence on the papermaking properties of printing and writing papers were determined.

2. The results showed that colloidal PCC consisted of nano PCC crystals agglomerated into an ellipsoidal shape on the surface of cellulose fibrils. Rhombohedral PCC and scalenohedral types of PCC formed a spider network with the fibrils. In the production of scalenohedral PCC crystals we found that particles had ellipsoidal shape and some of the particles had malformed structure.

3. First-pass retention was highest for colloidal PCC. At high filler contents, film-forming fibrillar fines increased the moisture content of wet pressed handsheets. Mixing of filler with fines results in higher retention compared to the mineral filler added alone due to the trapping of filler into the fines network.

4. Among composites, at all filler contents, colloidal PCC and rhombohedral PCCs added to paper showed minimum and maximum internal bond strength, respectively. At constant light scattering, handsheets that had been prepared with s- and r-composite PCC showed significantly higher density in contrast to the reference.

5. Print rub fastness increased with increased amounts of fibrillar fines in the handsheets.

ACKNOWLEDGEMENTS

The authors are grateful to Dr.Maloney, T.C, KCL, Finland and Taegeun, K, Laboratory of Paper and Printing Technology, TKK, Finland, for their contributions and support to this work.

This work was presented at the 6th Scientific and Technical Advances in Wet End Chemistry Conference, Madrid, 26-27 November, 2006, and the publication of this manuscript has been approved by the conference organiser, PIRA International.

REFERENCES CITED

Alince, B., and Lepourtre, P. (1985). "Light scattering in filled sheets – separating the contribution of the pigment and of fibre debonding", *Tappi J*. 68(4), 122-123.

Alince, B. (1986). "Light scattering of pigments in papermaking," *Paperi ja Puu*, 68(8), 545-547.

Alince, B., Porubska, J., and Van de Ven, T. G. M. (2002). "Light scattering and microporsity in paper," *J. Pulp Paper Sci*. 28(3), 93-98.

Allan, G. G., Carroll, J. P., Jimenez, G., and Negri, A. R. (1998). "Enhancement of the optical properties of a bagasse newsprint furnish by fibre-wall-filler, *Cellulose Chemical Technology* 32(3-4), 339-347.

Bown, R. (1996), *Paper Chemistry*, J. C. Roberts (ed.), Published by Blackie Academic & Professional, 202.

Bown, R. (1997). "A review of the influence of pigments on papermaking and coating," *Transactions of the 11th Fundamental Research Symposium*, Vol.1, Cambridge, Pira International Publications, UK, 83-137.

Fairchild, G. H. (1992). "Increasing the filler content of PCC-filled alkaline papers," *Tappi J*. 75(8), 85-90.

Gane, P. A. C., Ridgway, C. J., and Gliese, T. (2006). "A re-evaluation of factors controlling print rub on matt and silk coated papers" In: *Proceedings of TAPPI Coating and Graphic Arts Conference*, Atlanta, USA.

Holik, H. (2006). *Handbook of Paper and Board*, published by Wiley- VCH Verlag GmbH & Co. KGaA, Weinheim, Germany, 33.

Kang, T., and Paulapuro, H. (2004). "New mechanical treatment of chemical pulp," In: *Proceedings of Progress in Paper Physics Seminar*, Trondheim, Norwary, p. 11-13. NTNU and PFI, edited by Gregersen, O.W., Extended abstract.

Klungness, J. H., Caulfield, D. F., Sachs, I. B., Skyes, M. S., Tan, F., and Shilts, R. W. (1993). "Method of fibre loading a chemical compound," US Patent 5,223,090.

Maloney, T. C., Ataide J., Kekkonen J., Forsmand H., and Hoeg-Petersen H. (2005). "Changes to PCC structure in papermaking" In: *Proceedings of XIX National Technicelpa Conference*, Lisbon, Portugal

Meuronen, Jari (1997). "The precipitation of calcium carbonate to the fines fraction of chemical pulp and properties as a filler in papermaking" Master of Science thesis, Lappeenranta University of Technology, Finland

Middleton, S. R., and Scallan, A. M. (1985). "The preparation of lumen-loaded pulp," *Transactions of the 8th Fundamental Research Symposium*, Oxford, Mechanical Engineering Publications Limited, London, Vol. 2, 613-630.

Retulainen, E. (1997). "The role of fibre bonding in paper properties," Doctoral thesis, Helsinki University of Technology, Laboratory of Paper Technology, Espoo, Finland, Report Series A7, 63p.

Seth, R.S. (2003). "The measurement and significance of fines" *Pulp and Paper Canada* 104(2), T47.

Silenius, P. (2002). "Improving the combinations of critical properties and process parameters of printing and writing paper and paperboards by new paper-filling methods, Doctoral thesis, Helsinki University of Technology, Laboratory of Paper Technology, Espoo, Finland, Report Series A14, 129p.

Solberg, D. (2003). "Adsorption kinetics of cationic polyacrylamides on cellulose fibres and its influence on fibre flocculation" Licentiate thesis, Royal institute of technology, department of fibre and polymer technology, Stockholm, Sweden, TRITA PMT Report 2003:13.

Subramanian, R., Maloney, T., and Paulapuro, H. (2005). "Calcium carbonate composite fillers," *Tappi J.* 4 (7), 23-27.

Xu, Y., Chen, X., and Pelton, R. (2005_a). "How polymers strengthen filled papers," *Tappi J.* 4(11), 8-12.

Xu, Y., and Pelton, R. (2005_b). "A new look at how fines influence the strength of filled papers," *J. Pulp Paper Sci*. 31(3):147-152.

Yamada, H., and Hara, N. (1985_a). "Formation process of colloidal calcium carbonate in the reaction of the system $Ca(OH)_2$-H_2O-CO_2" *Gypsum & Lime,* No 194, 3-12.

Yamada, H., and Hara, N. (1985_b). "Synthesis of basic $CaCO_3$ from the reaction of the system $Ca(OH)_2$-H_2O-CO_2" *Gypsum & Lime,* No 196 , 12-22.

Yamada, H., and Hara, N. (1985_c). "Transformation of amorphous $CaCO_3$ from the reaction of the system $Ca(OH)_2$-H_2O-CO_2" *Gypsum & Lime,* No 203 , 25-32.

Article submitted: Nov. 28, 2006; First round of reviewing completed: Jan. 22, 2007;
Revised version accepted: Feb. 22, 2007; Published: Feb. 24, 2007

PAPER'S RESISTANCE TO WETTING – A REVIEW OF INTERNAL SIZING CHEMICALS AND THEIR EFFECTS

Martin A. Hubbe

This review considers research related to internal sizing agents. Such chemicals, when added as emulsions or in micellar form to slurries of cellulosic fibers before paper is made, can make the product resist water and other fluids. Significant progress has been achieved to elucidate the modes of action of alkylketene dimer (AKD), alkenylsuccinic anhydride (ASA), rosin products, and other sizing chemicals. Recent findings generally support a traditional view that efficient hydrophobation requires that the sizing chemicals contain hydrophobic groups, that they are efficiently retained on fiber surfaces during the papermaking process, that they become well distributed on a molecular scale, and that they need to be chemically anchored. A variety of studies have quantified ways in which internal sizing treatments tend to be inefficient, compared to what is theoretically possible. The inefficient nature of chemical and physical processes associated with internal sizing, as well as competing reactions and some interfering or contributing factors, help to explain apparent inconsistencies between the results of some recent studies.

Keywords: Internal sizing, Hydrophobicity, Cellulosic fibers, Paper, Mechanisms, Curing, Liquid penetration, Rosin, ASA, AKD

Contact information: Department of Forest Biomaterials Science and Engineering, North Carolina State University, Campus Box 8005, Raleigh, NC 27695-8005 USA, hubbe@ncsu.edu

INTRODUCTION

The term "internal sizing" is used by paper technologists to describe the practice of adding chemicals to aqueous slurries that contain cellulosic fibers, so that the resulting paper is able to resist water or other fluids (Davison 1975, 1986; Keavney and Kulick 1981; Reynolds 1989; Crouse and Wimer 1990; Eklund and Lindström 1991; Hodgson 1994; Roberts 1997; Neimo 1999; Hubbe 2000, 2005). The process can seem like magic. Very small amounts of additives are able to overcome the inherent wettability of the cellulose and hemicellulose (Hansen and Björkman 1998), two of the main chemical components of ordinary paper. The widespread success of internal sizing can seem even more improbable when one considers the fact that a typical sheet of copy paper has a thickness equivalent to the widths of only about seven layers of cellulosic fibers, and over half of the space within a typical sheet of paper or paperboard is occupied by air (Scott et al. 1995). Various other authors have reviewed ways in which changes in the free energy of surfaces is likely to affect the passage of liquids through the tiny pores that exist within a sheet of paper (Davison 1975; Keavney and Kulick 1981; Eklund and Lindström 1991). To add to the challenge, the chemical additives need to be formulated in such a way that they are compatible with the aqueous mixture, something that would appear to contradict the stated objective of being able to make the paper resist aqueous fluids. Typical

addition levels of the most efficient internal sizing agents lie in the range of 0.05 to 0.25%, based on the dry weight of paper. These tiny amounts of additives explain the wetting characteristics of paper cups and inkjet printing papers, making such products very different from paper towels and blotter paper.

Why Treat the Fiber Slurry to Hydrophobize Paper?

In the broadest sense, paper products can serve three main functions. They can be used for communication, for containing materials, and for absorbing or wiping liquids. Sometimes two of these functions are combined, as in the case of the cereal boxes, which use multi-color graphics to grab your attention. All of these functions can be highly dependent upon the degree to which fluids are able to spread onto or penetrate through the material. What is often overlooked is that internal sizing agents also can have a large effect on the paper manufacturing process itself. The process efficiency can be affected, and sizing can affect the hold-out materials, such as starch solutions, which are applied to the surface of paper.

Ironically, the end-use performance of absorbent paper products often can be improved by treating the fiber mixture so that the final product is somewhat less absorbent. Excessively rapid wetting can cause a paper towel to come apart before its job of wiping and absorbing is complete. Though wet-strength agents (Wågberg and Björklund 1993; Espy 1995) are widely used for many such applications, such chemicals have limited applicability for paper products that are likely to become disposed in septic systems. A well-chosen treatment with a sizing chemical, at the wet-end of the paper machine, can provide a few seconds of delay in wetting.

More obvious motivations to resist fluid penetration into paper or paperboard can be found in the case of products that are designed to act as containers, but even in those cases, the reasons can be subtle. Modern paper-based cartons for milk and juices have plastic laminate layers on each side. These layers perform the main job of resisting fluid penetration. To save costs, however, most milk cartons have unprotected edges of paperboard that remain exposed to the liquid. The paperboard needs to be internally sized to limit the rate of edge-wicking (Avitsland and Wågberg 2005). Internal sizing also is needed in order to deal with liquid that may pass through pinhole defects in the plastic laminate layers. Requirements for internal sizing of paper are more obvious in such cases as paper cups, paper bags that need to be able to contain wet grocery items, and packing boxes that may be exposed to the rain.

Not all printing processes require that the paper or paperboard be able to resist wetting. For instance, the word "xerography," which describes the operation of common photocopy machines (Borch 1986), means "dry writing." However, many users of xerographic printing paper choose to use the same paper in their ink-jet printers. Insufficient internal sizing can result in feathering of the ink-jet fluid, depending on the type of printer and the amounts of liquid transferred to the page (Barker et al. 1994). Holdout of the colorants in inkjet fluid, near to the surface of paper, is desirable in order to achieve the desired density of print images, while minimizing the cost of the ink.

The efficiency of the papermaking process can be highly dependent on the internal sizing of paper in paper machine systems where the web of product has to pass through a puddle or bath of liquid solution, as in cases where a starch film is applied to

the paper surface (Klass 1990). For example, most paper intended for offset or xerographic printing applications passes through a size press, in which the paper surface is exposed to a hot starch solution. Excessive penetration, before the paper has been dried again, can weaken the structure to such an extent that the frequency of web breaks can increase significantly, hurting the economic viability of the operation. Though size-press breaks are a critical issue for many paper machine operations, the issue has become less important in state-of-art paper machine systems that employ film-press technology (Klass 1990). In such operations, a solution of starch or other hydrocolloid is metered as a thin film onto a roll and then the film is transferred to the paper surface.

Finally, internal sizing can influence the structural characteristics of paper. The best example of this involves the effect of internal sizing on the degree of penetration of size-press starch, which is applied to paper's surface (Barker et al. 1994; Aloi et al. 2001). Such starch can act as a binder, increasing paper's modulus of elasticity. By concentrating such effects near to the paper's surface, one can achieve an "I-beam effect," maximizing the starch's contribution to stiffness (Lee et al. 2002; Lipponen et al. 2005). Starch near to paper's surface also can decrease paper's tendency to transfer lint or mineral components during printing operations (Fineman and Hoc 1978), or to fail when contacted by tacky inks during multi-color lithographic printing operations. The sizing performance of hydrophobic copolymers added at the size press also tends to have a synergistic relationship to internal sizing (Barker et al. 1994; Latta 1994).

What Internal Sizing Does *Not* Accomplish

As a general rule, internal sizing agents generally do *not* contribute significantly to any of the following effects:

- Provide any barrier to vapor, except as an indirect consequence of holding out size-press starch or other water-soluble polymers (Aloi et al. 2001)
- Affect the tendency of fibers in paper to change dimensions in response to changes in humidity (Page and Tydeman 1962; Gallay 1973; Lyne et al. 1996)
- Provide any strength to paper that has become completely soaked with water (Wågberg and Björklund 1993; Espy 1995)

With respect to vapor transport, papermakers can rely on other approaches, including the use of laminated films, as mentioned earlier. High levels of refining, yielding highly dense paper, as well as certain size-press treatments can decrease the vapor permeability of paper (Aloi et al. 2001), though not nearly to the same degree as plastic film.

The reason why internal sizing treatments don't tend to have much effect on paper's dimensional stability, especially under challenging conditions of humidity and temperature, will be considered again towards the end of this discussion. Briefly stated, the effect can be attributed to (a) the tendency of internal sizing treatments to affect mainly the outer surfaces of fibers, and (b) the ability of water vapor to diffuse within the interior of cellulosic fibers, causing them to swell (Page and Tydeman 1962; Gallay 1973; Nanri and Uesaka 1993; Chatterjee et al. 1997).

The Technical Challenges of Internal Sizing

Before considering theories related to the action of internal sizing agents, one can list some challenges that any successful internal sizing system will need to address. A

key challenge consists of the high surface area of the materials that constitute paper. There is a relationship between the required amount of sizing agent and the surface area of the solid materials in paper (Davison 1986; Lindström and Söderberg 1986b). Dried cellulosic fibers often have an air-accessible surface area of about 1-2 m^2/g (Haselton 1955). Much higher values have been found for the accessible surface area of the same fibers before they are dried.

Papermakers use fine mineral particles, *i.e.* "fillers," to achieve opacity, smoothness, and brightness goals. Another common goal of filler use is to decrease the net cost per mass of materials in paper. The dry surface area of filler is typically in the range of 4-20 m^2/g (Bown 1996). As has been shown (Marton and Marton 1983; Riebeling et al. 1996; Voutilainen 1996; Petander et al. 1998), the higher surface area per unit mass of fillers, relative to dry fibers, can lead to a higher uptake of papermaking additives, though the uptake is not necessarily directly proportional to surface area. The amount of chemical required to achieve desired levels of sizing tends to increase with increasing surface area per unit mass of filler (Ozment and Colasurdo 1994) and cellulosic material (Yang et al. 1999; Ramamurthy et al. 2000). As will be discussed, high-area calcium carbonate fillers appear to be somewhat incompatible with certain sizing agents (Moyers 1992). To overcome such problems, it is sometimes recommended to cover up the mineral surfaces with other materials before their addition to the paper machine system (Kurrle 1995). Alternatively, the order of addition of chemical additives and fillers to the papermaking process can be adjusted such that other materials cover the mineral surfaces before the sizing agent is introduced (Moyers 1992).

Surface-active materials, some of which originate in the pulpwood, are well known to counter-act the effects of internal sizing agents (Lindström and Söderberg 1986b; Moyers 1992; Proverb 1997; Yang et al. 1999; Zeno et al. 2005). Avitsland et al. (2006) recently quantified the effects of wood extractives relative to the efficiency of alkylketene dimer (AKD) sizing, depending on how the fibers had been bleached. Other researchers have attributed such effects of bleaching practices to differences in retention efficiency of the sizing agents (Laine et al. 2004).

When kraft fibers swell in water, the pore volume within paper can increase by a factor of four, greatly increasing the size of passages through which water can flow (Avitsland and Wågberg 2005). This effect is especially important in the case of chemithermomechanical pulp (CTMP) fibers.

HOW SIZING WORKS: THEORY

A general hypothesis can be proposed to account for the ability of chemical additives to the papermaking furnish to produce resistance to aqueous fluids in the final paper. A subsequent section will then evaluate these ideas relative to findings in the case of four main types of internal sizing agents – alkenylsuccinic anhydride (ASA), alkyl-ketene dimer (AKD), rosin products, and copolymer products.

Many aspects of the hypothesis to be described already have been discussed in previous reviews of the subject (Davison 1975, 1986; Keavney and Kulick 1981; Ehrhardt 1987; Reynolds 1989; Crouse and Wimer 1990; Gess 1991; Eklund and

Lindström 1991; Roberts 1991, 1997; Hodgson 1994; Neimo 1999; Hubbe 2000). It is generally agreed that resistance to the spreading or penetration of water requires a reduction in the free energy of paper's surface (Krueger and Hodgson 1995; Irvine et al. 1999). Aqueous fluids spread and penetrate with relative ease in the case of "bare" cellulosic surfaces, due to the ability of water to form hydrogen bonds with the surface hydroxyl groups of the polysaccharide-rich material. The relatively high energy of interaction results in relatively low contact angles of water with cellulosic materials (where, by convention, the angle of contact is drawn through the liquid phase). By contrast, when a drop of water is placed onto a flat, non-wetting plastic surface, by definition, the angle of contact is greater than 90 degrees. Thus, the internal sizing of paper can be envisioned as a way to transform the paper surface from a relatively high-energy state, rich in groups capable of hydrogen bonding, to a modified state in which the free energy of the surface is reduced.

To account for this transformation, the following general hypothesis can be proposed for the action of an effective internal sizing additive:

1. A hydrophobic entity, such as an alkyl group having about 16 or more carbons, must be included in the active ingredient of the sizing agent.
2. The active ingredient must become well dispersed after its addition to the fiber-containing suspension, for instance as an emulsion or micellar solution.
3. The sizing agent must remain in its active form up to a critical point in the papermaking process.
4. The sizing agent must be retained efficiently in the wet-web of paper.
5. The sizing agent must become molecularly well distributed on the outer surfaces of the paper by the time it is dried.
6. Individual molecules of the sizing agent must become anchored and oriented in order to achieve a stable and efficient sizing effect.

Retain in the Wet Web

To be effective, it is essential that sizing additives become retained on solid surfaces within the paper, as it is being formed. Non-retained sizing materials either may pass out of the system with the excess water sent to the waste treatment system, or they may circulate long enough in the process so that they suffer physical or chemical changes, making them less effective. Unretained sizing agents also may deposit onto wetted surfaces within the paper machine system (Petander et al. 1998). Though some kinds of sizing additives are formulated in such a way that they have a natural attraction for cellulosic materials, it is often satisfactory if the material is capable of being retained by commonly used coagulants and retention aid polymers (Norell et al. 1999).

Distribute on Surfaces

Divergent opinions have been offered regarding how internal sizing agents become distributed over the surfaces of fibers as paper is being made. The broad term "distribute" has been chosen in order to encompass various explanations. In the case of rosin soap sizes there is general agreement that the active ingredient usually becomes chemically precipitated onto surfaces as a consequence of treatment with soluble

aluminum species (Back and Steenberg 1951; Strazdins 1977, 1984; Ehrhardt 1987; Marton 1989). In the case of other sizing agents, such as rosin emulsion products, ASA, and AKD, one traditional explanation is that the active ingredients of size are in liquid form under the conditions prevailing during the drying of paper, allowing them to flow and spread over paper's surface (Dumas 1981; Davison 1986; Fischer 1999; Lindfors et al. 2005). More recently, much attention has been paid to factors affecting the diffusion of monomolecular or multi-layer films adjacent to a liquid droplet of sizing agent (Seppänen and Tiberg 1999; Garnier and Godbout 2000; Shen and Parker 2003; Shen et al. 2003). In addition to these possible mechanisms, there also is good evidence that molecules of certain sizing agents become vaporized under drying conditions, making it possible for them to recondense onto adjacent surfaces (McCarthy and Stratton 1987; Back and Danielsson 1991; Gess 1991; Yu and Garnier 1997; Shen et al. 2001; Gess and Rende 2005). The latter mechanism is sometimes disputed, possibly due to the fact that some sizing agents can decompose to non-sizing species while in a humid vapor (Akpabio and Roberts 1987; Laitinen 1999; Hutton and Shen 2005; Shen et al. 2005). As will be discussed, it appears likely that two or more of these mechanisms contribute to effects that are commonly observed during production of a typical sized paper product.

In addition to the question of "how," it is also important to ask "when" do typical sizing agents, other than rosin soap products, become distributed over the surfaces in a sheet of paper. An important clue is provided by the fact that heat and time are required, and sizing does not develop significantly until after the paper has become dry (Davis et al. 1956; Lindström and Söderberg 1986). It has been suggested that the presence of liquid water blocks the spreading of sizing agent species over paper's surface (Lindström and Söderberg 1986; Eklund and Lindström 1991). A happy consequence of this situation is that sizing tends to develop only on the outer surfaces of paper, not within bonded areas, where the effect would be expected to adversely affect paper strength.

Anchor and Orient

Why is it the case that the most effective sizing agents – rosin, ASA, and AKD – all happen to have some means by which they might become chemically anchored to solid surfaces? Such anchoring ability appears to be essential in order to maintain an efficient barrier to wetting of paper surfaces (Davison 1975; Dumas 1981; Davison 1986). The idea is that there needs to be some kind of ionic or covalent bonding so that the sizing molecules don't simply diffuse away when confronted by an approaching meniscus of aqueous fluid (Davison 1975). Also, it would make sense that the hydrophobic groups on the sizing agent ought to be kept facing outwards from the surface. Paraffin wax is an inefficient sizing agent, despite the low free energy of its surface (Davison 1986). This lack of effectiveness has been attributed to wax's inability to anchor itself to solid surfaces. As will be seen from the later discussions of ASA, AKD, and rosin emulsion sizing technologies, there is a surprising lack of agreement regarding the degree to which, and even the possibility of various chemical reactions between sizing agents and the solid surfaces of paper. Nevertheless, strong evidence still supports the "anchor and orient" concept as an essential step in the action of efficient sizing agents.

HOW SIZING WORKS: PRACTICE

To support the general sizing hypothesis, as described above, this section considers published findings related to four main types of sizing agents, ASA, AKD, rosin products, and copolymer products. As will be seen, each class of sizing agents shows somewhat unique characteristics. Readers are forewarned not to expect complete agreement among the apparent findings of all of these studies. Some disagreements may be attributed to differences in conditions of treatment or analysis. In other cases there appear to be opportunities for researchers to make further progress in evaluating different molecular explanations of the action of sizing agents.

Case 1: ASA

The use of alkenylsuccinic anhydride (ASA) as an internal sizing agent for paper has grown rapidly since its introduction in the early 1960s (Wurzburg and Mazzarella 1963; Gess and Rende 2005). The active ingredient, in its most commonly available form, exists as an oily liquid at room temperature. The chemical is usually formed by reacting maleic anhydride with an isomerized mixture of linear alkenes having chain lengths in the range of about 16 to 22 carbon atoms. ASA has a relatively high chemical reactivity, making it possible to achieve most of the hydrophobizing effect before the size press of a typical paper machine (Wasser 1986; Daud 1993; Gess and Rende 2005). ASA's high reactivity sometimes has been attributed to the ring strain within the cyclic anhydride group (Davis and Hogg 1983). Reactivity also has been found to depend on the proximity of the anhydride group to other unsaturated groups, which may or may not be in conjugated systems (Rossall and Robertson 1975). As illustrated in Fig. 1, it is generally believed that ASA achieves its most efficient and most permanent sizing effect by forming ester bonds with hydroxyl groups on the polysaccharide components of paper during the drying process.

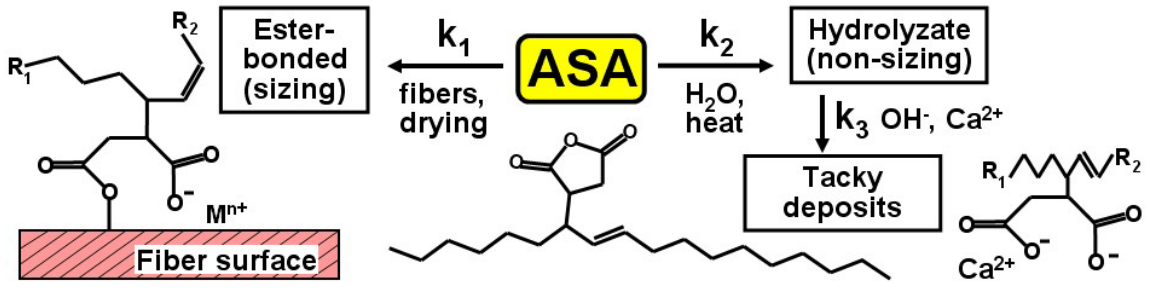

Fig. 1. Summary of main reactions affecting use of alkenylsuccinic anhydride (ASA) size

ASA can be classed as an "alkaline sizing agent," meaning that it can be used effectively in systems containing substantial proportions of calcium carbonate filler. Optimum sizing often is observed at $7.5 < pH < 8.4$ (Savolainen 1996). To be effective under such conditions, the oil needs to be formed into an emulsion before its addition to the paper machine system. Proximity to water during preparation and storage of emulsions, and especially after the material has been added to the paper machine, makes

it impossible to completely avoid an undesired hydrolysis reaction. The hydrolyzed form of ASA, often present as the calcium or magnesium salt of the diacid, cannot be effectively distributed over paper surfaces and tends to form tacky deposits on papermaking equipment. According to Wasser and Brinen (1998), the calcium salt of ASA does not contribute to sizing of paper, whereas the soap form of the ASA hydrolyzate actually tends to reverse the desired sizing effect. Recently it was reported that tackiness could be reduced when ASA was formed from the ethyl esters of mono-unsaturated fatty acids (Isogai and Morimoto 2004).

Cationic starch and related stabilizers

Much effort has gone into optimizing the preparation of emulsions of ASA, usually with cationic starch solutions and controlled hydrodynamic shear (Chen and Woodward 1986; Lee and Shin 1991; Isogai et al. 1996; Proverb 1997; Guan 2002). The cationic starch not only keeps the dispersed droplets from colliding and coalescing; it also helps attach the droplets to the surfaces of cellulosic fibers, fines, and other negatively charged surfaces in the papermaking suspension (Isogai et al. 1996). The word heterocoagulation has been used to describe the retention of positively charged particles of sizing chemicals onto negatively charged surfaces (Lindström and Söderberg 1986b; Robert 1991). Best performance requires that the emulsion droplets be controlled to an optimum diameter, usually near 1 μm (Chen and Woodward 1986). Because excessive hydrodynamic shear can reduce the molecular mass of cationic starch, it is sometimes recommended to initially emulsify the ASA with a minimum amount of cationic starch solution, and then, after the high shear zone, add enough starch to achieve a ratio of about 3-5 parts of starch per part of ASA.

Different types of cationic starch have been found to give very different performance of the sizing agent, when using a specific set of equipment and procedures (Guan 2002). Cationic potato starches were used almost exclusively during the early alkaline conversions of paper machines in the 1980s, but more recently a variety of corn starches, including waxy maize, also have been employed as sources of cationic starch for ASA emulsification. Lee and Shin (1991) found that higher-charged cationic starch tended to achieve higher efficiency of ASA emulsions, when they were used immediately, but the higher-charged starches also tended to speed up the hydrolytic decomposition of dispersed ASA. Lee et al. (2004) observed that a hydrophobically modified cationic starch outperformed ordinary cationic starch, in terms of ASA sizing efficiency. The increased sizing effectiveness was attributed to a smaller droplet size.

Not all paper mills have starch cooking equipment. In addition to pregelatinized cationic starches, which do not require cooking, various synthetic polyelectrolytes have been used for ASA emulsification. Rendé and Breslin (1987) patented the use of various cationic copolymers, including acrylamide products, for use as ASA stabilizers. Shigeto and Umekawa (1992) claimed the use of amphoteric acrylamide for similar applications, and reported good storage stability and sizing performance of the emulsions.

Hydrolysis and its consequences

One reason why the size of droplets plays such an important role in the optimization of ASA systems is that smaller droplets have higher surface area, making the

anhydride more susceptible to the undesired reaction with water, before the material can be retained in the paper web and cured in the dryer section of the paper machine. Wasser (1987) showed that the rate of ASA hydrolysis during storage of emulsions tended to increase with increasing pH and temperature. An observed acceleration with time of the hydrolysis reaction (Wasser 1987) suggests that the decomposition products accelerate the reaction. This makes sense, since carboxylate species would be expected to increase the concentration of water that diffuses within a droplet of ASA.

To slow down the rate of hydrolysis, some papermakers employ strategies in which the starch solution, to be used for ASA emulsification, is buffered into the acidic range by addition of such substances as adipic or citric acid or aluminum sulfate (papermakers' alum). Scalfarotto (1985) found that the presence of aluminum species in the process water also tends to reduce the tackiness of any ASA hydrolyzate that happens to form. Thus it was possible to overcome picking problems at the wet press by alum addition to the paper machine. At the same time, the aluminum salts also tended to boost the sizing efficiency of ASA (Scalfarotto 1985; Zandersons et al. 1993; Lee and Shin 1991).

Vapor Distillation

McCarthy and Stratton (1987) reported that ASA can volatilize during the drying of paper. Papermakers using ASA often find evidence of vapor-phase transport of the sizing agent. ASA byproducts can be found on the hoods of paper machines, either in isolation, or mixed with other materials (Gess and Rende 2005). The amounts of such deposits could be reduced by increasing the molecular mass of the ASA, *i.e.* by increasing the lengths of the alkenyl groups. Back and Danielson (1991) showed that ASA sprayed onto one side of a paperboard sheet was able to migrate and develop hydrophobicity throughout the thickness of the product. The ability to size the opposite side of the sheet increased with increasing temperature and time.

Ester bond evidence

Though various methods are available for detection of ester bonds, such as those most likely to form between ASA molecules and the hydroxyl groups of cellulose, hemicellulose, and starch molecules on fiber surfaces, it has been very challenging to quantify such reactions. One faces the problem of trying to observe a relatively small quantity of bonds formed at an interface. Meanwhile, the most commonly used analysis methods, such as infrared (IR) absorption spectroscopy, also detect signals that result from the adjacent bulk phase or phases (Dumas and Evans 1986). The problem of sensitivity is compounded by the fact that relatively little ASA is needed in order to size paper, *e.g.* of the order of magnitude 0.1% addition on a solids basis. Even to quantify the amount of ASA that is retained in paper, it is necessary to use methods that are ultrasensitive to surface-bound features, *i.e.* surfaced-ionization mass spectrometry (SIMS) (Brinen and Kulick 1996). McCarthy and Stratton (1987) carried out reactions in dimethylsulfoxide (DMSO), using Fourier-transform infrared (FTIR) spectroscopy to show that ASA is capable of forming ester bonds with cellulosic hydroxyl groups. Subsequently they and others showed that ester bonds also can form under realistic conditions of ASA sizing (McCarthy and Stratton 1987; Zandersons et al. 1993).

Isogai and coworkers, using a variety of experimental approaches, found little or no evidence of ester bond formation during ASA sizing. Though some of their results probably can be attributed to the sensitivity issues mentioned earlier, much of the added ASA was converted to the hydrolysis product during sizing, and only a small proportion, if any, formed an ester bond with the fiber (Nishiyama et al. 1996a; Isogai and Onabe 1996). Most of the ASA products could be removed from sized sheets by a hot aqueous micellar solution of nonionic surfactant, an observation that would not be expected in the case of ester bonds to a surface (Isogai 1998). To explain why unreacted ASA was required in order to achieve sizing, it was proposed that only the anhydride form can be efficiently distributed onto fiber surfaces (Isogai and Onabe 1996; Nishiyama et al. 1996b; Isogai 1998). Another explanation is that the authors sometimes may have employed conditions in which the ASA had a greater opportunity to react with water, relative to typical conditions in the dryer section of a paper machine, *i.e.* relatively large ASA dosages and relatively slow rates of drying.

Theories proposing that ASA achieves sizing by means of the diacid form of the chemical may receive some measure of credibility by reference to work carried out under acidic conditions. Hatanaka et al. (1991) showed that it is possible to employ the diacid soap of ASA in very much the same manner that one would size with rosin soap products (see later). The pH needed to be below 5.5 and at least 1% alum addition produced the most effective sizing, even exceeding the effect of a fortified rosin soap product. One might expect such a reaction to be possible, even under alkaline papermaking conditions, if the surfaces have sufficient coverage by aluminum or calcium species, capable of forming the stable, insoluble salts with the additive. Novak and Rendé (1993) suggested, however, that ASA molecules adsorbed onto calcium carbonate surfaces can more easily revert to a non-sizing form during storage of the paper. In summary, though there is good evidence that ASA forms ester bonds at the paper surface during drying, there is also evidence that much of the ASA can end up in an unbonded or weakly bonded state.

Assuming, for the moment, that ASA's contribution to sizing is mainly due to ester formation, it still remains unclear whether or not much of the esterification takes place between ASA and starch products, rather than with cellulose or hemicellulose. No study addressing this point was located while searching the literature for this review. Factors suggesting a significant role for ASA-starch reactions include (a) the proximity of ASA and starch, following preparation of starch-based emulsions, (b) the flexibility and non-crystalline nature of starch chains, which would be expected to make the hydroxyl groups available for reaction, and (c) the fact that ASA sizing efficiency often increases with increasing ratios of cationic starch that is added concurrently with the ASA.

Molecular architecture effects: Sweeping and protection

At the start of this discussion of ASA characteristics it was mentioned that the alkenes from which ASA is synthesized typically are isomerized. This is done to obtain a mixture of products having their double bonds usually located towards the central part of the molecule. From a practical standpoint, the transformation reduces the melting point of ASA, so that ASA emulsions can be prepared at relatively low temperatures. In addition, the isomerized form of ASA tends to out-perform ASA that has been prepared from primary alkenes (Roberts et al. 1993; Smith 1999). The higher performance of the

commonly used isomerized form of ASA was attributed to the shape of the molecule, roughly resembling a "T," bound to the fiber at its base. The alkyl group, situated above the anchoring group of the ASA, can be expected to protect the ester bond, as well as the carboxyl group that becomes left over during the proposed ester-forming reaction with the fiber surface (see Fig. 1). The alkyl group also may be able to sweep itself around, preventing the advance of a front of aqueous solution over that part of the fiber.

Case 2: AKD

Alkylketene dimer (AKD) products, which usually are prepared by dimerization of stearoyl chloride (Hodgson 1994), provide a second set of examples that can be used when attempting to define the essential characteristics and actions of efficient sizing agents. Already at the time of its introduction, the inventors of AKD sizing technology were convinced that a chemical reaction takes placed between the active ingredient and hydroxyl groups at the fiber surface (Davis et al. 1956). Similarly to the ASA products just discussed, AKD needs to be emulsified in the presence of cationic starch or other cationic polymers, before it can be added to paper machine systems. But AKD is so much less reactive than ASA that the emulsification can be carried out at a central facility, allowing shipment of ready-to-use AKD dispersions to paper mills. Like ASA, AKD tends to perform best at neutral to weakly alkaline pH, making the product suitable for making paper that contains calcium carbonate filler. Due to AKD's relatively low reactivity, papermakers often over-dry paper before the size press to cure the size. In many cases, full sizing is achieved only after the reels and rolls of paper have gradually cooled for several hours or days (Kamutzki and Krause 1983; Roberts and Garner 1985).

Some differences in performance of AKD and ASA sizing agents can be traced to differences in the physical state of the active ingredient. Neat AKD is a waxy solid at room temperature. Not surprisingly, over-use of AKD can result in slippery paper (Hoyland and Neill 2001; Karademir and Hoyland 2003), though some researchers blame a breakdown product of AKD, rather than AKD itself for observed decreases in the coefficient of friction (Karademir et al. 2004). As delivered to the paper mill it is expected that AKD dispersion can contain the ketone byproduct of hydrolysis (Asakura et al. 2006b), as well as oligomers of alkylketenes (Asakura et al. 2006a) and fatty acids (Asakura et al. 2005). Most sources agree that such impurities decrease the overall effectiveness of AKD products (Isogai et al 1992; Asakura et al. 2006ab) and make it more difficult to prepare stable dispersions of AKD (Asakura et al. 2005). One study found, on the contrary, that sizing efficiency improved as the content of hydrolyzed products increased to about 25% (Isogai et al. 1994). Impurities, as well as the chain lengths of the alkyl groups within AKD can affect the melting point of the material, a factor that has been found to correlate well with certain deposit problems if the melting point is close to the temperature of the process water (Knubb and Zetter 2002). AKD having a somewhat higher molecular mass, *i.e.* having longer alkyl groups, has been found to form dispersions with higher stability, presumably due to the less tacky nature of the active ingredient (Chew et al. 2004).

The theory that slipperiness problems with AKD-sized paper are due to AKD itself, rather than due to byproducts, finds support in observations that the problems can be substantially overcome if there are unsaturated groups within the hydrocarbon tails of

the reagent. Alkenylketene dimer (AnKD) products have been used effectively for the sizing of paper products intended for precision sheet-fed printing, an application that can be highly sensitive to slippage (Brungardt and Gast 1996; Kenton 1996).

Figure 2 summarizes commonly held concepts of how AKD molecules become distributed and bound to cellulosic fiber surfaces. Issues related to distribution pathways and relative rates of reaction will be discussed later. It is widely believed that the fraction of AKD molecules that are able to form β-keto ester bonds with hydroxyl groups at the surfaces of papermaking materials play a central role in achieving the observed increases in resistance to aqueous fluids (Davis et al. 1956; Karademir et al. 2004). By contrast, efforts to make paper hydrophobic by treating it with the ketone byproduct of AKD usually fail (Karademir et al. 2004), and unreacted AKD does not appear to contribute significantly to the sizing effect (Karademir and Hoyland 2003).

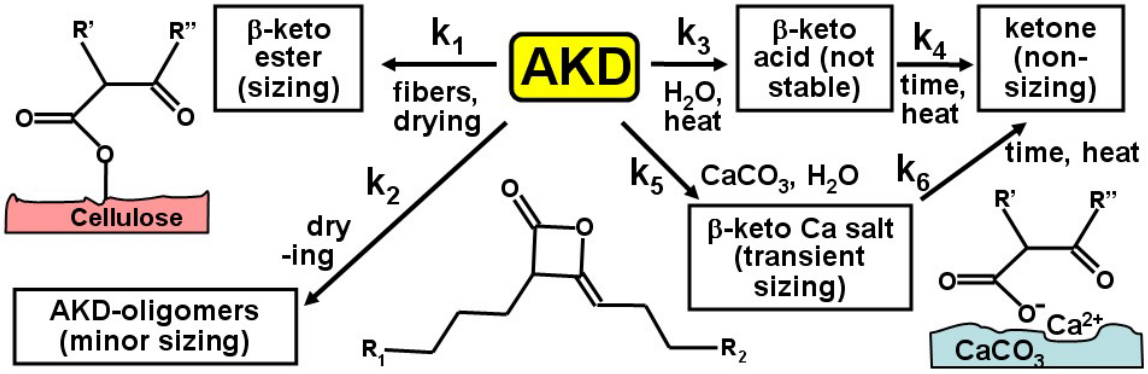

Fig. 2. Summary of main reactions affecting alkylketene dimer (AKD) sizing agents

Emulsification at the supplier plant

Dispersions of AKD particles are often called "emulsions," due to the fact that the active ingredient is melted just before the process of dispersion. The term "dispersions" will be used here, in recognition of the fact that AKD exists as solid particles in the formulations that are received by papermakers. The most commonly used stabilizers for AKD include cationic starch products (Knubb and Zetter 2002; Chew et al. 2004), cationic amido-amine epichlorohydrin products, which are well known as wet-strength agents (Espy 1995), and other cationic synthetic polyelectrolytes (Esser and Ettl 1997). The function of the stabilizers is to prevent particles of AKD from colliding and sticking together. The effectiveness of starch products in maintaining stable dispersions has been found to increase with increasing molecular mass (Chew et al. 2004). A severe way to evaluate the effectiveness of different stabilizing systems involves subjecting AKD emulsions to thermal shock cycles; such tests have shown that the presence of fatty acids (Asakura et al. 2005) and stearic anhydride (Asakura et al. 2006b) tend to make AKD dispersions less stable. Asakura et al. (2006b) found evidence that the presence of impurities in AKD wax tended to accelerate further hydrolysis, an effect that mirrors some findings in the case of ASA (Wasser 1987).

Even with a good stabilizing system and use of refrigeration, excessively long storage of AKD emulsions can be expected to result in significant hydrolysis, reducing

the efficiency of sizing (Isogai et al. 1992). Esser and Ettl (1997) found that the rate of hydrolysis of AKD tended to be faster in the case of dispersions stabilized by polyethyleneimine (PEI), in comparison to cationic starch as a stabilizer.

Retention of AKD during paper forming

Because AKD usually is added to paper machine systems having neutral to alkaline pH, conditions under which hydrolysis is accelerated, it is important that the product be retained efficiently (Davison 1986; Cooper et al. 1995; Esser and Ettl 1997). Material that is not retained during the first pass through the forming section will tend to break down, to some degree, as it remains an unnecessarily long time in contact with the alkaline process water.

Electrostatic factors appear to play important roles in AKD retention (Lindström and Söderberg 1986b, Isogai 1997; 2004a; Ravnjak 2006). Thus, negatively charged colloidal materials in the paper machine process water are expected to neutralize the cationically stabilized AKD particles, interfering with their adsorption onto cellulosic solids. The importance of negatively charged groups on fiber surfaces in retention of AKD particles stabilized by cationic polyelectrolytes was demonstrated by selectively blocking carboxylate groups (Isogai et al. 1997); less of the AKD was retained on aminated pulp. Similarly, Johansson and Lindström (2004a) found increasing retention efficiency of AKD onto fibers having increasing negative charge density. Though specific cationic polymers have been found to promote retention of AKD products (Moyers 1992; Hasegawa et al. 1997; Isogai 1997), it is usually sufficient just to aim for relatively high overall retention of fines, using conventional retention aid products (Johansson and Lindström 2004ab). As shown by Marton (1991), the amount of AKD that becomes attached to fiber fines and fillers tends to be out of proportion to the mass of those solids. Riebeling et al. (1996) observed that sequential treatment of the furnish with a hydrophobically modified amphoteric polymer was able to direct more of the AKD onto cellulosic surfaces, rather than the surfaces of calcium carbonate.

Composition and migration of AKD vapors

Though there is good reason to expect that vapor migration plays some role in AKD sizing, various studies have suggested that much of the material may be converted to the non-sizing ketone form, perhaps as a consequence of being present in a humid vapor phase. Akpabio and Roberts (1987) concluded that there was sufficient water even in "dry" paper to be able to convert palmitic AKD to palmitone. The vapor-phase treatment did not result in a significant hydrophobic effect, even though byproducts of AKD could be detected in the treated paper. Likewise, Hutton and Shen (2005) saw no development of sizing when AKD-saturated paper was separated from untreated paper by an air gap and heated to 105 ^{o}C or 175 ^{o}C. Results were consistent with the transfer of ketone, rather than active AKD. Laitinen (1999) observed considerable migration of ketone byproducts of AKD to an untreated sheet of wet paper applied to the wet web of AKD-treated paper on a pilot paper machine. Shen et al. (2005) observed that the vapor above heated AKD consisted mainly of fatty acids, rather than AKD or its ketone byproduct. It appears that similar chemical phenomena may underlie the ineffectiveness of AKD as a sizing agent under conditions of impulse drying, especially in the case of

relatively long pressing times (Mendes et al. 2003ab). Rather than proving that AKD does not migrate in vapor, as part of the sizing mechanism, the observations cited above suggest that effective AKD sizing requires a relatively narrow range of conditions. Such conditions might be achieved more easily in a real paper machine system, in contrast to artificial curing conditions that have been used in certain mechanistic studies.

Evidence favoring vapor deposition, as a mechanism of distributing AKD to sites on the paper surface where it can contribute to sizing, was provided by Davis et al. (1956). Sizing was achieved throughout paper's thickness when it was applied just to one side. Yu and Garner (1997) demonstrated vapor-phase sizing by AKD in sealed tubes. Increased bicarbonate alkalinity and polyethyleneimine (PEI) treatment of the paper, during its initial preparation, tended to increase the rate at which water contact angles increased, due to the vapor-phase sizing. Shen et al. (2001ab) observed sizing on uncovered surfaces that were heated adjacent to AKD-sized paper sheets.

Vapor distribution appears to play a further role in the development of AKD sizing effects after a size press. Brungardt (1997) reported cases in which over-drying of AKD-sized paper before a size press resulted in *less* sizing effects after starch had been applied and the paper had been redried. The effects were attributed to the ability of unreacted AKD in the paper to diffuse through the sheet and react with the starch layer on the paper in the after-size-press dryers. At high levels of AKD treatment there was no advantage of under-drying the paper before the size press, since there was always plenty of unreacted AKD in the paper, ready to take part in the proposed vapor-phase effect.

Before leaving the subject of vaporization, some comment should be made regarding molecular mass. If one were to form both ASA and AKD from 18-carbon alkanes and alkenes, the molecular mass of each AKD molecule would be about 1.5 times that of each ASA molecule. Each AKD molecule, being a dimer, contains two of the alkyl chains, whereas the ASA contains only one. All things being equal, higher molecular mass implies a lower partial pressure as a function of temperature. On that somewhat discouraging note, with respect to vapor-phase sizing with AKD, it makes sense to inquire about other possible mechanisms. Likewise, according to Dumas (1981) the relatively low volatility of stearic anhydride has been one of the primary reasons why it failed to achieve widespread use, in competition with ASA and AKD.

Spreading evidence

Considerable progress has been achieved recently with respect to evaluating the extent to which AKD is capable of spreading on heated cellulosic surfaces, either by bulk-phase flow or as a thin film. Though the results of bulk-phase surface tension measurements might suggest complete wetting of cellulosic surfaces by molten AKD, results of spreading experiments on smooth surfaces suggest otherwise (Seppänen and Tiberg 1999; Garnier and Yu 1999). For instance, Garnier and Yu (1999) observed isolated patches of AKD on a sized surface by means of atomic force microcopy (AFM). Researchers have observed finite angles of contact between droplets of AKD and various model surfaces representing the fiber (Garnier et al. 1999; Garnier and Godbout 2000).

Given the limited spreading tendency of liquefied AKD onto dry cellulosic surfaces, as just mentioned, researchers have suggested that AKD mainly moves in the form of thin "precursor" films adjacent to the bulk liquid (Seppänen and Tiberg 1999;

Garnier and Godbout 2000). Such spreading may involve multi-layer, in addition to monolayer flow (Shen et al. 2003). In theory, such films may have a lower surface energy than AKD itself, thus impeding spreading of the liquid phase. The advance of molecular films over higher-energy surfaces has been shown to be sensitive to surface imperfections. General roughness, including features perpendicular to the direction of migration, can be expected to halt, or at least slow the progress of a precursor film. In principle, tiny, deep grooves parallel to the direction of migration are expected to promote spontaneous spreading (Garnier and Godbout 2000). However, the cited authors did not expect such a mechanism to be rapid enough, under realistic conditions of paper manufacture, to have a significant effect.

In principle, the spreading within a very thin film would be expected to depend on the effective melting point of the material, the value of which might differ from the bulk melting point. Shen and Parker (2003) detected evidence to support this theory, showing that the freezing point of AKD in a thin film was lower than its bulk value. However, the ketone byproduct of AKD hydrolysis has a higher melting point than AKD itself, and the presence of the ketone appears to impede spreading of AKD precursor films (Shen et al. 2002). Though the ketone has a low surface energy, it apparently does not orient itself in a way such as to be able to achieve effective sizing (Shen et al. 2003). Similarly, the fatty acid component of wood resins can impede AKD sizing, possibly due to their adverse effect on spreading of AKD films (Lindström and Söderberg 1986b; Eklund and Lindström 1991).

To help explain the apparent disagreement among various findings, it has been found that areas of cellulosic surface covered by AKD products tend to be non-uniform, based on dynamic contact angle tests (Shen et al. 2001). Results suggested that much of the AKD-related material became deposited onto fibers as islands, overlying a mono-molecular film at the cellulosic surface. Such an explanation can explain why contact angle tests showed a uniformly hydrophobic surface only after solvent extraction to remove unbound materials (Shen et al. 2001). Taniguchi et al. (1993) found that AKD sizing often improved after treatment of the paper with either solvent or water, followed by redrying. In principle, such procedures can lead to a better distribution of sizing materials.

Covalent reactions

As was made apparent already in Fig. 2, there are various ways in which AKD may potentially react covalently in the course of paper production. Table 1 lists various species that have been detected after the AKD sizing of paper or model substrates, along with literature references tending to support the existence of various species.

The first three AKD-related chemical species listed in Table 1 appear to contribute to the hydrophobation of paper. Support for the formation of covalently bound AKD, the first item in the table, includes the fact that the paper's resistance to water usually cannot be removed by solvent extraction (Davis et al. 1956; Roberts and Garner 1981; Karademir et al. 2004; Avitsland et al. 2006). Ödberg et al. (1987) showed that bound AKD could be removed only when the solvent conditions favored hydrolysis of ester bonds. Bottorff (1993) observed ester peaks in solid-state ^{13}C NMR spectra after extraction of sized paper with tetrahydrofuran (THF).

Table 1. AKD-related Chemical Species Observed after Treatments of Paper or Model Substrates

Chemical Species	Literature Citations
β-keto esters of AKD bound the substrate	Davis et al. 1956; Roberts and Garner 1981, 1985; Lindström and O'Brian 1986; Lindström and Söderberg 1986a; Dumas and Evans 1986; Nahm 1986; Ödberg et al. 1987; Marton 1991; Bottorff 1993; Bottorff and Sullivan 1993; Marton 1995; Chen and Biermann 1995; Karademir and Hoyland 2003; Lee and Luner 2005; Avitsland et al. 2006
Oligomeric species	Roberts and Garner 1985; Bottorff 1993; Hardell and Woodbury 2002
Unreacted AKD	Bottorff 1993; Bottorff and Sullivan 1993; Jaycock and Roberts 1994; Karademir et al. 2004; Lee and Luner 2005
β-keto acids or salts	Rohringer et al. 1985; Bottorff 1993 (minor)
Ketone (hydrolysis product)	Akpabio and Roberts 1987; Bottorff 1993; Marton 1995; Karademir et al. 2004; Seo and Cho 2005

Various authors, using extraction and spectroscopic methods, estimated the proportion of AKD added to paper that eventually forms covalent bonds at fiber surfaces. The fraction of bound AKD was estimated as 34-78% (Dumas and Evans 1986), or up to 60-85% under the most favorable conditions (Lindström and O'Brian 1986). Slow drying conditions seem to favor AKD hydrolysis reactions over esterification (Mendes et al. 2003ab). This can explain why drying temperatures of 120 ^{o}C and above were required to achieve efficient AKD sizing under conditions employed by Kamutzki and Krause (1983). The presence of water appears to impede the distribution of the sizing agent during the early phases of drying (Lindström and Söderberg 1986a), allowing hydrolysis to take place while the sizing reaction is not yet enabled. Under more favorable conditions of drying the activation energy for ester bond formation has been found to be lower than that of the hydrolysis reaction (Lindström and O'Brian 1986), though the difference was found to narrow with increasing temperature (Marton 1995). Seo and Cho (2005) observed mainly formation of the ketone when AKD was reacted with cotton linter cellulose in an ionic liquid solvent system. However, such conditions do not provide any mechanism by which the AKD can be shielded from hydrolysis during a period in which water remains a dominant species in the mixture.

Estimates of the minimum theoretical amounts of sizing agent able to make paper hydrophobic can be obtained from certain studies in which the paper was extracted after treatment with AKD. In theory, solvent extraction is able to remove unbound materials, including unreacted AKD and the ketone hydrolysis product. Though it is less clear whether solvents are able to remove oligomerized AKD or the calcium salts of β-keto acids (see Fig. 2), one usually makes the assumption that the residual concentrations of the latter materials can be neglected. On this basis, Roberts and Garner (1985) found that 0.006 to 0.010% of AKD products, by mass, remained after extraction of sized paper. Dumas and Evans (1986) concluded that between 0.01 and 0.07% coverage of the paper surface by bound AKD molecules was sufficient to achieve sizing. Lindström and Söderberg (1986) reported that between 0.008 and 0.038% of bound AKD, on a mass basis, was sufficient. The lower end of this range was estimated to correspond to just 4% of a monolayer of coverage. The ability of the sizing agent to be effective at such low levels was attributed to rotation and "sweeping" of bound AKD molecules, affecting an

area considerably larger than is occupied by the molecule at any one moment. Marton (1991) estimated that just 20-38% of added AKD ended up becoming chemically bound to the paper surface under practical conditions of manufacture. Cooper et al. (1995) estimated that between 17 and 27% of the added AKD reacted with the paper surface.

Several researchers did not succeed in detecting covalent bonds between AKD and paper surfaces, and they concluded that such bonds may not play an essential role in paper sizing. Isogai (1999), using solid-state NMR, did not detect ester bonds after handsheets formed with AKD addition were dried at 20% or 50% relative humidity, or alternatively in an oven at 105 ^{o}C. Follow-up work (Isogai 2000) showed that if β-ketoester bonds had been able to form, they would have been stable to the conditions of enzymatic treatment that were used in the analysis. Likewise Rohringer et al. (1985) failed to detect ester absorbances in IR spectra. Drying was delayed by placing the test samples between pieces of blotter paper. A possible explanation for the results is that the hydrolysis reaction was favored by relatively low temperatures and long exposure times.

In related work, Lee and Luner (2005) observed that non-bound species, such as unreacted AKD, were able to contribute significantly to sizing when there was at least some bound AKD present. The unbound material made its greatest relative contribution to sizing when the bound material was about 0.025% on a mass basis. The synergistic effect, involving bound and unbound molecules to achieve sizing, suggests that the hydrophobic molecules associate with each other at the paper surface. Nahm (1986) observed a related effect in which bound AKD molecules tended to be clustered together on surfaces, suggesting that association between the hydrophobic groups helps to direct unreacted AKD molecules towards hydroxyl groups at the paper surface.

Lee and Luner (2005) also observed that AKD's reaction tended to be more efficient in the presence of humidity, compared to completely dry conditions. Their observations suggest that the presence of moisture increases the availability of surface hydroxyl groups to react with the AKD molecules. In principle, hydrogen bonds that are engaged in intra-molecular or intra-fiber hydrogen bonding would not be available the react with AKD. It would make sense that water molecules, in a humid environment, can displace some of these cellulose-to-cellulose hydrogen bonds, forming structures more accessible to AKD. Similar considerations also can help to explain the greater ease of sizing of never-dried fibers, in comparison to fibers that have been dried one or more times (Davis et al. 1956). Drying results in formation of an increased proportion of intra-fiber hydrogen bonds, and the process is not completely reversible (Stone and Scallan 1966; Hubbe et al. 2003).

Because the hydroxyl groups on paper's surfaces are assumed to play a major role in the formation of any ester bonds with sizing agents, one would expect coverage of those groups with other materials to make paper more difficult to size. Accordingly, Avitsland et al. (2006) observed that wood extractives tended to reduce the amount of AKD that was able to react with bleached kraft pulps.

Oligomers formed during the heating of AKD have been found to contribute to hydrophobicity (Bottorff and Sullivan 1993). However, the effectiveness of AKD oligomers is sufficiently low that their presence in AKD wax was found to have a net negative effect on sizing, in comparison with relatively pure AKD (Asakura et al. 2006).

Cure promoters

If one starts with the assumption that AKD needs to form ester bonds in order to size paper efficiently, as demonstrated by various studies cited above, then if follows that paper technologist are likely to seek ways to encourage such reactions. Investigators have shown that polymeric amines can promote AKD curing (Lindström and Söderberg 1986; Thorn et al. 1993; Kondo and Makino 1993; Cooper et al. 1995; Marton 1995; Mendes et al. 2003c). The fact that the most effective cure promoters of this type contain secondary or other non-quaternary amine groups (Thorn et al. 1993; Kondo and Makino 1993; Cooper et al. 1995), suggests that AKD reacts with such groups during the drying of paper. Some of these studies showed that the same cationic polymers that tended to promote the reaction of AKD in paper sizing also tended to hasten hydrolytic decomposition of AKD after its formulation (Colasurdo and Thorn 1992; Marton 1995). After curing, it has been found that the sizing effects resulting from "promoted" AKD tend to be stable over time, not suffering the "reversion" problems, which will be discussed next (Bottorff 1993). Cooper et al. (1995) suggested, however, that some of the apparent "promoting" effect of amine-type polymers may be due to increased or more uniform retention of the AKD during paper formation.

Increasing bicarbonate alkalinity also promotes the sizing reaction of AKD (Lindström and Söderberg 1986c; Jiang and Deng 2000). Results have been attributed either to a pH buffering effect (Jiang and Deng 2000) or to a lower-energy transition state in the reaction, involving the bicarbonate ion (Lindström and Söderberg 1986).

Sizing reversion

Though only a few authors have offered evidence for the presence of β-keto acids and the corresponding salt forms in paper (Rohringer et al. 1985; Bottorff 1993), it is logical to expect such bonds to form initially when AKD first encounters calcium carbonate surfaces when paper is dried. Bottorff (1993) observed transient calcium salts of β-keto acids in freshly-sized paper, but the material reverted to a keto form during storage. This concept can help to explain why AKD-sized papers made with calcium carbonate filler often show significant loss of sizing effects in the days and weeks after the paper is made (Patton 1991; Colasurdo and Thorn 1992; Novak 1993; Bartz et al. 1994; Esser and Ettl 1997). The effect has been found to be more pronounced in the case of precipitated calcium carbonate (PCC) filler (Colasurdo and Thorn 1992; Bartz et al. 1994; Esser and Ettl 1997), an observation that is consistent with the higher surface area of many PCC products, compared to typical ground $CaCO_3$ fillers. Bartz et al. (1994) observed increasingly severe sizing reversion with decreasing particle size and increasing surface area of PCC. Transient salts of β-keto acids can help to explain why the size can be extracted from calcium carbonate surfaces (Voutilainen 1996). Sizing reversion problems often can be reduced by increasing the distance between addition points for AKD and $CaCO_3$, allowing cationic starch or other species to adsorb onto the mineral surfaces ahead of the sizing agent (Esser and Ettl 1997).

Isogai and Asakura (1999) explored other aspects of size reversion, showing that the unsaturated form of AKD tends to be more susceptible to sizing loss when exposed to air-blowing and UV light. Such treatments might be expected to attack the double bonds

within ester-bonded alkenylketene dimer molecules at the paper surface, especially if the electric motor used to blow the air is a significant source of ozone.

Case 3: Rosin Sizes

Rosin-type sizing agents are often called "acidic sizes." They tend to be most efficient in pH ranges of about 4 to 6, depending on the type of rosin and various other factors. Rosin products usually require higher levels of addition, compared to the ASA and AKD sizing agents just discussed. Most rosin is sold either as a dispersion (or "emulsion") of rosin acid particles or as a micellar soap solution. The formulation of dispersion-type rosin products (Ehrhardt and Gast 1988; Shen et al. 2004) is not unlike that of ASA or AKD, except that there is no need to be concerned about hydrolysis. Both forms of rosin product require use of a mordant, such as alum, to fix the hydrophobic molecules to the paper surface (Strazdins 1977, 1984; Marton 1989). In the case of dispersion-type products, interaction with alum mainly takes place during the drying of paper (Ehrhardt and Gast 1988). By contrast, soap rosin products already become precipitated onto fiber surfaces by addition of alum at the wet end of the paper machine (Back and Steenberg 1951). These differences are illustrated in Fig. 3, which uses a fortified rosin molecule for purposes of illustration (see later).

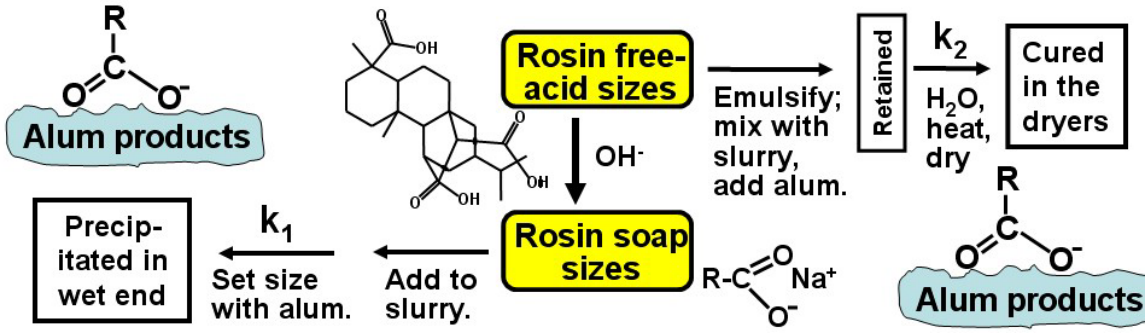

Fig. 3. Summary of the main sizing pathways for two types of rosin sizing agents

The active ingredient of rosin products usually is obtained as a byproduct of kraft pulping. The tall oil that separates from the aqueous phase after a kraft cook can be fractionated, making it possible to collect a mixture that is rich in terpenoids, including abietic acid (Strazdins 1989; Lee et al. 2006). Abietic acid is a multi-ring compound. It is generally hydrophobic, except that it contains a carboxylic acid group. Most rosin used in papermaking has been partially "fortified" by treatment with either maleic or fumaric anhydride (Strazdins 1977). Fortification introduces two more carboxyl groups, after reaction with water. The carboxyl groups appear to facilitate either formation of a stable soap and more stable emulsions (Davison 1975). Fortification also inhibits crystallization of rosin products. Best results usually are obtained when only a small proportion of the abietic acid molecules are fortified (Eklund and Lindström 1991). Before forming an emulsified product, a slightly saponified mixture of partially fortified rosin is heated above its melting point.

The somewhat uncontrolled manner in which rosin soap size becomes precipitated (Strazdins 1977, 1981, 1984), and also the relatively high melting point of the aluminum

rosinates that form (Strazdins 1981) have been cited to help explain the relatively inefficient nature of this traditional sizing technology. Reaction of rosin soap and alum has been shown to yield mixtures of aluminum diresinate and free rosin (Davison 1975; Eklund and Lindström 1991). Sizing performance sometimes can be improved by adding coordinating ions such as citric acid, which lowers the melting point of the size particles (Strazdins 1981). If the paper mill's process water is hard, containing a relatively high level of calcium or magnesium, these ions can cause premature agglomeration of the rosin soap without significant contribution to water resistance (Strazdins 1977). To avoid this, papermakers often add aluminum compounds to the system before the rosin, even in the case of soap sizing. It has been reported that esterified rosin products (see later) are less sensitive to water hardness and other issues affecting electrostatic inter-actions during rosin sizing (Nitzman and Royappa 2003). Though rosin is the best-known product for soap sizing, the soaps of other materials such as fatty acids (Eklund and Lindström 1991, Shimada et al. 1997), and hydrolyzed ASA (Hatanaka et al. 1991) also are known to develop sizing upon the addition of alum or polyaluminum chloride (PAC).

Rosin dispersion products are capturing an increasing share of the rosin size market. When stabilized with a cationic polymer, rosin dispersion products offer advantages of self-retention onto fiber surfaces, lower melting points compared to precipitated soap size particles, and tolerance of somewhat higher pH values (Ehrhardt and Gast 1988; Lauzon 1997).

Self-sizing

Clues to the mechanisms involved in rosin sizing can be found in a phenomenon known as "self-sizing." Especially in the case of paper and paperboard made under acidic conditions from relatively high-yield fibers, the paper can gradually develop water-repellency over time, even without the addition of rosin (Galvin 1988; Hodgson and Ness 1999). Such uncontrolled hydrophobicity can become a serious problem, as in the case of corrugating medium, which needs to be sufficiently absorptive in order for gluing to be effective (Galvin 1988).

The role of wood extractives in self-sizing is shown by the fact that solvent extraction of pulp, before papermaking, can eliminate the effect (Swanson and Cordingly 1956; Soteland and Loras 1976). Swanson and Cordingly (1956) and Swanson (1978) proposed that self-sizing occurs as a result of vapor-phase diffusion of extractable materials during storage of paper. Sizing was observed in untreated sheets that were heated in sealed tubes, adjacent to wood pitch samples (Swanson and Cordingly 1956). Alum appears to accelerate self-sizing by providing anchoring sites at the paper surface, upon which resin acid and fatty acid molecules can become anchored and oriented (Swanson and Cordingly 1959; Aspler et al. 1985; Hodgson and Ness 1999). The fact that self-sizing becomes more rapid at high temperatures, for instance during the gradual cooling of a freshly-made roll of paper (Hodgson and Ness 1999), is consistent with these suggested mechanisms. One practical way to combat self-sizing effects is to add a surfactant to the paper (Aspler et al. 1985).

Though rosin size products ordinarily are not considered to be "reactive", there is evidence that, given sufficiently high temperature and time, the carboxyl groups on rosin can form esters with the hydroxyl groups on fiber surface (Swanson 1978; Zhuang et al.

1997; Hodgson and Ness 1999; Ness and Hodgson 1999). Such ester-bound rosin cannot be extracted. Under ordinary conditions of paper drying, such covalent bonds are not expected to play a major role.

Given the relative non-reactivity of rosin products, in comparison to ASA and AKD already described, it is perhaps surprising that both rosin dispersions and rosin soap products tend to be intolerant of very high temperatures within the paper machine system (Marton 1989). In the case of dispersed free-acid rosin products, there are two likely explanations. First, increasing temperatures above about 50 ^{o}C can make the particles excessively tacky, resulting in agglomeration and less uniform distribution within the paper. Second, the higher temperature itself, as well as the resulting more liquid-like state of the rosin, will tend to speed up undesired conversion of the free acid to the soap form, which requires pH values below about 5 to react efficiently with alum (Marton 1989). In the case of soap sizing, the effect may be related to agglomeration, leading to increasing sizes of precipitated aluminum rosinate particles, again leading to inefficient coverage of the paper surface (Strazdins 1977).

Mordants for fixing and orienting adsorbed rosin molecules

If one excludes conditions so vigorous as to produce ester bonding, as just cited, then it is generally agreed that effective rosin sizing requires that a strongly positively charged species be present to anchor and orient molecules of rosin. In other words, there needs to be a mordant. Aluminum sulfate, or "papermaker's alum" is well known as an inexpensive and effective mordant for rosin sizing, especially in a pH range between about 4 and 5.5 (Back and Steenberg 1951; Strazdins 1977). It has been shown that aluminum species adsorb mainly on carboxylated sites at the fiber surface, thereby providing anchoring sites for rosin, which becomes distributed over the surfaces as paper is dried (Kitaoka et al. 1995). Alum-induced sizing appears to involve coordination-type bonds (Hodgson and Ness 1999). This assertion is supported by the fact that rosin sizing can be defeated by aluminum-complexing ions (Chen and Biermann 1995). Recent research has shown that alum is just one of many possible mordants. In Table 2 these candidate materials are listed roughly in order of the pH ranges in which the added materials have been found to function best in the promotion of rosin sizing.

Although Table 2 shows a pH range up to about 7.5 in the case of poly-aluminum chloride (PAC), such high pH values tend to convert aluminum ionic species to neutral alum floc, $Al(OH)_3$. Rosin acid molecules are expected to react with aluminum products attached to fiber surfaces as they become distributed during drying of the paper (Ehrhardt 1987; Marton 1989). However, the neutral species of alum are not expected to be very effective for retaining rosin particles when paper is being formed (Poppel and Bobu 1987). Thus, when paper technologists want to employ rosin products and aluminum products at neutral to weakly alkaline conditions, it makes sense to minimize the length of time that the aluminum product is in contact with the furnish (Ehrhardt and Gast 1988). Alternatively, some researchers have investigated sizing strategies involving pre-mixing of PAC or other aluminum products with rosin (Liu 1993; Peck and Markillie 1994; Zou et al. 2004), and then adding the mixture to the fiber furnish.

Table 2. Chemicals Having Ability to Act as Mordants for Rosin Sizing

Type of Mordant	Most Favorable pHs	Literature References
Aluminum sulfate	4 – 4.5 (soap sizing) 4.5 – 5.5 (dispersed rosins)	Back and Steenberg 1951; Strazdins 1977
Poly-aluminum Chloride (PAC)	5 – 7.5	Traugott 1985; Isolati 1989; Liu 1993; Chen et al. 2001
Metals that form hydroxides	Depends on the metal	Strazdins 1963; Subramanyam and Biermann 1992; Zhuang and Beirmann 1995
Poly-ethyleneimine (PEI)	Near-neutral	Li et al. 2003; Hartong and Deng 2004
Linear polyamines	Near-neutral	Wu et al. 1997
Cationic amides of low charge density	Neutral – weakly alkaline	Wang and Tanaka 2001

With respect to inorganic ions, as mordants, Zhuang and Biermann (1995) observed that the most efficient rosin sizing tended to be achieved near to the pK_a value of the species under consideration.

In the case of the amine-type polymers listed in Table 2, the published evidence suggests that the sizing mechanism may involve some formation of covalent bonds between rosin molecules and the polymer (Hartong and Deng 2004). The mechanistic role of cationic polymers is somewhat hard to pin down, however, since the same additives can play a significant role in retaining the size particles as the paper is being formed (Norell et al. 1999). Similarly, Hedborg and Lindström (1993) showed that efficient rosin sizing could be achieved under neutral conditions by use of a retention aid system that contained colloidal aluminum compounds as one of the additives.

Sizing contribution of non-bound species

Recent work showed, in the case of sizing with dispersed rosin, that much of the sizing agent remained in an unreacted, free-acid form, even after the paper was dried (Kitaoka et al. 1997). In apparent contradiction of the theory that aluminum in the sheet ought to be binding rosin to the paper surface (Marton 1989), no evidence of aluminum rosinate formation was found (Kitaoka et al. 1997). Such observations provide a lead-in to the topic of esterified rosin sizing agents. By esterification, many of the carboxyl groups on rosin essentially become blocked, no longer able to participate in interactions with any of the mordant materials just described. Nevertheless, esterified rosins have extended the range of rosin sizing to somewhat higher pH values (Fallmann and Bernardis 1997; Iwasa 1999; Ito et al. 1999; Fischer 1999; Nitzman and Royappa 2003; Liu et al. 2004). A likely explanation for these effects is that a degree of ionic binding involving far lower than 100% of the hydrophobic molecules may be sufficient to achieve a stable sizing effect. Thus, it is not surprising that superior results often are achieved with optimized mixtures of esterified and conventional partially fortified rosin products (Iwasa 1999), only the latter of which have a mechanism that allows strong anchoring of the molecules. In theory, the bound molecules will tend to hold the unbound molecules in place by hydrophobic association. Such a mechanism also can help explain why rosin esters, by themselves, sometimes show almost no sizing effect (Wang et al. 1999).

Case 4: Polymeric Sizing Agents

Though copolymers of various sorts are more often used at the size-press of paper machines to impart water repellency (Batton 1995; Garrett and Lee 1998), their use at the wet end can provide us with further insights, especially when contrasted with the ASA, AKD, and rosin sizes just discussed. Polymeric wet-end hydrophobic agents can include ethylene-acrylic acid copolymers (Finlayson et al. 1996; Wang et al. 1997; Hodgson 1997), styrene-maleic-anhydride (SMA) copolymers (Batton 1995), when used at the wet end, cationic styrene copolymers (Ono and Deng 1997; Yang and Deng 2000), derivatized acrylamides (Takai et al. 1997), and derivatized starch (Yang et al. 1999). Products having cationic groups (Ono and Deng 1997; Yang and Deng 2000; Valton et al. 2003) generally can be efficiently retained during papermaking without depending on other additives. By contrast, anionic copolymers are used in sequence with cationic additives such as alum (Takai et al. 1997; Wang et al. 1997) or cationic copolymer retention aids (Finlayson et al. 1996). Polymeric sizes tend to be less efficient on a mass or cost basis, compared to the amounts of ASA or AKD to achieve a given level of hydrophobicity. On the plus side, they have potential to offer a more precise and reliable gradation of sizing, and they don't suffer from any size-reversion issues. When properly formulated, polymeric sizing agents can have a long shelf-life (Finlayson et al. 1996).

Accounts of sizing with polymeric materials provide various examples in which it is clear that distribution over the fiber surfaces tends to be patch-like, or at least non-uniform on a molecular scale. For instance, Carceller and Juppo (2005) observed that the amphiphylic copolymers they studied tended to form 30 nm particles. The dried film resulting from such treatment showed a network pattern. Garnier et al. 2000 showed that SMA macromolecules tend to self-associate, especially under pH conditions such that about half of the carboxyl groups were in their ionic form. Others have achieved sizing effects with materials consisting of latex-like particles or microaggregates (Ono and Deng 1997; Yang and Deng 2000; Finlayson et al. 1996).

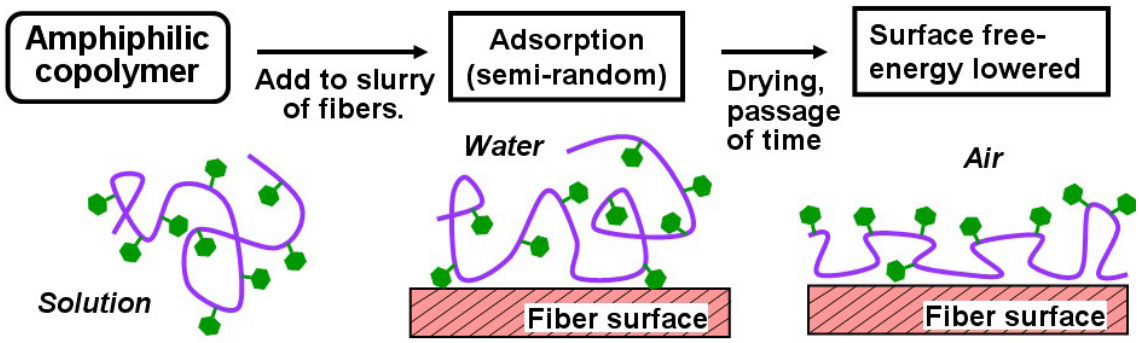

Fig. 4. Concept of rearrangement upon drying of amphiphilic copolymer, such that more hydrophobic groups end up facing the air phase and more hydrophilic groups end up facing the fiber

Although copolymeric sizing agents cannot migrate through the vapor phase or as monomeric films, it is reasonable to expect that they change their molecular conformations when paper is dried. As illustrated in Fig. 4, it would be expected that water-hating groups would tend to orient themselves facing outwards from the paper surface during

the final stages of drying, thus decreasing the interfacial free energy of the system (Garnier et al. 2000). Garrett and Lee (1998) suggested that the copolymers may be able to gradually rearrange their conformation upon exposure to water, such that an increasing proportion of hydrophilic groups face the aqueous phase. Yasuda et al. (1995) confirmed such rearrangement by ESCA analysis for another type of amphiphilic copolymer. Such conformational adjustments may provide a mechanism by which to achieve intermediate levels of resistance to fluids in a reliable way.

ADDING UP THE EVIDENCE

Based on work cited in the preceding section it is possible to claim general support for the hypothesis proposed earlier. Thus, the hydrophobic active ingredient of the sizing agent must contain a hydrophobic group, it must become well dispersed, it must remain in its active form up to a critical point in the papermaking process, it must be retained efficiently in the wet-web of paper, it must become well distributed on the outer surfaces of the paper by the time it is dried, and individual molecules of the sizing agent must become anchored and oriented in order to achieve a stable and efficient sizing effect. However, sizing systems are subject to a variety of interferences, competing reactions, and unique properties of the sizing molecules. Some of these complicating factors will be highlighted here.

Sizing Can Be Blocked or Covered

Studies of the fundamentals of paper sizing sometimes may be misleading in cases where the systems under investigation are artificially "clean." Various studies have shown that solvent-extractable materials in papermaking furnish can adversely affect sizing treatments (Johansson and Lindström 2004a; Liden and Tollander 2004). Some of the evidence suggests that anionic colloidal material, such as extractives, can interfere with the retention of sizing agents during papermaking (Mikkonen and Eklund 1998). In other cases, surface-active materials in the furnish just act as wetting agents, presumably because they lack a mechanism that would anchor them in position, orienting the molecules in the manner of an effective sizing agent (Moyers 1992; Brinen and Kulick 1995, 1996; Boone 1996).

In other cases extractives on the surfaces of paper appear to block sites that otherwise could become occupied by molecules of a sizing agent (Zeno et al. 2005; Avitsland et al. 2006). A similar phenomenon may explain the adverse effect of aluminum sulfate on AKD sizing (Kamutzki and Krause 1983). Moderate amounts of alum decreased the effectiveness of AKD, despite the fact that retention efficiency of the sizing agent was greatly improved. The effect suggests that the fiber surfaces became covered by a film of oligomeric hydrated aluminum species (Strazdins 1984), and that AKD was not able to form covalent bonds to such species. A similar explanation can be offered to explain the difficulties of obtaining stable sizing in the presence of high levels of PCC filler (Patton 1991; Moyers 1992; Bartz et al. 1994; Esser and Ettl 1997).

It Doesn't Take Much

Another take-away message from the published literature, especially as it pertains to ASA and AKD, is that very little hydrophobic material is required, if only it could be distributed in an ideal way and reacted at 100% efficiency. As discussed earlier, researchers have achieved sizing effects with as little as 0.006 to 0.01% of sizing materials remaining in paper after solvent extraction (Roberts and Garner 1985; Dumas and Evans 1986; Lindström and Söderberg 1986). Advanced methods are required even to quantify the presence of sizing agents in paper, let alone determine the manner in which they are bound (Dart 1990; Sundberg et al. 1999; Vrbanac et al. 1999; Yano et al. 2000; Odermatt et al. 2003). Davison (1986) estimated that it takes about 1 mg of sizing agent per square meter of surface to form half of a contiguous monolayer. If one assumes that the surface area of dry paper lies within 1-3 m^2/g, it follows that a loading of 0.05 to 0.15% sizing agent in paper ought to be enough to size paper. It is reasonable to expect less than a molecular layer of sizing agent to be effective, due to the fact that a molecule attached at one end can be expected to "sweep" a larger area than it occupies at any instant (Lindström and Söderberg 1986).

It Doesn't Have to be Uniform

The effectiveness of low levels of sizing agents also can be attributed to hysteresis effects, *i.e.* the reluctance of a liquid meniscus to advance across rough, porous, or heterogeneous surfaces (von Bahr et al. 2004). Matsuyama et al. (2006) found support for the theories of Cassie and Baxter (1944), showing that it is difficult for a meniscus of water to advance across a dry, porous surface. These researchers were able to achieve a high degree of hydrophylicity by covering just 20% of a hydrophilic substrate with hydrophobically modified colloidal gold particles. The study also demonstrated the validity of early work by Wenzel (1936), related to the equilibrium contact angles of fluids on surfaces having a very fine scale of roughness. Wenzel's main conclusion can be summarized by stating that fine-scale roughness can greatly increase the contrast between wettable and hydrophobic surfaces, and one can expect a relatively sharp transition from one state to the other at a certain level of treatment with a hydrophobic agent. All of the effects mentioned above help to explain why significant sizing often is observed only after the amount of sizing agent has reached a threshold, whereas further increases in size dosage often yield sharp increases in fluid resistance (Dumas and Evans 1986; Wasser 1986; Crouse and Wimer 1991; Esser and Ettl 1997; Johansson and Lindström 2004b; Isogai and Morimoto 2004).

On a micrometer scale, various studies have shown non-uniformity in the surface distribution of sizing agents. Such observations have been reported especially in the case of rosin sizing (Davison 1975; Strazdins 1981; Ozaki and Sawatari 1997; Wang et al. 2000), and excessively non-uniform coverage has been correlated to inefficient sizing (Lee 1936; Strazdins 1981). In the early work by Lee (1936) the most efficient sizing with rosin soap was achieved when the size particles were the smallest, achieving a better distribution. More recent work shows, however, that microscopic studies may miss an important part of the story; Ozaki and Sawatari (1997), using electron probe micro-analysis (EPMA), detected an uneven distribution of rosin. However, the same samples, when studied by time-of-flight surface ionization mass spectroscopy (TOF-SIMS)

revealed a molecular layer of rosin covering essentially the whole surface. Related results were obtained by Shen et al. (2001) in the case of AKD sizing. Dynamic contact angle analysis of AKD-sized fibers revealed a high degree of heterogeneity. However, steady contact angles and a high degree of hydrophobicity were observed after solvent extraction to remove unbound material.

Airborne Distribution Supplements Partial Spreading

Vapor-phase transport of sizing agents is relatively easy to demonstrate by solvent-treatment of one sheet, and then placing the treated sheet in a foil wrapper with a stack of untreated sheets. In the case of reactive sizing agents such as ASA, AKD, and stearic anhydride, sizing effects develop in untreated sheets, even when they are separated by several layers from the treated sheet. Vapor-phase transport of various compounds related to sizing agents have been demonstrated (Davis et al. 1956; Swanson 1978; McCarthy and Stratton 1987; Back and Danielsson 1991; Yu and Garnier 1997; Shen et al. 2001; Gess and Rende 2005).

Though the traditional explanations for sizing effects often assume melting and spreading of droplets of sizing agents on the solid surfaces of paper (Davison 1986), we have seen earlier in this review that most evidence suggests rather limited spreading of liquid sizing agents (Seppänen and Tiberg 1999; Garnier et al. 1999; Garnier and Godbout 2000; Lindfors et al. 2005). Likewise, the spreading of monomolecular "precursor" films appears to be rather inefficient (Garnier and Godbout 2000). Evidence for and against a vapor-phase mechanism of size distribution is sometimes clouded by competing reactions. Thus, attempts to find evidence for AKD migration through the vapor phase sometimes show only the hydrolysis product on the target surfaces (Akpabio and Roberts 1987; Hutton and Shen 2005).

Non-bound Materials Can Contribute

Another general conclusion that can be drawn from published literature already cited is that although unbound hydrophobic species *can* contribute to sizing, as long as conditions are favorable, these contributions tend to be supplemental, rather than central to efficient sizing practices. As was noted, such contributions can depend strongly on having a certain amount of bound sizing agent present (Lee and Luner 2005). Lindström and Söderberg (1986a) obtained an especially convincing set of data, showing very high correspondence between the amounts of chemically bound AKD and the degree of water hold-out, irrespective of the presence or absence of other chemical species related to AKD. Some researchers have described unbound hydrophobes as inefficient sizing agents, compared to those molecules that are properly anchored and oriented (Lindström and Söderberg 1986; Bottorff and Sullivan 1993). Other research found little or no contribution to sizing effects due to unreacted AKD (Karademir 2002).

To present a balanced picture, some researches have noted cases where the contribution of unbound hydrophobic materials appeared to be important. Significant contributions to sizing have been reported for unreacted AKD (Lindström and Söderberg 1986; Colasurdo and Thorn 1992), as well as unbound oligomers of AKD (Bottorff 1993; Bottorg and Sullivan 1993). Colasurdo and Thorn (1992) demonstrated the sizing effect of unreacted AKD by showing cases in which solvent extraction made the paper wettable

again. In the case of rosin, Kitaoka et al. (1997) estimated that 80% of the added rosin remained in an unchanged, free-acid chemical form, following sizing with a dispersed rosin product. Subsequent solvent extraction eliminated the sizing effect. Aluminum rosinates were not detectable, despite the fact that without aluminum salts in the system, no sizing was observed.

PATHS TOWARDS HIGHER SIZING EFFICIENCY

Major increases in the efficiency of sizing systems are possible, relative to today's technology, at least in theory. The rather inefficient nature of the available sizing technologies has been documented in earlier sections of this article. Though there is no assurance that the theoretical limits of sizing efficiency ever can be achieved in practice, one can point to a number of variables that will need to be considered. Among these are the design of the hydrophobic group, the nature of the anchoring group, and the sizing agent's vapor pressure as a function of temperature. For sake of discussion, let us assume that issues related to retention of the sizing agent and avoidance of the effects of interfering substances, such as surface-active materials, can be addressed by known technologies, such as pulp washing and the use of retention aid systems.

With respect to the design of hydrophobic groups, both the size and the shape can be expected to be important. Various studies have shown increasing effectiveness of sizing agents with increasing chain length of alkyl groups, assuming that curing conditions are sufficient to achieve good distribution and reaction (Roberts et al. 1993; Smith 1999). A somewhat bulky, centrally-attached hydrophobic group, as in the case of rosin (Shimada et al. 1997) or isomerized ASA (Roberts et al. 1993; Smith 1999) can be expected to protect the bond by which the sizing molecule is attached and oriented. An isomerized alkenyl group, in the case of ASA, also is expected to hide the extra carboxylate group that results during the formation of an ester bond (Roberts et al. 1993). However, the currently available sizing agents do not come close to exhausting the possible kinds of hydrophobic groups that could be used in the future to better meet the needs of end-users. For example, it may be possible to achieve superior adhesion of inks and toner particles to sized paper (Borch 1986), if a reactive sizing agent were prepared with a hydrophobic group related to either styrene or rosin.

Researchers hoping to find a more effective reactive group, in comparison to ASA or AKD, face considerable challenge. Many alternative reactive chemistries have been considered, but none of them have achieved long-term commercial success (Dumas 1981; Jing et al. 1998). Not only must the active material be able to form a stable attachment to fiber surfaces, but it also has to resist adverse side reactions during storage and during production of the paper (Robert 1997). Work by Rossall and Robertson (1975) suggests that the reactivity of sizing chemicals towards hydroxyl groups at the fiber surface and towards water might be fine-tuned by varying the size of anhydride rings and by judicious use of conjugated double bonds associated with those rings. Another possible approach would be to encapsulate sizing agents, such that the active ingredient is released only after most of the moisture has been dried from a sheet of paper (Hunkeler 2006).

Relative to the importance of the subject, little published work has touched upon optimization of the partial pressure of sizing agents as a function of temperature. Adverse effects of excessively volatile sizing agents include deposits in the hoods of paper machine drier sections (Gess and Rende 2005) and the concurrent inefficiencies. At the other extreme, AKD products are typically about 1.5 times the molecular mass of an ASA molecule. This circumstance may help explain why over-drying of paper is often required to achieve sizing ahead of a size press (Roberts 1997), and why full AKD sizing often is not achieved until after storage of paper rolls. An AKD product having a single alkyl chain might come closer to the optimum in terms of vapor pressure, though someone needs to figure out what to do with the other end of the molecule. This question, as well as a great many questions related to addition strategies and interactions with other wet-end additives can be expected to keep paper technologists occupied for a long time to come.

REFERENCES CITED

Akpabio, U. D., and Roberts, J. C. (1987). "Alkylketene dimer sizing: Vapor-phase deposition of tetradecylketene dimer on paper," *Tappi J.* 70(12), 127-129.

Aloi, F., Trksak, R. M., and Mackwicz, V. (2001). "The effect of base sheet properties and wet end chemistry on surface-sized paper," *Proc. TAPPI 2001 Papermakers Conf.*, electronic document.

Asakura, K., Iwamoto, M., and Isogai, A. (2005). "Effects of fatty acid components present in AKD wax on emulsion stability and paper sizing performance," *J. Wood Chem. Technol*. 25(1-2), 13-26.

Asakura, K., Iwamoto, M., and Isogai, A. (2006a). "The effects of AKD oligomers present in AKD wax on dispersion stability and paper sizing performance," *Nordic Pulp Paper Res. J.* 21(2), 245-252.

Asakura, K., Iwamoto, M., and Isogai, A. (2006b). "Influences of fatty acid anhydride components present in AKD wax on emulsion stability and paper sizing performance," *Appita J.* 59(4), 285-290.

Aspler, J. S., Chauret, N., and Lyne, M. B. (1985). "Mechanism of self-sizing in paper," in *Papermaking Raw Materials*, Punton (ed.), Mechan. Eng. Publ., England, Vol. 2, 707-727.

Avitsland, G. A., Sterner, M., Wågberg, L., and Ödberg, L. (2006). "AKD sizing of TCF and ECF bleached birch pulp characterized by peroxide edge wicking index," *Nordic Pulp Paper Res. J.* 21(2), 237-244.

Avitsland, G. A., and Wågberg, L. (2005). "Flow resistance of wet and dry sheets used for preparation of liquid packaging board," *Nordic Pulp Paper Res. J.* 20(3), 345-353.

Back, E., and Steenberg, B. (1951). "Isolation and properties of aluminum di- and mono-abietate," *Svensk Papperstidn.* 54, 510-516.

Back, E. L., and Danielsson, S. (1991). "Hot extended press nips as gas-phase reactors: Hydrophobation with ASA," *Tappi J.* 74(9), 167-174.

Barker, L. J., Proverb, R. J., Brevard, W., Vazquez, I. J., dePierne, O. S., and Wasser, R. B. (1994). "Surface absorption characteristics of ASA paper: Influence of surface

treatment on wetting dynamics of ink-jet ink," *Proc. TAPPI 1994 Papermakers Conf.*, TAPPI Press, Atlanta, 393-397.

Bartz, W. J., Darroch, M. E., and Kurrle, F. L. (1994). "Alkyl ketene dimer sizing efficiency and reversion in calcium carbonate filled papers," *Tappi J.* 77(12), 139-149.

Batten, G. L., Jr. (1995). "The effects of SMA surface sizes on paper end-use properties," *Tappi J.* 78(1), 142-146.

Boone, S. R. (1996). "How does the use of recycled fiber affect sizing chemistry – Both internal sizing and surface or on-machine sizing?" *Prog. Paper Recycling* 5(2), 99-102.

Borch, J. (1986). "Sizing and its effect on paper-polymer adhesion," *Paper Technol. Ind.* 26(8), 388-395.

Bottorff, K. J. (1993). "The AKD sizing mechanism: A more definitive description," *Proc. TAPPI 1993 Papermakers Conf.*, TAPPI Press, Atlanta, 441-450.

Bottorff, K. J., and Sullivan, M. J. (1993). "New insight into the AKD sizing mechanism," *Nordic Pulp Paper Res. J.* 8(1), 86-95.

Bown, R. (1996). "Physical and chemical aspects of the use of fillers in paper," in *Paper Chemistry*, 2nd Ed., J. C. Roberts (ed.), Blackie Academic & Professional, London, Ch. 11, 194-230.

Brinen, J. S., and Kulick, R. J. (1995). "SIMS imaging of paper surfaces. Part 4. The detection of design agents on hard-to-size paper surfaces," *Int. J. Mass Spectroscopy Ion Proc.* 143, 177-190.

Brinen, J. S., and Kulick, R. J. (1996). "Detection of ASA and desizing agents in hard to size paper surfaces by SIMS," *Proc. 1996 International Paper and Coating Chemistry Symp.*, CPPA, 125-129.

Brungardt, B. (1997). "Improving the efficiency of internal and surface sizing agents," *Pulp Paper Can.* 98(12), T480-T483.

Brungardt, C. L., and Gast, J. C. (1996). "Alkenyl-substituted sizing agents for precision converting grades of fine paper," *Proc. TAPPI Papermakers Conf.*, TAPPI Press, Atlanta, 297-308.

Carceller, F., and Juppo, A. (2005). "Nanostructures in aqueous dispersions for surface sizing," *Paperi Puu* 87(1), 35-37.

Cassie, A. B. D., and Baxter, S. (1944). "Wettability of porous surfaces," *Trans. Faraday Soc.* 40, 546-551.

Chatterjee, S. G., Ramarao, B. V., and Tien, C. (1997). "Water-vapor sorption equilibria of a bleached-kraft paperboard – A study of the hysteresis region," *J. Pulp Paper Sci.* 23(8), J366-J373.

Chen, G. C. I., and Woodward, T. W. (1986). "Optimization of alkenyl succinic anhydride emulsification and sizing," *Tappi J.* 69(8), 95-97.

Chen, M., and Biermann, C. J. (1995). "Investigation of the mechanism of paper sizing through a desizing approach," *Tappi J.* 78(8), 120-126.

Chen, Y., Long, Z., Xie, L., and Fang, B. (2001). "The factors affecting rosin neutral sizing," *China Pulp Paper* 2001(2), 20-24.

Chew, Y. S., Peng, G., Roberts, J. C., Xiao, H., Nurmi, K., and Sundberg, K. (2004). "Characteristics of AKD emulsions prepared using cationic starches with well-

defined structures," *Proc. Wet End Chemistry*, May 11-12, 2004, Nice, France, Pira International, Leatherhead, Surrey, UK.
Colasurdo, A. R., and Thorn, I. (1992). "The interactions of alkylketene dimer with other wet-end additives," *Tappi J.* 75(9), 143-149.
Cooper, C., Dart, P., Nicholas, J., and Thorn, I. (1995). "The role of polymers in AKD sizing," *Paper Technol.* 36(4), 30-34.
Crouse, B., and Wimer, D. G. (1990). "Alkaline sizing: An overview," *TAPPI Neutral/Alkaline Short Course Notes*, TAPPI Press, Atlanta, 5-39.
Dart, P. J. (1990). "Determination of alkylketene dimer sizing agent products in paper by capillary gas chromatography," *Analyst* 115(1), 13-16.
Daud, W. R. W. (1993). "Fundamental aspects of alkenyl succinic anhydride sizing," *Proc. APPITA Annual General Conf.*, Vol. 2, Paper No. 3B23, 567-572.
Davis, K. R., and Hogg, J. L. (1983). "Transition-state structures for the hydrolysis of cyclic and acyclic carboxylic acid anhydrides," *J. Org. Chem.* 48, 1041-1047.
Davis, J. W., Roberson, W. H., and Weisgerber, C. A. (1956). "A new sizing agent for paper – Alkylketene dimers," *Tappi* 39(1), 21-23.
Davison, R. W. (1976). "The sizing of paper," *Tappi* 58(3), 48-57.
Davison, R. W. (1986). "A general mechanism of internal sizing," *Proc. TAPPI 1986 Papermakers Conf.*, TAPPI Press, Atlanta, 17-27.
Dumas, D. H. (1981). "An overview of cellulose-reactive sizes," *Tappi* 64(1), 43-46.
Dumas, D. H., and Evans, D. B. (1986). "AKD-cellulose reactivity in papermaking systems," *Proc. TAPPI 1986 Papermakers Conf.*, TAPPI Press, Atlanta, 31-35.
Ehrhardt, S. M. (1987). "The fundamentals of sizing with rosin," *TAPPI 1987 Sizing Short Course Notes*, TAPPI Press, Atlanta.
Ehrhardt, S. M., and Gast, J. C. (1988). "Cationic dispersed rosin sizes," *Proc. TAPPI 1988 Papermakers Conf.*, TAPPI Press, Atlanta, 181-186.
Eklund, D., and Linström, T. (1991). *Paper Chemistry, An Introduction*, DT Paper Science Publ., Grankulla, Finland.
Espy, H. H. (1995). "The mechanism of wet-strength development in paper: A review," *Tappi J.* 78(4), 90-99.
Esser, A., and Ettl, R. (1997). "On the mechanism of sizing with alkyl ketene dimer (AKD): Physico-chemical aspects of AKD retention and sizing efficiency," *The Fundamentals of Papermaking Materials*, Trans. 11th Fundamental Res. Symp., Cambridge,1997, Pira International, Leatherhead, Surrey, UK, 997-1020.
Fallmann, J., and Bernardis, M. (1997). "Progress in paper sizing," *Wochenbl. Papierfabr.* 125(18), 878-883.
Fineman, I., and Hoc, M. (1978). "Surface properties, especially linting, of surface-sized fine papers – Influence of starch distribution and hydrophobicity," *Tappi J.* 61(5), 433-46.
Finlayson, M. F., Hodgson, K. T., Cooper, J. L., Gathers, J. J., and Springs, K. E. (1996). "Internal sizing of paper and paperboard with ethylene copolymers," *Proc. TAPPI 1996 Papermakers Conf.*, TAPPI Press, Atlanta, 309-314.
Fischer, K. (1999). "Improvement of rosin sizes by esterification and new emulsification techniques," *Proc. Scientific and Technical Advances in the Internal and Surface*

Sizing of Paper and Board, Florence, Italy, Dec. 2-3, 1999, Pira International, Leatherhead, Surrey, UK, Paper 14.

Gallay, W. (1973). "Stability of dimensions and form of paper," *Tappi* 56(11), 54-95.

Galvin, D. H. (1988). "Shedding light on water absorption rates," *Tappi J.* 71(12), 188-189.

Garnier, G., Berlin, M., and Smrckova, M. (1999). "Wetting dynamics of alkylketene dimer on cellulosic model surfaces," *Langmuir* 15(22), 7863-7869.

Garnier, G., Duskova-Smrckova, M., Vyhnalkova, R., van de Ven, T. G. M., and Revol, J.-F. (2000). "Association in solution and adsorption at an air-water interface of alternating copolymers of maleic anhydride and styrene," *Langmuir* 16(8), 3757-3763.

Garnier, G., and Godbout, L. (2000). "Wetting behavior of alkyl ketene dimer on cellulose and model surfaces," *J. Pulp Paper Sci.* 26(5), 194-199.

Garnier, G., and Yu, L. (1999). "Wetting mechanism of a starch-stabilized alkylketene dimer emulsion: A study by atomic force microscopy," *J. Pulp Paper Sci.* 25(7), 235-242.

Garrett, P. D., and Lee, K. I. (1998). "Characterization of polymers for paper surface sizings using contact angle methods," *Tappi J.* 81(4), 198-203.

Gess, J. M. (1991). "The sizing of paper with rosin and alum at acid pHs," in *Paper Chemistry*, 2nd Ed., J. C. Roberts, ed., Blackie Academic and Professional, London, Ch. 8, 120-139.

Gess, J., and Rende, D. S. (2005). "Alkenyl succinic anhydride (ASA)," *Tappi J.* 4(9), 25-30.

Guan, Y. (2002). "Effect of cationic starch on ASA emulsification," *China Pulp Paper* 2002(5), 17-20.

Hansen, C. M., and Björkman, A. (1998). "The ultrastructure of wood from a solubility parameter point of view," *Holzforschung* 52 (4), 335-344.

Hardell, H. L., and Woodbury, S. E. (2002). "A new method for the analysis of AKD oligomers in papermaking systems," *Nordic Pulp Paper Res. J.* 17(3), 340-345.

Hartong, B., and Deng, Y. (2004). "Evidence of ester bond contribution to neutral to alkaline rosin sizing using polyethylenimine-epichlorohydrin as a mordant," *J. Pulp Paper Sci.* 30(7), 203-209.

Hasegawa, M., Isogai, A., and Onabe, F. (1997). "Alkaline sizing with alkylketene dimers in the presence of chitosan salts," *J. Pulp Paper Sci.* 23(11), J528-J531.

Haselton, W. R. (1955). "Gas adsorption by wood, pulp, and paper. II. The application of gas adsorption techniques to the study of the area and structure of pulps and the unbonded and bonded area of paper," *Tappi* 38(12), 716-723.

Hatanaka, S., Takahashi, Y., and Roberts, J. C. (1991). "Sizing with saponified alkenyl succinic acid," *Tappi J.* 74(2), 177-181.

Hedborg, F., and Lindström, T. (1993). "Alkaline rosin sizing using microparticulate aluminum-based retention aid systems in a fine paper stock containing $CaCO_3$," *Nordic Pulp Paper Res. J.* 8(3), 331-336.

Hodgson, K. T. (1994). "A review of paper sizing using alkyl ketene dimer versus alkenyl succinic anhydride," *Appita* 47(5), 402-406.

Hodgson, K. (1997). "Other alkaline-sizing chemistries," *TAPPI 1997 Sizing Short Course Notes*, TAPPI Press, Atlanta, Session 4, Paper 3.

Hodgson, K. T., and Ness, J. M. (1999). "Self-sizing mechanisms of thermomechanical pulps used in newsprint production," *Proc. Scientific and Technical Advances in the Internal and Surface Sizing of Paper and Board*, Florence, Italy, Dec. 2-3, 1999, Pira International, Leatherhead, Surrey, UK, Paper 15.

Hoyland, R. W., and Neill, M. P. (2001). "Factors affecting the frictional properties of paper – The effect of AKD neutral size," *Paper Technol.* 42(3), 45-373.

Hubbe, M. A. (2000). "Wetting and penetration of liquids into paper," *Encyclopedia of Materials Technologies*, Elsevier, Oxford, UK, 6735-6739.

Hubbe, M. A. (2005). "Acidic and alkaline sizings for printing, writing, and drawing papers," *The Book and Paper Group Annual* 23, 139-151.

Hubbe, M. A., Venditti, R. A., Barbour, R. L., and Zhang, M. (2003). "Changes to unbleached kraft fibers due to drying and recycling," *Prog. Paper Recycling* 12(3), 11-20.

Hunkeler, D. (2006). "Value added polyelectrolytes: Novel polymers and micro-capsules," *Proc. Wet End Chemistry 2006*, Madrid, Pira International, Leatherhead, UK, Paper 6.

Hutton, B., and Shen, W. (2005). "Sizing effects via AKD vaporization," *Appita J.* 58(5), 367-373.

Isolati, A. (1989). "The use of aluminum polychloride for internal rosin sizing of paper," *Paperi Puu* 66(9), 521-2, 525-6, 529-30.

Irvine, J. A., Aston, D. E., and Berg, J. C. (1999). "The use of atomic force microscopy to measure the adhesive properties of size and unsized papers," *Tappi J.* 82(5), 172-174.

Isogai, A. (1997). "Effect of cationic polymer addition on retention of alkylketene dimer," *J. Pulp Paper Sci.* 23(6), J276-J281.

Isogai, A. (1998). "Sizing behavior of paper by ASA and extractability of ASA components from sheets," *Proc. 1998 65th Pulp Paper Res. Conf.*, 178-181.

Isogai, A. (1999). "Mechanism of paper sizing by alkylketene dimers," *J. Pulp Paper Sci.* 25(7), 251-255.

Isogai, A. (2000). "Stability of AKD-cellulose β-ketoester bonds to various treatments," *J. Pulp Paper Sci.* 26(9), 330-334.

Isogai, A., and Asakura, K. (1999). "Retention and sizing behavior in AKD (liquid-type ketene dimer) sizing," *Proc. Scientific and Technical Advances in the Internal and Surface Sizing of Paper and Board*, 1999, Florence, Italy, Pira International, Leatherhead, Surrey, UK, Paper 5.

Isogai, A., Kitaoka, C., and Onabe, F. (1997). "Effects of carboxyl groups in pulp on retention of alkylketene dimer," *J. Pulp Paper Sci.* 23(5), J215-J219.

Isogai, A., and Morimoto, S. (2004). "Sizing performance and hydrolysis resistance of alkyl oleate succinic anhydrides," *Tappi J.* 3(7), 8-12.

Isogai, A., Nishiyama, M., and Onabe, F. (1996). "Mechanism of paper sizing with ASA; Mechanism of retention of alkenyl succinic anhydride (ASA) on pulp fibers at the wet end of papermaking," *Sen'i Gakkaishi* 52(4), 195-201.

Isogai, A., and Onabe, F. (1996). "Structures of alkenyl succinic anhydride (ASA) components in ASA-sized paper sheet," *Sen'i Gakkaishi* 52(4), 180-188.

Isogai, A., Onabe, F., Taniguchi, R., and Usuda, M. (1992). "Sizing mechanism of alkylketene dimers. Part 2. Deterioration of alkylketene dimer emulsion," *Nordic Pulp Paper Res. J.* 7(4), 205-211.

Isogai, A., Taniguchi, R., and Onabe, F. (1994). "Sizing mechanism of alkylketene dimers. Part 4. Effects of AKD and Ketone in emulsions on sizing," *Nordic Pulp Paper Res. J.* 9(1), 44-48.

Ito, K., Isogai, A., and Onabe, F. (1999). "Rosin-ester sizing of alkaline papermaking," *J. Pulp Paper Sci.* 25(6), 222-226.

Iwasa, S. (1999). "Application of rosin size for acid to alkaline papermaking," *Proc. Scientific and Technical Advances in the Internal and Surface Sizing of Paper and Board,* Florence, Italy, Dec. 2-3, 1999, Pira International, Leatherhead, Surrey, UK, Paper 13.

Jaycock, M. J., and Roberts, J. C. (1994). "A new procedure for the analysis of alkyl ketene dimers in paper," *Paper Technol.* 35(4), 38-42.

Jiang, H., and Deng, Y. (2000). "The effects of inorganic salts and precipitated calcium carbonate filler on the hydrolysis kinetics of alkylketene dimer," *J. Pulp Paper Sci.* 26(6), 208-213.

Jing, Q., Chen, M., and Biermann, C. J. (1998). "Octadecylamime as an internal sizing agent," *Tappi J.* 81(4), 193-197.

Johansson, J, and Lindström, T. (2004a). "A study on AKD-size retention, reaction, and sizing efficiency. Part 1: The effects of pulp bleaching on AKD-sizing," *Nordic Pulp Paper Res. J.* 19(3), 330-335.

Johansson, J, and Lindström, T. (2004b). "A study on AKD-size retention, reaction, and sizing efficiency. Part 2: The effects of electrolytes, retention aids, shear forces, and mode of addition on AKD-sizing using anionic and cationic AKD dispersions," *Nordic Pulp Paper Res. J.* 19(3), 336-344.

Kamutzki, W., and Krause, T. (1983). "Mechanisms during the neutral sizing with alkyldiketenes," *Wochenbl. Papierfabr.* 111(7), 215-222.

Karademir, A. (2002). "Quantitative determination of alkyl ketene dimer (AKD) retention in paper made on a pilot paper machine," *Turk. J. Agric. For.* 26, 253-260.

Karademir, A., and Hoyland, D. (2003). "The sizing mechanism of AKD and its effect on paper friction," *Appita J.* 56(5), 380-384.

Karademir, A., Hoyland, D., Wiseman, N., and Xiao, H. N. (2004). "A study of the effects of alkyl ketene dimer and ketone on paper sizing and friction properties," *Appita J.* 57(2), 116-120.

Keavney, J. J., and Kulick, R. J. (1981). "Internal sizing," in *Pulp and Paper Chemistry and Chemical Technology*, 3rd Ed., J. P. Casey, ed., Wiley-Interscience, New York, Vol. 3, Ch. 16, 1547-1592.

Kenton, J. (1996). "Sizing history: From evolution to revolution," *PaperAge* 112(6), 32-33.

Kitaoka, T., Isogai, A., and Onabe, F. (1995). "Sizing mechanism of emulsion rosin size-alum systems. Part 1. Relationships between sizing degrees and rosin size or

aluminum content in rosin-sized handsheets," *Nordic Pulp Paper Res. J.* 10(4), 253-260.

Kitaoka, T., Isogai, A, and Onabe, F. (1997). "Sizing mechanism of emulsion rosin size-alum systems. Part 2. Structures of rosin size components in the paper sheet," *Nordic Pulp Paper Res. J.* 12(1), 26-31.

Klass, C. P. (1990). "Trends and developments in size press technology," *Tappi J.* 73(12), 69-75.

Knubb, S., and Zetter, C. (2002). "Deposit study of alkylketene dimer dispersions," *Nordic Pulp Paper Res. J.* 17(2), 164-167.

Kondo, N., and Makino, S. (1993). "Neutral/alkaline papermaking system by using specialized cationic polymers. Mechanism of enhancing AKD sizing," *Kami Pa Gikyoshi* 47(2), 234-238.

Krueger, J. J., and Hodgson, K. T. (1995). "The relationship between single fiber contact angle and sizing performance," *Tappi J.* 78(2), 154-161.

Kurrle, F. L. (1995). "Process for enhancing sizing efficiency in filled papers," *U.S. Pat.* 5,411,639.

Laine, J., Mattson, F., and Swerin, A. (2004). "The effect of bleached pulp type on AKD internal sizing – An EuroFEX experimental paper machine study," *Appita J.* 57(4), 327-327.

Laitinen, R. A. (1999). "Quantitative analysis of AKD and ASA distribution in paper," *Proc. Scientific and Technical Advances in the Internal and Surface Sizing of Paper and Board,* 1999, Florence, Italy, Pira International, Leatherhead, Surrey, UK, Paper 6.

Latta, J. L. (1994). "Practical applications of styrene maleic anhydride surface treatment resins for fine paper sizing," *Proc. TAPPI 1994 Papermakers Conf.*, TAPPI Press, Atlanta, 399-406.

Lauzon, R. V. (1997). "New cationic dispersed rosin size – Field trials and successes," *Proc. TAPPI 1997 Engineering & Papermakers Conf.*, TAPPI Press, Atlanta, 819-836.

Lee, G. H., and Shin, D. S. (1991). "Effects of degree of substitution of cationic starches on ASA sizing in alkaline papermaking," *J. TAPPIK* 23(2), 5-14.

Lee, H. L., Kim, J. S., and Youn, H. Y. (2004). "Improvement of ASA sizing efficiency using hydrophobically modified and acid-hydrolyzed starches," *Tappi J.* 3(12), 3-6.

Lee, H. L., and Luner, P. (2005). "Effect of relative humidity and unreacted AKD on AKD sizing," *Nordic Pulp Paper Res. J.* 20(2), 227-231.

Lee, H. L., Shin, J. Y., Koh, C.-H., Ryu, H., Lee, D.-J., and Sohn, C. (2002). "Surface sizing with cationic starch: Its effect on paper quality and papermaking process," *Tappi J.* 1(1), 34-40.

Lee, H. N. (1936). "The microscopical mechanism of rosin sizing," *Paper Trade J.,* 103(TAPPI Sec.), T386-390.

Lee, S. Y., Hubbe, M. A., and Saka, S. (2006). "Prospects for biodiesel as a byproduct of wood pulping – A review," *BioResourses* 1(1), 150-171.

Li, H., Ni, Y., and Sain, M. (2003). "Further understanding of polyethyleneimine-induced rosin ester sizing," *Nordic Pulp Paper Res. J.* 18(1), 5-9.

Liden, T., and Tollander, M. (2004). "Extractives in totally chlorine free bleached birch pulp and their effect on alkylketene dimers and alkenyl succinic anhydrides sizes," *Nordic Pulp Paper Res. J.* 19(4), 466-469.

Lindfors, J., Ahola, S., Kallio, T., Laine, J., Stenius, P., and Danielsson, M. (2005). "Spreading and adhesion of ASA on different surfaces present in paper machines," *Nordic Pulp Paper Res. J.* 20(4), 453-458.

Lindström, T., and O'Brian, H. (1986). "On the mechanism of sizing with alkylketene dimers. Part 2. The kinetics of reaction between alkylketene dimers and cellulose," *Nordic Pulp Paper Res. J.* 1(1), 34-42.

Lindström, T., and Söderberg, G. (1986a). "On the mechanism of sizing with alkylketene dimers. Part 1. Studies on the amount of alkylketene dimer required for sizing different pulps," *Nordic Pulp Paper Res. J.* 1(1), 26-33,42.

Lindström, T., and Söderberg, G. (1986b). "On the mechanism of sizing with alkylketene dimers. Part 3. The role of pH, electrolytes, retention aids, extractives, Ca-lignosulfonates and mode of addition on alkylketene dimer retention," *Nordic Pulp Paper Res. J.* 1(2), 31-38.

Lindström, T., and Söderberg, G. (1986c). "On the mechanism of sizing with alkylketene dimers. Part 4. The effects of HCO_3^- ions and polymeric reaction accelerators on the rate of reaction between alkylketene dimers and cellulose," *Nordic Pulp Paper Res. J.* 1(2), 39-45.

Lipponen, J., Pakarinen, J., Jaaskelainen, J. and Gron, J. (2005). "Mechanical properties of woodfree paper sheets at different surface size starch amounts," *Paperi Puu* 87(3), 170-175.

Liu, J. (1993). "Sizing with rosin and alum at neutral pH," *Paper Technol.* 34(8), 20-24.

Liu, Y., Niu, M., and Zhang, Y. (2004). "The research of rosin ester neutral sizing agent," *Proc. 2nd ISTPPBFP*, Oct. 13-14, 2004, Nanjing Forestry University, China, 441-443.

Lyne, Å. L., Fillers, C., and Kolseth, P. (1996). "The effect of filler on hygroexpansivity," *Nordic Pulp Paper Res. J.* 11(3), 152-156.

Marton, J. (1989). "Mechanistic differences between acid and soap sizing," *Nordic Pulp Paper Res. J.* 4(2), 77-80.

Marton, J. (1991). "Practical aspects of alkaline sizing: Alkyl ketene dimer in mill furnishes," *Tappi J.* 74(8), 187-191.

Marton, J. (1995). "Kinetic aspects in furnish interactions. Sizing as an example," *Proc. TAPPI 1995 Papermakers Conf.*, TAPPI Press, Atlanta, 97-99.

Marton, J., and Marton, T. (1983). "Effect of fillers on rosin sizing of paper," *Tappi J.* 66(12), 68-71.

Matsuyama, K., Yokota, S., Kitaoka, T., and Wariishi, H. (2006). "Surface morphology and wetting characteristics of sized cellulose imitations," *Sen'i Gakkaishi* 64(4), 89-94.

McCarthy, W. R., and Stratton, R. A. (1987). "Effects of drying on ASA esterification and sizing," *Tappi J.* 70(12), 117-121.

Mendes, P., Xiao, H., Belgacem, M. N., and Costa, C. A. V. (2003a). "Potential limitations of impulse drying of AKD-containing paper," *Appita J.* 56(1), 46-52.

Mendes, P., Costa, C. A. V., Xiao, H. N., Belgacem, M. N., and Roberts, J. C. (2003b). "Influence of impulse drying on the retention and sizing of paper with alkyl ketene dimer," *Appita J.* 56(3), 241.

Mendes, P., Xiao, H., Costa, C. A. V., Belgacem, M. N., and Roberts, J. C. (2003c). "Influence of impulse drying on the retention and sizing of paper with alkyl ketene dimer," *Tappi J.* 2(2), 25-29.

Mikkonen, M., and Eklund, D. (1998). "The adsorption of different polyacrylamides on thermomechanical pulp in the presence of dissolved and colloidal substances," *Wochenbl. Papierfabr.* 126(2), 50-53.

Moyers, B. M. (1992). "Diagnostic sizing loss problem solving in alkaline systems," *Tappi J.* 94(1), 111-115.

Nahm, S. H. (1986). "Evidence for covalent bonding between ketene dimer sizing agents and cellulose," *J. Wood Chem. Tech.* 6(1), 89-112.

Nanri, Y., and Uesaka, T. (1993). "Dimensional stability of mechanical pulps – drying shrinkage and hygroexpansivity," *Tappi J.* 76(6), 62-66.

Ness, J., and Hodgson, K. T. (1999). "The effects of peroxide bleaching on thermo-mechanical pulp self-sizing," *Nordic Pulp Paper Res. J.* 14(2), 111-115.

Neimo, L. (1999). "Internal sizing of paper," in *Papermaking Chemistry*, L. Neimo (ed.), Fapet Oy, 151-203.

Nishiyama, M., Isogai, A., and Onabe, F. (1996a). "Mechanism of paper sizing with ASA; Structures of alkenyl succinic anhydride (ASA) components in ASA-sized paper sheet," *Sen'i Gakkaishi* 52(4), 180-188.

Nishiyama, M., Isogai, A., and Onabe, F. (1996b). "Mechanism of paper sizing with ASA; Roles of reactive alkenyl succinic anhydride (ASA) is paper sizing," *Sen'i Gakkaishi* 52(4), 189-194.

Nitzman, A. F., and Royappa, A. T. (2003). "Sizing variations of dispersed rosin sizes with fortification, hardness, pH, and temperature," *Tappi J.* 2(4), 8-11.

Norell, M., Johansson, K., and Persson, M. (1999). "Retention and drainage," in *Papermaking Chemistry*, L. Neimo (ed.), Fapet Oy, Helsinki, Ch. 3, 42-93.

Novak, R. W., and Rende, D. S. (1993). "Size reversion in alkaline papermaking," *Tappi J.* 76(8), 117-120.

Ödberg, L., Lindström, T., Liedberg, B., and Gustavsson, J. (1987). "Evidence for β-ketoester formation during the sizing of paper with alkylketene dimers," *Tappi J.* 70(4), 135-139.

Odermatt, J., Meyer, R., Meier, D., and Ettl, R. (2003). "Identification and quantification of alkylketene dimers by pyrolysis-gas chromatography/ mass spectrometry and pyrolysis-gas chromatography/ flame ionization detection," *J. Pulp Paper Sci.* 29(1), 1-6.

Ono, H., and Deng, Y. (1997). "Cationic polystyrene-based paper sizing agents," *Proc. TAPPI 1997 Engineering and Papermakers Conf.*, TAPPI Press, Atlanta, 837-849.

Ozaki, Y., and Sawatari, A. (1997). "Surface characterization of a rosin sizing agent in paper by means of EPMA, ESCA, and TOF-SIMS," *Nordic Pulp Paper Res. J.* 12(4), 260-266.

Ozment, J. L., and Colasurdo, A. R. (1994). "AKD sizing with blended PCC morphologies at high filler loading," *Proc. TAPPI 1994 Papermakers Conf.*, TAPPI Press, Atlanta, 169-172.

Page, D. H. and Tydeman, P. A. (1962). "A new theory of the shrinkage, structure, and properties of paper," in *Formation and Structure of Paper*, F. Bolam (ed.), Tech. Sect. British Paper and Board Makers Assoc., London, Vol. 1., 397-425.

Patton, P. A. (1991). "On the mechanisms of AKD sizing and size reversion," *Proc. TAPPI 1991 Papermakers Conf.*, TAPPI Press, Atlanta, 415-423.

Peck, M. C., and Markillie, M. A., "Practical applications of neutral papermaking with rosin size," *Proc. TAPPI 1994 Papermaker's Conf.*, TAPPI Press, Atlanta, Vol. 1, 165-168.

Petander, L., Ahlskog, T., and Juppo, A. J. (1998). "Strategies to reduce AKD deposits on paper machines," *Paperi Puu* 80(2), 100-103.

Poppel, E., and Bobu, E. (1987). "Some aspects of neutral/alkaline sizing of calcium carbonate-filled paper," *Proc. Pira Chem. Neutral Pmkg. Sem.*, Pira International, Leatherhead, Surrey, UK, Session 3, Paper 10.

Proverb, R. (1997). "Troubleshooting sizing problems; Alkaline papermaking," *TAPPI 1997 Sizing Short Course Notes*, TAPPI Press, Atlanta, Paper No. 8.1.

Ramamurthy, P., Vanerek, A., and van de Ven, T. (2000). "Efficiency of AKD sizing in mixed hardwood-softwood furnishes," *J. Pulp Paper Sci.* 26(2), 72-75.

Ravnjak, D. (2006). "Deposition kinetics of AKD size on pulp fibers," *Proc. Wet End Chemistry 2006*, Madrid, Pira International, Leatherhead, UK, Paper 7.

Rende, D. S., and Breslin, M. D. (1987). "Paper sizing method and emulsion," *U.S. Pat.* 4,657,946.

Reynolds, W. F., ed., *The Sizing of Paper*, 2nd Ed., TAPPI Press, Atlanta, USA.

Riebeling, U., Jeurissen, H. F. M., de Clercq, A., and Prinz, M. (1996). "A new internal sizing concept – Enhanced performance of AKD through use of hydrophobically modified amphoteric polymers," *Wochenbl. Papierfabr.* 124(22), 997-1002.

Roberts, J. C. (1991). "Neutral and alkaline sizing," in *Paper Chemistry*, 2nd Ed., J. C. Roberts, ed., Blackie Academic and Professional, London, Ch. 9, 140-160.

Roberts, J. C. (1997). "Chemical control of water penetration in paper," *Proc. SPIE – Iont. Soc. Optical Engineering* (3227), 20-39.

Roberts, J. C., and Garner, D. N. (1985). "The mechanism of alkyl ketene dimer sizing of paper. Part 1," *Tappi J.* 68(4), 118-121.

Roberts, J. C., Takahashi, Y., Hatanaka, S., and Takeda, Y. (1993). "The effect of substituted alkaline structure on ASA sizing," *Proc. The Chemistry of Papermaking*, 1993, Pira International, Leatherhead, Surrey, UK, Paper 10.

Rohringer, P, Bernheim, M., and Werthmann, D. P. (1985). "Are so-called reactive sizes really cellulose reactive?" *Tappi J.* 68(1), 83-86.

Rossall, B., and Robertson, R. E. (1975). "Neutral solvolysis of acyl carbon and temperature dependence of kinetic solvent isotope effect," *Can. J. Chem.* 53, 869-877.

Savolainen, R. M. (1966). "The effects of temperature, pH, and alkalinity on ASA sizing in alkaline papermaking," *Proc. TAPPI 1996 Papermakers Conf.*, TAPPI Press, Atlanta, 289-295.

Scalfarotto, R. E. (1985). "Remedies for press picking boost efficiency of ASA synthetic sizing," *Pulp Paper* 59(4), 126-129.

Scott, W. E, Abbott, J. C., and Trosset, S. (1995). *Properties of Paper: An Introduction*, 2nd Ed., TAPPI Press, Atlanta, see pp. 53-67.

Seo, W.-S., and Cho, N.-S. (2005). "Effect of water content on cellulose/AKD reaction," *Appita J.* 58(2), 122-126.

Seppänen, R., and Tiberg, F. (1999). "AKD sizing – spreading mechanism and influence on paper properties," *Proc. Scientific and Technical Advances in the Internal and Surface Sizing of Paper and Board*, 1999, Florence, Italy, Pira International, Leatherhead, Surrey, UK, Paper 2.

Shen, J., Liu, W., and Li, C. (2004). "Effect of cationic polymers on rosin emulsification and sizing efficiency," *Proc. 2nd ISTPPBFP*, Nanjing, China, Oct. 13-14, 2004, Nanjing Forestry Univ., Nanjing, China, 363-366.

Shen, W., Brack, N., Huy, L., Parker, I. H., Pigram, P. J., and Liesegang, J. (2001a). "Mechanism of AKD migration studied on glass surfaces," *Colloids Surf. A* 176(2-3), 129-137.

Shen, W., and Parker, I. (2003a). "A study of the non-solid behavior of AKD wax," *Appita J.* 56(6), 442-356.

Shen. W., Parker, I. H., Brack, N., and Pigram, P. J. (2001b). "A simplified approach to understanding the mechanism of AKD sizing," *Appita J.* 54(4), 352-356.

Shen, W., Xu, F., and Parker, I. H. (2002). "The effect of the melting of AKD and its corresponding ketone on spreading behavior," *Appita J.* 55(5), 375-381.

Shen, W., Xu, F., and Parker, I. H. (2003). "An experimental investigation of the redistribution behaviour of alkyl ketene dimers and their corresponding ketones," *Colloids Surf. A* 212(2-3), 197-209.

Shen, W., Zhang, H. L., and Ettl, R. (2005). "Chemical composition of 'AKD vapor' and its implication to AKD vapor sizing," *Cellulose* 12(6), 641-652.

Shigeto, H., and Umekawa, H. (1992). "Alkenyl succinic acid emulsion sizing agent," *U.S. Patent* 5,391,225.

Shimada, K., Dumas, D., and Biermann, C. (1997). "Properties of candidate internal sizing agents versus sizing performance," *Tappi J.* 80(10), 171-174.

Smith, D. (1999). "ASA components: Their synthesis and relative sizing performance," *Proc. Scientific and Technical Advances in the Internal and Surface Sizing of Paper and Board,* Pira International, Leatherhead, Surrey, UK, Paper 8.

Soteland, N., and Loras, V. (1976). "Self-sizing of mechanical pulp," *Svensk Papperstid.* 79(9), 203-202 sic.

Stone, J. E., and Scallan, A. M. (1966). "Influence of drying on the pore structures of the cell wall," in *Consolidation of the Paper Web*, F. Bolam (ed.), Tech. Sec. British Paper and Board Makers Assoc., London, Vol. 1, 145-174.

Strazdins, E. (1963). "Interaction of rosin with some metal ions," *Tappi* 46(7), 432-437.

Strazdins, E. (1977). "Mechanistic aspects of rosin sizing," *Tappi* 60(10), 102-105.

Strazdins, E. (1981). "Chemistry of rosin sizing," *Tappi* 64(1), 31-34.

Strazdins, E. (1984). "Critical phenomena in rosin sizing," *Tappi J.* 67(4), 110-113.

Strazdins, E. (1989). "Paper sizes and sizing," in *Naval Stores: Production, Chemistry, Utilization*, D. F. Zinkel and J. Russell (eds.), Pulp Chem. Assoc., New York, Ch. 16, 575-624.

Subramanyam, S., and Biermann, C. J. (1992). "Generalized rosin soap sizing with coordinating elements," *Tappi J.* 75(3), 223-228.

Sundberg, K., Holmbom, B., Ekman, R., Nyman, J., and Axberg, J. (1999). "Determination of alkenyl succinic anhydride (ASA) in pulp and paper samples," *Proc. Scientific and Technical Advances in the Internal and Surface Sizing of Paper and Board*, 1999, Florence, Italy, Pira International, Leatherhead, Surrey, UK, Paper 7.

Swanson, R. E. (1978). "Mechanism of cellulose sizing produced by vapor phase adsorption," *Tappi* 61(7), 77-80.

Swanson, J. W., and Cordingly, S. (1959). "Surface chemical studies of pitch. 2. The mechanism of self-sizing in papers made from wood pulps," *Tappi* 42(10), 812-819.

Takai, T., Ooyanagi, S., Tanabe, M., and Itoh, H. (1997). "Sizing mechanism of hydrophobically modified polyacrylamides," *Kami Pa Gikyoshi* 51(2), 286-291.

Taniguchi, R., Isogai, A., Onabe, F., and Usuda, M. (1993). "Sizing mechanism of alkylketene dimers. Part 3. Appearance of sizing features of AKD-sized sheets," *Nordic Pulp Paper Res. J.* 8(4), 352-357.

Thorn, I., Dart, P. J., and Main, S. D. (1993). "The use of cure promoters in alkaline sizing," *Paper Technol.* 34(1), 41-45.

Traugott, W. (1985). "Rosin sizing in the neutral to weakly alkaline range," *Wochenbl. Papierfabr.* 113(1), 1-4.

Valton, E., Sain, M., and Schmidhauser, J. (2003). "Performance of cationic styrene maleimide copolymer in wet-end papermaking," *Proc. TAPPI Spring Tech. Conf.*, TAPPI Press, Atlanta, electronic doc.

Von Bahr, M., Seppänen, R., Tiberg, F., and Zhmud, B. (2004). "Dynamic wetting of AKD-sized papers," *J. Pulp Paper Sci.* 30(3), 74-81.

Voutilainen, P. (1996). "Competitive adsorption of alkyl ketene dimer (AKD) on pulp fibers and $CaCO_3$ fillers," *Proc. 1996 International Paper and Coating Chemistry Symposium*, 195-204.

Vrbanac, M. D., Bogar, R. G., Dixon, D. H., Thomsonn, S. L., and Clawson, C. M. (1999). "Analysis of paper sizing and wet strength chemicals," *Proc. Scientific and Technical Advances in the Internal and Surface Sizing of Paper and Board,*" Florence, Italy, 1999, Pira International, Leatherhead, Surrey, UK, Paper 3.

Wågberg, L., and Björklund, M. (1993). "On the mechanism behind wet strength development in papers containing wet strength resins," *Nordic Pulp Paper Res. J.* 8(1), 53-58.

Wang, F., and Tanaka, H. (2001). "Mechanisms of neutral-alkaline paper sizing with usual rosin size using alum-polymer dual retention aid system," *J. Pulp Paper Sci.* 27(1), 8-13.

Wang, F., Tanaka, H., Kitaoka, T., and Hubbe, M. A. (2000). "Distribution characteristics of rosin size and their effect on the internal sizing of paper," *Nordic Pulp Paper Res. J.* 15(5), 416-421.

Wang, F., Wu, Z., and Tanaka, H. (1999). "Preparation and sizing mechanisms of neutral rosin size. 2: Functions of rosin derivatives on sizing efficiency," *J. Wood Sci.* 45, 475-480.

Wang, T., Simonsen, J., and Biermann, C. J. (1997). "A new sizing agent: Styrene-maleic anhydride copolymer with alum or iron mordants," *Tappi J.* 80(1), 277-282.

Wasser, R. B. (1986). "The penetration of aqueous liquids into ASA sized paper," *Proc. TAPPI 1986 Papermakers Conf.*, TAPPI Press, Atlanta, 1-6.

Wasser, R. B. (1987). "The reactivity of alkenyl succinic anhydride: Its pertinence with respect to alkaline sizing," *J. Pulp Paper Sci.* 13(1), J29-J32.

Wasser, R. B., and Brinen, J. S. (1998). "Effect of hydrolyzed ASA on sizing in calcium carbonate filled paper," *Tappi J.* 81(7), 139-144.

Wenzel, R. N. (1936). "Resistance of solid surfaces to wetting by water," *Indust. Eng. Chem.* 28(8), 988-994.

Wu, Z.-H., Chen, S.-P., and Tanaka, H. (1997). "Effects of polyamine structure on rosin sizing under neutral papermaking conditions," *J. Appl. Polymer Sci.* 65(11), 2159-2163.

Wurzburg, O. B., and Mazzarella, E. D. (1963). "Novel paper sizing process," *U.S. Pat.* 3,102,064.

Yang, L., Pelton, R., McLellan, F., and Fairbank, M. (1999). "Factors influencing the treatment of paper with fluorochemicals for oil repellency," *Tappi J.* 82(9), 128-135.

Yang, N., and Deng, Y. L. (2000). "Paper sizing agents from micelle-like aggregates of polystyrene-eased cationic copolymers," *J. Appl. Polymer Sci.* 77(9), 2067-2073.

Yano, T., Ohtani, H., and Tuge, S., "Determination of neutral sizing agents in paper by pyrolysis-gas chromatography," *Analyst* 117(5), 849-852.

Yasuda, H., Okuno, T., Sawa, Y., and Yasuda, T. (1995). "Surface configuration change observed for Teflon-PFA on immersion in water," *Langmuir* 11(8), 3255-3260.

Yu, L., and Garnier, G. (1997). "Mechanism of internal sizing with alkyl ketene dimers: The role of vapor deposition," *The Fundamentals of Papermaking Materials*, Trans. 11th Fundamental Res. Symp, 1997, Cambridge, Pira International, Leatherhead, Surrey, UK, 1021-1046.

Zandersons, Y. G., Tardenaka, A. T., and Zhurin'sh, A. I. (1993). "Reactivity of alkenylsuccinic anhydrides and factors affecting paper sizing in neutral and alkaline media," *Khim. Drev.* (6), 46-52.

Zeno, E., Carré, B., and Mauret, E. (2005). "Influence of surface active substances on AKD sizing," *Nordic Pulp Paper Res. J.* 20(2), 253-258.

Zhuang, J., and Biermann, C. J. (1995). "Neutral to alkaline rosin soap sizing with metal ions and polyethyleneimine as mordants," *Tappi J.* 78(4), 155-162.

Zhuang, J., Chen, M., and Biermann, C. J. (1997). "Rosin soap sizing without mordants by immersion in size solution," *Tappi J.* 80(1), 271-276.

Zou, Y., Hsieh, J. S., Wang, T. S., Mehnert, E., and Kokoszka, J. (2004). "The mechanism of premixing rosin sizes for neutral-alkaline papermaking," *Tappi J.* 3(9), 16-18.

Article submitted: Oct. 7, 2006; First round of reviewing completed: November 28, 2006; Publication: Feb. 24, 2007.